TU WIEN Technische Universität Wien Vienna University of Technology

ALDIS

Master Thesis

Extreme Lightning Parameters in Austria

Master's degree in Electrical Engineering

Director of Master Thesis:

Ao.Univ.Prof.i.R. Dipl.-Ing. Dr.techn.

Wolfgang Hadrian

E373 - Institute of Power Systems and Energy Economics

Supervisor:

Dipl.-Ing. Dr.techn. Wolfgang Schulz

Dipl.-Ing. Dr.techn. Gerhard Diendorfer

Austrian Lightning Detection and Information System (ALDIS)

Submitted at:

Vienna University of Technology

Faculty of Electrical Engineering and IT

June 2009

Master Thesis of:

BSc. Hubert Umprecht

Matr.-Nr. 0225409

Hauptstraße 30, 2463 Stixneusiedl

Abstract

The main goal of this diploma thesis is to perform a comprehensive study of the lightning activity in Austria in the time interval from 1998 to 2007. Additionally some important lightning parameters of the flashes located in Austria are analysed. The used data have been collected by the Austrian Lightning Location System called Austrian Lightning Detection and Information System (ALDIS). The first analysis determines the lightning density of Austria. There are a few hot spots which are described in more detail. The location with the highest flash density is the 2166 m high mountain Dobratsch where a radio transmitter tower is situated, with a value of 85.6 flashes per square kilometer and year. The second part of this diploma thesis provides information about the highest flash multiplicities observed in Austria between 2002 and 2007. The highest multiplicity had a flash detected at the Dobratsch with 45 strokes on the 18th September 2007. The next analysis shows a study of strokes with extremely high peak currents located in Austria and Middle Europe. Aim is to find the stroke with the highest peak current and a serious detection quality in the time interval between 2000 and 2007. We found a stroke with a peak current of about 550 kA detected by 11 sensors and with a degree of freedom of 5. Finally the influence of the radio transmitter tower located on the Gaisberg to the lightning density in the proximity is analysed. The directly measured tower impacts are subtracted from the strokes detected by the Lightning Location System in a 20 km × 20 km area with the Gaisberg in the center. Additionally the Appendix shows a detailed collection of photos and maps of the described locations.

Acknowledgements

First of all, I want to warmly thank my parents who supported me during my whole study.

My deep gratitude goes to Prof. Wolfgang Hadrian from Vienna University of Technology who made it possible for me to write a diploma thesis about a very interesting topic. Additionally he introduced me to the people from ALDIS.

I wish to thank Dr. Gerhard Diendorfer from ALDIS who supported me developing my diploma thesis.

My warmest thanks go to the supervisor of my diploma thesis Dr. Wolfgang Schulz from ALDIS who has collaborated with me in a very pleasant atmosphere. He introduced me in different software programs as well as in Lightning Location System technology and supported me at every difficult situation.

Additionally thanks to the Technical Committee BL "Lightning Protection" which allowed me presenting my diploma thesis at their 193. meeting on the 12th May 2009 in Puch bei Weiz (styria).

Also thanks to Natascha Liebhart, Stephan Willinger and Thomas Kropej who joined and supported me on my different travels through Austria, investigating the "lightning-interesting" areas.

Stixneusiedl, 29th May 2009

Hubert Umprecht

Table of contents

1. Introduction

A cloud to ground discharge, also known as lightning or flash is one of the most interesting natural spectacles around the world. This phenomenon fascinates the mankind for a long time, from the mythology of ancient Greece, where lightning was considered as punishment sent by Zeus, up to the triggering of lightning with special rockets in U.S. for research purposes in the present. But the biggest interest in lightning is based on its danger including the threat for humans, buildings, electronic transmission and distribution and electronic devices. Actually everything on the earth surface, above it[1] or even below[2] could be target of a cloud to ground discharge and this fact leads to the importance of the lightning protection. Such a lightning can cause destruction of electronic devices, power blackouts and fire on buildings or forests. That means one lightning discharge and certainly the consequences can affect a lot of humans at the same time.

Up to now the incident lightning is not completely explored but it is possible to measure the lightning characteristic and its location. Using the records of so called lightning flash counters (LFC) and especially lightning location systems (LLS) we obtain lightning density maps showing the geographical distribution of lightning flashes. The knowledge of locations with higher flash density in addition with real time data from the LLS can be very useful for different applications, as:

- Helping insurance companies to proof whether a given damage is caused by a lightning or not
- Find coherences between lightning density and local conditions or atmospheric influences
- Buildings with sensitive equipment can be built in areas with lower lightning density to reduce the likelihood of a stroke
- Forecast of forest fire ignition due to lightning strokes
- Effects of lightning to the atmosphere and global warming
- Surveillance of airports and electric power utilities

The name of the cooperation which runs the largest lightning location system in Europe is EUCLID (**EU**ropean **C**ooperation for **LI**ghtning **D**etection). The aim of EUCLID is to identify and detect lightning over the European area. The involved countries are: Austria, Czech Republic, Denmark, Finland, France, Germany, Holland, Hungary, Italy, Norway, Slovakia, Slovenia, and Sweden. The whole network consists of 135 sensors contributing the detection of lightning [*www.euclid.org, March 2009*]. The Austrian part of EUCLID, called ALDIS (**A**ustrian **L**ightning **D**etection & **I**nformation **S**ystem), exists since 1991 and is a joint project of the Austrian Electrotechnical Association (ÖVE), the Austrian Electricity Board (VERBUND) and Siemens AG Austria. The Austrian lightning detection system consists of eight LS7000 sensors and a central lightning processor [*www.aldis.at, March 2009*].

[1] E.g. Aircraft
[2] E.g. Subway

In the following list a few important lightning parameters are given:

- peak current (kA)
- average current slope (kA/µs)
- flash/stroke charge transfer (C)
- duration (ms)
- flash/stroke energy (J)
- current rise time (µs)
- current fall time (µs)
- channel length (m)
- channel temperature (K)
- channel radius (m)
- propagation speed (m/s)
- number of strokes
- interstroke interval (ms)

These and more lightning parameters can be determined by measurements of rocket triggering lightning or lightning to tall towers as well as by optical methods like photography [*Rakov and Uman, 2003*].

In this diploma thesis I am going to analyse the following topics:

- Lightning density in Austria as well as analyses of so called "hot spots" (see chapter 5.)
- Investigate flashes with highest multiplicities located in Austria (see chapter 6)
- First attempt to find located strokes with the highest peak currents and an appropriate detection quality in Austria and Middle Europe (see chapter 7)
- Investigate the influence of the Gaisberg-tower on the local ground flash density (see chapter 8)

First I am giving an overview about the theory of lightning (chapter 2), the principles of lightning detection (chapter 3) and the Austrian Lightning Detection and Information System ALDIS (chapter 4).

2. The Lightning Phenomenon

In this chapter the basics of the lightning phenomenon will be discussed. Although all the details of a lightning discharge are not completely known and understood, in this chapter I will try to answer the following questions:

- What is a lightning discharge?
- What types of lightning exist?
- How does a lightning stroke occur?
- How are thunderclouds charged?
- How are the electromagnetic fields of a lightning stroke/flash?
- What are the parameters of a lightning stroke/flash?

A lightning discharge is a naturally generated high current discharge whose path length is measured in kilometers. The most common lightning sources are electric charges in ordinary thunderclouds (cumulonimbus). Other lightning like discharges, not associated with a thunderstorm, have been observed by volcanic eruptions [*e.g. Anderson et al., 1965; Brook et al., 1974; Pounder, 1980*], thermonuclear explosions [*e.g. Uman et al., 1972; Hill, 1973; Grover, 1981; Gardner et al., 1984*], sandstorms [*e.g. Kamra, 1972*] and earthquakes [*e.g. Finkelstein and Powell, 1970*]. This diploma thesis will focus on the most common lightning produced by thunderclouds.

According to measurements of cloud electric fields made inside and outside the cloud the electrical structure of a thundercloud is a double-dipole [*e.g. Byrne et al., 1983; Weber et al., 1982*] as illustrated in Figure 2.2. There are two distinguishable main cloud charge areas whereby the upper part of the cloud is positive and the lower part negative charged. The spatial distance between these charge-centers is a few kilometers. Additionally there is a small layer of positive charge in the lower part of the cloud. Basically there are two theories for the generation of the main cloud charge dipole [*Uman, 1987*]:

- Precipitation theories [*e.g. Sartor, 1967*]
- Convection theories [*e.g. Wagner and Telford, 1981*].

The first are viewed in the literature as the more significant, but both could play some part in the cloud electrification. The small positive charge at the bottom of the cloud could be produced by on or more of the following mechanisms [*Uman, 1987*]:

- Release of positive corona at the ground and its subsequent upward motion to the cloud base [*e.g. Malan and Schonland, 1951*]
- Deposition by lightning [*e.g. Marshall and Winn, 1982*]
- Mechanism similar to the producing of the main cloud charge dipole [*e.g. Jayaratne and Saunders, 1984*]

The fine-weather electric field is about 100 V/m and is pointing downward, which is due to the negative charge on the Earth and the positive charge distributed in the atmosphere. The electrical conductivity increases in an altitude of about 50 km, where

the atmosphere is a good conductor to slowly varying signals, this level is called the electrosphere. Between the Earth and the electrosphere in a fine weather region is a voltage of 300 kV. For this high voltage a negative surface charge of about 10^6 C and an equal positive charge distributed in the air are necessary. In fine-weather regions currents in the order of 1000 A are continuously depleting this charge. As illustrated in Figure 2.1 the thunderstorm system act as a type of battery to keep the fine-weather system charged [*Uman, 1987*].

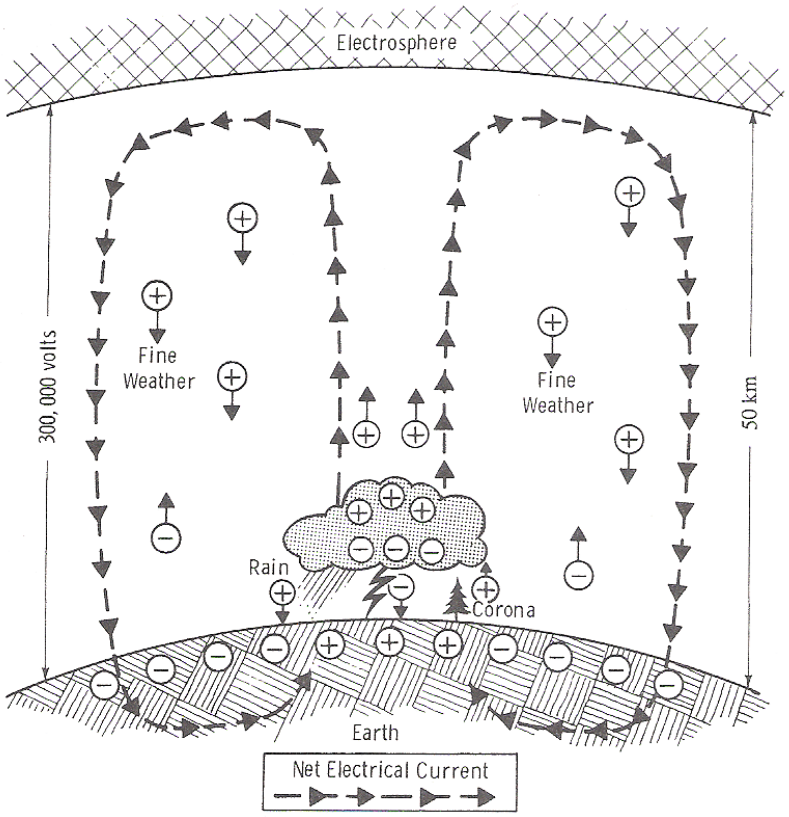

Figure 2.1: Electrical equilibrium between earth and atmosphere inclusive a thundercloud [*Uman, 1987*]

The positive orientated fine-weather electric field will switch the sign within a distance of about 10 km to a thunderstorm. The bottom side of the cloud is negative charged, this leads to an accumulation of positive charge below the thundercloud and to an electric field distribution at ground level as illustrated in Figure 2.2. With the detection of the sign switch of the electric field the sphere of influence of the thunderstorm can be realized.

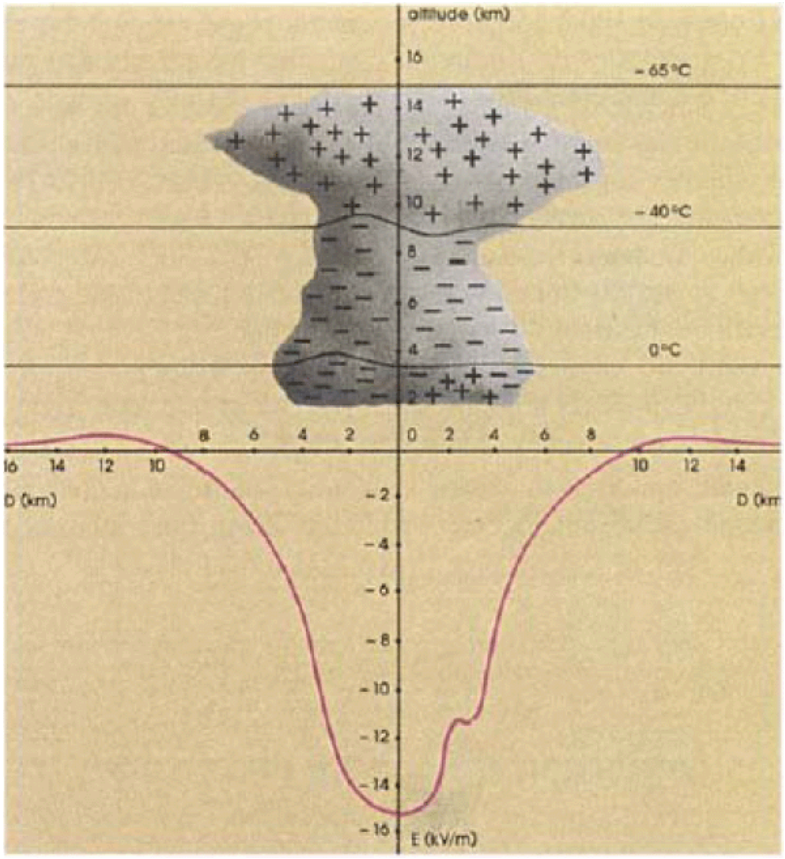

Figure 2.2: Charge of a thundercloud and the corresponding electric field at ground level [*Gary, 1995*]

If the electric field level reaches a value that the process of a lightning discharge can start the following scenarios are possible:

- Discharge between a cloud and another cloud (intercloud)
- Discharge within a cloud (intracloud)
- Discharge between a cloud and air
- Discharge between a cloud and ground

Cloud to Ground Discharges (CG) are not the most frequent discharges produced during a thunderstorm, but they are the most interesting ones, because they are responsible for lightning caused damages on earth. Furthermore CG strokes are the most studied because lightning channels below the cloud level are more easily photographed and studied with optical instruments. Additionally ground based lightning triggering systems (e.g. tower or rocket) allows a measurement and analysis of the CG lightning current. This diploma thesis will concentrate on discharges between thunderclouds and ground [*Uman, 1987*].

According to Berger (1978) four types of Cloud-Ground-Discharges are distinguished. The first criterion is the direction of motion of the so called leader that initiates the discharge and the second one is the polarity of the charge which is lowered to earth. These distinguishing characteristics lead to the following categorization of types of lightning as illustrated in Figure 2.3:

- **Downward negative lightning (a):** The initiated leader propagates downward, has a negative polarity and hence this lightning lowers negative charge to earth. This type is the most common CG discharge. About 90 % of the worldwide detected lightning flashes are downward and negative. A typical downward negative flash consists of a few strokes sometimes followed by a continuous current [*Uman, 1987*].
- **Downward positive lightning (c):** The initiated leader propagates also downward but the polarity is positive. Hence this type of lightning lowers positive charge to earth. Downward positive flashes contribute less than 10 % to the worldwide detected lightning. Positive flashes usually transport a higher amount of charge and are generally composed of a single stroke followed by a continuing current [*Uman, 1987*].
- **Upward negative and positive lightning (b + d):** These types of flashes are initiated by an upward propagating leader started from the earth and are called Ground to Cloud Discharges. These flashes are relatively rare and usually initiated by mountain summits or high structures like towers. An upward initiated negative flash has a positive leader which leads to lower negative charge to earth and an upward positive flash works with the inverse polarity [*Uman, 1987*].

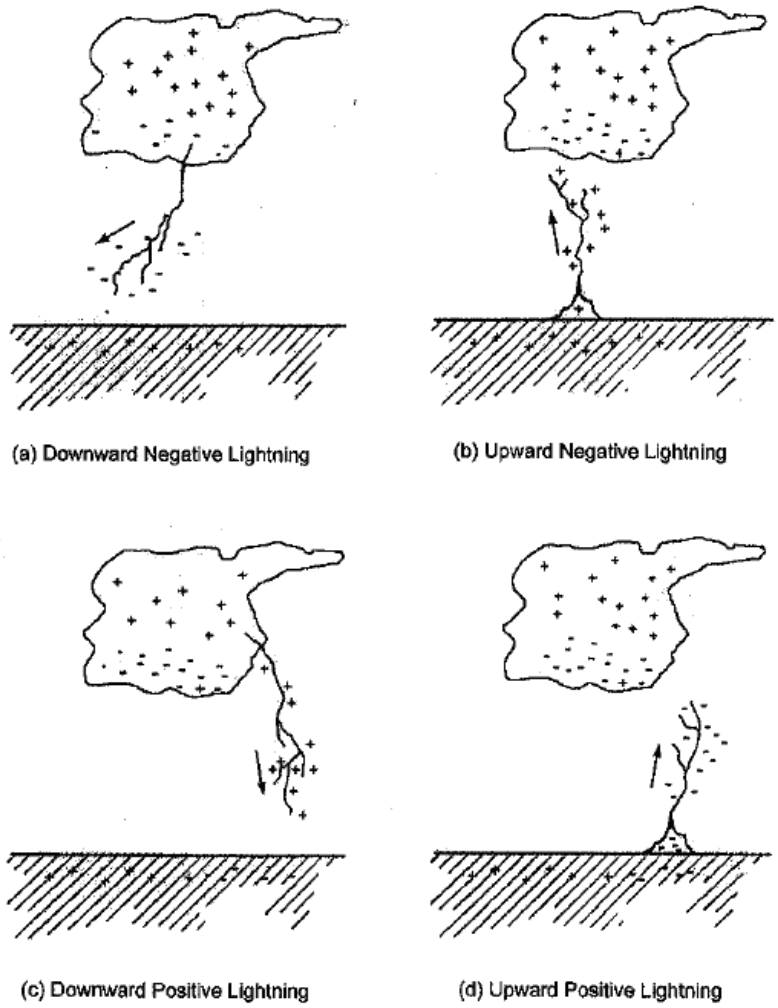

Figure 2.3: Categorization of the four types of lightning according to Berger (1978)

Now I will illustrate the lightning process based on the most common downward negative discharge according to Uman (1987) as seen in Figure 2.4 and Figure 2.5. The discharge starts in the cloud and can lower tens of coulomb of negative charge to earth. The whole discharge is termed a flash and the time duration is about 200-300 ms. The flash generally consists of three to five high current pulses, called strokes. The number of strokes inclusive the first one is known as the multiplicity of the flash. Because of the time between the strokes (interstroke time interval) in the order of 60 ms the human eye cannot resolve the individual strokes and the flash appears to flicker [*Rakov and Uman, 2003*].

If the cloud-charge-distribution generates high local electric fields a preliminary breakdown in the cloud initiate the so called stepped leader. This negative charged stepped leader moves downward and divides into several branches. The stepwise direction changes as well as the branching of the leader could be explained by the variation of conductivity in the air. The step length is about 50 m and the average propagation speed is about $2 \cdot 10^5$ m/s [*Rakov and Uman, 2003*]. When the stepped leader approaches ground, the electric field at sharp or pointed objects on the ground exceeds the breakdown value of the air and one or more upward moving discharges are initiated by those points and the so called attachment process begins. If one of the upward moving discharges contacts the downward moving stepped leader some tens meter above ground the leader channel is connected to ground potential. The negative ionized leader channel will be discharged while the so called first return stroke propagates upward. This pulse of high current moves upward although the negative charge flows downward resulting in the impression of an upward travelling flash. The propagation speed of the return stroke is about $1\text{-}2 \cdot 10^8$ m/s, the channel radius about 1-2 cm and the channel temperature about 30,000 K [*Rakov and Uman, 2003*]. This high channel temperature leads to an explosive extension of the surrounded air which is recognisable as thunder. After the return stroke current has ceased to flow the lightning may end as a single stroke flash. But if additionally charge is made available at the top of the channel, a second leader, called dart leader and initiated by so called J- and K- processes, occurs in the cloud. A dart leader propagates down the residual channel with usually no branches and initiates the second or any subsequent return stroke. The time between the strokes can be hundreds of milliseconds if a continuous current flows in the channel after a return stroke. Continuing current magnitudes are in the order of 100 A and represent a direct charge transfer from cloud to ground. This continuous current is the reason of fire ignition due to a lightning strike to ground and for example a strike to a tree can cause a forest fire. Figure 2.6 shows a streak-camera photograph of a 12-stoke lightning flash. The first stroke on the left is the only branched one and continuing current flows after the eleventh stroke.

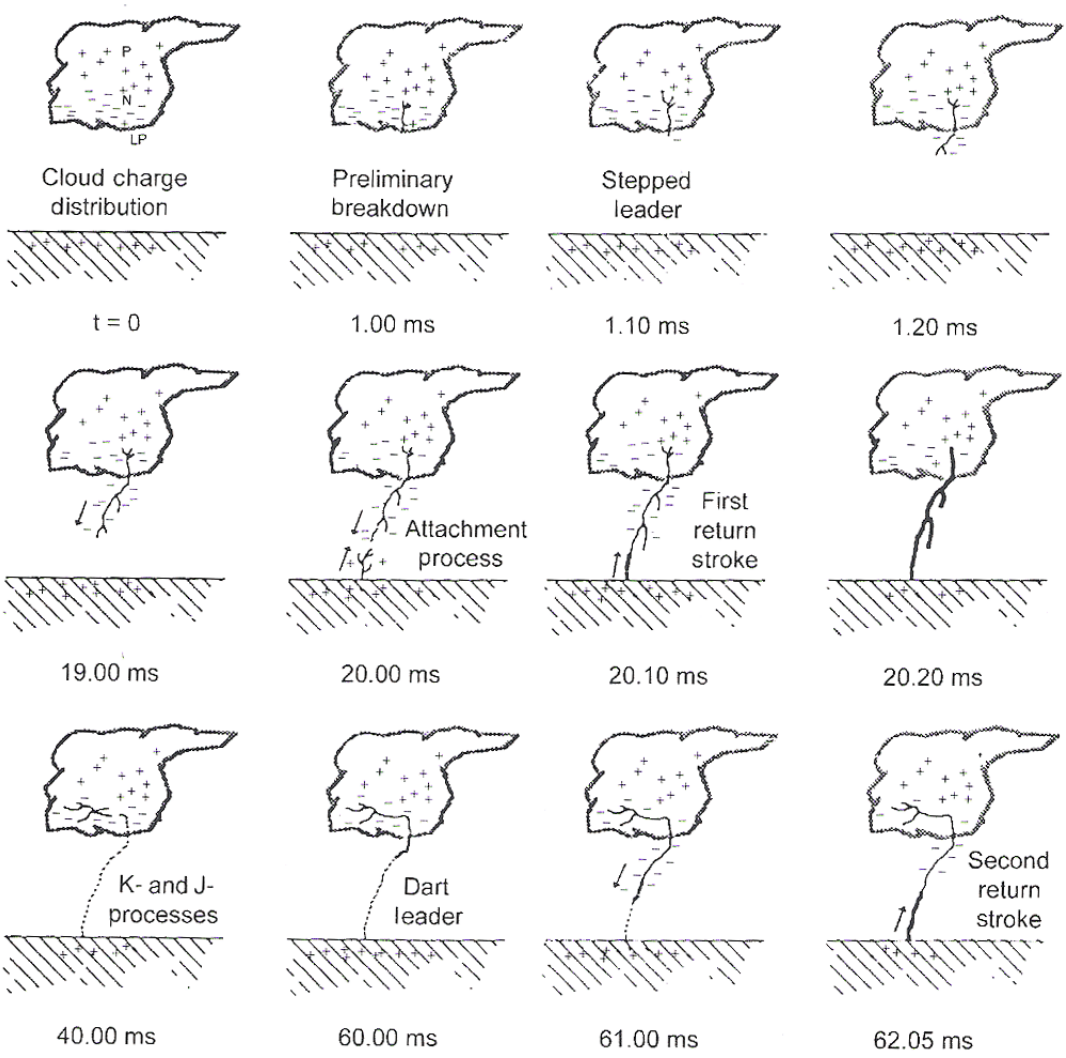

Figure 2.4: Illustration of the downward negative lightning process [*Uman, 1987*]

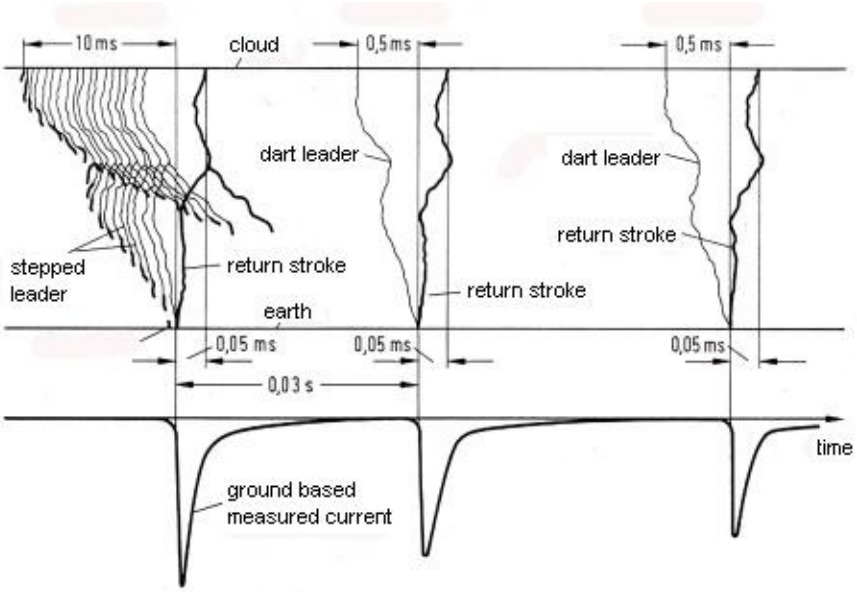

Figure 2.5: Multiple cloud to ground discharge [adapted from *www.sferics.physik.uni-muenchen.de, March 2009*]

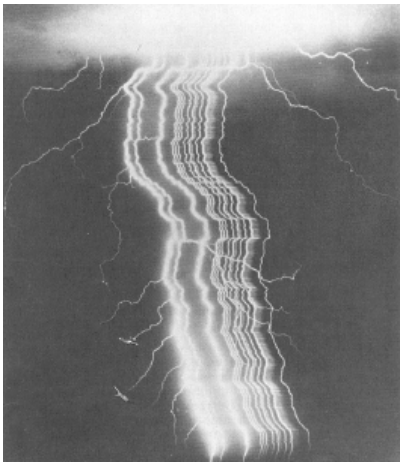

Figure 2.6: Streak-camera photograph of a 12-stroke lightning flash [*Uman, 1987*]

According to Rakov and Uman (2003) typical values of negative cloud to ground lightning parameters are given in Table 2.1:

Table 2.1: Characterization of negative cloud to ground lightning

Stepped leader	
Step length	50 m
Time interval between steps	20-50 μs
Step current	> 1 kA
Step charge	> 1 mC
Average propagation speed	$2 \cdot 10^5$ m/s
Overall duration	35 ms
Average current	100-200 A
Total charge	5 C
Electric potential	≈ 50 MV
Channel temperature	≈ 10,000 K

First return stroke	
Peak current	30 kA
Maximum current rate of rise	≥ 10-20 kA/μs
Current risetime (10-90 %)	5 μs
Current duration to half-peak value	70-80 μs
Charge transfer	5 C
Propagation speed	$1\text{-}2 \cdot 10^8$ m/s
Channel radius	≈ 1-2 cm
Channel temperature	≈ 30,000 K

Dart leader	
Speed	$1\text{-}2 \cdot 10^7$ m/s
Duration	1-2 ms
Charge	1 C
Current	1 kA
Electric potential	≈ 15 MV
Channel temperature	≈ 20,000 K

Subsequent return stroke	
Peak current	10-15 kA
Maximum current rate of rise	100 kA/μs
10-90% current rate of rise	30-50 kA/μs
Current risetime (10-90 %)	0.3-0.6 μs
Current duration to half-peak value	30-40 μs
Charge transfer	1 C
Propagation speed	$1\text{-}2 \cdot 10^8$ m/s
Channel radius	≈ 1-2 cm
Channel temperature	≈ 30,000 K

Continuing current (longer than 40ms)	
Magnitude	100-200 A
Duration	≈ 100 ms
Charge transfer	10-20 C

Overall flash	
Duration	200-300 ms
Number of strokes per flash	3-5
Interstroke interval	60 ms
Charge transfer	20 C
Energy	$10^9\text{-}10^{10}$ J

Every return stroke produces electric and magnetic fields which are measurable in different distances from the lightning channel. Typical waveforms are illustrated in Figure 2.7. The solid lines represent the typical vertical electric field intensity (left column) and the azimuthal magnetic flux density (right column) in consequence of the first return stroke and the broken line in consequence of the subsequent return stroke. The initial peak in the illustrated waveforms is used for identifying strokes in lightning location systems.

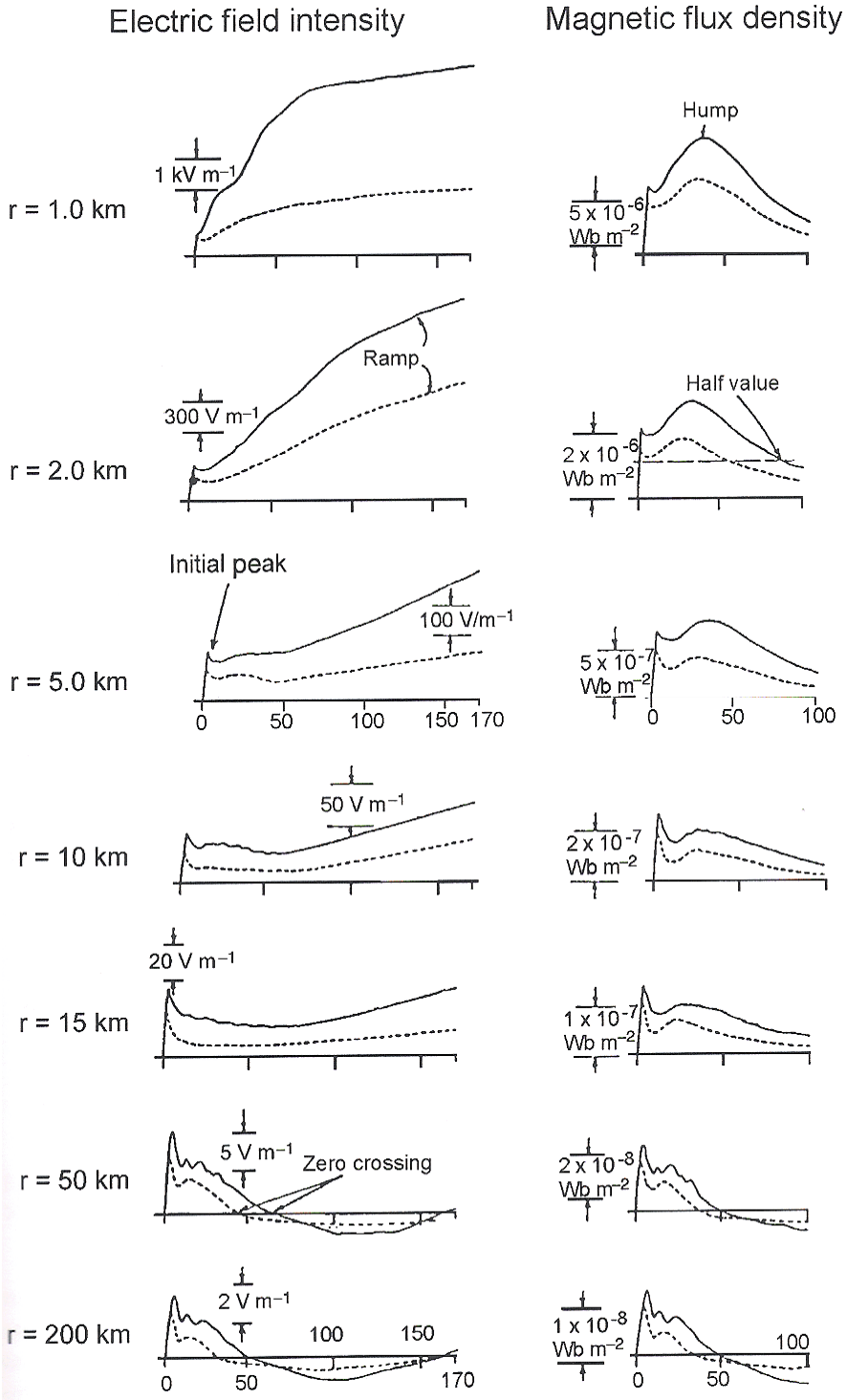

Figure 2.7: Electric field intensity and magnetic flux density of negative return strokes (time scales in µs) [*Rakov and Uman, 2003*]

According to Diendorfer (2007), Figure 2.8 (left) shows a typical current waveform of a lightning recorded on the Gaisberg tower. Almost all lightning strikes to the tower are upward initiated (ground to cloud discharges). Lightning to an elevated object like a tower typically starts with an upward leader represented in an initial continuous current (ICC) with a duration of some hundreds of milliseconds and an amplitude of some tens to some thousands of amperes. Often current impulses are superimposed on the slowly varying ICC and these pulses are called α-pulses. After the cessation of the ICC one ore more downward leader/upward return stroke sequences, similar to a subsequent return stroke of a cloud to ground lightning, may occur. The associated pulses are called β-pulses which are assumed to be very similar to subsequent strokes in natural cloud to ground lightning. Figure 2.8 (right) shows a higher resolution of a typical current waveform of a β-pulse measured at Gaisberg tower [*Diendorfer, 2007*; *CIGRE, 2008*].

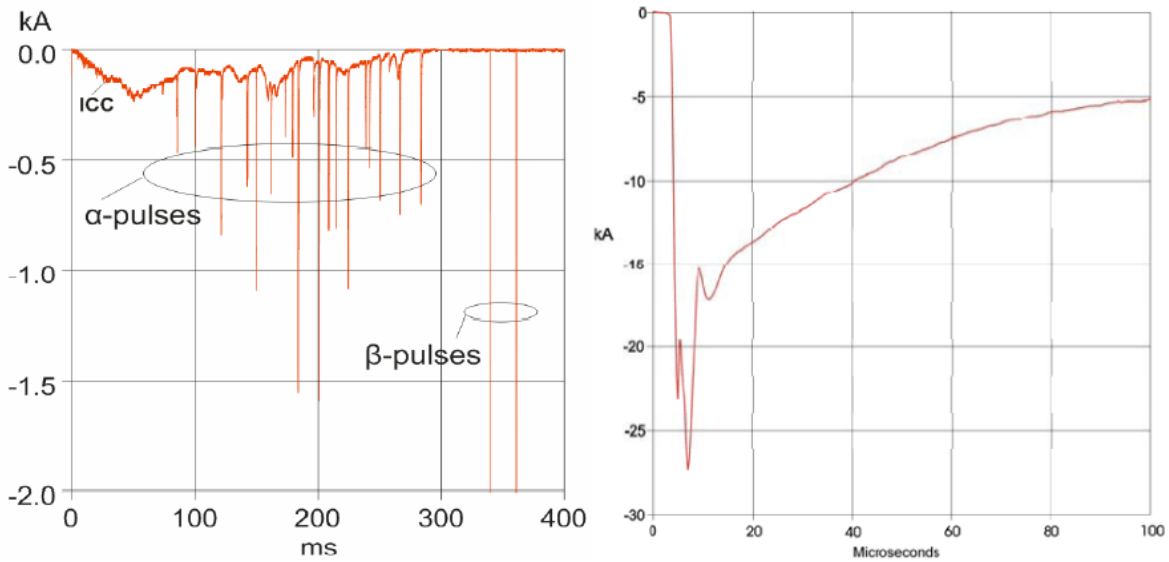

Figure 2.8: Typical current waveform of an upward initiated lightning measured at Gaisberg tower (left) and a higher resolution of a typical β-pulse (right) [*Diendorfer, 2007*]

3. Lightning Detection and Location

3.1. Introduction

Every lightning discharge emits a broadband electromagnetic field in the range of 1 Hz to about 300 MHz, with a peak in the frequency spectrum near 5 to 10 kHz for lightning at distances beyond 50 km. In the frequency range from 1 Hz to 300 MHz the significant electromagnetic energy of the radiated wave is coming from the discharge. But electromagnetic fields from lightning are detectable at even higher frequencies, for example microwaves[3] and of course visible light[4]. All these signals can be used for detection and location. Systems used for that purpose are mostly ground-based and called Lightning Location Systems (LLS) [*Rakov and Uman, 2003*].

With the help of the detected signals in the range of 30 to 300 MHz (very-high-frequency, VHF) it is possible to image the whole lightning channel in three dimensions. But in this case a small baseline sensor network is necessary. Very-low-frequency signals (VLF[5]) as well as low-frequency (LF[6]) signals produced by lightning are surface propagated and can be used to locate just one point. This could be the cloud-charge-point or better the ground-strike-point. Hence, this latter frequency range is most suitable to detect and locate the ground-strike-point of cloud to ground discharges. To obtain an appropriate accuracy, a network of sensors which are separated by 50-400 km is necessary. Those sensors measure the electric and/or magnetic field or determine the arrival time of the fields and send their data to a central unit which calculates the estimated strike point. Most common sensors are Magnetic Direction Finders (MDFs), Time of Arrival (TOA) sensors and a combination of both [*Rakov and Uman, 2003; CIGRE, 2008*].

Except MDF and TOA there are also other possibilities for lightning detection like Interferometry, Optical Direction Finding, Satellites and Radar. For more information I refer to *Rakov and Uman [2003]*.

3.2. Magnetic Direction Finders (MDFs)

A Magnetic Direction Finder is used to determine the direction from the sensor to the strike point of a CG stroke. It consists of two wide-band orthogonal loop antennas measuring the north-south (H_{NS}) and the east-west (H_{EW}) component of the magnetic field radiated from the stroke channel as illustrated in Figure 3.1.

[3] Frequency range is between 300 MHz and 300 GHz
[4] Frequency range is between 10^{14} and 10^{15} Hz
[5] Frequency range is between 3 and 30 kHz
[6] Frequency range is between 30 and 300 kHz

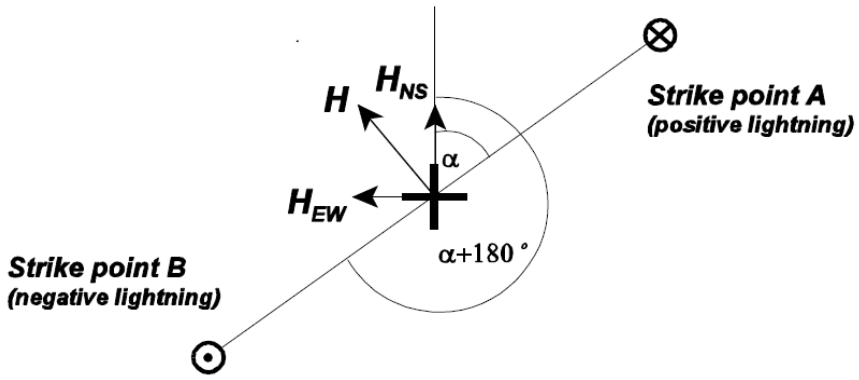

Figure 3.1: Determination of the magnetic field components and the azimuth angle [*Diendorfer and Schulz, 1998*]

The value which determines the direction is the azimuth angle α. This angle is calculated using the ratio of the measured H-components.

$$\alpha = \arctan \frac{H_{NS}}{H_{EW}} \tag{1}$$

The problem is that a positive discharge in strike point A and a negative one in strike point B are indistinguishable because they create the same azimuth angle. Therefore, in addition to the magnetic field, the electric field is also measured to determine the polarity of the discharge allowing to eliminate the 180° uncertainty. Signals radiated from CG strokes have a typical field waveform as seen in Figure 2.7. To ensure that a received signal comes from a CG stroke, a special algorithm called "waveform discrimination algorithm" [*Krider et al, 1980*] is used. Thus only real CG stroke signals satisfy the waveform criteria and will be separated from signals from cloud to cloud discharges and local noise. [*Diendorfer G. and Schulz W., 1998*]

Crossed-loop MDF can be divided into narrowband (tuned) DFs and gated wideband DFs. Both types have in common that the MDF technique involves the assumption that the radiated electromagnetic field comes from a vertical lightning channel producing a magnetic field which is horizontally orientated. Narrowband DFs are used for lightning detection since the 1920s [*Horner, 1957*] and work with a narrow frequency band with a center frequency in the range of 5 to 10 kHz. This frequency band was chosen because of the low attenuation of the earth-ionosphere waveguide and the high lightning signal energy in that range. A major disadvantage of this sensor type is that the detection of lightning within a range of 200 km has inherent azimuth errors called polarization errors of about 10°. These errors are caused by non-vertical channel sections as well as reflections by the ionosphere producing at the DF a non-horizontal magnetic field component [*Rakov and Uman, 2003*].

To solve the problem of large polarisation errors gated wideband DFs with a frequency range of a few kHz to about 500 kHz were developed in the early 1970s. This type of DF determines the direction by sampling (gating on) the initial peak (first 100 µs) of the return stroke magnetic field. The advantage is that this initial peak is radiated by the bottom few hundred meters of the lightning channel, which tends to be straight and vertical and hence the radiated magnetic field is horizontally oriented. Additionally the

ionospheric reflections will not be recorded because they usually arrive long after the initial peak. The inherent random errors in gated wideband DF are due to superimposed noise mainly appearing on the antennas outputs and due to imperfect instrumental processing and digitizing of the two signals. Additionally the wideband DF are, like the narrowband DF, susceptible to the so called site errors which can reach a value up to 30° (for narrowband DF). These errors are caused by the presence of unwanted magnetic fields due to non-flat terrain and due to nearby conducting objects such as underground and overhead power lines and structures, which are excited to radiate by the incoming lightning fields. To eliminate or better to minimize the site errors, the area surrounding a DF has to be as flat and uniform as possible and without significant conducting objects. The satisfaction of these requirements is usually difficult and so it is often easier to measure the site errors and compensate them mathematically [*Rakov and Uman, 2003*].

To determine a lightning stroke location we need at least the azimuth angle information from two MDFs. Figure 3.2 illustrates the intersection of two vectors provided by two MDFs. The solid lines represent the measured azimuth angle to the stroke and the broken lines represent the ±1° uncertainty resulting from the above mentioned angle errors. The shaded area shows the probable strike location.

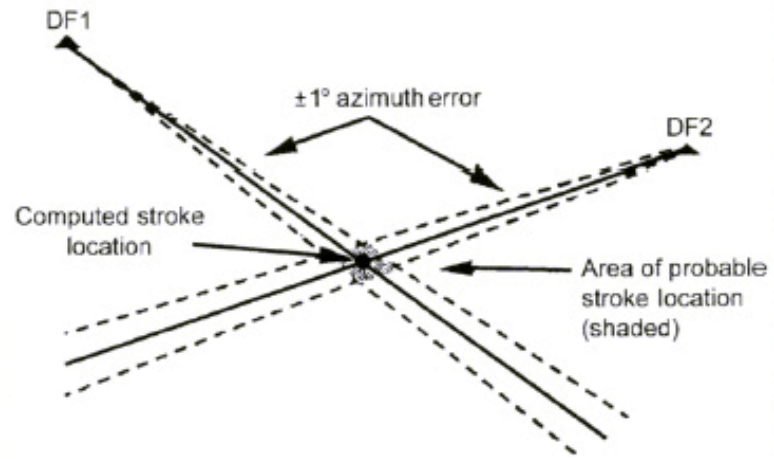

Figure 3.2: Determination of a stroke with two Magnetic Direction Finders [*Rakov and Uman, 2003*]

If three MDFs are involved, each pair of DFs provides a location. That means you get three points, as illustrated in Figure 3.3. The optimal stroke location is determined by minimizing a chi-square function (χ^2 function). You can see the optimal location in the intersection of the broken lines in Figure 3.3. The minimizing the χ^2 function technique is used when three or more MDFs detect a stroke.

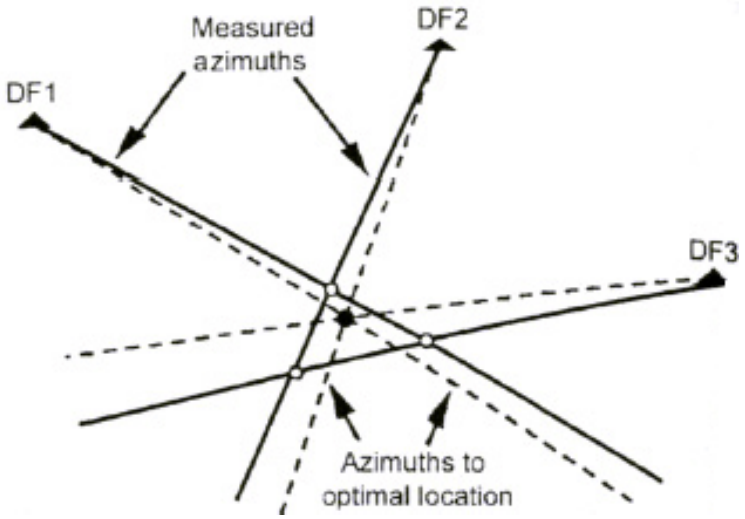

Figure 3.3: Determination of a stroke with three Magnetic Direction Finders [*Rakov and Uman, 2003*]

The following equation (2) shows the applied χ^2 function:

$$\chi^2 = \sum_{i=1}^{N}\left(\frac{\theta_{mi} - \theta i}{\sigma_{\theta i}}\right)^2 + \sum_{i=1}^{N}\left(\frac{E_{mi} - E_i}{\sigma_{Ei}}\right)^2 \qquad (2)$$

This χ^2 function technique works by iteratively varying all unknown values until χ^2 converges to a minimum. Θ_i and E_i are the unknown azimuth and electric field peak values, θ_{mi} and E_{mi} are the values measured by the i^{th} DF station and the σ's are the measurement error estimates. The unknown values found by this technique provide the most probable location of the lightning ground strike point and additionally an estimation of the error in this probable location. The error estimation is usually represented by an ellipse of a certain probability (for example 50 or 90 percent) that the true stroke location is within the area of this ellipse (see 3.8). According to the minimizing-the-χ^2-function-technique the smaller the ellipse and the χ^2 value, the higher is the location accuracy [*Rakov and Uman, 2003*].

3.3. Time of Arrival (TOA) Systems

A time of arrival (TOA) sensor provides the precise arrival time of a lightning electromagnetic field signal. Therefore an accurate time measurement is necessary. Since the implementation of global positioning systems (GPS), through earth orbiting satellites, the availability of accurate time synchronisation is given. A network of TOA sensors provides the location of the lightning ground strike point. Basically a TOA system can be divided into three types:

- Very-short-baseline[7]: ten to hundreds of meters (VHF – 30 to 300 MHz)
- Short-baseline: tens of kilometers (VHF)
- Long-baseline: hundreds to thousands of kilometers (VLF and LF – 3 to 300 kHz)

Very-short-baseline as well as short-baseline systems work in a very high frequency range, have a baseline up to a few kilometers and can provide images of lightning

[7] The baseline is the line connecting two sensors

channels. These system types are used to study the spatial and temporal development of discharges. The long-baseline system works in a frequency range between 3 and 300 kHz, has longer baselines up to thousands of kilometers and is used to identify the lightning ground strike point [*Rakov and Uman, 2003*].

Like mentioned above each sensor in a TOA system provides the arrival time of an electromagnetic field radiated by a lightning stroke. A given time difference between two sensors defines a hyperbola which represents all possible locations for the lightning ground strike point. Hence, three sensors deliver two hyperbolas which are at least necessary to get the real stroke location as illustrate in Figure 3.4.

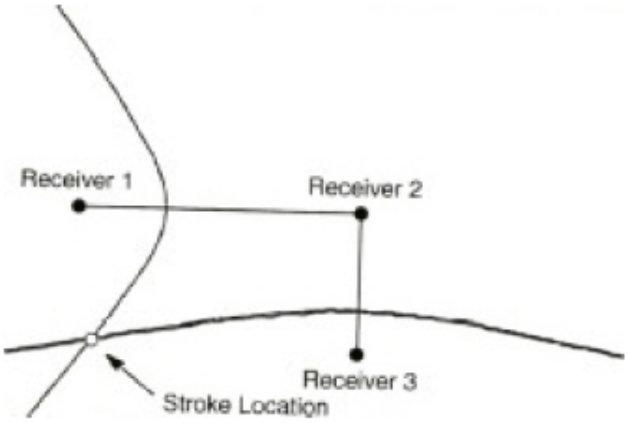

Figure 3.4: Intersection of two hyperbolas coming from three TOA sensors [*Rakov and Uman, 2003*]

Under some geometrical conditions the hyperbolas can cross twice and thus the system delivers two intersections which lead to an ambiguous location as seen in Figure 3.5. To avoid this ambiguous solution, a network of more than three sensors has to be installed [*Diendorfer, 2007*].

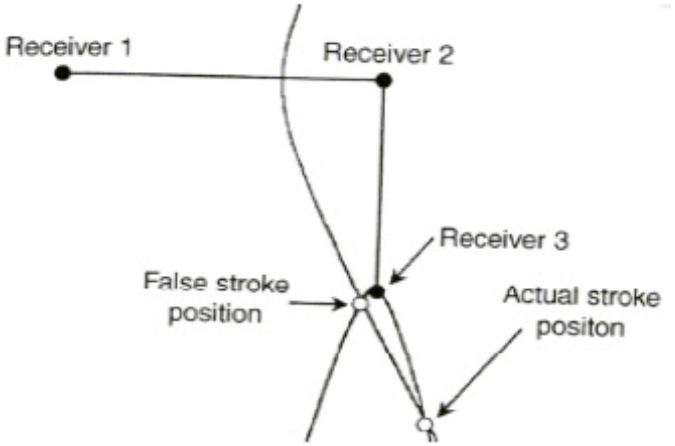

Figure 3.5: Example for an ambiguous location [*Rakov and Uman, 2003*]

Errors in location can be caused by anything that changes the arrival time of a signal such as path elongation due of mountains, inaccurate time synchronization and signal distortion due to propagation or other effects which can lead to identification problems at the sensor. A commercial long-baseline TOA system is the so called **L**ightning **P**ositioning **A**nd **T**racking **S**ystem (LPATS) which operates at LF and VLF with four or more stations 200 to 400 km apart. It was developed in the 1980s and determines the

ground strike location via time difference measurements of the received return stroke waveforms. The latest version operates with GPS clock synchronization and reaches location accuracies of less than 1 km [*Rakov and Uman, 2003*].

3.4. Combined Direction Finder and Time of Arrival (MDF+TOA)

The magnetic direction finder system provides the lightning location via azimuth angles and the time of arrival system via arrival time differences. In the early 1990s, Global Atmospherics found a way to combine these two systems. The new system was called **IMP**roved **A**ccuracy using **C**ombined **T**echnology (IMPACT) and every sensor delivers an azimuth angle and an arrival time. This system produces three estimated parameters: latitude, longitude and time of discharging. Thus the MDF+TOA method has redundant information which allows an optimized estimation of the ground strike location, even when only two sensors provide both values. The MDF+TOA location algorithm can use information from any kind of MDF, TOA or MDF+TOA [*CIGRE, 2008; Diendorfer, 2007*].

3.5. Grouping Strokes into Flashes

A large number of the worldwide occurring lightning flashes are multiple stroke flashes. Lightning location systems (LLS) locate every stroke independently and group the individual strokes into a flash. Most grouping algorithms use a spatial and temporal cluster algorithm illustrated in Figure 3.6. Strokes are added to an active flash in a specific time period (usually 1 second) after the first stroke, as long as the additional strokes are within a specific clustering radius (usually 10 km) of the first stroke and the time interval from the previous stroke is less than a maximum interstroke interval (usually 500 ms). In case when a stroke is a candidate for more than one flash it is assigned to the flash with the spatial closest first stroke. Additionally, in modern central processors developed by Global Atmospheric (LP2000) and Vaisala (CP8000), if a stroke is located beyond the clustering radius of the first stroke of a flash but is not separated from that stroke because their location confidence region overlap, then the stroke will be added to that flash. The maximum number of strokes in a flash is a configurable parameter of the system. Any stroke after that is considered to be member of a new flash [*CIGRE, 2008*].

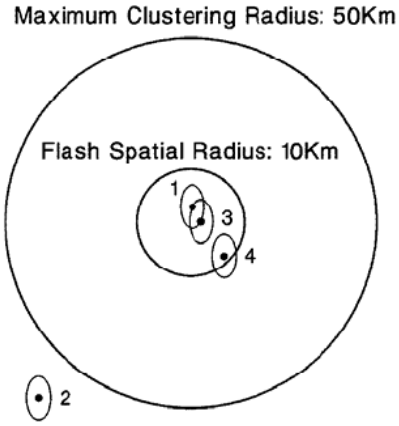

Figure 3.6: Spatial clustering method for grouping strokes into flashes [*Cummins et al., 1998*]

3.6. Peak Current Estimate

The estimation of the peak current of a cloud to ground flash by LLS is based on the transmission line model (TL) introduced by Uman et al. (1975). The following equation (3) shows the correlation between the measured field peak E_p and the peak current I_p.

$$I_p = \frac{2 \cdot \pi \cdot \varepsilon_0 \cdot c^2 \cdot D}{v} \cdot E_p \tag{3}$$

D is the horizontal distance between the lightning channel and the observation point, c is the speed of light and v is the velocity of the return stroke. With the assumption of a constant v (typically 10^8 m/s), a reference distance of D=100 km and a perfect conducting ground, equation (3) becomes

$$I_p[kA] = 5 \cdot E_p\left[\frac{V}{m}\right] \tag{4}$$

Not only the linear equation (4) is used to infer the lightning peak current from the measured electric field peak. The peak current is often inferred from the so called LLP[8]-Units which are directly proportional to the measured electric field peak. Equation (5) shows the correlation between the electric field peak in [V/m] and the sensor output signal in [LLP-Units].

$$52\left[\frac{V}{m}\right] \equiv 1158\,[LLP-Units] \tag{5}$$

Combining equation (4) and (5) leads to the often used direct conversion of the Range Normalized Signal Strength (RNSS[9]) in LLP-Units to peak current in kA which is shown in equation (6).

$$I_p[kA] \cong 0.23 \cdot \overline{RNSS}\,[LLP-Units] \tag{6}$$

The factor 0.23 is the so called Signal Normalization Factor (SNF) and $\overline{RNSS}$ is the mean value of all $RNSS_i$, which is the range normalized signal strength of the i^{th} sensor included in localisation [*CIGRE, 2008; Diendorfer, 2007*].

Due to the variability of the included parameters, like the velocity of the return stroke, an accurate determination of the lightning current based on a remotely measured magnetic and/or electric field is impossible. But Rachidi et al, 2004 showed that a statistical estimation of the mean values and standard deviations is possible [*CIGRE, 2008; Rachidi et al, 2004*].

3.7. Detection Efficiency

Detection Efficiency (DE) is defined as the percentage of the flashes or strokes occurring that are reported by the LLS. Every sensor in a LLS-network exhibits a DE, illustrated in Figure 3.7, which shows the DE as a function of the received signal

[8] Lightning Location and Protection
[9] Normalized to 100 km

strength. To guarantee a high DE, the received signal has to be stronger than a detection threshold to filter out the too small events. But if the signal is too strong the sensor will be "over-ranged" and the DE will go down rapidly. Since each sensor in a network detects a specific stroke at a different distance they may have different sensor DE values for this stroke. Hence the DE function of the whole LLS depends on the topology of the multiple sensor network [*Diendorfer, 2007*].

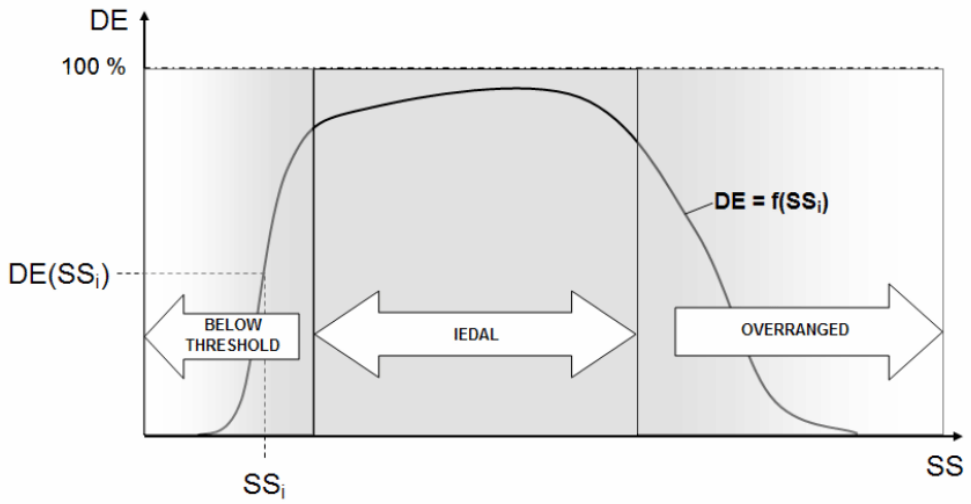

Figure 3.7: Sensor DE as a function of the received signal strength SS [*Diendorfer, 2007*]

3.8. Location Accuracy – Error Ellipse

Location accuracy is the distance between the estimated ground strike point determined by the LLS and the real strike point. Since usually the exact location of the strike point is unknown, a probability distribution is used to find a confidence area around the calculated strike point within the real strike point is located with a certain likelihood. According to *Gotthardt, 1968*, the confidence region of a calculated strike location is an ellipse for any optimization. Hence the aim is to find the parameters of such an ellipse within detected strokes are located with a certain probability. The location error distribution is a two-dimensional Gaussian distribution (Figure 3.8) when the following assumptions are valid:

- Random errors in time and angle measurements are uncorrelated
- Random errors in time and angle measurements are Gaussian
- Systematic site errors are corrected
- Propagation errors are small

Even if an assumption is not completely valid, the overall errors tend to be Gaussian when a large number of sensors are included in the calculation. The error ellipse is derived from a cross section of the two-dimensional Gaussian distribution at any desired probability value p. That means the real strike point is located within the obtained ellipse with the probability p. In the EUCLID network a probability p = 50 % is used to calculate the size of the error ellipse [*Cummins et al., 1998; Schulz, 1997*].

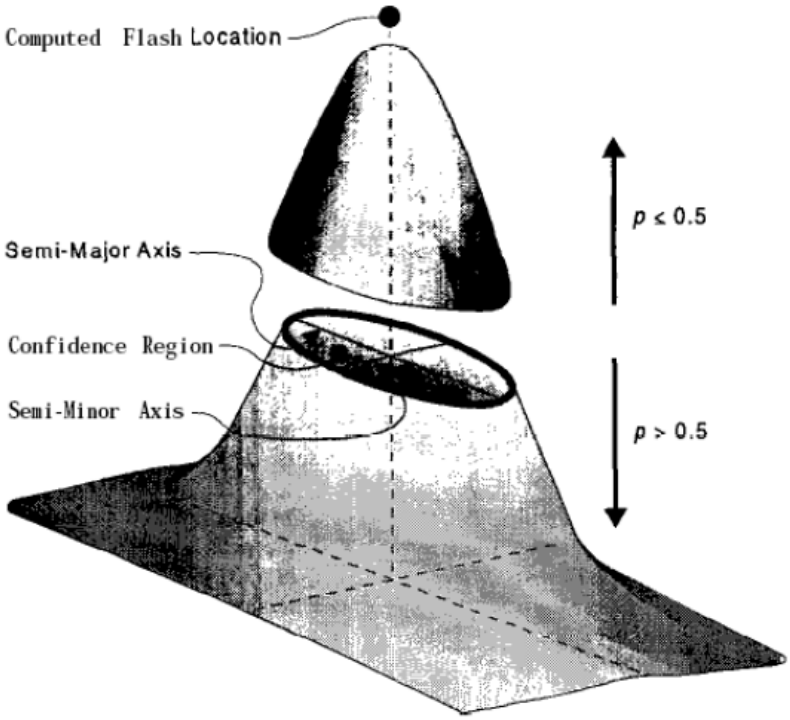

Figure 3.8: Two-dimensional Gaussian location error distribution [*Cummins et al., 1998*]

The error ellipse is defined by its semi-major axis (σ_{max}) and semi-minor axis (σ_{min}), the cross-section of them and the angle δ between the major axis and the north direction as illustrated in Figure 3.9 on a longitude-latitude map. The estimated strike point is in the center of the ellipse. Actually the lengths of the axes represent the standard deviation of the probability distribution at a certain probability in direction of the respective axis. The length of the semi-major axis is an important indicator of the location accuracy of the estimated ground strike point. Because it correlates with the maximum distance between the real strike point and the calculated point with a given probability [*Schulz, 1997*].

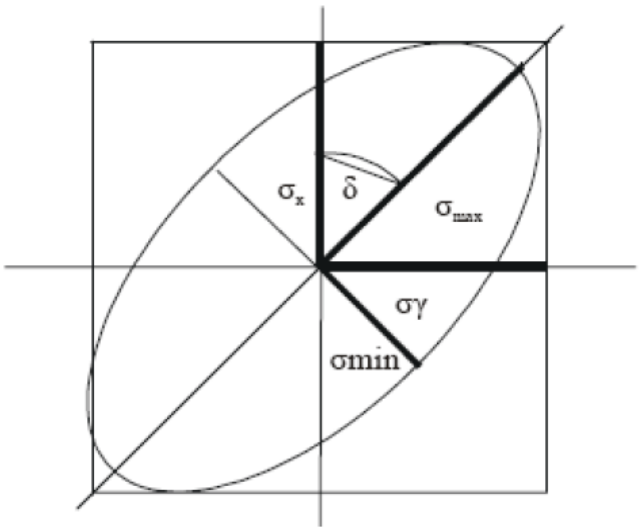

Figure 3.9: Error ellipse with corresponding parameters [*Schulz, 1997*]

4. Austrian Lightning Detection and Information System

4.1. ALDIS network

The **A**ustrian **L**ightning **D**etection and **I**nformation **S**ystem (ALDIS) is a cooperation between the Austrian Electrotechnical Association (ÖVE), the Austrian Electricity Board (VERBUND) and Siemens AG Austria. The purpose of ALDIS, which started operation in January 1992, is to detect lightning activity in Austria and store all the date in a database. Actual the network consists of eight LS7000[10] sensors employing to the MDF+TOA principle (see chapter 3.4). The main difference to the previously used IMPACT sensor is the fully digital signal processing. The mean baseline between the sensors is in the range of about 200 km and hence this network, illustrated in Figure 4.1 (left), has one of the smallest sensor baselines in the world. Due to this high sensor density the lightning detection system provides redundant information. A high number of flashes is located by four or more sensors.

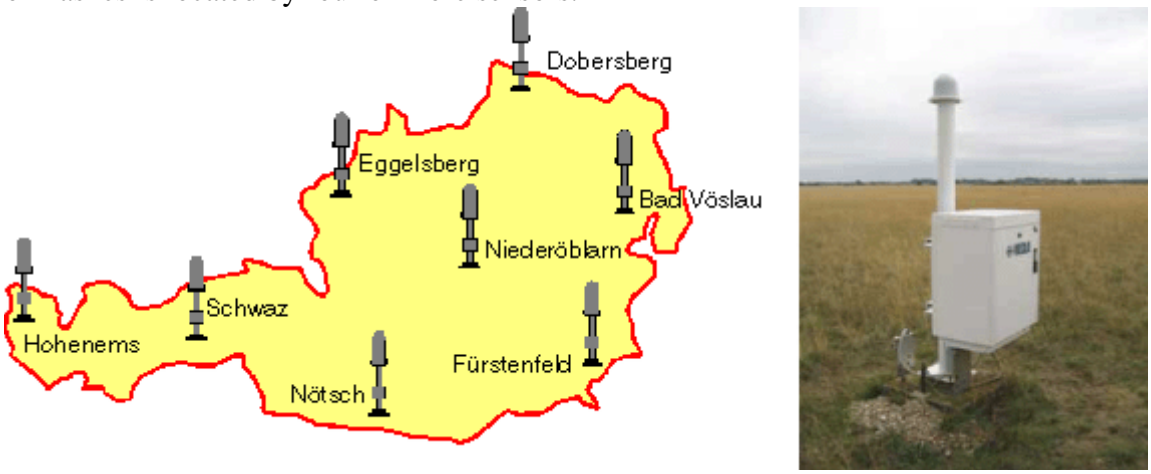

Figure 4.1: ALDIS network (left) and LS7000 (right) [*www.aldis.at, March 2009*]

If a sensor detects a lightning electromagnetic field pulse the processed and time stamped data will be transmitted to a central Lightning Processor (LP2000) by ADSL communication. This processor determines the estimated ground strike location with the help of at least two sensors and groups the strokes into flashes. The more sensors deliver data, the higher is the degree of freedom (redundant information) and the more likely is a high location accuracy. The LP2000 provides the following information of the cloud to ground discharge:

- Location of the ground strike point
- Time of the event
- Polarity of the stroke (positive/negative)
- Peak current of the stroke

Furthermore the LP2000 generates a few parameters which are related to the accuracy of the detection, for instance the χ^2 value (see 3.2) and the major and minor axis of the

[10] Manufactured by VAISALA Inc.

error ellipse (see 3.8). All the data provide by the LP2000 are stored on a UNIX-workstation by the software package CATS (**C**omputer **A**ided **T**hunderstorm **S**urveillance System), which was developed by the company METEORAGE. There is also a display system employed which allows the graphical presentation of the detected lightning activity [*CIGRE, 2008; www.aldis.at, March 2009*].

4.2. EUCLID network

The ALDIS sensors are also integrated in a European network called EUCLID (**EU**ropean **C**ooperation for **LI**ghtning **D**etection). EUCLID is a cooperation of national lightning detection networks with the aim to identify and detect lightning in the whole European area. The whole network consists of 135 sensors and the countries involved are illustrated in Figure 4.2 [*www.aldis.at, March 2009; www.euclid.org, March 2009*].

Figure 4.2: EUCLID network [*www.aldis.at, March 2009*]

4.3. Austrian Lightning Research Station Gaisberg

The Gaisberg is a mountain east of the city of Salzburg with a high lightning density (according to analysis of ALDIS data in the years 1992 to 1997). The radio transmitter tower on the summit of the Gaisberg is also used for lightning research since 1998. This project is a cooperation of ALDIS and Vienna University of Technology. Lightning rods and a measurement system are installed on the top of the tower (Figure 4.4). This

100 m high structure is triggering lightning and the measurement system records the current waveform. The following lightning parameters can be determined:

- Lightning peak current
- Charge transfer per stroke and per flash
- Time derivative of current [di/dt]

Figure 4.3: The Gaisberg with the radio transmitter tower [*Hubert Umprecht; www.wabweb.net*]

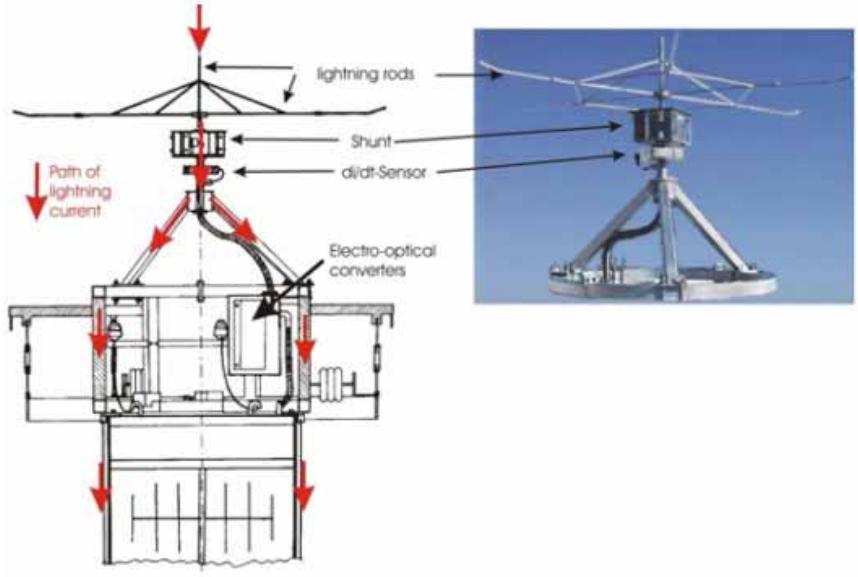

Figure 4.4: Measurement system on the Gaisberg tower [*www.aldis.at, March 2009*]

4.4. Location Accuracy in the EUCLID network

Based on the data from the Gaisberg lightning research project, the location accuracy of the EUCLID network can be analysed. Because every triggered stroke should be located by EUCLID exact at the Gaisberg coordinates, if the accuracy would be perfect. During the period 2000-2005 a total of 110 flashes with at least one β-pulse were measured at the Gaisberg tower. The smallest peak current was 2.1 kA and the highest was above 40 kA (40 kA is the measuring limit). 108 of those flashes were detected by the EUCLID network confirming a flash Detection Efficiency of 98%. The two missed flashes were not detected because of a GPS failure at the Gaisberg site. Regarding the location accuracy, EUCLID provides a median location error of 368 m and a standard deviation of 768 m as illustrated in Figure 4.5. The main cluster is shifted by about 300 m to the

north of the Gaisberg tower. The reasons for that bias (systematic error) are assumed to be a combination of the following effects [*Diendorfer, 2007; Schulz und Diendorfer, 2000*]:

- Time errors due to elongation of the signal propagation path caused by mountains
- Time errors introduced by a propagation velocity smaller than the speed of light due to finite ground conductivity

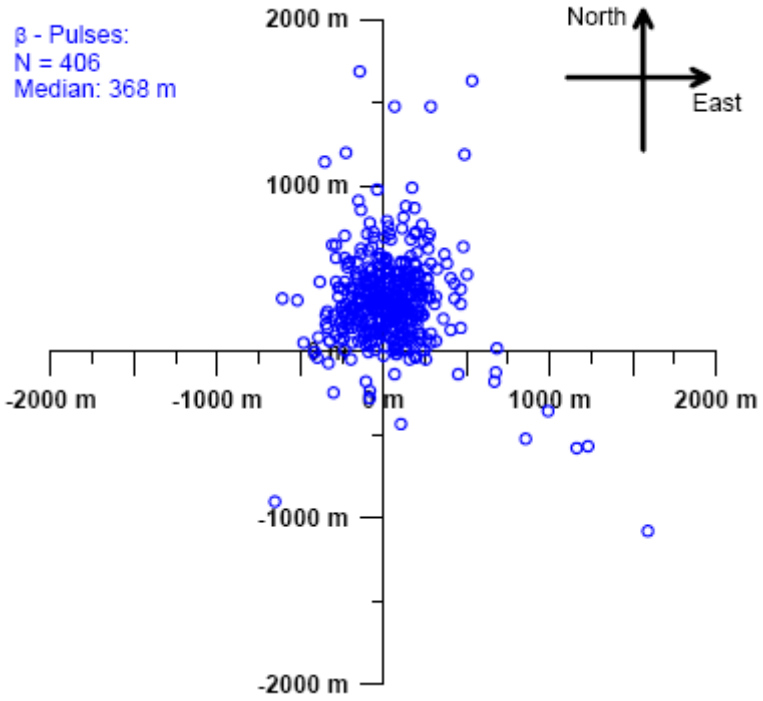

Figure 4.5: Plot of the EUCLID stroke locations [*Diendorfer, 2007*]

5. Lightning Density of Austria

5.1. Introduction

In this chapter I will analyse the lightning density of Austria during the time period from first January of 1998 till 31. December of 2007. A lightning density map shows the number of cloud to ground discharges per square kilometre per year and points out, over a longer time period, the probability of lightning strokes. All lightning data come from the ALDIS database and the evaluation has been executed with the program STATVIEW, which generates the density map. On the basis of the density maps I have analysed the locations with above-average lightning density. My aim was to find out the reason for that high density level.

Figure 5.1 shows the ground flash density map of Austria for the time period from 1998 till 2007. The average value of lightning density is between two and three flashes per square kilometer and year. But there are a few regions with a density of more than five flashes per square kilometer and year. Such locations are red inked and most of them appear in Styria, Carinthia and in the south of Lower Austria. Clearly visible is the area in the surrounding of Udine (Italy) which is the area with the highest thunderstorm activity in Europe.

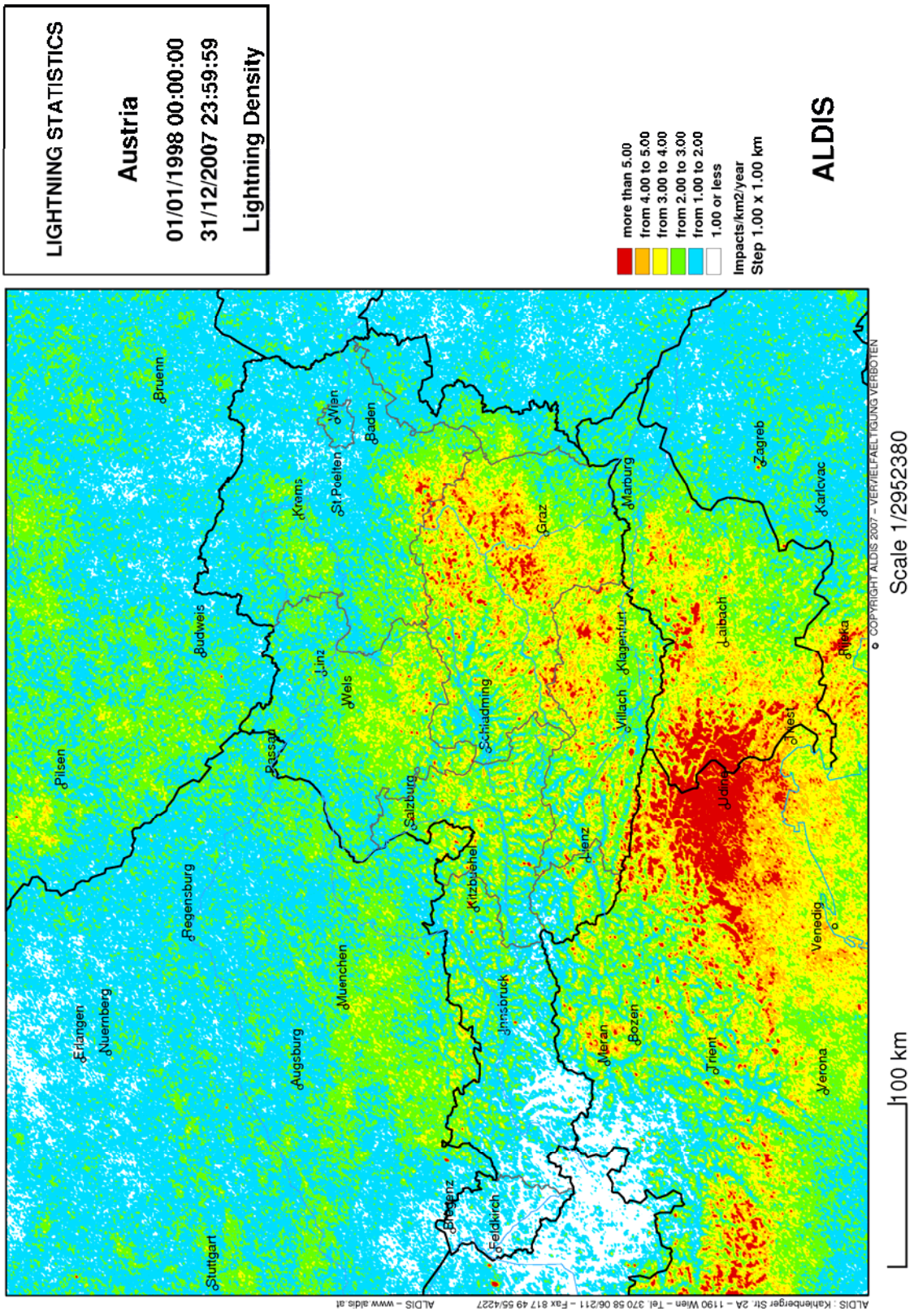

Figure 5.1: Ground flash density of Austria based on a 1 km x 1km grid

Figure 5.3 till Figure 5.10 represent the ground flash density maps of the particular counties of Austria. These maps have a different scaling (see color code legend at lower

right side of figure) to show only the locations with a density of more than six flashes per square kilometer and year. The most interesting regions in lightning activity have been marked with black circles or ellipses. Comparing the different figures it is noticeable that a few regions appear on different maps with a different ground flash density. These maps are based on a grid of squares and every square has been evaluated by itself. The problem is that the grid of the different maps is somewhat different and creates overlapping zones (see Figure 5.2). Thus when flashes strike in a location which lays in an overlap zone the flash will be counted on different squares. This is the explanation for the small variations of the flash densities for different maps. Despite of little differences between the maps the interesting areas remain the same.

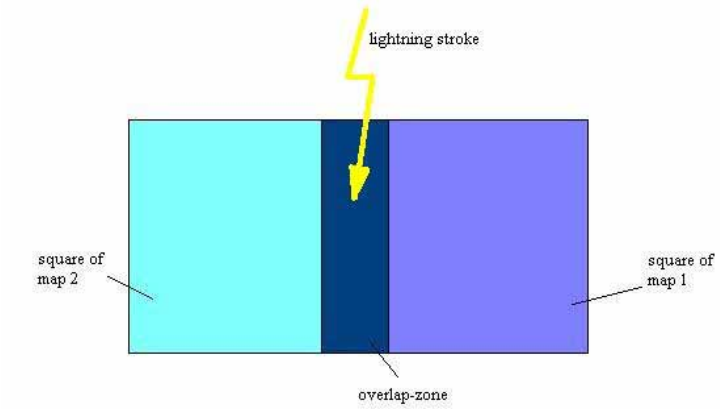

Figure 5.2: Overlap-zone between two maps

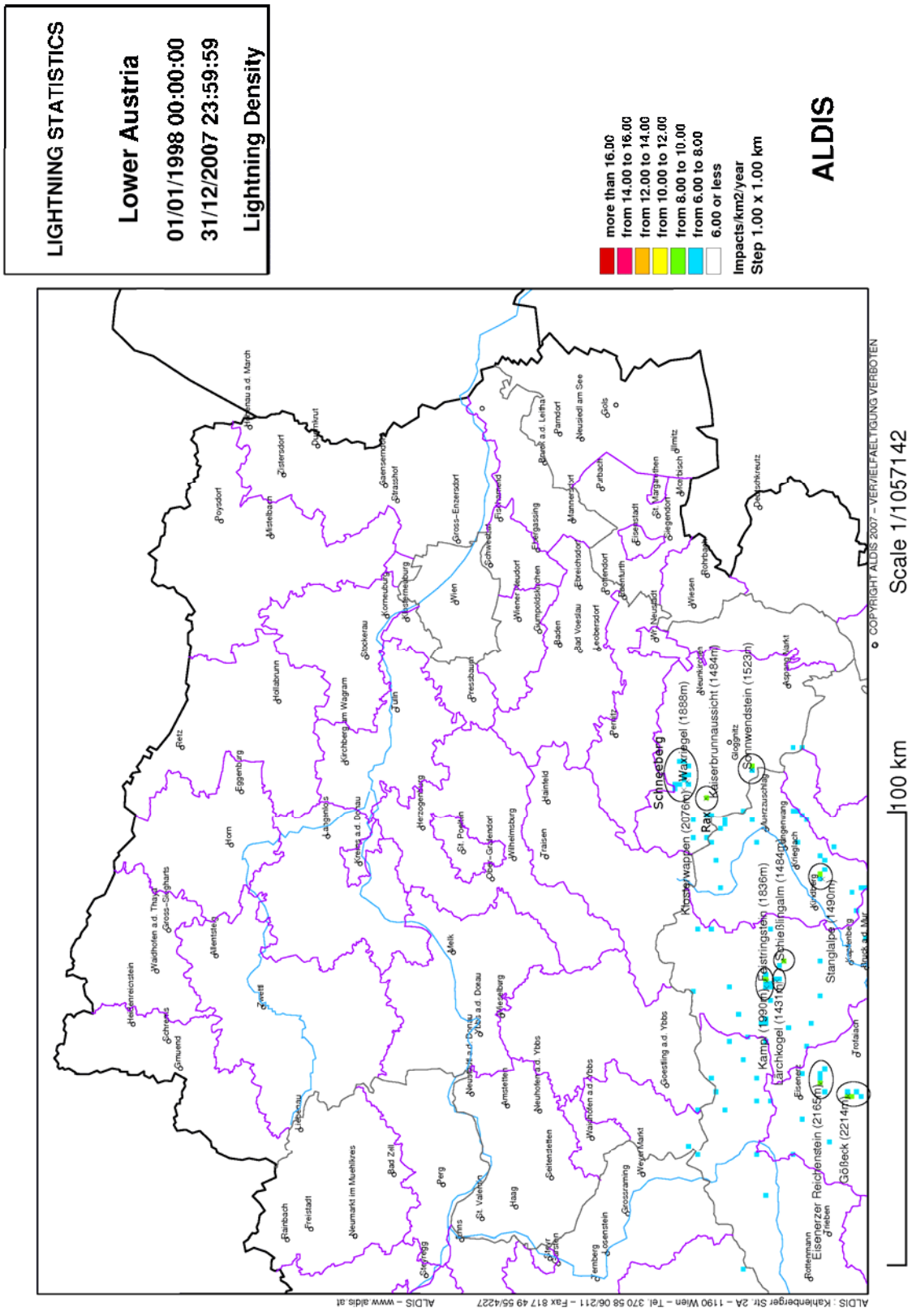

Figure 5.3: Ground flash density of Lower Austria and Vienna

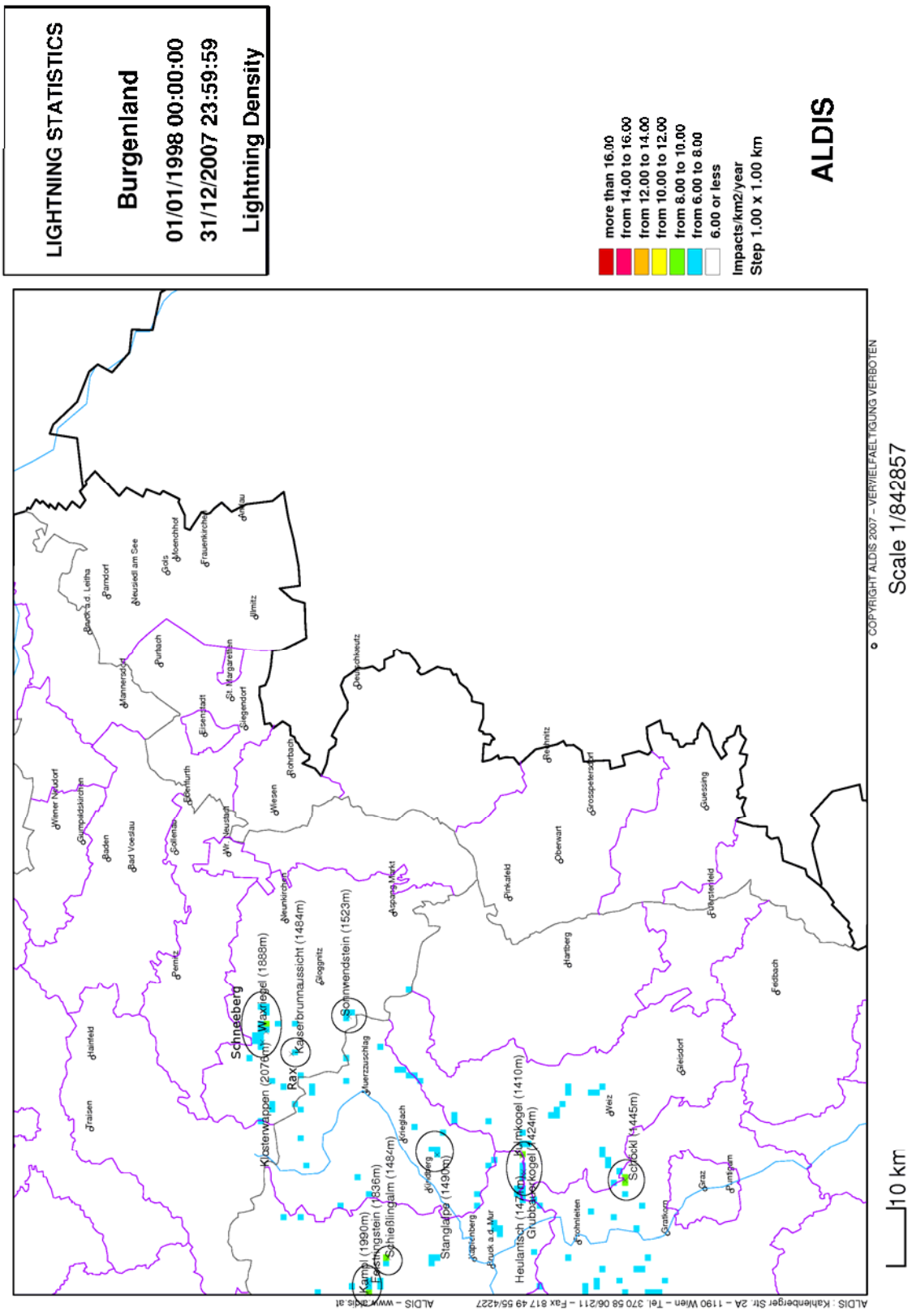

Figure 5.4: Ground flash density of Burgenland

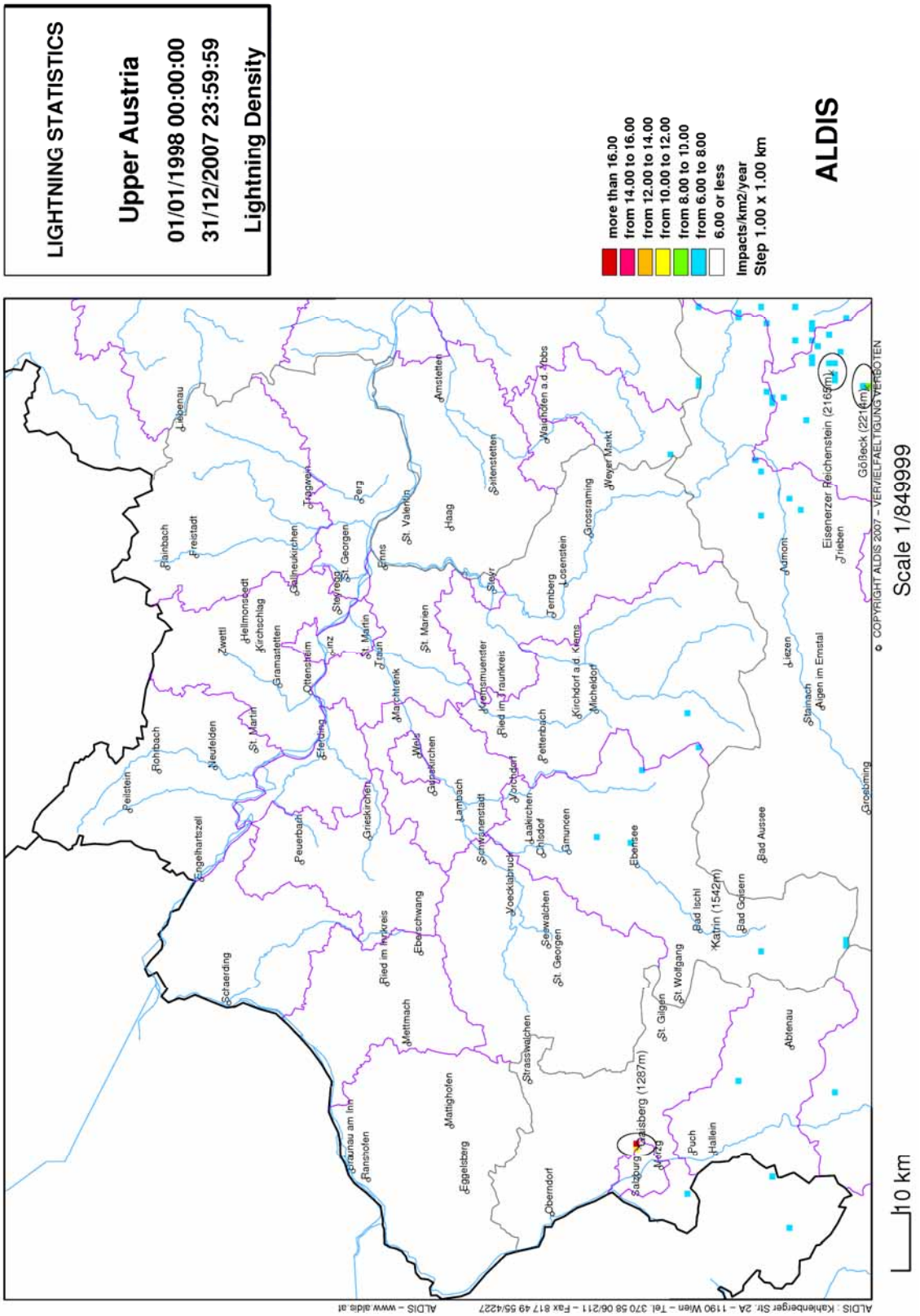

Figure 5.5: Ground flash density of Upper Austria

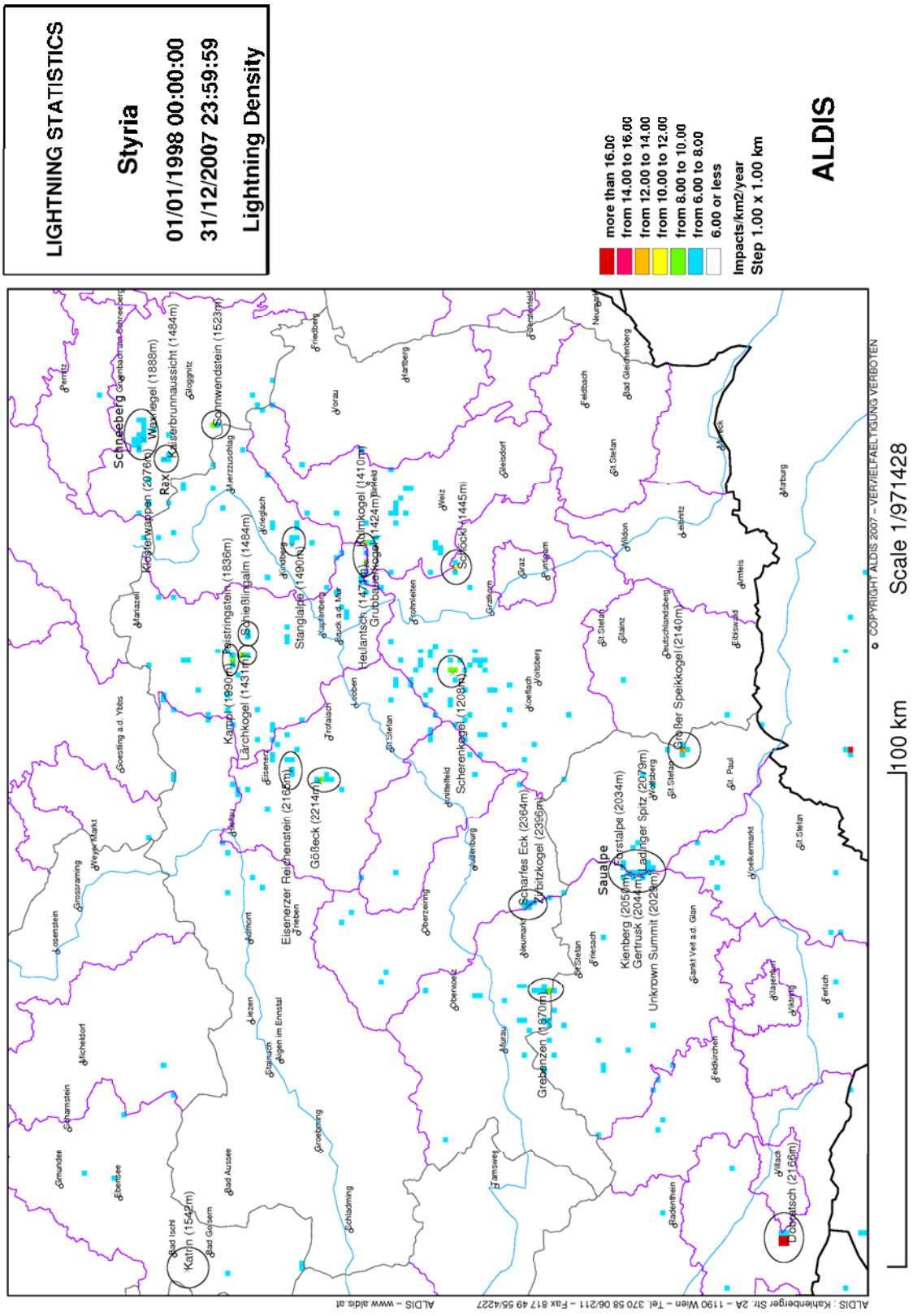

Figure 5.6: Ground flash density of Styria

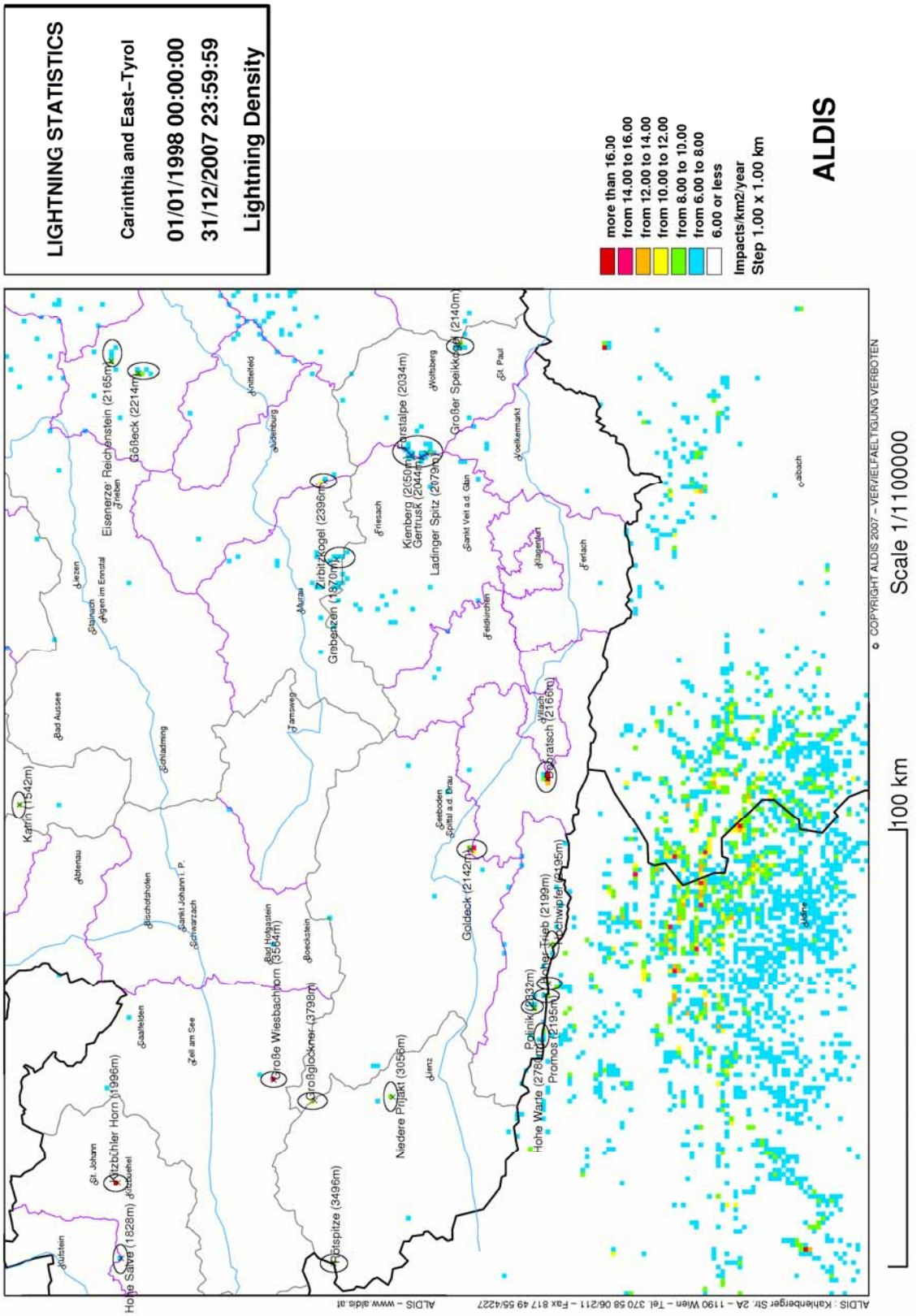

Figure 5.7: Ground flash density of Carinthia and East-Tyrol

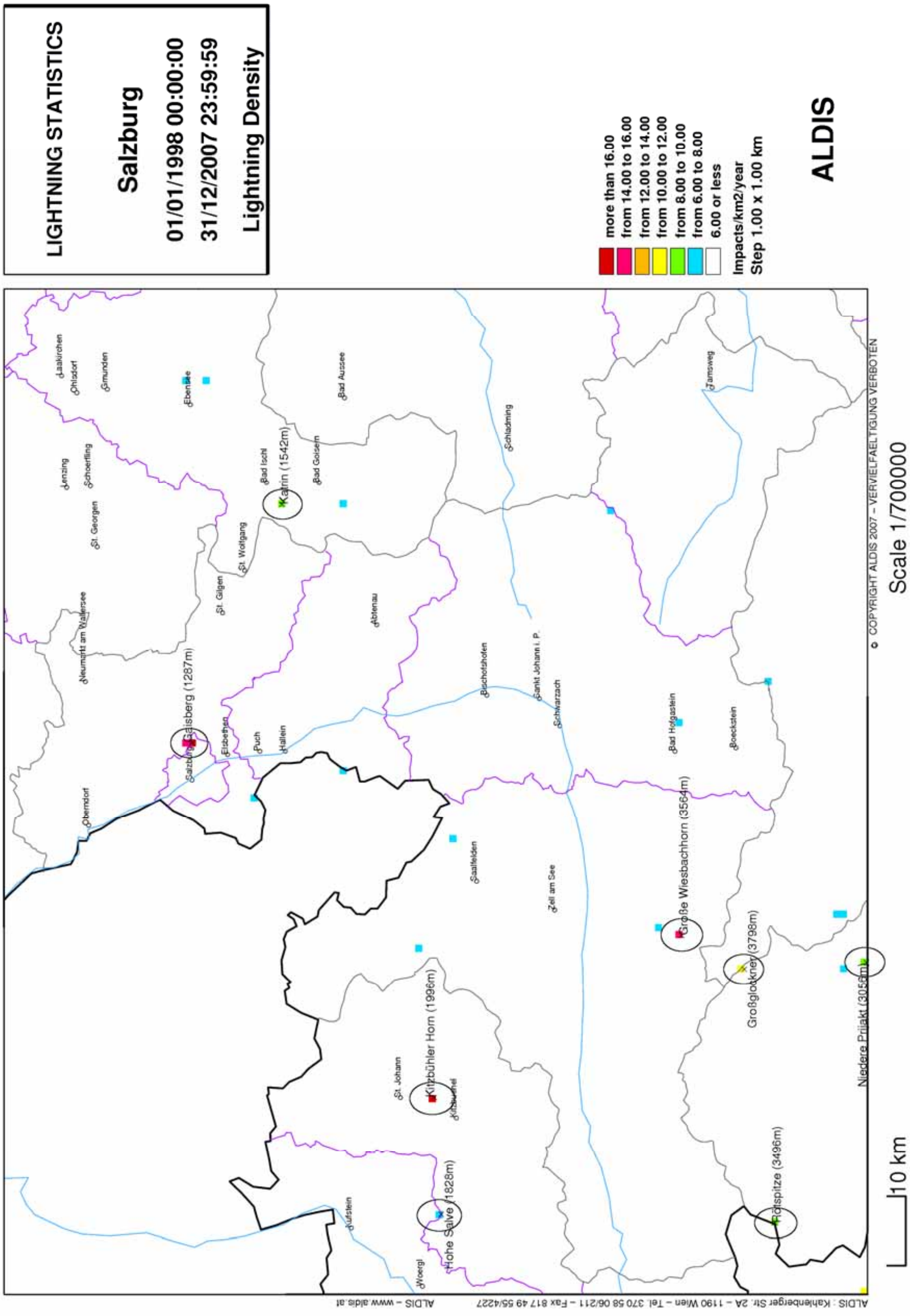

Figure 5.8: Ground flash density of Salzburg

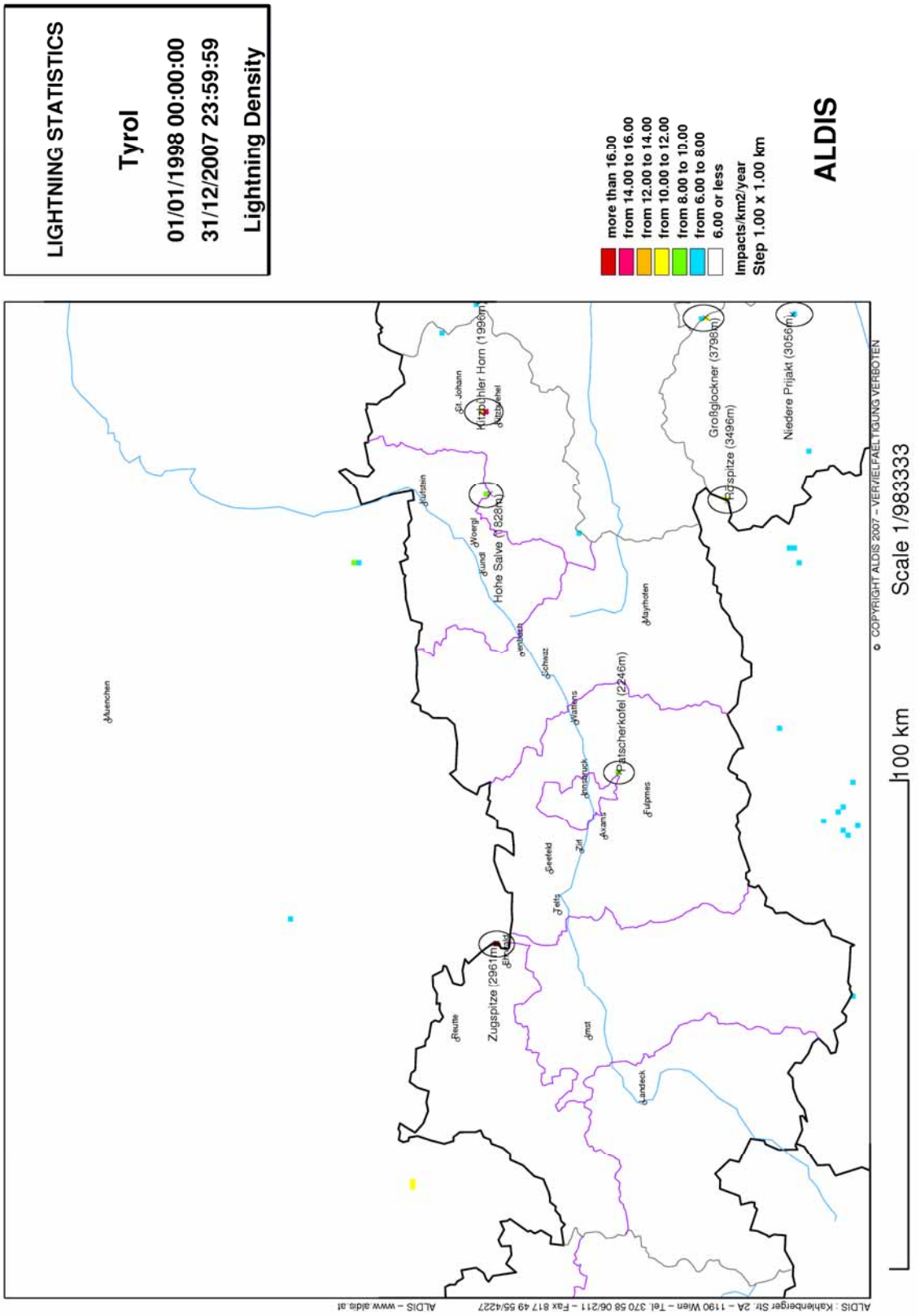

Figure 5.9: Ground flash density of Tyrol

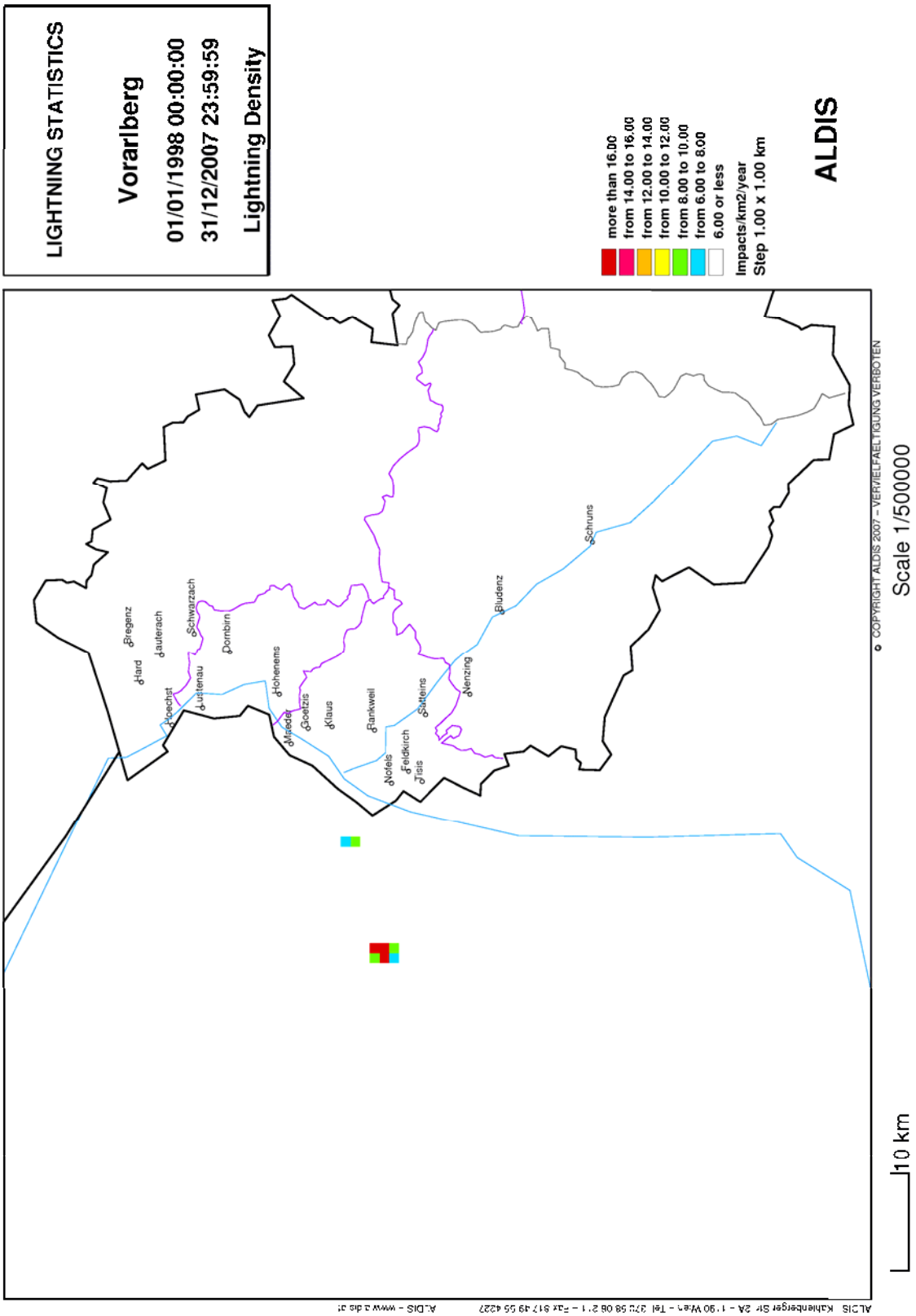

Figure 5.10: Ground flash density of Vorarlberg

In the following chapters I will discuss in more detail some of the locations with high lightning density. Additional analysis with photos and maps can be found in Appendix A. I have also analysed with the help of the program EXPERT the surrounding of the interesting points within a radius of 0.564[11] kilometer around the location in a time interval from 1998 to 2007. The program EXPERT allows to display every single stroke on a map and the disadvantage of the griding is dropped.

5.2. Lower Austria

The areas with the highest lightning activity of Lower Austria are in the south. Especially the surrounding of Schneeberg and Semmering are interesting regions.

- **Rax**
  The "Kaiserbrunnaussicht" is part of the mountain Rax and the altitude is 1484 m. 500 m south of it is a higher wooded summit (1547m) with a summit cable railway station (Rax-cable-railway) which is part of a big building named Gasthof Bergstation. Hundred meters north is a radio transmitter tower maintained by ORS[12], which is the main trigger of lighting occurred in that area, according to Rax-cable-railway staff. In the western surrounding is also a drag lift situated. According to the analysis with the EXPERT program the region of highest lightning activity is located about 250 m east of the radio transmitter tower. We assume that actual striking point of all these flashes was the radio tower and the 250 m shift is a result of systematic location error as observed at the Gaisberg tower.
  We have to note, that in case of lightning to a tower the given values of ground flash density in flashes per km^2 and used for larger areas are not correct. All those flashes struck the same location (tower top) and they are not more or less equal distributed over the area of 1 km^2.

Table 5.1: Data from the EXPERT analysis

	Kaiserbrunnaussicht	Ghf. Bergstation	250 m east*)
Negative flashes	66	71	84
Positive flashes	9	6	6
Total flashes	75	78	90
Calculated density [km^{-2} yr^{-1}]	7.5	7.8	9.0

*) Centre of located high flash density

- **Sonnwendstein:**
  The Sonnwendstein is a 1523 m high mountain next to the Semmering mountain pass. Two radio transmitter towers are located on the summit operated by ORF and Telekom Austria. There is also a shelter named Pollereshütte next to a former summit station of a meanwhile removed chairlift and a small chapel on the mountain. According to the EXPERT program the point of highest lightning activity is about 300 m east of the summit.

[11] Corresponding an area of 1 km^2
[12] Austrian Broadcasting Services

Table 5.2: Data from the EXPERT analysis

	Sonnwendstein	300 m east
Negative flashes	80	97
Positive flashes	12	11
Total flashes	92	108
Calculated density [km^{-2} yr^{-1}]	9.2	10.8

- **Schneeberg:**
  The "Klosterwappen" (2076 m), which is the highest summit in Lower Austria, as well as the "Waxriegel" (1888 m) are parts of the mountain called Schneeberg. The high lightning activity is distributed on almost the whole Schneeberg massif. But there is a point with a peak in the lightning density according to the EXPERT program. This location is at the "Nördliche Grafensteig" about one kilometer north-eastern of the "Waxriegel". On the top of the Klosterwappen are a big cross, a small radio transmitter tower and a radar station. A shelter called Fischerhütte is located near the summit "Kaiserstern" (2061 m) about 800 m north-eastern of the "Klosterwappen". On the summit "Waxriegel" is a cross and in the surrounding there are two shelters called Damböckhaus and Berghütte Hochschneeberg and the chapel Elisabethkirchlein. Next to those is the end of the rack railway named Schneebergbahn with a small train station. That railway has a length of 9.85 km and connects the town Puchberg with the Schneeberg since 1897 [*www.schneebergbahn.at, November 2008*].

Table 5.3: Data from the EXPERT analysis

	Klosterwappen	Waxriegel	Nördl. Grafensteig
Negative flashes	44	56	77
Positive flashes	16	9	14
Total flashes	60	65	91
Calculated density [km^{-2} yr^{-1}]	6.0	6.5	9.1

5.3. Vienna

Vienna has a relative low lightning activity. The lightning density is approximately 1.5 flashes per square kilometer and year.

5.4. Burgenland

Burgenland has also no appreciable lightning activity. There is no point with a ground flash density higher than 5 flashes per square kilometer and year.

5.5. Upper Austria

The overall lightning activity of Upper Austria is higher than of Burgenland. Primarily in the south are a few locations with a ground flash density above the average. But there is only one real "hot spot" in this county I want to consider more precise.

- **Katrin:**
  The "Katrin" is a 1542 m high summit part of a mountain range called Katergebirge. The mountain is located south-west of the town Bad Ischl. A radio transmitter tower operated by ORS and a big metal cross called Kaiser Franz Josef Kreuz are situated on the summit. Beneath the "Katrin" is a shelter called Katrinalm and the summit station of a cable railway starting in Bad Ischl. Next to those is a chair lift too, which is used for winter sport. A second smaller cross is located on an elevation called "Elferkogel", which is opposite of the Katrin.

Table 5.4: Data from the EXPERT analysis

	Katrin
Negative flashes	81
Positive flashes	5
Total flashes	86
Calculated density [km^{-2} yr^{-1}]	8.6

5.6. Styria

Styria is the county with the highest lightning activity in Austria. In Styria there are a lot of interesting locations, which are analyzed in more detail in the following.

- **Feistringstein / Kampl:**
  The "Feistringstein" (1836 m) is part of the Hochschwab mountain massif and the "Kampl" (1990 m) is a summit 1.5 kilometer west of the "Feistringstein". The only mentionable things are the steep stony hillsides and a cross on the top of the "Feistringstein". Centre of highest lightning activity is about 300 m east of the "Kampl" according to the EXPERT program.

Table 5.5: Data from the EXPERT analysis

	Feistringstein	Kampl	300 m east
Negative flashes	66	60	75
Positive flashes	6	18	15
Total flashes	72	78	90
Calculated density [km^{-2} yr^{-1}]	7.2	7.8	9.0

- **Lärchkogel:**
  The "Lärchkogel" (1713 m) is also part of the Hochschwab mountain range in the south of "Feistringstein". There is no man made construction in the closer surrounding of that summit. About one kilometer away is a shelter called Schönleitenhaus and a chair lift station on a summit named "Windgrube" (1809 m). In winter the surrounding of "Windgrube" is a skiing region called Bürgeralm-Aflenz, but that location has no relevant lightning activity[13]. Point of highest lightning activity is about 300 m south of the "Lärchkogel" according to the EXPERT program.

[13] Lightning density of 3.6 flashes km^{-2} yr^{-1} with the Windgrube in the centre (radius equal 564 m)

Table 5.6: Data from the EXPERT analysis

	Lärchkogel	300 m south
Negative flashes	65	74
Positive flashes	12	7
Total flashes	77	81
Calculated density [km^{-2} yr^{-1}]	7.7	8.1

- **Schießlingalm:**
  The last interesting location in the Hochschwab mountain range is the small village Schießlingalm (1484 m) south-east of the summit "Schießling" (1667 m). This village consists of about 30 wooden cottages and is on the top of an elevation in a wooded area situated.

Table 5.7: Data from the EXPERT analysis

	Schießlingalm
Negative flashes	92
Positive flashes	9
Total flashes	101
Calculated density [km^{-2} yr^{-1}]	10.1

- **Eisenerzer Reichenstein:**
  The Eisenerzer Reichenstein is the most known part of the Eisenerzer Alps with an altitude of 2165 m. There is a big metal cross on the summit and a shelter named Reichensteinhütte next to it. Mentionable is also the steep stony hillside in the surrounding of the summit.

Table 5.8: Data from the EXPERT analysis

	Eisenerzer Reichenstein
Negative flashes	81
Positive flashes	16
Total flashes	97
Calculated density [km^{-2} yr^{-1}]	9.7

- **Reiting / Gößeck:**
  The "Gößeck" is with 2214 m part of the Reiting and the highest summit of the Eisenerzer Alps. On the summit is a big metal cross and in the surrounding is a second one. A lower summit of that mountain is called "Grieskogel" (2148 m), about 700 m south of the highest peak, which has the highest lightning activity in that area according to the EXPERT program.

Table 5.9: Data from the EXPERT analysis

	Gößeck	Grieskogel
Negative flashes	75	78
Positive flashes	12	17
Total flashes	87	95
Calculated density [km^{-2} yr^{-1}]	8.7	9.5

- **Stanglalpe:**
  The "Stanglalpe" is part of the Fischbacher Alps with an altitude of 1490 m. In the surrounding of the summit is a shelter named Leopold-Wittmaier Hütte, a cross, a chapel and a monument. But the location of highest lightning activity according to the EXPERT program is the wooded area about one kilometer north-east of the "Stanglalpe" without any particularity in the surrounding.

Table 5.10: Data from the EXPERT analysis

	Stanglalpe	1 km north-east
Negative flashes	64	73
Positive flashes	7	13
Total flashes	71	86
Calculated density [km^{-2} yr^{-1}]	7.1	8.6

- **Kulmkogel (Sommeralm):**
  The "Kulmkogel" is an elevation part of the Fischbacher Alps. The altitude is 1410 m and the whole area is an alp with wooded parts. Point of highest lightning activity in that area is located at an unknown summit (1367 m) in the west of the Kulmkogel according to the EXPERT program. In the surrounding called Sommeralm is a wind power turbine situated (1.5 km south-east of the 1367m high unknown summit) but with a lower lightning density.

Table 5.11: Data from the EXPERT analysis

	Kulmkogel	unknown summit (1367 m)
Negative flashes	48	66
Positive flashes	13	12
Total flashes	61	78
Calculated density [km^{-2} yr^{-1}]	6.1	7.8

- **Heulantsch / Grubbauerkogel (Teichalm):**
  The "Heulantsch" (1471 m) and "Grubbauerkogel" (1424 m) are also parts of the Fischbacher Alps about three kilometer west of the "Kulmkogel" and the distance between the summits is about 800 m. This area called Teichalm is an alp with wooded parts and in the west of the "Heulantsch" is a drag lift located. Point of highest lightning activity is between those two summits according to the EXPERT program analysis.

Table 5.12: Data from the EXPERT analysis

	Heulantsch	Grubbauerkogel	between the summits
Negative flashes	53	64	71
Positive flashes	8	8	9
Total flashes	61	72	80
Calculated density [km^{-2} yr^{-1}]	6.1	7.2	8.0

- **Schöckl:**
  The Schöckl (1445 m) is a mountain part of the Grazer Bergland in the north of the city Graz. In winter the Schöckl is used for winter sports and hence there are two drag lifts situated. On the summit plateau are three radio transmitter towers maintained by ORS, a monument, a cable railway station, a cross, a few houses and the shelter Stubenberghaus located. The highest tower has an altitude of 96.5 m [*www.ors.at, November 2008*]. The point of the highest lightning activity according to the EXPERT program is about 200 m south-east of the summit.

Table 5.13: Data from the EXPERT analysis

	Schöckl	200 m south-east
Negative flashes	86	98
Positive flashes	17	18
Total flashes	103	116
Calculated density [km^{-2} yr^{-1}]	10.3	11.6

- **Schererkogel:**
  The mountain "Schererkogel" (1208 m) is in the east of the Gleinalpen mountain range north-east of Graz and the whole surrounding is a forest. On the peak there is just one cross but one kilometer away is a bigger cross called Schererkreuz hidden on the wooded summit. About 500 m to the south of that Schererkreuz the highest lightning activity is observed in that area according to the EXPERT program. There are scattered farms in the surrounding of the Schererkogel and about 800 m south-east of that summit is also a high lightning activity area but there is no mentionable thing regarding flashes in that area.

Table 5.14: Data from the EXPERT analysis

	Schererkogel	south of Schererkr.	south-east of Schererkg.
Negative flashes	54	80	79
Positive flashes	7	15	8
Total flashes	61	95	87
Calculated density [km^{-2} yr^{-1}]	6.1	9.5	8.7

- **Zirbitzkogel / Scharfes Eck:**
  The natural reserve Zirbitzkogel is with 2396 m the highest elevation of the Seetaler Alps. On the summit is a big cross, a small bell and a shelter called Zirbitzkogelhaus. One kilometer north is a summit called "Scharfes Eck" (2364 m) with a radio transmitter tower and a weather radar station. Centre of the

highest lightning activity in that area is about 300 m east of the summit "Scharfes Eck" according to the EXPERT program.

Table 5.15: Data from the EXPERT analysis

	Zirbitzkogel	Scharfes Eck	300 m east of Scharfes Eck
Negative flashes	60	104	118
Positive flashes	7	7	8
Total flashes	67	111	126
Calculated density [km^{-2} yr^{-1}]	6.7	11.1	12.6

- **Grebenzen:**
  The natural reserve Grebenzen (1870 m) is about 20 km west of the Zirbitzkogel and the region is used for winter sport. On the summit plateau and in the surrounding is a cross, a small weather station, two drag lifts, a small monument and the shelter Dreiwiesenhütte next to a chapel called Hubertuskapelle. The surroundings of two upper summits, called Zweite Grebenzenhöhe (1874 m) and an unknown summit (1892 m) are almost 1 and 1.5 kilometer south of the Grebenzen and have higher lightning activity according to the EXPERT program.

Table 5.16: Data from the EXPERT analysis

	Grebenzen	Zweite Grebenzenhöhe	unknown summit
Negative flashes	57	67	68
Positive flashes	11	13	12
Total flashes	68	80	80
Calculated density [km^{-2} yr^{-1}]	6.8	8.0	8.0

5.7. Carinthia

Like Styria Carinthia has a high lightning activity with numerous "hot spots", which will be discussed in the following.

- **Großer Speikkogel:**
  The Großer Speikkogel is with an altitude of 2140 m the highest peak of the Koralpe mountain massif east of the town Wolfsberg. The area around the Speikkogel is touristically developed. A road leads to the summit where two radar stations and a cross are located. One of these is part of the Austrian air defensive system called Goldhaube and the other one is a civil radar. The road is closed for public traffic, but there is also a public road reaching 1627 m altitude where a ski-center operates a few skiing lifts. About one kilometer north-west of Großer Speikkogel is the shelter Koralpenhaus and a radio transmitter station on the summit named "Steinschneider" (2020 m). But that part has a much smaller lightning activity[14] than the Speikkogel itself. The last mentionable attribute is a small cross on a ridge 500 m east of the Speikkogel called "Seespitz" (2066 m).

[14] Lightning density of 4.7 flashes km^{-2} yr^{-1} with the Steinschneider in the centre (radius equal 564m)

Centre of highest lightning activity in that area is about 200 m east of the Großer Speikkogel according to the EXPERT program analysis.

Table 5.17: Data from the EXPERT analysis

	Großer Speikkogel	200 m east
Negative flashes	131	137
Positive flashes	7	7
Total flashes	138	144
Calculated density [km^{-2} yr^{-1}]	13.8	14.4

- **Saualpe:**
  Almost the whole area of the central Saualpe mountain range western of the town Wolfsberg has a lightning activity larger than the Austrian average. This area stretches from the summit "Forstalpe" (2034 m) in the north over "Kienberg" (2050 m), "Gertrusk" (2044 m) and "Ladinger Spitz" (2079 m), which is the highest peak of that mountain range, to an unknown summit (2029 m) in the south. Centre of highest lightning activity in that whole area is between the unknown summit and the Ladinger Spitz. The following mentionable attributes are located on the interesting area of the Saualpe:

  - A cross named Zingerlekreuz and the shelter Wolfsberger Hütte in the south of the unknown summit
  - A cross on the "Ladinger Spitz"
  - A cross on the "Gertrusk" and one named Eisernes Kreuz in the north of that
  - The shelter Schmiedbauerhütte south-east of the Forstalpe

Table 5.18: Data from the EXPERT analysis

	2029m	Ladinger Spitz	between those summits
Negative flashes	62	56	72
Positive flashes	5	9	7
Total flashes	67	65	79
Calculated density [km^{-2} yr^{-1}]	6.7	6.5	7.9
	Gertrusk	Kienberg	Forstalpe
Negative flashes	60	57	61
Positive flashes	7	10	13
Total flashes	67	67	74
Calculated density [km^{-2} yr^{-1}]	6.7	6.7	6.4

- **Dobratsch:**
  The mountain Dobratsch, also called Villacher Alp, has steep hillsides and is located in the west of the city of Villach. That mountain massif is accessible by a toll road reaching 1733 m. The highest peak of the Dobratsch has an altitude of 2166 m where a 165 m high radio transmitter tower is situated. That tower is

maintained by ORS and with an ERP[15] of 125,000 watts it is the strongest transmitter of Austria [*www.ors.at, November 2008*]. A non public cable railway, starting in the town Bad Bleiberg, is used for the employees to reach the tower. Close to the tower are two chapels, two crosses, a small weather station and the shelter Ludwig Walter Haus. That area, actually the radio transmitter tower, is the place with the highest lightning density recorded in Austria. The lightning detection system ALDIS measured the most interesting point about 200m south-east of the tower.

Table 5.19: Data from the EXPERT analysis

	Dobratsch	200 m south-east
Negative flashes	725	839
Positive flashes	10	17
Total flashes	735	856
Calculated density [km^{-2} yr^{-1}]	73.5	85.6

- **Goldeck:**
  The mountain Goldeck with an altitude of 2142 m is part of the mountain range Gailtaler Alps. Goldeck is situated in the south of the town Spittal an der Drau and in winter the mountain is used for winter sports. Hence there are a few skiing lifts reaching the summit, which is also accessible by a toll road leading to 1883 m. On the summit are a few lift summit stations, a shelter, a cross and particularly a radio transmitter tower maintained by ORS. In the surrounding of the summit are more skiing-lifts, three crosses and three shelters[16] situated. Highest lightning activity is about 200 m south of the summit according to the EXPERT program.

Table 5.20: Data from the EXPERT analysis

	Goldeck	200 m south
Negative flashes	202	212
Positive flashes	9	9
Total flashes	211	221
Calculated density [km^{-2} yr^{-1}]	21.1	22.1

- **Hochwipfel:**
  The Hochwipfel is a mountain with steep hillsides in the south auf the town Kirchbach. The summit with an altitude of 2195 m is part of the mountain range Karnische Alps. On the peak is a big iron cross. Centre of highest lightning activity in that area is about 300 m south of the summit Hochwipfel according to the EXPERT program.

[15] Effective Radiated Power
[16] Gasthof Krendlmaralm, Goldeckhütte, Gasthof Seetal

Table 5.21: Data from the EXPERT analysis

	Hochwipfel	300 m south
Negative flashes	51	70
Positive flashes	12	12
Total flashes	63	82
Calculated density [km^{-2} yr^{-1}]	6.3	8.2

- **Hoher Trieb:**
  The Hoher Trieb (2199 m) and the Kleiner Trieb (2096 m) are two mountains with steep hillsides and they are part of the Karnische Alps. The two summits are close together on the national border between Austria and Italy and on each peak is a cross. About one kilometer north-east of the Kleiner Trieb is the shelter Dr. Steinwender Hütte and a chapel.

Table 5.22: Data from the EXPERT analysis

	Hoher Trieb	Kleiner Trieb
Negative flashes	78	72
Positive flashes	7	6
Total flashes	85	78
Calculated density [km^{-2} yr^{-1}]	8.5	7.8

- **Promos:**
  The Promos, also known as Blaustein, is part of the Karnische Alps. That mountain is located on the national border between Austria and Italy and has an altitude of 2195 m. According to the EXPERT program the highest lightning activity in that area is about 500 m south of the summit on the Italian side close to the mountain Pizzo Di Timau[17]. The whole area consists of steep hillsides.

Table 5.23: Data from the EXPERT analysis

	Promos	500 m south-west
Negative flashes	55	69
Positive flashes	17	13
Total flashes	72	82
Calculated density [km^{-2} yr^{-1}]	7.2	8.2

- **Polinik:**
  The Polinik is with 2332 m also part of the Karnische Alps. This mountain has steep hillsides, is in the south of the town Kötschach-Mauthen and on the summit is a big iron cross. According to the EXPERT program the centre of highest lightning activity is about 400 m south-west of the summit.

[17] In German named Hocheck

Table 5.24: Data from the EXPERT analysis

	Polinik	400 m south-west
Negative flashes	64	89
Positive flashes	8	7
Total flashes	72	96
Calculated density [km^{-2} yr^{-1}]	7.2	9.6

- **Hohe Warte:**
  The Hohe Warte is a small mountain massif with steep hillsides on the border between Austria and Italy and is part of the Karnische Alpen. The highest point is the Hohe Warte itself with an altitude of 2780 m and a cross close to a small bell on the top. Another important summit is the "Kollinkofel" (2742 m) about 1.5 kilometer east of the highest peak. 400 m east of that summit is the centre of highest lightning activity in that area according to the EXPERT program.

Table 5.25: Data from the EXPERT analysis

	Hohe Warte	Kollinkofel	400 m east
Negative flashes	63	75	84
Positive flashes	13	9	6
Total flashes	76	84	90
Calculated density [km^{-2} yr^{-1}]	7.6	8.4	9.0

- **Großglockner:**
  The Großglockner (3798 m) is the highest mountain in Austria with a big metal cross on the top and steep hillsides in the proximity. The summit is part of the so-called Glocknergruppe which lies in the mountain range Hohe Tauern. About 700 m south-east of the peak is the highest-situated shelter in Austria called Erzherzog-Johann Hütte connected to valley with a material cable railway. Centre of highest lightning activity is about 300 m north of the summit according to the EXPERT program.

Table 5.26: Data from the EXPERT analysis

	Großglockner	300 m north
Negative flashes	93	110
Positive flashes	13	13
Total flashes	106	123
Calculated density [km^{-2} yr^{-1}]	10.6	12.3

5.8. East Tyrol

In East Tyrol, which is part of the county Tyrol, are two "hot spots" regarding lightning activity.

- **Hoher / Niedere Prijakt:**
  The Prijakt is a mountain part of the so-called Schobergruppe with two summits consist of steep hillsides, the Niedere Prijakt with an altitude of 3056 m and a cross on the top and the higher Hoher Prijakt with 3064 m. An important shelter called Hochschoberhütte is located in the north of the mountain.

Table 5.27: Data from the EXPERT analysis

	Niedere Prijakt	Hoher Prijakt
Negative flashes	67	75
Positive flashes	12	13
Total flashes	79	88
Calculated density [km^{-2} yr^{-1}]	7.9	8.8

- **Rötspitze:**
  The Rötspitze is located at the border between Austria and Italy in the western Venedigergruppe which is part of the mountain range Hohe Tauern. The altitude is 3496 m and there is a cross on the peak which is located on a ridge. Maximum of analysed lightning activity is about 300 m north-east of the summit.

Table 5.28: Data from the EXPERT analysis

	Rötspitze	300m north-east
Negative flashes	75	100
Positive flashes	3	4
Total flashes	78	104
Calculated density [km^{-2} yr^{-1}]	7.8	10.4

5.9. Salzburg

Salzburg is fourth smallest county in Austria according to covered area (after Vienna, Vorarlberg and Burgenland) and is located in the Alps region. Despite the mountainous area there are just two remarkable points of high lightning activity.

- **Großes Wiesbachhorn:**
  The Großes Wiesbachhorn with 3564 m and steep hillsides is the third highest mountain of the Glocknergruppe, which is part of the mountain range Hohe Tauern. On the summit of the Wiesbachhorn is a metal cross. The chains fixing the cross are in consequence of lightning strikes quite affected (partial melted). The centre of highest lightning activity in that area is about 500 m north of the peak according to the EXPERT program.

Table 5.29: Data from the EXPERT analysis

	Großes Wiesbachhorn	500m north
Negative flashes	91	140
Positive flashes	6	5
Total flashes	97	145
Calculated density [km^{-2} yr^{-1}]	9.7	14.5

- **Gaisberg:**
  The Gaisberg (1287 m) is a wooded mountain east of the city Salzburg. On the summit is a radio transmitter station with a 100 m tall tower [*www.ors.at, November 2008*] maintained by ORS. On the Gaisberg Tower direct lightning current measurements are done by ALDIS. The high lightning activity observed around the Gaisberg was the reason why the Gaisberg was chosen for the measurements. The summit is accessible by a public road and on the plateau is a shelter, a cross and a monument. Centre of highest lightning activity is about 400 m north of the tower according to the EXPERT program.

Table 5.30: Data from the EXPERT analysis

	Gaisberg	200 m north	400 m north
Negative flashes	217	252	262
Positive flashes	11	11	14
Total flashes	228	263	276
Calculated density [km^{-2} yr^{-1}]	22.8	26.3	27.6

5.10. Tyrol

The county Tyrol is also situated in the alpine region of Austria. In that area there are a few points with high lightning activity. The whole average lightning density is lower than in Salzburg, but there are more "hot spots" I am going to analyse them more closely.

- **Kitzbühler Horn:**
  The Kitzbühler Horn is a 1996 m high summit which is a significant part of the mountain range Kitzbühler Alps. On the summit there are a cable railway station, a chair lift station, a shelter, a chapel and especially a radio transmitter tower maintained by ORF with a tower height of 102 m. There is also a cross next to the summit. Centre of highest lightning activity in that area is about 400 m north of the tower according to the EXPERT program.

Table 5.31: Data from the EXPERT analysis

	Kitzbühler Horn	400 m north
Negative flashes	178	222
Positive flashes	8	9
Total flashes	186	231
Calculated density [km^{-2} yr^{-1}]	18.6	23.1

- **Hohe Salve:**
  The Hohe Salve (1828 m) is part of the Kitzbühler Alps, about 10 km east of the town Wörgl. That mountain is used for winter sports and hence there are several buildings located on the top. On the summit there are two shelters, a chapel, a cable railway station, a drag lift, a cross and a radio transmitter mast. According to the EXPERT program the centre of highest lightning activity is about 500m north-west of the summit.

Table 5.32: Data from the EXPERT analysis

	Hohe Salve	500 m north-west
Negative flashes	71	89
Positive flashes	4	7
Total flashes	75	96
Calculated density [km^{-2} yr^{-1}]	7.5	9.6

- **Patscherkofel:**
  The Patscherkofel (2246 m) is the local mountain near the city of Innsbruck and is part of the Tuxer Alps. The mountain is used for winter sports and due to the specific position there are a lot of radio-, radar- and measuring stations on the summit plateau. On that plateau is especially a large radio transmitter tower maintained by ORS with a tower height of 67 m[18] [*www.ors.at, November 2008*]. Furthermore there are a smaller transmitter tower by "KroneHit", a weather radar station by Austro Control, a shelter, a summit station of a chair lift, a cross and several smaller measuring sensors as well as transmitter stations. According to the EXPERT program the location of highest lightning activity is about 300 m north-east of the summit.

Table 5.33: Data from the EXPERT analysis

	Patscherkofel	300m north-east
Negative flashes	89	103
Positive flashes	2	4
Total flashes	91	107
Calculated density [km^{-2} yr^{-1}]	9.1	10.7

- **Zugspitze:**
  The Zugspitze is the highest peak of the mountain massif Zugspitze and is part of the Wettersteingebirge in the northern Kalkalps. The mountain is situated on the boarder between Germany and Austria and has an altitude of 2961 m. On the peak of the summit, close to steep hillsides, are a meteorological observatory, two cable railway stations, a restaurant, a cross and diverse transmitters and sensors inclusive a radio transmitter mast on the top. Centre of highest lightning activity is about 200 m south of the summit.

[18] without antenna on the top

Table 5.34: Data from the EXPERT analysis

	Zugspitze	200 m north
Negative flashes	141	153
Positive flashes	8	6
Total flashes	149	159
Calculated density [km^{-2} yr^{-1}]	14.9	15.9

5.11. Vorarlberg

The county Vorarlberg has a low lightning activity with no noteable hot spots.

5.12. Comparison of locations and conclusion

At almost all locations described above there is a difference between the summit and/or tower position and the point of highest lightning activity according to ALDIS. This difference is the bias (systematic error) as described in 4.4. In the following a summary of the most important attributes for all locations described above is given.

Table 5.35: Comparison of locations

		highest lightning density [km^{-2} $year^{-1}$]	altitude of the summit	transmitter tower on the summit	radar station on the summit	cross on the summit	shelter on the summit	chapel on the summit	cable railway summit station	skiing lift on the summit	ridge or steep hillside on the summit	wooded summit	village and/or scattered houses
1.	Dobratsch	85.6	2166 m	X		X	X	X	X		X		
2.	Gaisberg	27.6	1287 m	X		X	X					X	
3.	Kitzbühler Horn	23.1	1996 m	X		X	X	X	X	X	X		
4.	Goldeck	22.1	2142 m	X		X	X			X	X		
5.	Zugspitze	15.9	2961 m	X		X	X		X		X		
6.	Großes Wiesbachhorn	14.5	3564 m			X					X		
7.	Großer Speikkogel	14.4	2140 m		X	X					X		
8.	Zirbitzkogel / Scharfes Eck	12.6	2396 m	X	X	X	X				X		
9.	Großglockner	12.3	3798 m			X					X		
10.	Schöckl	11.6	1445 m	X		X	X		X	X		X	
11.	Sonnwendstein	10.8	1523 m	X		X	X	X				X	
12.	Patscherkofel	10.7	2246 m	X	X	X	X			X			
13.	Rötspitze	10.4	3496 m			X					X		
14.	Schießlingalm	10.1	1484 m									X	X
15.	Eisenerzer Reichenstein	9.7	2165 m			X	X				X		
16.	Polinik	9.6	2332 m			X					X		
16.	Hohe Salve	9.6	1828 m	X		X	X	X	X	X			
18.	Schererkogel	9.5	1208 m			X[19]						X	
18.	Gößeck	9.5	2214 m			X					X		
20.	Schneeberg	9.1	2076 m		X	X	X	X			X		
21.	Kaiserbrunnaussicht	9.0	1484 m	X			X		X	X		X	
21.	Hohe Warte	9.0	2780 m			X					X		
21.	Feistringstein/Kampl	9.0	1990 m			X					X		
24.	Hoher / Niederer Prijakt	8.8	3064 m			X					X		
25.	Stanglalpe	8.6	1490 m									X	
25.	Katrin	8.6	1542 m	X		X	X		X	X	X	X	
27.	Hoher / Kleiner Trieb	8.5	2199 m			X					X		
28.	Promos	8.2	2195 m								X		
28.	Hochwipfel	8.2	2195 m			X					X		
30.	Lärchkogel	8.1	1431 m									X	
31.	Heulantsch/Grubbauerkogel	8.0	1471 m									X	
31.	Grebenzen	8.0	1870 m			X	X	X		X		X	
33.	Saualpe	7.9	2079 m			X	X						
34.	Kulmkogel	7.8	1410 m									X	

[19] The cross is hidden in a forest

The Question is: Why do these locations have an increased lightning strike probability? All 34 locations have in common that they are mountains or at least elevated areas. The altitudes are between 1208 m (Schererkogel) and 3798 m (Großglockner). Hence it is obvious that there is a correlation between altitude and lightning density. An explanation would be that the altitude of an area, reduces the distance between the charged thundercloud and the ground level and this increases the probability of a lightning strike.

But beside the altitude every area with high lightning density has also special attributes, listed in Table 5.35, which can lead to potential correlations to lightning density. We can divide the characteristics of the "hot-spot" locations into the following categories:

- **Category I:** Locations with a radio transmitter tower or a radar station on the summit.
- **Category II:** Locations with only a cross on the summit and/or a ridge and/or a steep hillside
- **Category III:** Locations with only buildings like shelters, chapels, skiing lifts or cable railways on the summit
- **Category IV:** Locations with no man made constructions but a forest

Figure 5.11 shows the distribution of the assignment to the four categories. 41 % of the given locations are assigned to category I. The average lightning density of those locations is 19.3 flashes per square kilometer and year and the average altitude is 1945 m. To category II are 38 % of the given locations are assigned. The average lightning density is 9.7 flashes per square kilometer and year and the average altitude is 2621 m. The first two categories correspond 79 % of all interesting locations. Hence it appears that radio transmitter towers, radar stations and crosses and/or ridges or steep hillsides on mountain summits are the most important lightning triggers. Because of the difference between the average lightning densities of the first two categories it is clear that radio transmitter towers as well as radar stations are the main lightning triggers.

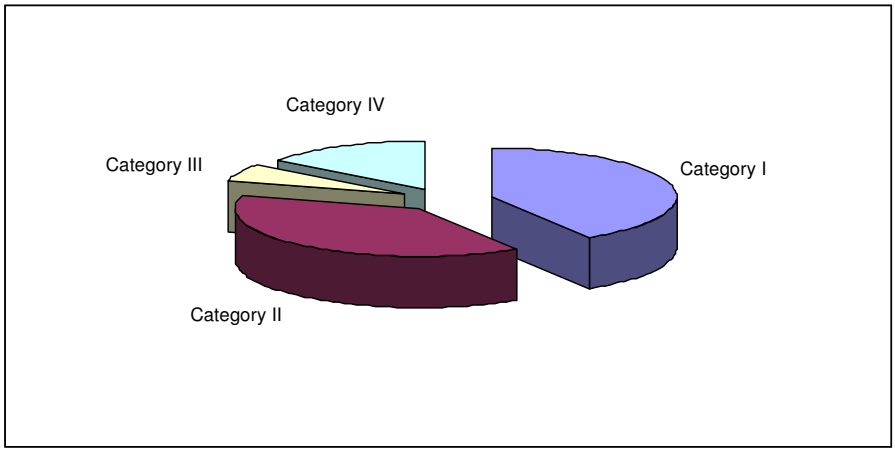

Figure 5.11: Distribution of the categories

To the remaining two categories III and IV 21 % of the locations are assigned. Category III (6 %) has an average lightning density of 9.1 flashes per square kilometer and year and an average altitude of 1677 m. To those locations count the Schießlingalm and the

Grebenzen. The lightning trigger at those areas can be small buildings like houses (Schießlingalm) or skiing lifts (Grebenzen). The last category (IV-15%) includes the Schererkogel, Stanglalpe, Lärchkogel, Heulantsch/Grubbauerkogel and Kulmkogel. The average lightning density is 8.4 flashes per square kilometer and year and the average altitude is 1402 m. As there are no man made elevated objects, lightning at those locations can only be trigger by trees.

Figure 5.12 and Figure 5.13 shows a comparison of the average lightning density and the average altitude of the individual categories. The average lightning density of category I is because of the radio transmitter towers as well as the radar stations distinct higher than of the other categories which have similar average values.

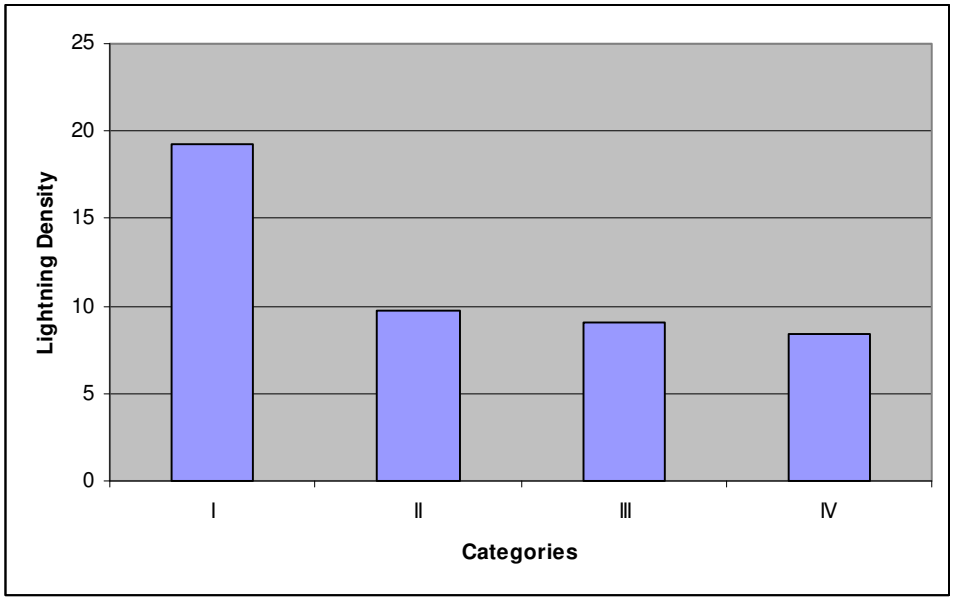

Figure 5.12: The average lightning density for the 4 categories I, II, III and IV

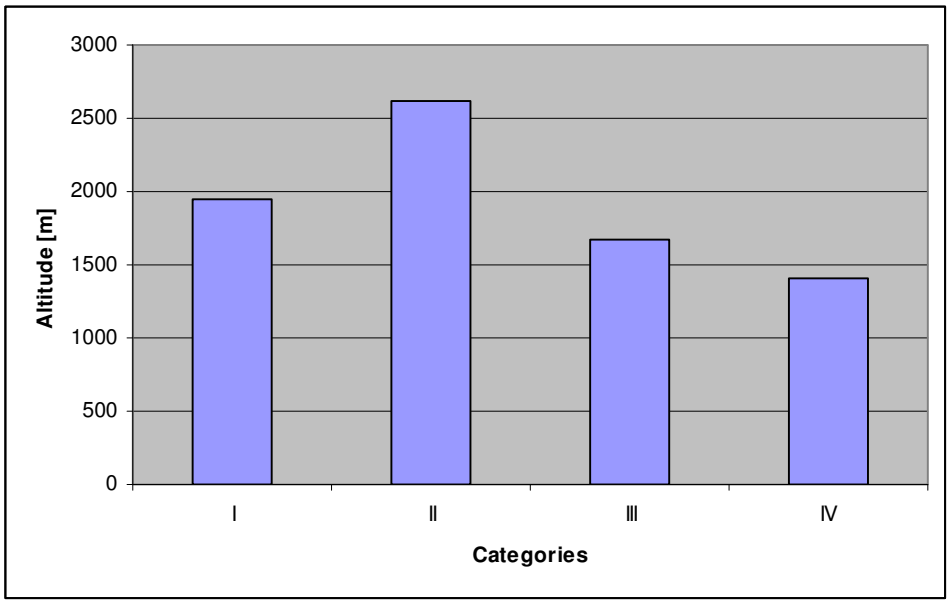

Figure 5.13: The average altitude for the 4 categories I, II, III and IV

Table 5.36 shows the locations of highest lightning density for each category.

Table 5.36: Most important locations of each category

category	lightning density	location	county	altitude
I	85.6	Dobratsch	Carinthia	2166 m
II	14.5	Großes Wiesbachhorn	Salzburg	3364 m
III	10.1	Schießlingalm	Styria	1484 m
IV	9.5	Schererkogel	Styria	1208 m

Finally a short explanation for the increase of the electrostatic field at elevated objects which leads to an increase of the lightning strike probability is given in Figure 5.14. The vertical lines represent the electric flux while the horizontal lines are the equipotential surfaces (surfaces with the same electric potential). The distance between the equipotential surfaces represents the strength of the local electric field. Hence at the tops of objects like mountains, radio transmitter towers, trees and buildings exists a higher electric field than across the lower surrounding and the probability of triggering a lightning strike is increased.

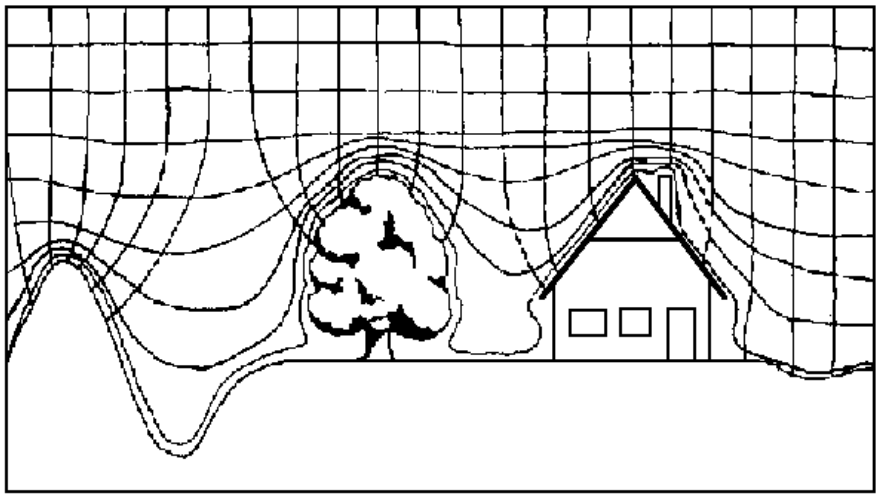

Figure 5.14: Electrostatic field [*www.igte.tugraz.at, March 2009*]

6. High multiplicity flashes in Austria

6.1. Introduction

In this chapter we will analyse the flashes in Austria with a multiplicity greater than 25. Furthermore the locations of these flashes will be examined to find possible reasons for such high multiplicities. The flash multiplicity represents the number of strokes in a flash. According to 3.5 the determination of the multiplicity of a flash is given by a grouping algorithm implemented in the LLS which groups the located strokes to a flash. Hence the parameter flash multiplicity is very sensitive to the performance of the LLS. Since 1998 the performance of ALDIS increased as a result of interconnection to neighbouring systems as well as through improvements of the used sensors. To guarantee suitable lightning data, the period under review is restricted to a time period from January 1st, 2002 till December 31st 2007. The particular strokes are again visualised with the help of the program EXPERT and in Appendix B details of the multiple stroke flashes and photos of the locations are given.

In Figure 6.1 to Figure 6.5 the striking locations of the multi-stroke-flashes with a multiplicity greater than 25 in the particular counties of Austria are shown. Interesting locations are emphasized with black ellipses.

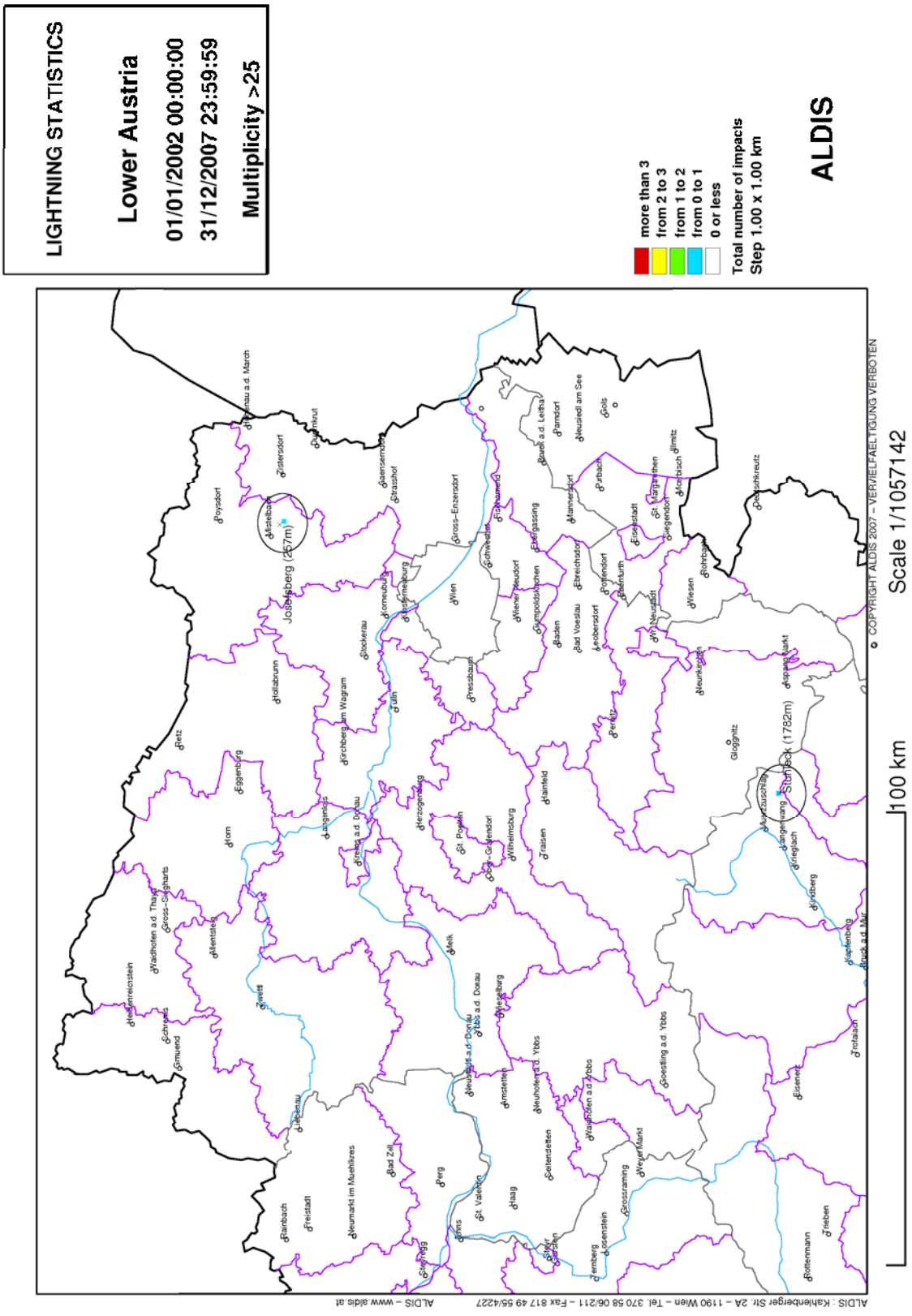

Figure 6.1: Locations of flashes with multiplicity >25 in Lower Austria

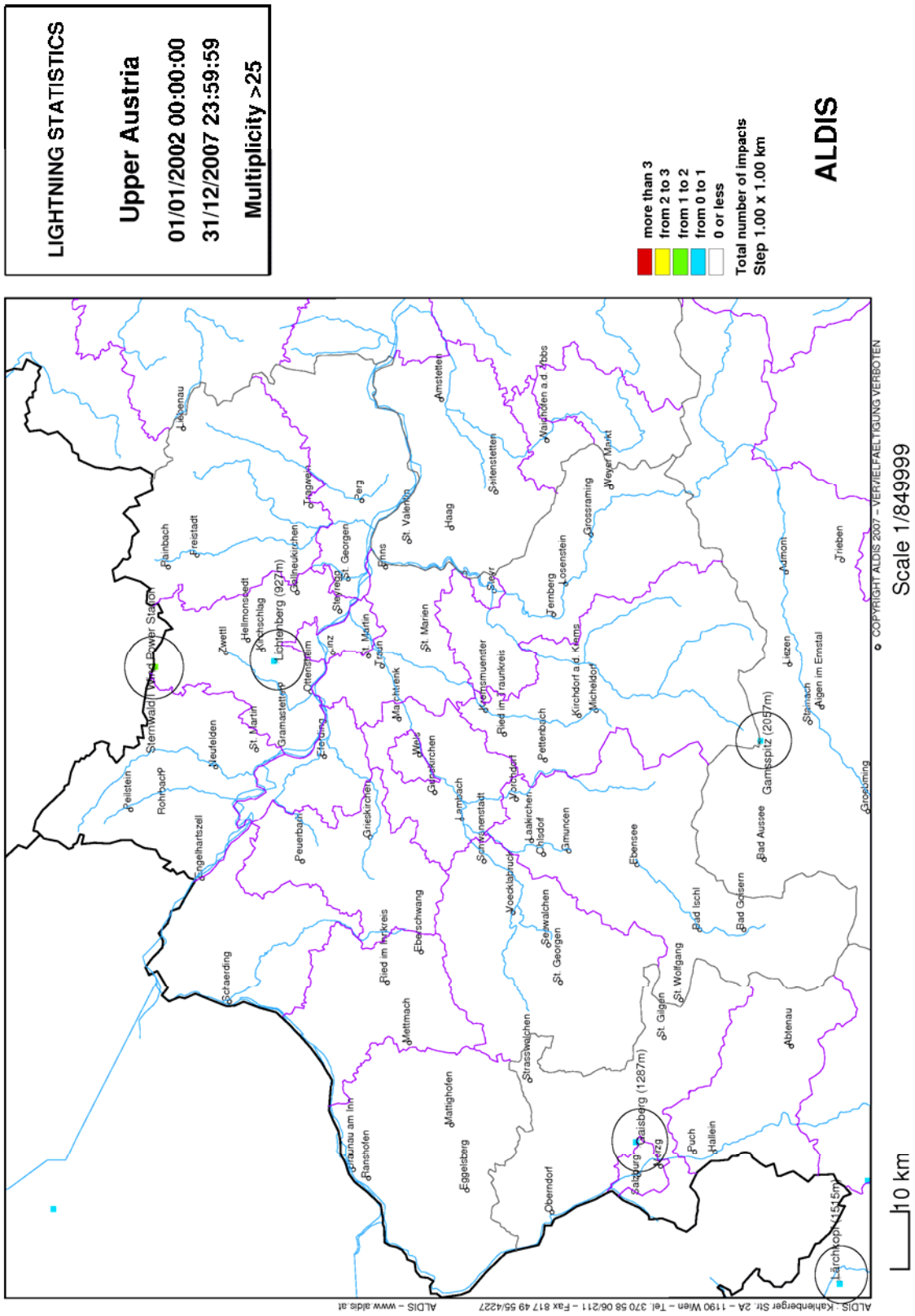

Figure 6.2: Locations of flashes with multiplicity >25 in Upper Austria

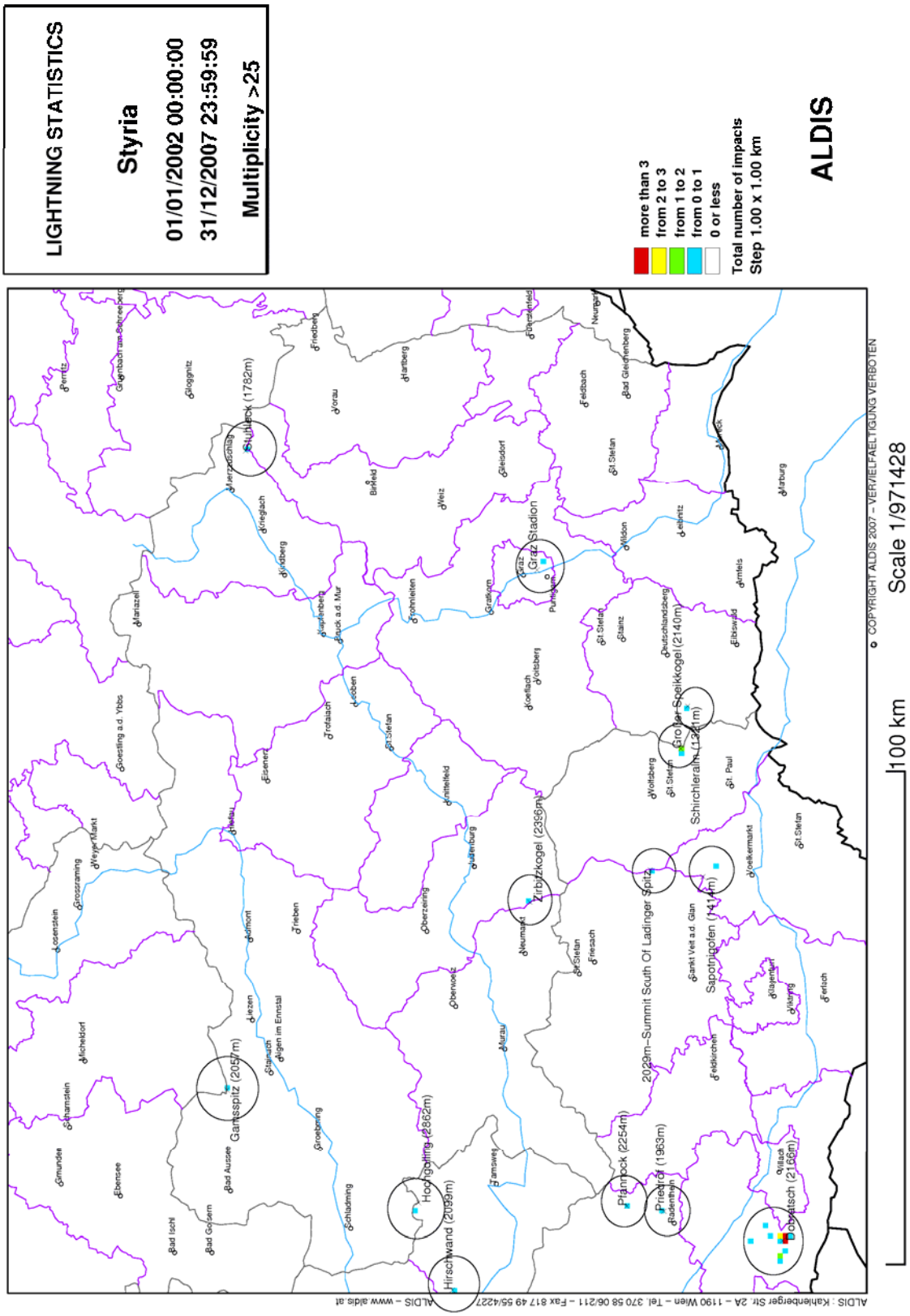

Figure 6.3: Locations of flashes with multiplicity >25 in Styria

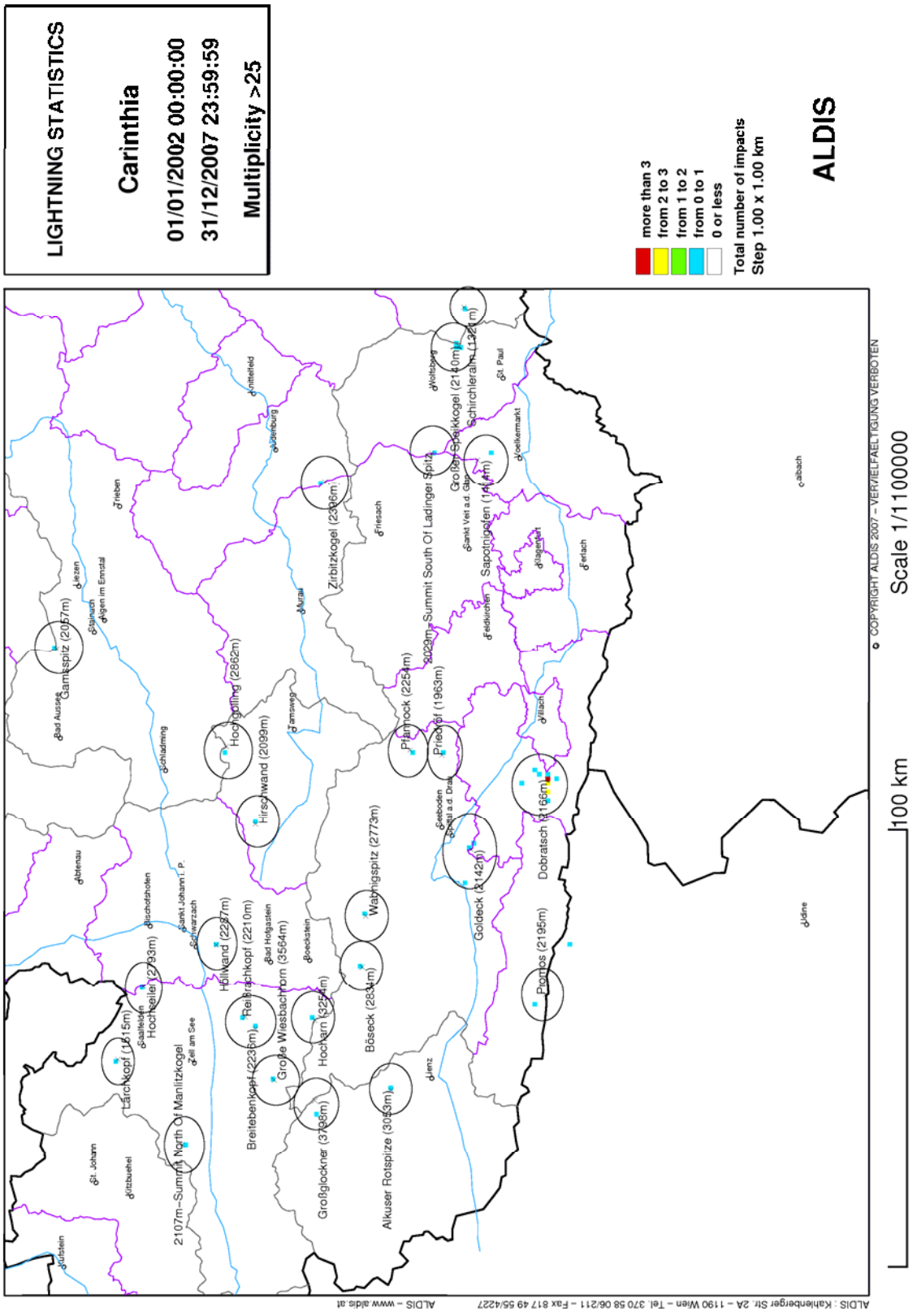

Figure 6.4: Locations of flashes with multiplicity >25 in Carinthia

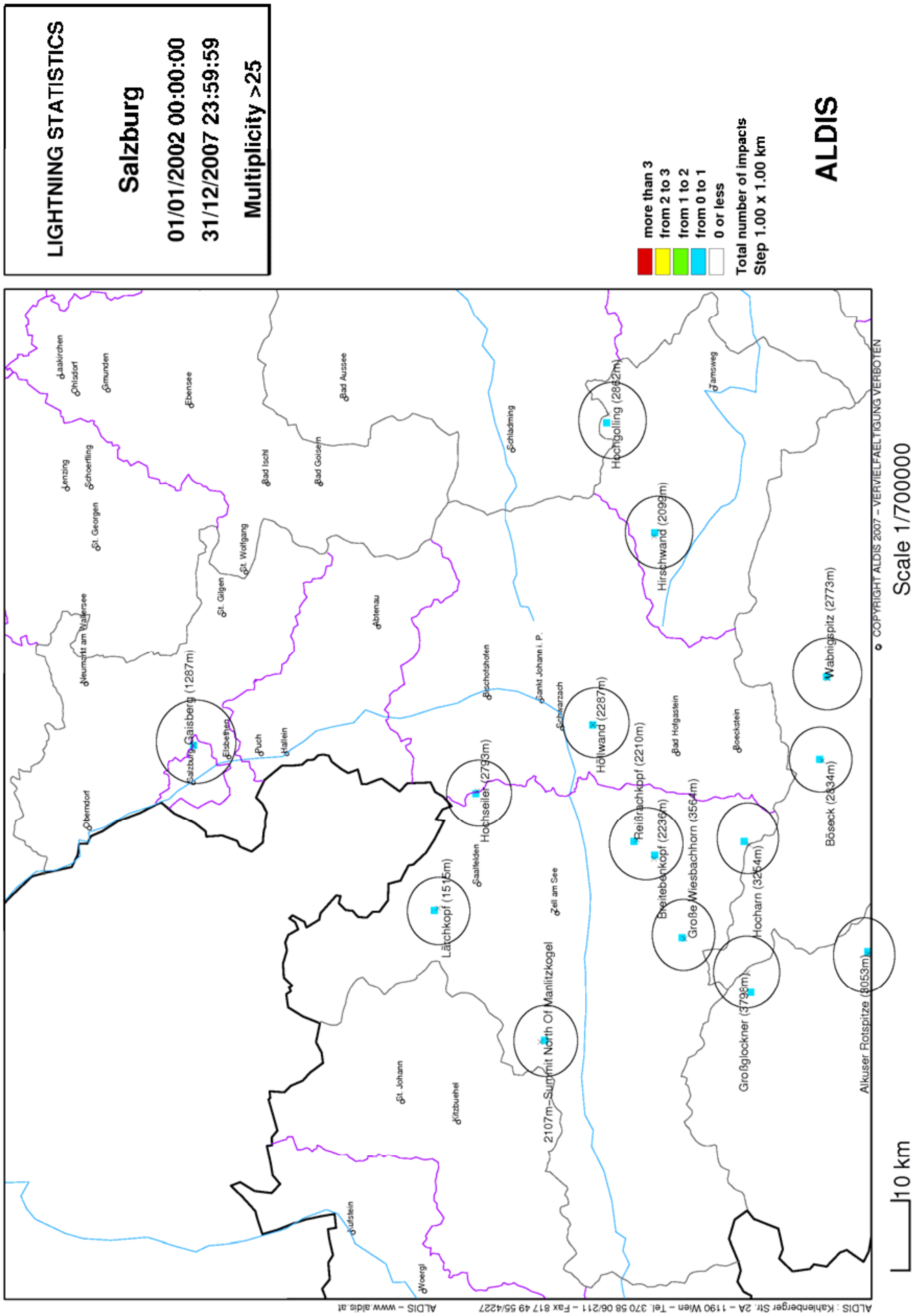

Figure 6.5: Locations of flashes with multiplicity >25 in Salzburg

6.2. Lower Austria

- **Mistelbach / Josefsberg:**
  The Josefsberg (257 m) is a small hill east of the town Mistelbach. On 21st June 2007 ALDIS detected a 29 stroke flash in the surrounding of that hill. But a detailed analysis shows two clusters of strike points at a distance of about 12 kilometer as shown in Figure 6.6. Three possible explanations are given below:

  - Two different flashes occurred almost at the same time
  - A single flash with more than one ground strike point occurred
  - One ground strike point with huge detection deviation (not very likely)

  The two strike point clusters are in the area around the villages Höbersbrunn[20] and Maustrenk[21]. In the surrounding of the villages several wind turbines are installed. On the highest point in the proximity of the north-eastern cluster (Steinberg, 320 m) is also a radio transmitter mast located. One of the wind turbines or the radio transmitter tower could have triggered that flash. Stroke number two exhibits the highest peak current with an amplitude of 33.7 kA. The first two strokes are positive discharges while the remaining strokes are negative discharges (see Figure 6.7). Hence this ambiguous flash was changing its polarity between the strokes. This type of flashes is called a bipolar flash and has been observed also at the Gaisberg tower [*Schulz W. und Diendorfer G. 2003*].

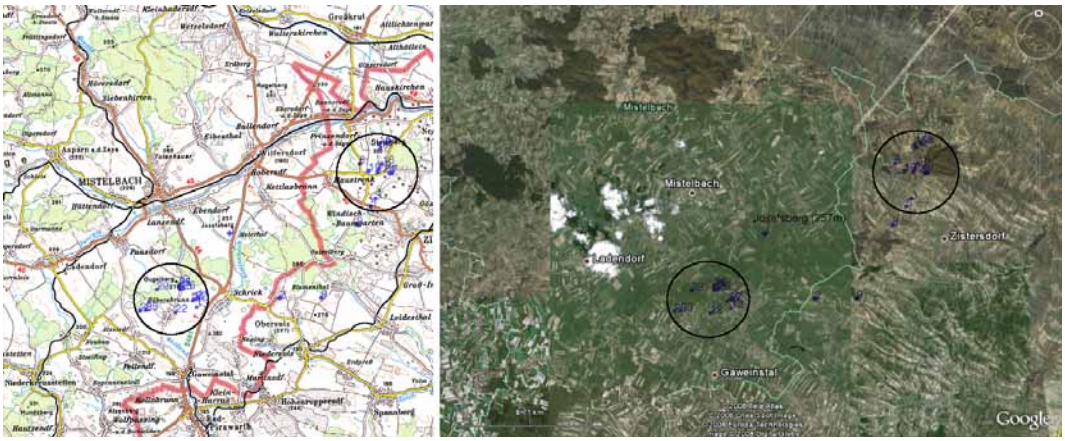

Figure 6.6: Map (22 km × 22 km) of the surrounding of Mistelbach (left) with the two clusters of located strike points grouped to and a satellite image of that area by Google Earth (right)

[20] About 14 strokes
[21] About 15 strokes

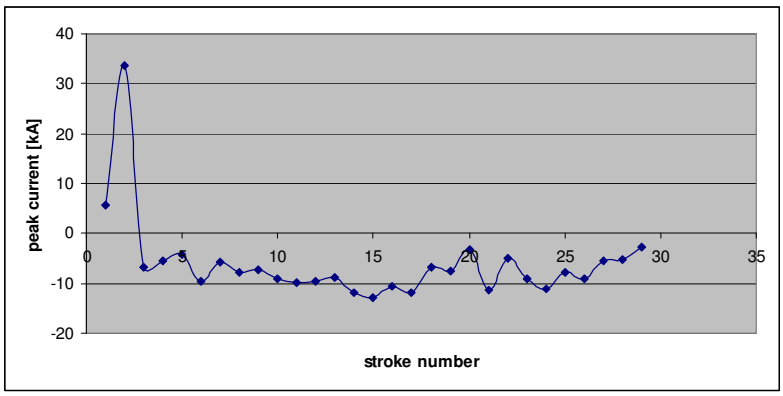

Figure 6.7: Distribution of stroke peak currents

6.3. Upper Austria

- **Sternwald I Wind Power Station:**
  The wind farm Sternwald I is about 30 kilometer north of the city Linz at the border between Austria and Czech Republic. Sternwald I consists of several wind turbines installed on an about 1000 m high wooded plateau. On 14th December 2003 and 14th January 2004 two flashes with 30 (-9 kA average peak current[22]) and 27 strokes (-7.3 kA average peak current), respectively, struck the wind turbines with the notation V17708 as viewed in Figure 6.8 and Figure 6.9. The highest current amplitudes are -30.7 kA (stroke number 25 in the 30 stroke flash) and -15.4 kA (stroke number 12 in the 27 stroke flash) as seen in Figure 6.10 and Figure 6.11.

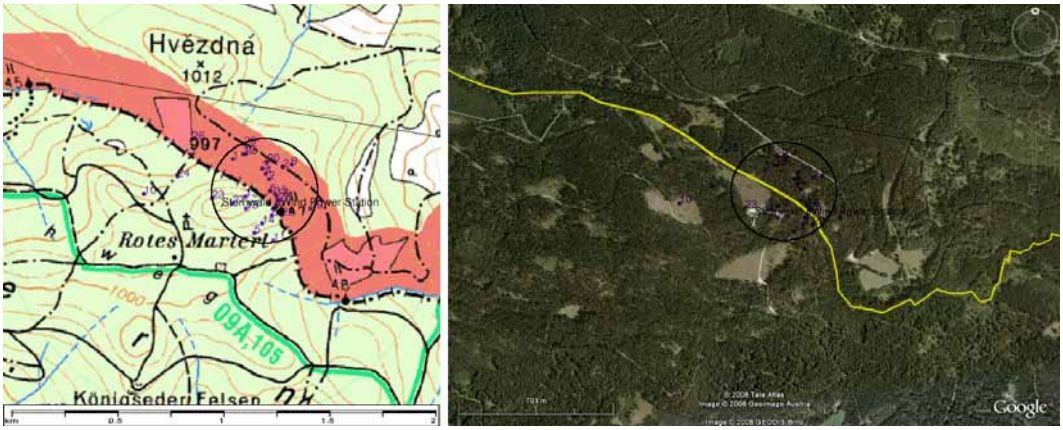

Figure 6.8: Map (left) and satellite image (right) of the area where the 30 stroke flash was located on 14th December 2003

[22] For the evaluation of the average peak current only the negative strokes are used, because the detected positive strokes could be misclassified cloud discharges.

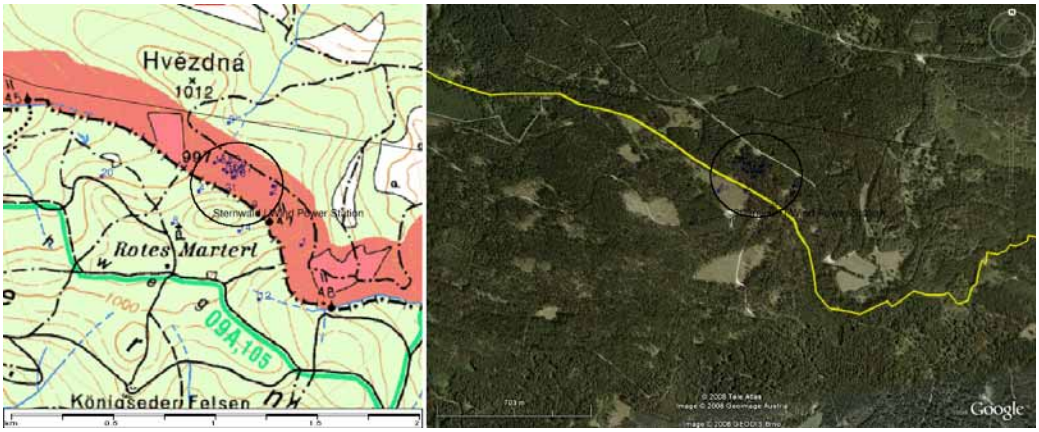

Figure 6.9: Map (left) and satellite image (right) of the area where the 27 stroke flash was located on 14th January 2004

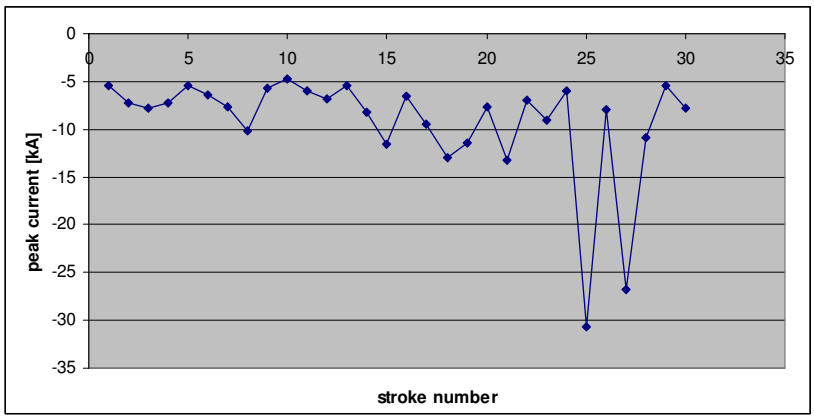

Figure 6.10: Distribution of stroke peak currents of the flash on 14th December 2003

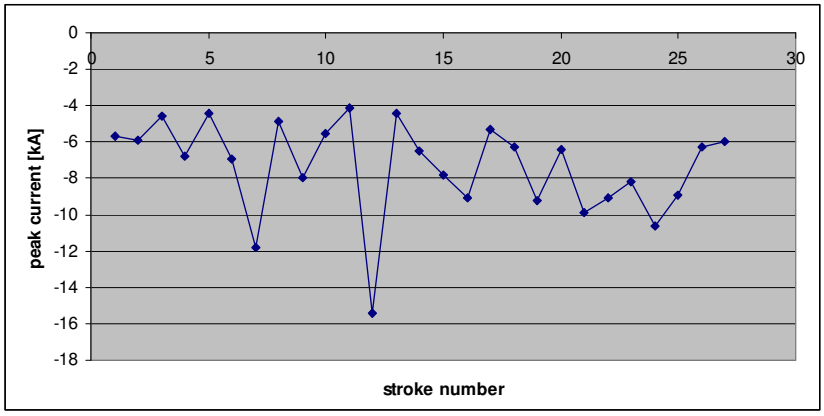

Figure 6.11: Distribution of stroke peak currents of the flash on 14th January 2004

- **Lichtenberg:**
  The Lichtenberg is a 927 m high wooded elevation about 5 km north of the city of Linz. Amidst the forest is an about 156 m high radio transmitter tower next to a 20 m high look-out called Giselawarte. On 11th November 2007 ALDIS detected a multiple lightning flash with 29 strokes in that area as seen in Figure 6.12. The maximum peak current stroke is number 22 with an amplitude of -16.5 kA as shown in Figure 6.13 and the average peak current of the whole flash is -

8.1 kA. The probability is high that the multiple-flash was triggered by the transmitter tower.

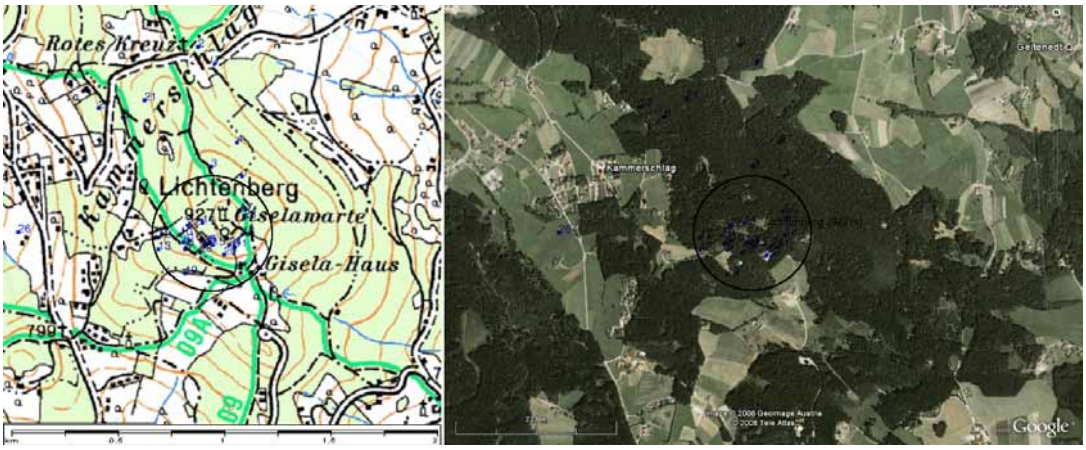

Figure 6.12: Map (left) and satellite image (right) with the area where the 29 strokes flash was located in the proximity of the Lichtenberg

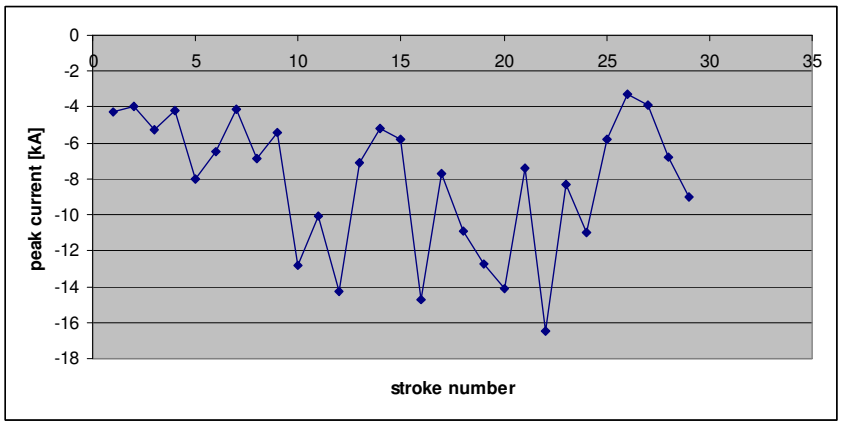

Figure 6.13: Distribution of stroke peak currents

- **Gamsspitz:**
  The "Gamsspitz" is a 2057 m high summit part of the mountain range Totes Gebirge. On 2nd August 2007 a 29 strokes lightning flash with an average peak current of -10.5 kA has been detected in the northern surrounding of that area as shown in Figure 6.14. In the surrounding of the located flash is a stony steep hillside, which could have triggered the flash. Stroke number 12 is the strongest one with a peak current of -40.6 kA (see Figure 6.15).

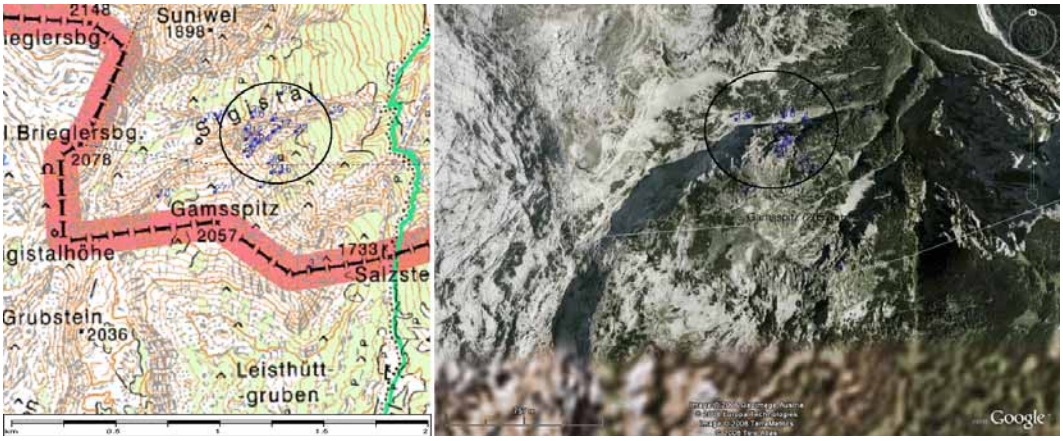

Figure 6.14: Map (left) and satellite image (right) of the area Gamsspitz with the individual stroke locations

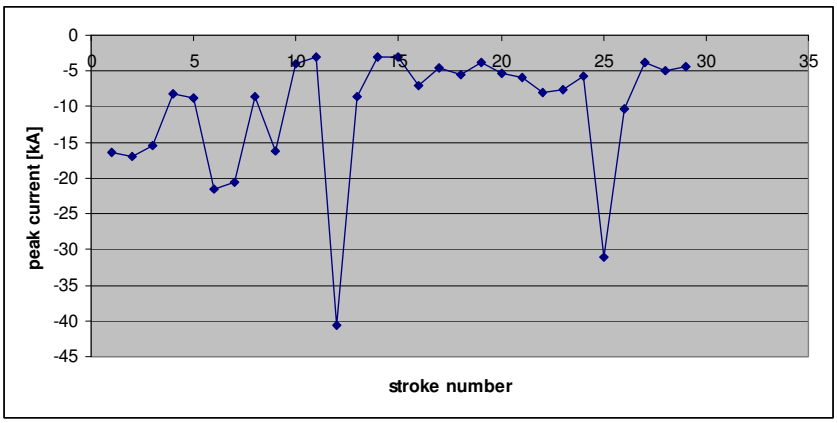

Figure 6.15: Distribution of stroke peak currents

6.4. Styria

- **Stuhleck:**
  The Stuhleck with an altitude of 1782 m is the highest mountain of the Fischbacher Alpen. On the summit are a cross, a chair lift and a shelter called Alois-Günther-Haus. ALDIS detected a bipolar flash with 27 strokes and an average peak current of -8.9 kA on 9th July 2007 in the western surrounding of that summit (see Figure 6.16 left[23]), more precisely in the proximity of the chair lift, which could have triggered the flash. The strongest stroke is number 11 with a peak current of -21.3 kA. Noteable is that in contrast to the other strokes, the two last strokes were of positive polarity as shown in Figure 6.16 (right image). Those positive strokes are very small and they are most likely misclassified cloud discharges.

[23] The chair lift is not visualised

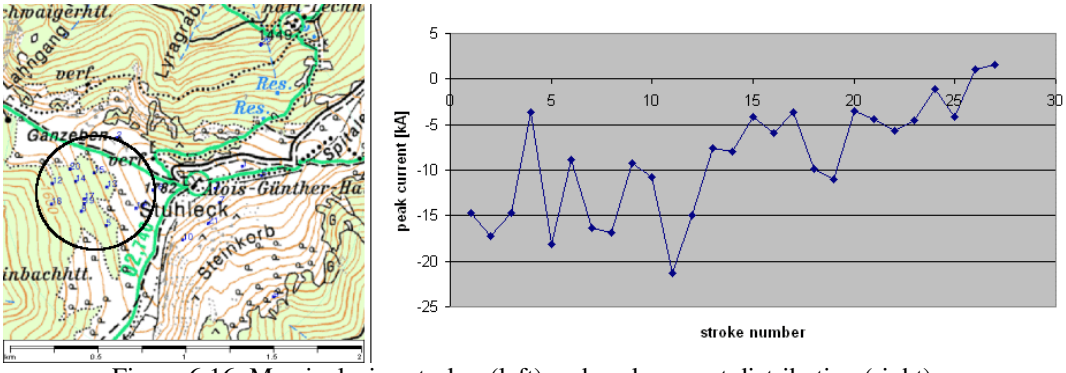

Figure 6.16: Map inclusive strokes (left) and peak current distribution (right)

- **Graz / St.Peter:**
  Graz is the main town of the Austrian province Styria. On 29th June 2006 ALDIS detected a 26 stroke flash with an average peak current of -8.9 kA in the area of the district called St.Peter as shown in Figure 6.17. The strongest stroke had a peak current of -47.5 kA (stroke number 1) as shown in Figure 6.18. The individual strokes are located around the church St.Peter, which was with high probability trigger of that flash.

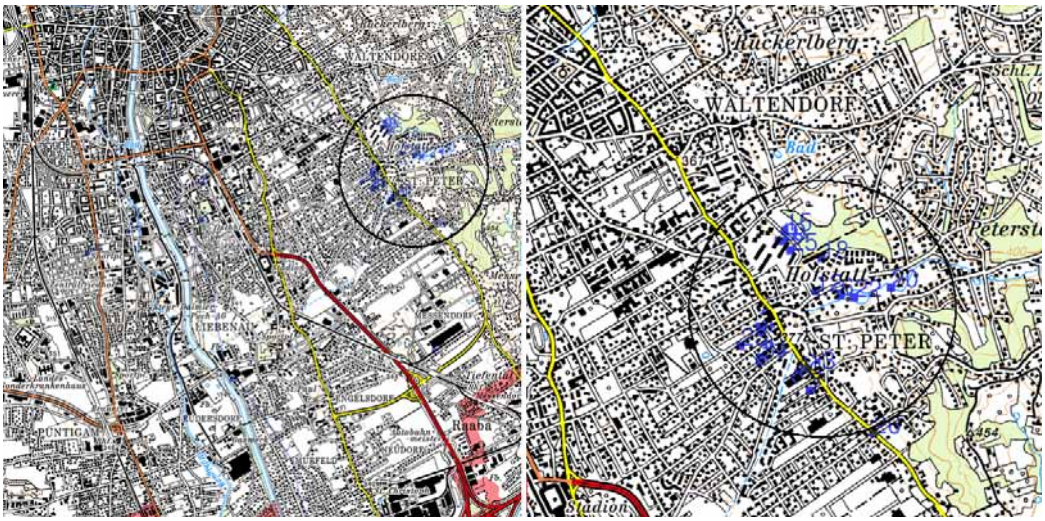

Figure 6.17: Maps (left: 6×6km, right: 3×3km) of a part of Graz inclusive detected strokes

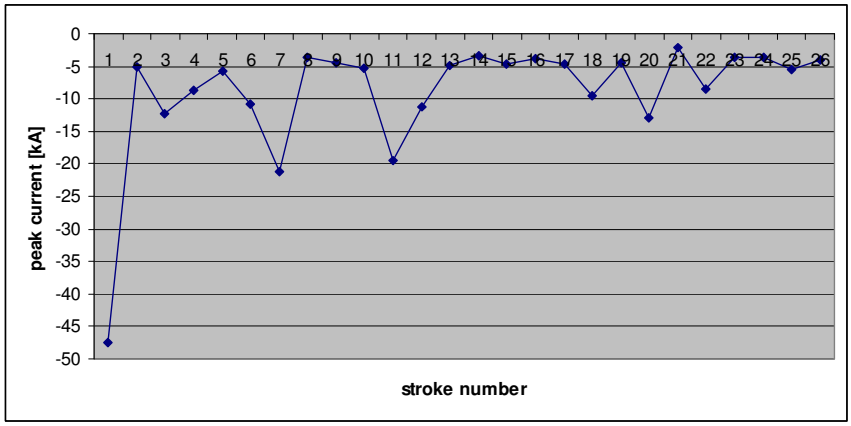

Figure 6.18: Distribution of stroke peak currents

- **Zirbitzkogel / Scharfes Eck:**
  On 29th June 2006 ALDIS detected a flash with 37 strokes at the neighbour summit of the Zirbitzkogel called "Scharfes Eck" as shown in Figure 6.19. The description of this area is given in chapter 5.6. The multiple-stroke flash had an average peak current of -6.8 kA and stroke number 2 and 5 had the highest current amplitude with -14.7 kA as shown in Figure 6.20. This flash could have been triggered by the local transmitter tower, by the weather radar station or by the steep hillside which are all located in the proximity of the summit.

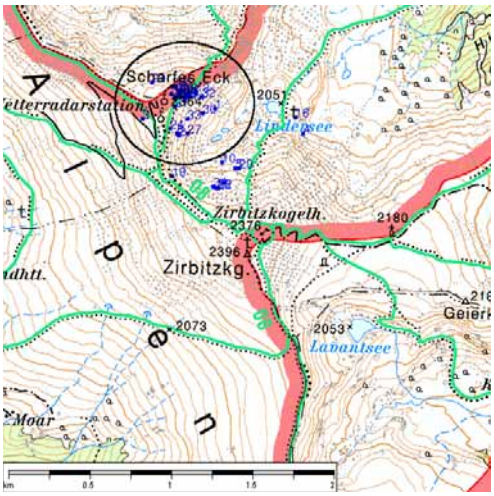

Figure 6.19: Map of the surrounding of the Zirbitzkogel with located strokes

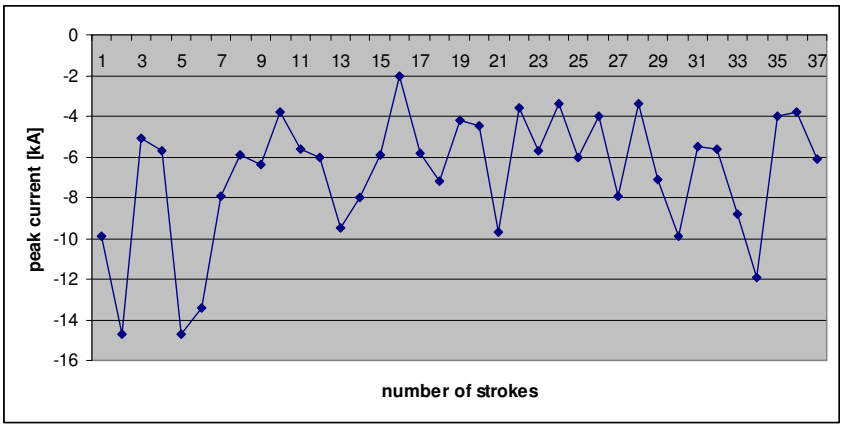

Figure 6.20: Distribution of stroke peak currents

- **Schirchleralm:**
  The "Schirchleralm" (1321 m) is an alp-plant in a wooded area about 9 km west of the Großer Speikkogel and about 10 km south-west of the town Deutschlandsberg. Figure 6.21 shows the bipolar flash detected in the western surrounding of the Schirchleralm on 9th July 2006 with a multiplicity of 28. The average peak current is -11 kA and stroke number 6 had the highest current amplitude with -36.7 kA as shown in Figure 6.22. Additionally two strokes had positive polarity with small amplitudes. But those positive strokes are very small

and probably misclassified cloud discharges. The trigger of that flash was with high probability a tree.

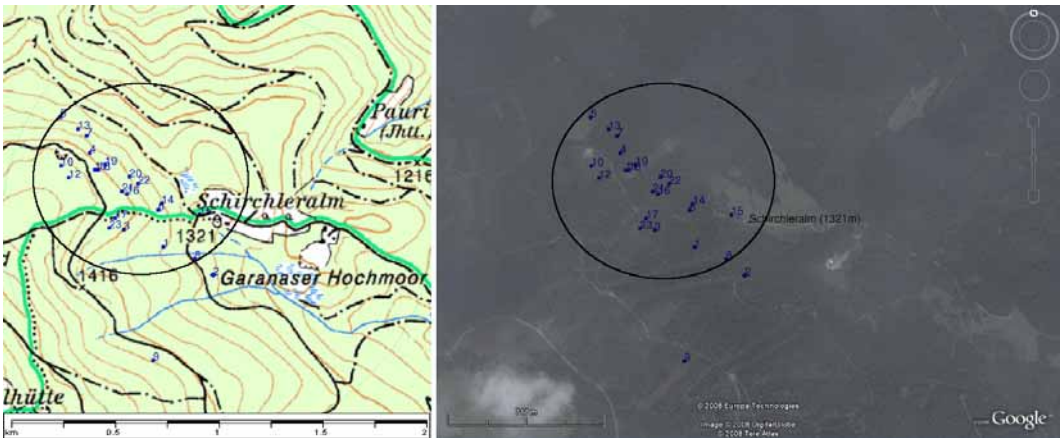

Figure 6.21: Map (left) and satellite image (right) of the Schirchleralm showing the individual ALDIS stroke locations

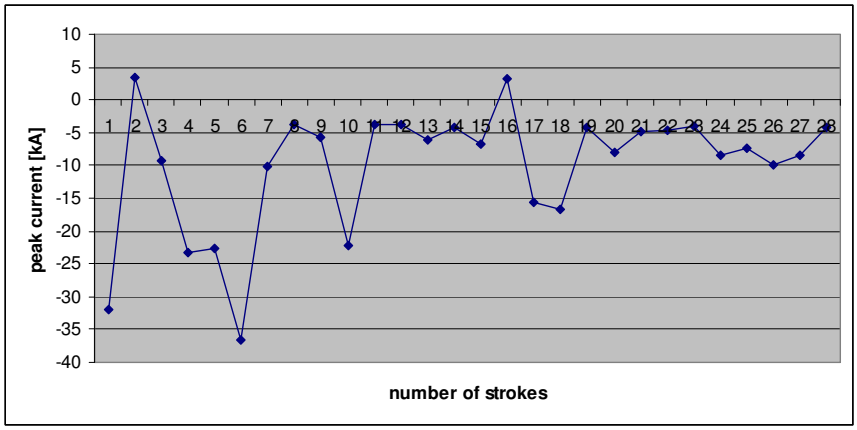

Figure 6.22: Distribution of stroke peak currents

6.5. Carinthia

- **Großer Speikkogel:**
  The description of that area can be found in chapter 5.7. Table 6.1 shows three high multiplicity flashes detected by ALDIS at that summit. The trigger sources of these flashes are with high probability the two radar stations located at the summit of the Großer Speikkogel.

Table 6.1: Detected multiple-stroke flashes

date	time	number of strokes	average peak current	highest peak current	stroke number of stroke with highest peak current
24.09.2004	09:11:55	30	-8.1 kA	-17.6 kA	16
24.09.2004	09:16:29	36	-8.8 kA	-19.5 kA	36
04.07.2007	12:21:27	32	-5.6 kA	-20.3 kA	23

The stroke peak current distribution of the 32-strokes flash on 4thJuly 2007 is illustrated in Figure 6.23. The average peak current is -5.6 kA and the highest

current amplitude is -20.3 kA. Figure 6.24 shows a comparison of the stroke peak currents of the three multiple-stroke flashes.

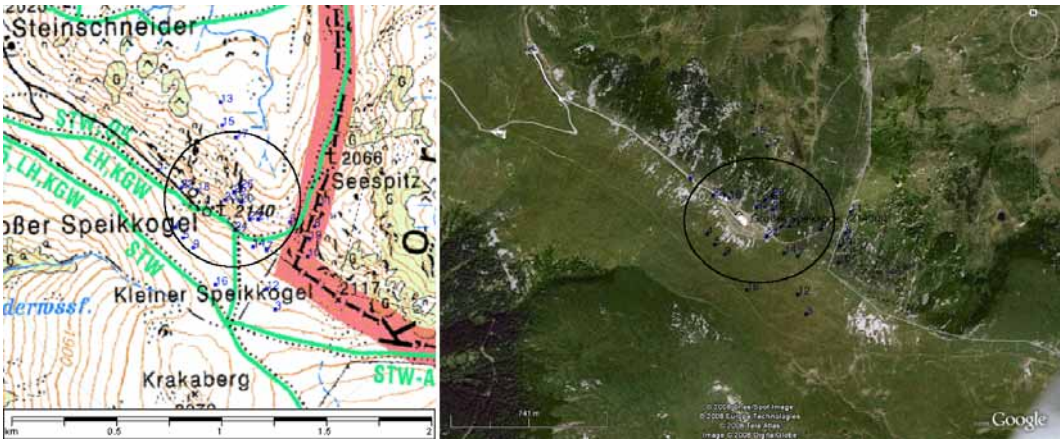

Figure 6.23: Map of the surrounding of the Großer Speikkogel inclusive the strokes of the multiple-stroke flash in the year 2007

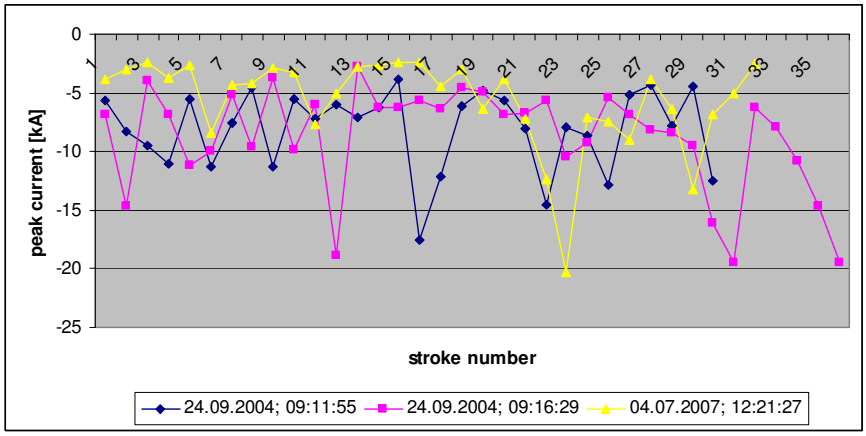

Figure 6.24: Distribution of stroke peak currents of the three multiple-stroke flashes

- **Saualpe - Nameless Summit 2029 m:**
  Figure 6.25 shows the locations of a 26 stroke flash from 19th July 2004 in the southern proximity of a nameless summit (2029 m) south of the Ladinger Spitz (highest summit of the Saualpe; see chapter 5.7). This area is just an alp with heaps of stones on the 2029 m summit and in the proximity, which could have triggered the flash. The average peak current of that flash is -8.7 kA and the stroke with the highest current amplitude is stroke number 9 with -16.4 kA as shown in Figure 6.26.

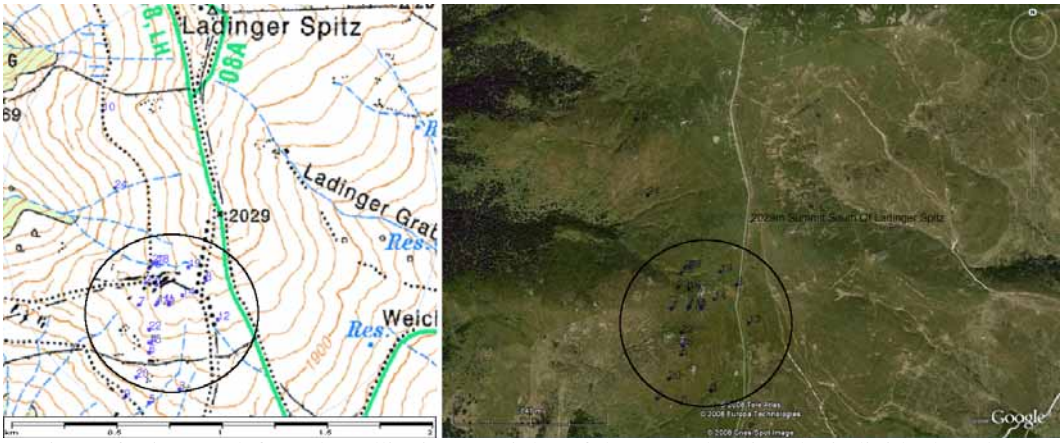

Figure 6.25: Map (left) and satellite image (right) of that area showing the individual stroke locations

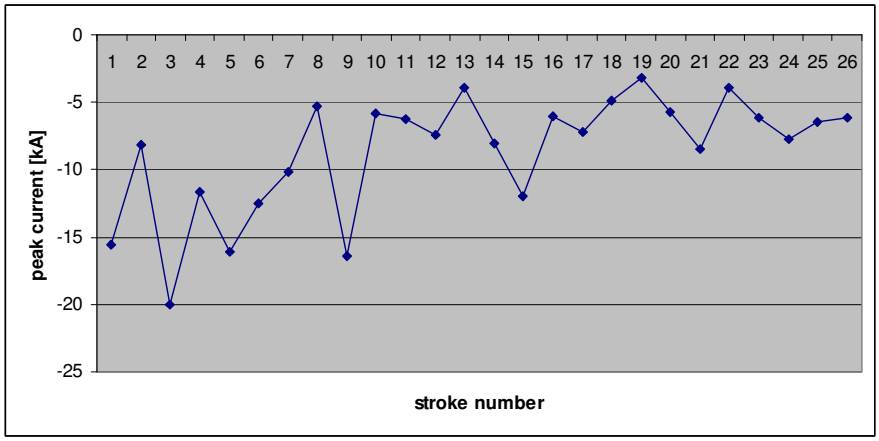

Figure 6.26: Distribution of stroke peak currents

- **Sapotnigofen:**
  Sapotnigofen is a 1474 m high wooded hill 1.5 km north-east of the village Diex, located about 9 km north of the town Völkermarkt. On 14th August 2007 ADLIS detected a flash with 26 strokes in the proximity of Sapotnigofen as shown in Figure 6.27. The cluster of strike points is about 400 m south-east of Sapotnigofen, where there is no special object except a forest and a small village at the foot of the hill. The average peak current of that flash is -9.7 kA and the highest current amplitude (-47.3 kA) was inferred for stroke number 1 as shown in Figure 6.28.

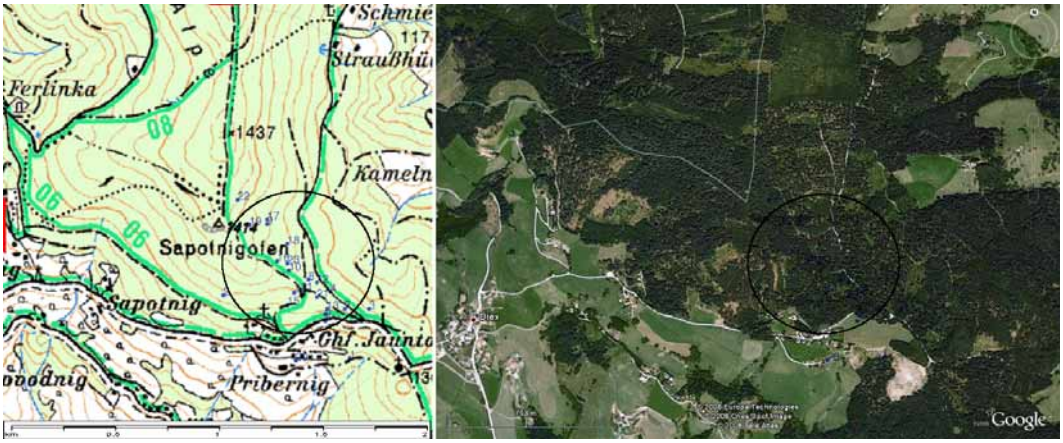

Figure 6.27: Map (left) and satellite image (right) of the proximity of Sapotnigofen showing the individual stroke locations

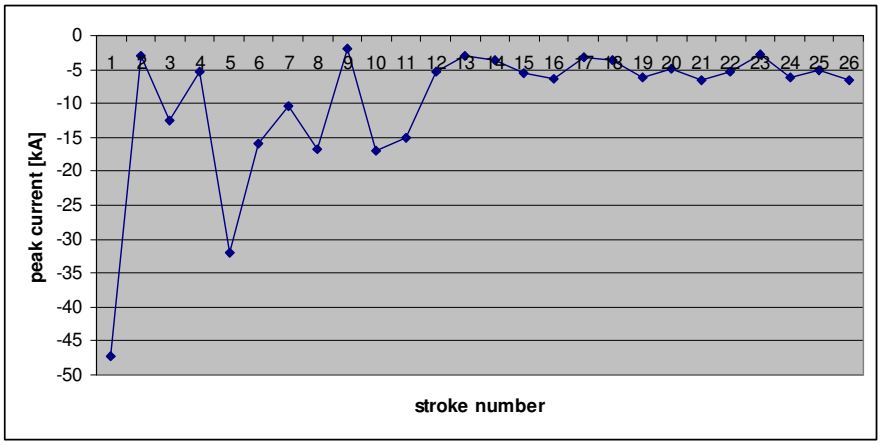

Figure 6.28: Distribution of stroke peak currents

- **Pfannock:**
  The Pfannock is a 2254 m high mountain and part of the national park Nockberge in the Gurktaler Alps. The summit has a metal cross on the top and is situated about 10 km north of the town Radenthein. On 29th June 2006 ALDIS detected a 26 stroke flash in the southern proximity of the Pfannock where a ridge is located (see Figure 6.29). It is probable that the ridge was the trigger of that flash. The average peak current is -5.7 kA and the highest current amplitude of -18.1 kA was inferred for stroke number 21 as seen in Figure 6.30.

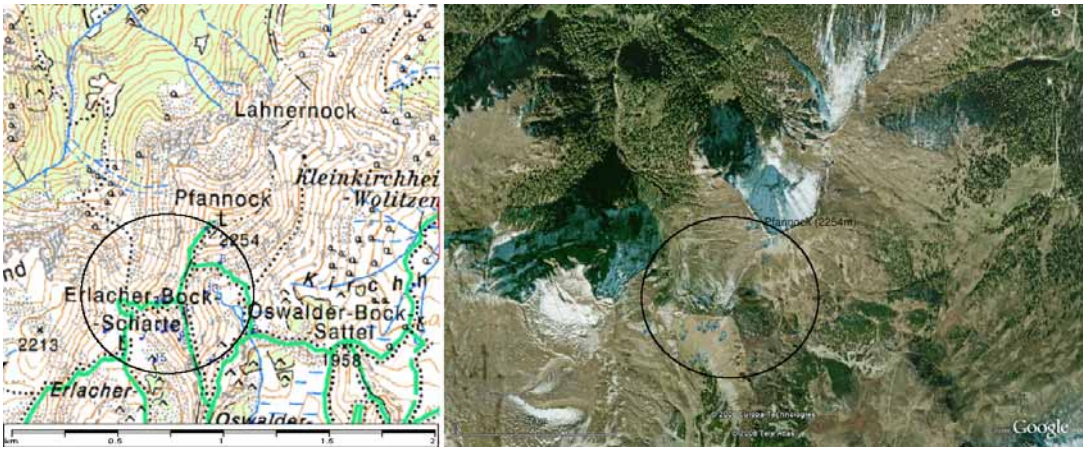

Figure 6.29: Map (left) and satellite image (right) of the proximity of the Pfannock showing the individual stroke locations

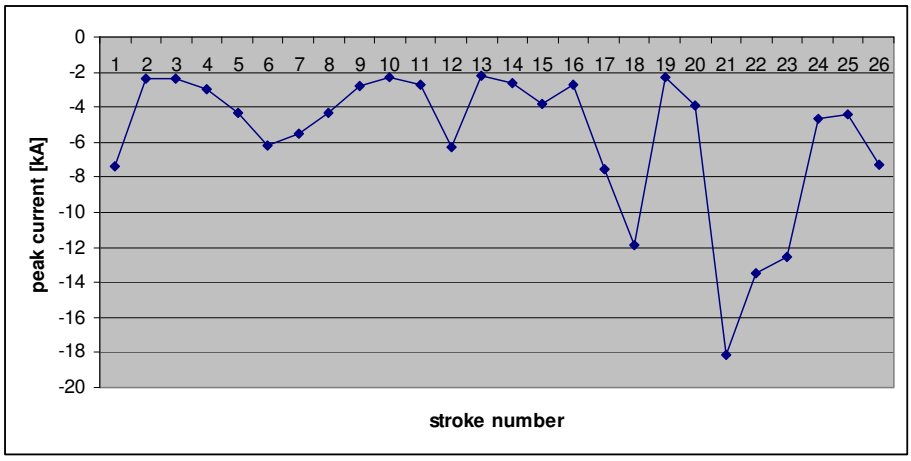

Figure 6.30: Distribution of stroke peak currents

- **Priedröf:**
  The Priedröf is a 1963 m high wooded mountain and part of the Gurktaler Alps. This mountain is about 8 km south of the Pfannock, on the top of the summit is a wooden cross and in the proximity are two drag-lifts used for ski-sport[24]. Furthermore in the surrounding, within about one km, are a few shelters called Nockalmhütte and Brentlerhütte. On 14th June 2003 ALDIS detected a multiple-stroke flash with 28 strokes at the summit of the Priedröf as shown in Figure 6.31. The flash has an average peak current of -8.6 kA and stroke number 1 has the highest peak current with -28.9 kA as seen in Figure 6.32. It is probable that the flash was triggered by a local drag-lift.

[24] Ski-sport region Bad Kleinkirchheim

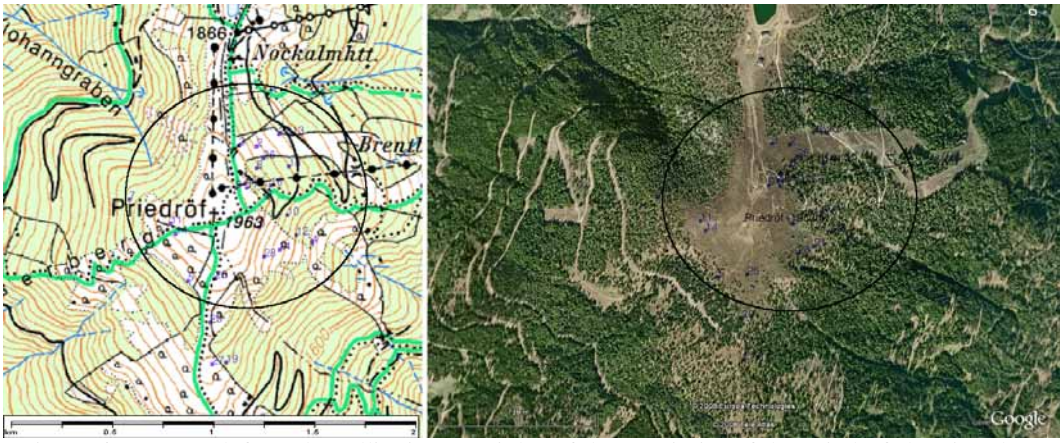

Figure 6.31: Map (left) and satellite image (right) of the proximity of the Priedröf showing the individual stroke locations

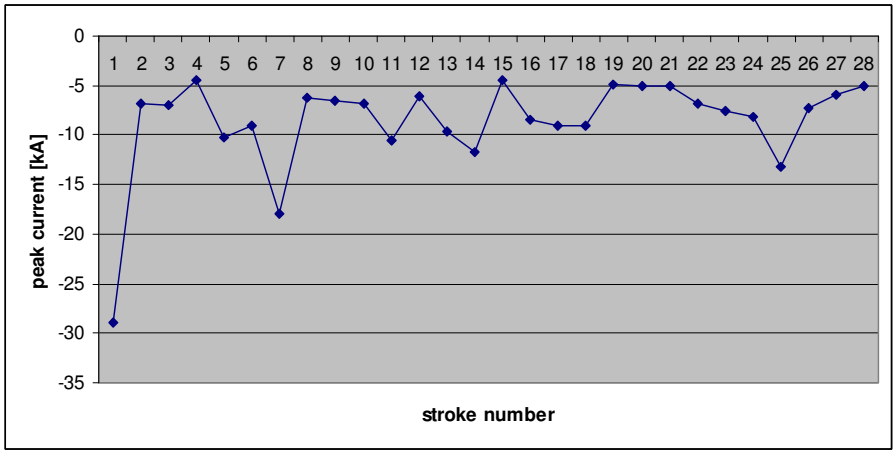

Figure 6.32: Distribution of stroke peak currents

- **Dobratsch:**
  The Dobratsch (2166 m) is the point with the highest lightning activity in Austria according to chapter 5. The radio transmitter tower which is located on the summit also triggered 20 multi-stroke flashes seen in Table 6.2, whereby 6 of these flashes are bipolar multiple-strokes.

Table 6.2: Detected multiple-stroke flashes

date	time	number of strokes	average peak current [kA]	highest peak current [kA]	stroke number of stroke with highest peak current
06.08.2003	21:40:53	30	-10.6	-17.3	12
20.06.2004	03:19:38	30	-8.3	-29.4	29
26.12.2004	13:50:54	28	-9.0	-17.8	28
16.07.2005	16:42:15	29	-12.1	-36.7	27
04.10.2006	19:10:05	33	-5.9	-14.1	27
02.07.2007	18:05:15	38	-6	-17.8	32
02.07.2007	18:06:20	34	-9.5	-20.8	28
02.07.2007	18:07:18	32	-8.0	-21.7	28
02.07.2007	18:23:33	28	-8.4	-16.9	24
02.07.2007	18:24:48	35	-6.5	-14.8	12
09.07.2007	19:07:04	43	-11.4	-66.8	23
09.07.2007	19:15:55	27	-6.7	-13.9	19
09.07.2007	19:17:12	26	-10.5	-22.4	13
09.07.2007	19:29:50	27	-5.9	-19.1	25
09.07.2007	19:31:33	37	-9.2	-23.9	32
24.07.2007	16:03:16	35	-5.6	-14.5	28
30.07.2007	06:44:09	27	-6.5	-20.9	22
18.09.2007	17:19:06	45	-7.6	-17.3	41
18.09.2007	17:49:48	28	-7.8	-23.1	26
26.09.2007	16:14:41	32	-6.3	-14.6	24

Figure 6.33 shows the stroke locations of a bipolar multiple-stroke flash that struck the tower on 9th July 2007 at 19:07. This flash had 43 strokes with an average current of -10.1 kA. The peculiarity of this lightning is stroke number 23 that had a peak current of -66.8 kA. This is the highest value in all the analysed multi-stroke flashes and in contrast to the other strokes in the flash strokes number 20 and 22 had positive polarity as shown in Figure 6.34. This flash could be a real bipolar flash because of the peak current values being greater than +10 kA.

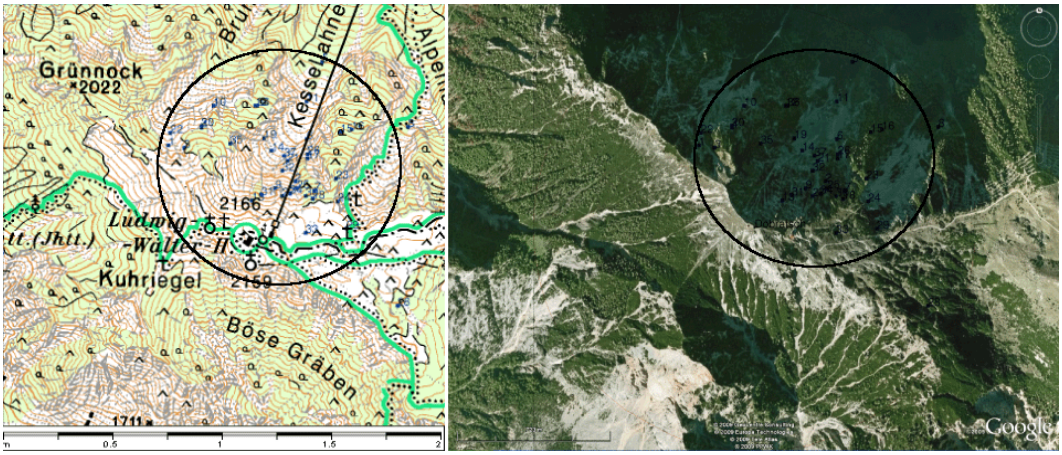

Figure 6.33: Map (left) and satellite image (right) of the proximity of the Dobratsch showing the individual stroke locations of the flash occurred on 9th July 2007 at 19:07

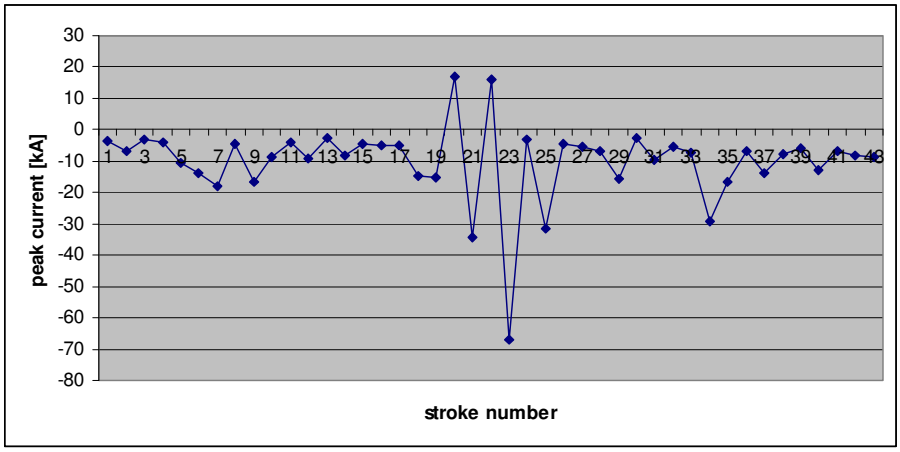

Figure 6.34: Distribution of stroke peak currents of the flash occurred on 9th July 2007 at 19:07

The pecularity of the multi-stroke flash shown in Figure 6.35 and Figure 6.36 is that this flash with 45 strokes has the highest number of strokes of all the multi-stroke flashes analysed in this thesis. The flash occurred on 18th September 2007 at 17:19 with an average peak current of -7.6 kA and with -17.3 kA stroke number 41 had the highest amplitude.

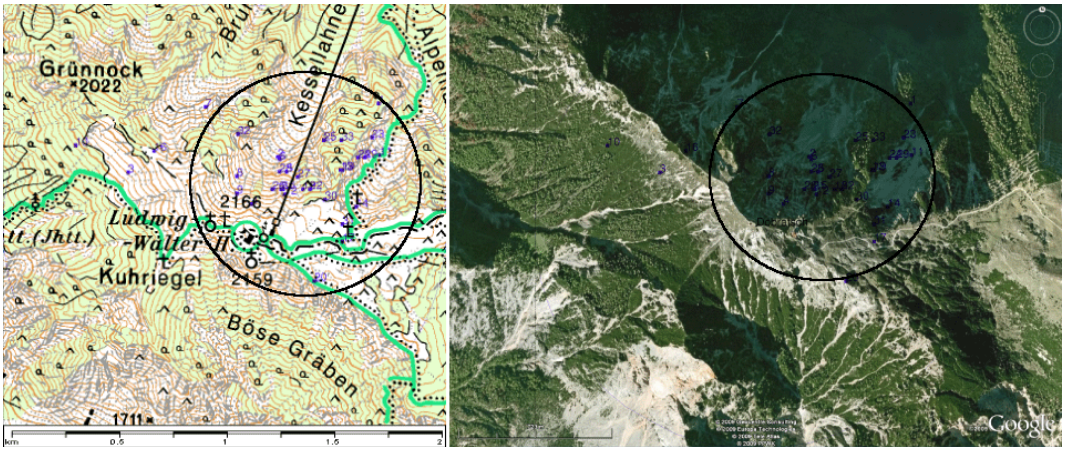

Figure 6.35: Map (left) and satellite image (right) of the proximity of the Dobratsch showing the individual stroke locations of the flash occurred on 18th September 2007 at 17:19

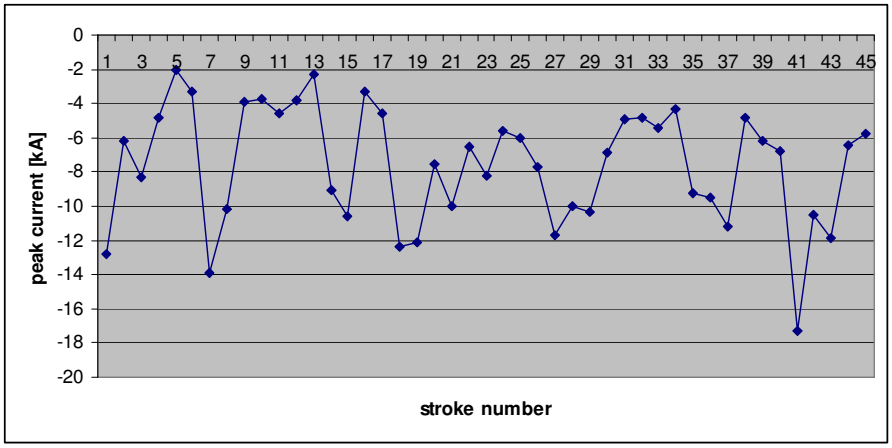

Figure 6.36: Distribution of stroke peak currents of the flash occurred on 18th September 2007 at 17:19

- **Goldeck:**
  The Goldeck is a 2142 m high mountain described in 5.7. The radio transmitter tower located on the summit is with high probability the trigger source of three multiple-stroke flashes summarized in Table 6.3.

Table 6.3: Detected multiple-stroke flashes:

date	time	number of strokes	average peak current [kA]	highest peak current [kA]	stroke number of stroke with highest peak current
02.07.2007	17:43:56	31	-6.1	-13.5	21
02.07.2007	17:53:19	31	-6.1	-14	28
02.07.2007	17:54:59	27	-6.7	-18.4	23

The stroke distribution of the 31-strokes flash on 2nd July 2007 at 17:53 is illustrated in Figure 6.37. The average peak current is -6.1 kA and the highest peak current is -14 kA. Figure 6.38 shows a comparison of the peak currents of the three multiple-stroke flashes occurred within a few minutes.

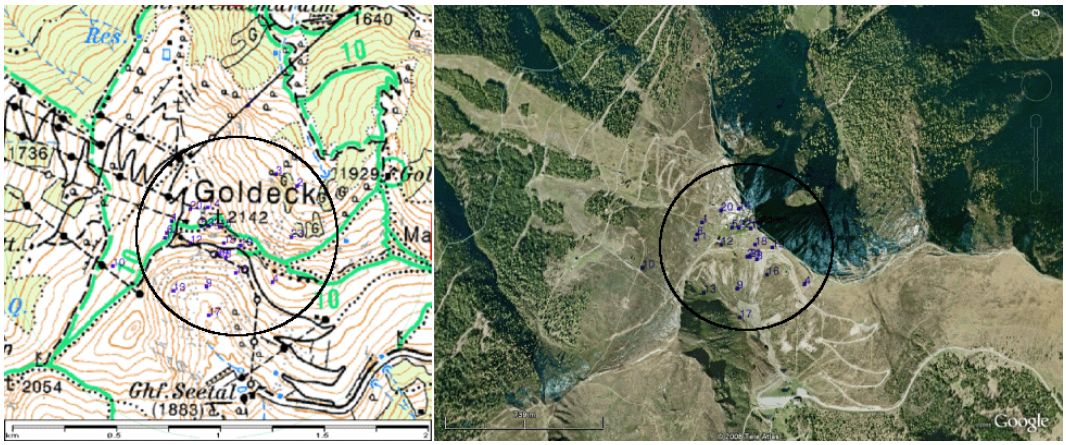

Figure 6.37: Map (left) and satellite image (right) of the proximity of the Goldeck showing the individual strokes of the flash occurred on 2nd July 2007 at 17:53:19

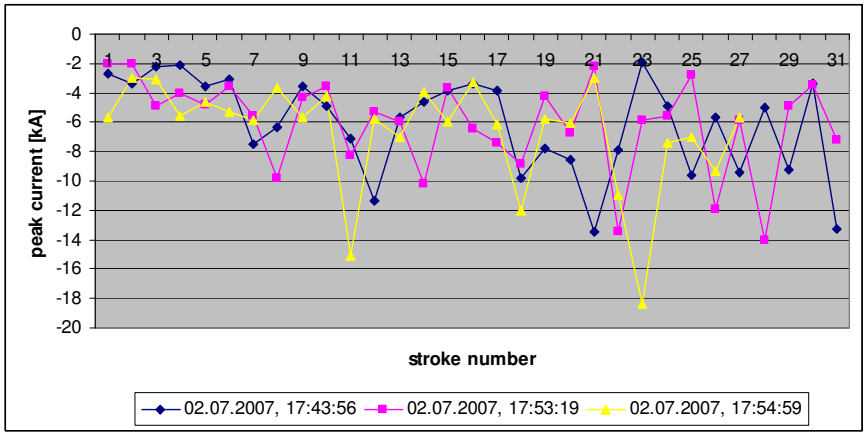

Figure 6.38: Distribution of stroke peak currents of the three multiple-stroke flashes

- **Wabnigspitz:**
  The "Wabnigspitz" is a 2773 m high summit along a ridge part of the Reißeckgruppe which is part of the Ankogelgruppe. Both mountainsides are steep stony hillsides. In the eastern proximity of the Wabnigspitz ALDIS detected a bipolar flash consisting of 26 strokes on 29th June 2006 as shown in Figure 6.39. The average peak current is -7.7 kA and the highest peak current with -44.6 kA was assigned to stroke number 1. Noteable is stroke number 5 of positive polarity (see Figure 6.40). This flash could be a real bipolar flash because of a peak current value of greater than +10 kA.

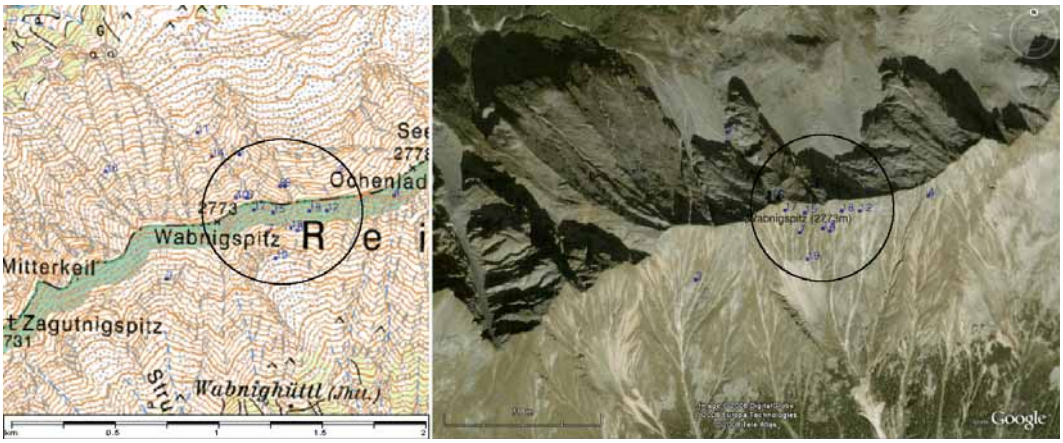

Figure 6.39: Map (left) and satellite image (right) of the proximity of the Wabnigspitz showing the individual stroke locations

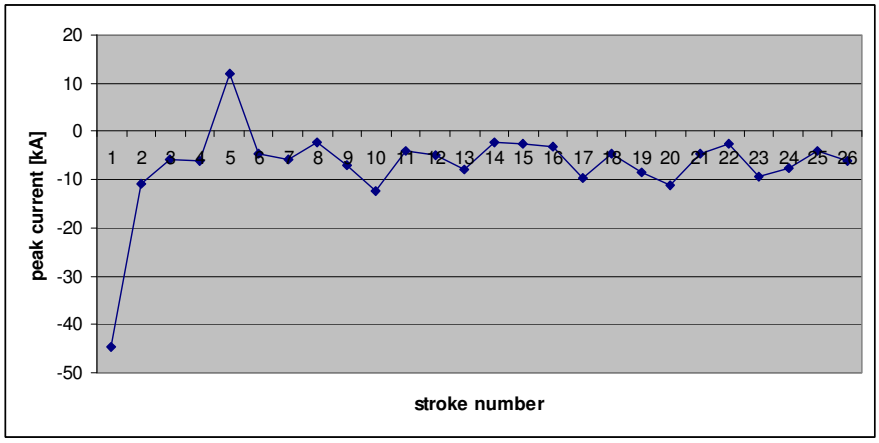

Figure 6.40: Distribution of stroke peak currents

- **Böseck:**
  The Böseck is a 2834 m high summit about 12 km west of the Wabnigspitz. In the west of the Böseck is an impounding reservoir called Oscheniksee for a hydro storage power plant and in the west is a small cottage named Böseckhütte. In the north-eastern proximity of the summit are steep hillsides where ALDIS detected a flash with 27 strokes on 18th July 2005 as shown in Figure 6.41. The average peak current is -8.2 kA and the highest peak current of -28.8 kA is assigned to stroke number 8 (see Figure 6.42).

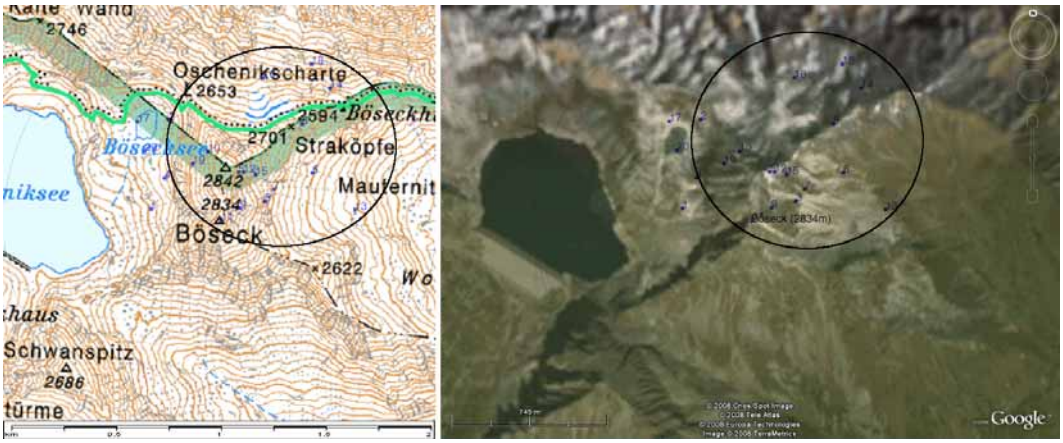

Figure 6.41: Map (left) and satellite image (right) of the proximity of the Böseck showing the individual stroke locations

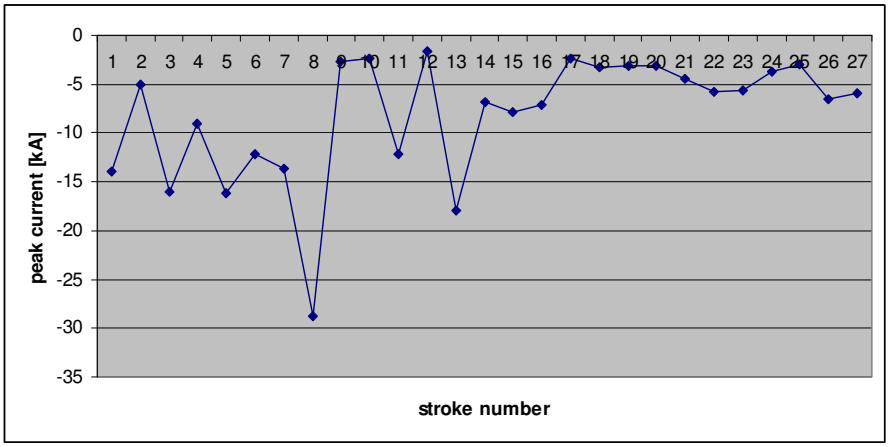

Figure 6.42: Distribution of stroke peak currents

- **Promos / Köderhöhe:**
  The Promos is a 2195 m high mountain part of the Karnische Alps as described in chapter 5.7. On a ridge about 1.5 km north-west of the Promos, in the proximity of a summit called Köderhöhe, ALDIS detected on 29th August 2003 a flash with 26 strokes as seen in Figure 6.43. Figure 6.44 shows the distribution of the strokes with an average peak current of -12.2 kA. Stroke number 1 with -41.7 kA had the highest peak current.

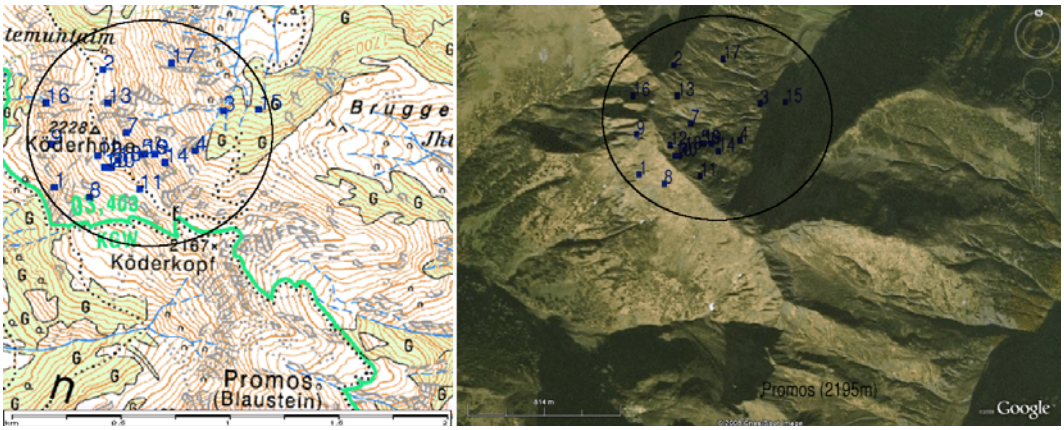

Figure 6.43: Map (left) and satellite image (right) of the northern proximity of the Promos showing the individual stroke locations

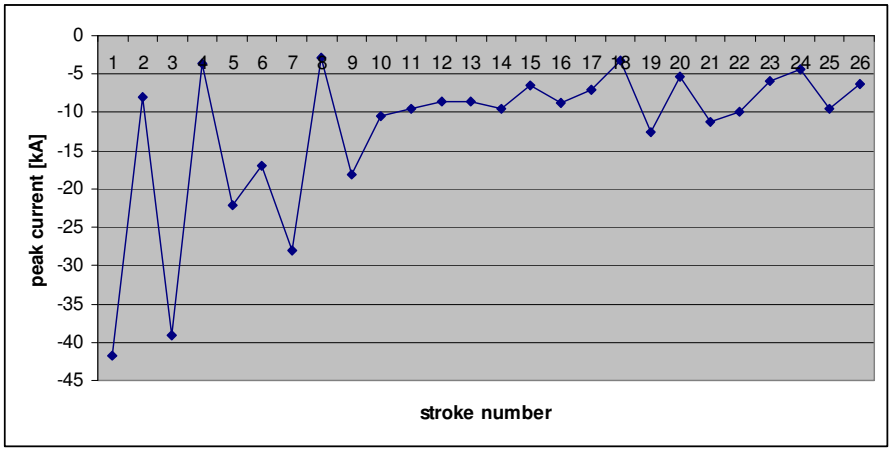

Figure 6.44: Distribution of stroke peak currents

- **Großglockner:**
  The Großglockner is with 3798 m the highest elevation in Austria. A closer description is given in chapter 5.7. On 20th June 2007 ALDIS detected a multiple-flash with 35 strokes in the proximity of that summit. The cross as well as the steep hillsides could be the trigger of that flash. The maps and the peak current distribution of the strokes are shown in Figure 6.45 and Figure 6.46, respectively. The multiple-stroke flash had a relatively small average peak current of -3.4 kA and the highest peak current of -6.6 kA (stroke number 23) is also relatively small.

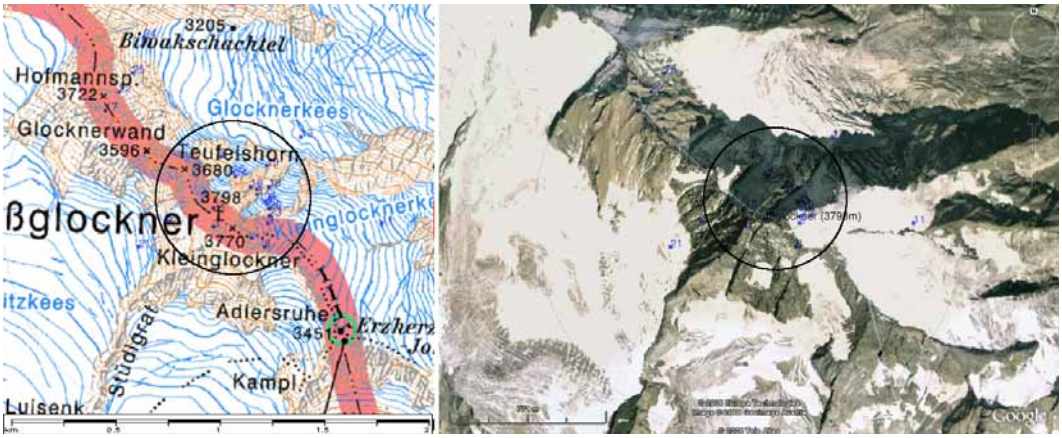

Figure 6.45: Map (left) and satellite image (right) of the proximity of the Großglockner showing the individual stroke locations

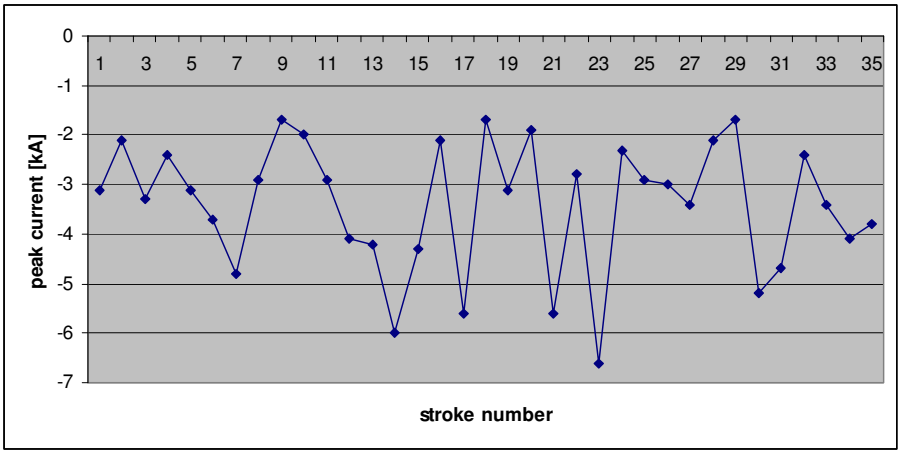

Figure 6.46: Distribution of stroke peak currents

6.6. East Tyrol

- **Alkuser Rotspitze:**
  The Alkuser Rotspitze is a 3053 m high mountain and part of the Schobergruppe. On the top of the summit is a cross and in the north-west as well as in the south-east is a ridge. The Hohe- and Niedere Prijakt, described in chapter 5.8, is only 1.5 km in the west of the Alkuser Rotspitze. On 9th July 2007 ALDIS detected in the proximity of the considered mountain a flash with 44 strokes shown in Figure 6.47. This is the second highest multiplicity of all analysed multiple-stroke flashes. The average peak current was -6.5 kA and the highest peak current exhibited stroke number 16 with -15.5 kA as shown in Figure 6.48.

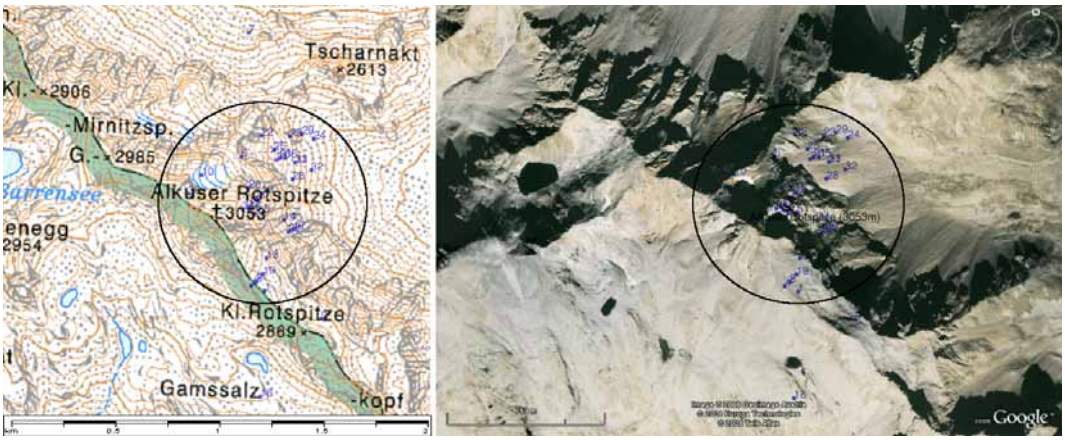

Figure 6.47: Map (left) and satellite image (right) of the proximity of the Alkuser Rotspitze showing the individual stroke locations

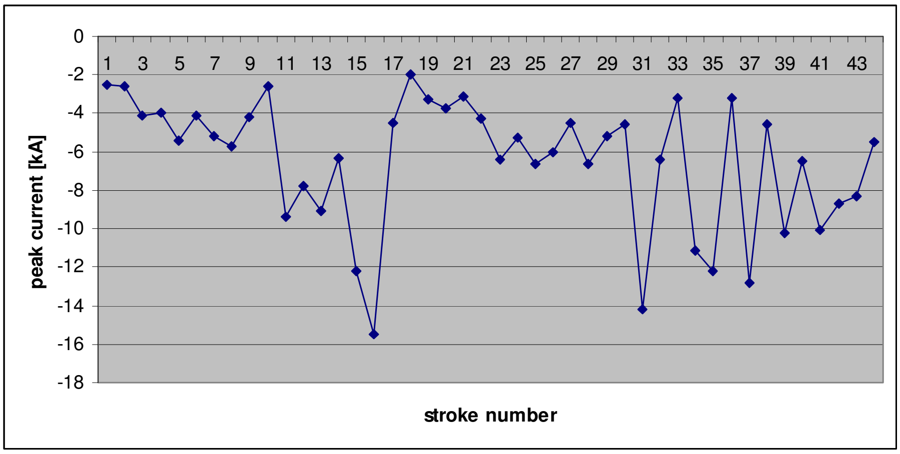

Figure 6.48: Distribution of stroke peak currents

6.7. Salzburg

- **Gaisberg:**
  The Gaisberg is a 1287 m high mountain next to the town Salzburg with a radio transmitter tower on the summit as described in detail in chapter 5.9. This tower triggered a 28 stroke flash on 16th December 2005 as illustrated in Figure 6.49. The average peak current is -10.6 kA and the highest peak current exhibited stroke number 18 with -23.1 kA as shown in Figure 6.50.

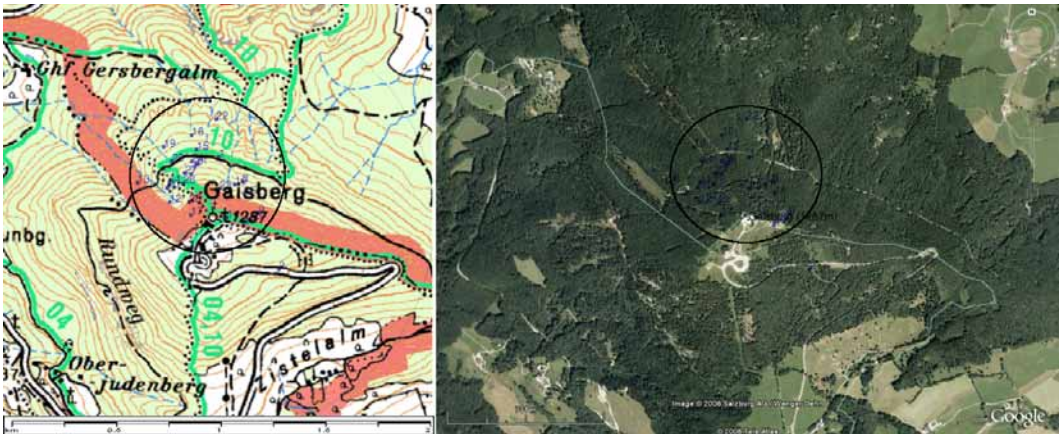

Figure 6.49: Map (left) and satellite image (right) of the proximity of the Gaisberg showing the individual stroke locations

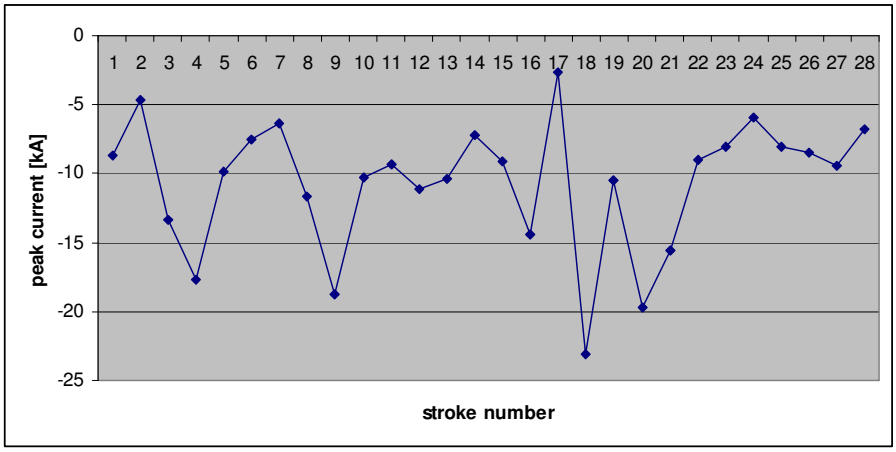

Figure 6.50: Distribution of stroke peak currents

- **Hochseiler:**
  The "Hochseiler" is a 2793 m high summit and part of the mountain massif Hochkönig about 2.5 km north-west of the highest peak also called Hochkönig. This mountain massif is about 40 km south of the town Salzburg and is part of the Berchtesgadener Alps. On the summit is a metal cross and in the surrounding steep hillsides. Both could be the trigger of the multiple stroke flash. On 13th June 2007 ALDIS detected a flash with 27 strokes in the northern proximity of the "Hochseiler" as shown in Figure 6.51. The average peak current is -2.5 kA which is, as well as the highest stroke peak current (-4.5kA of stroke number 16), a relatively small value.

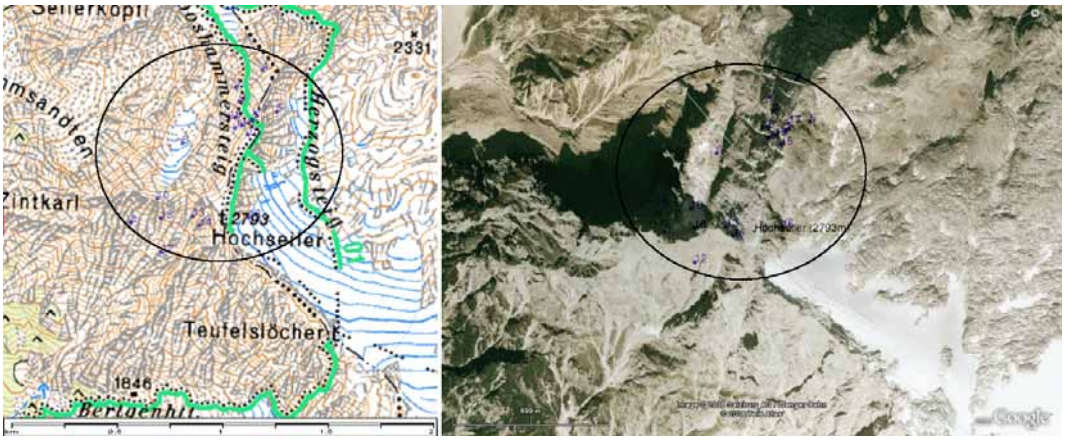

Figure 6.51: Map (left) and satellite image (right) of the proximity of the Hochseiler showing the individual stroke locations

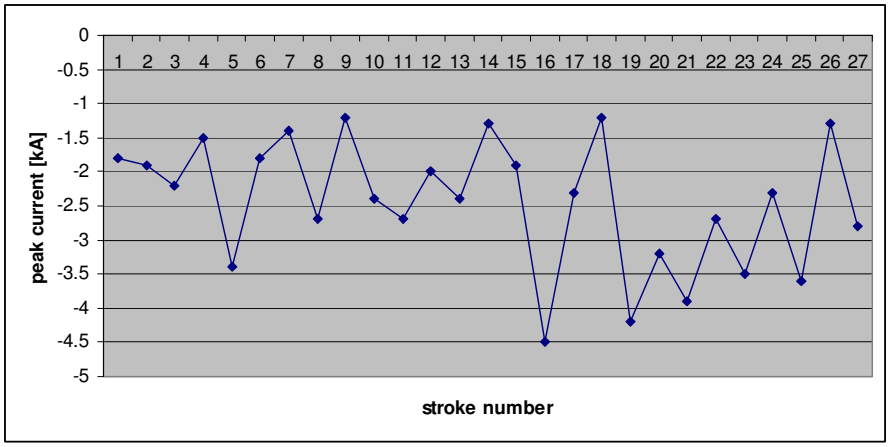

Figure 6.52: Distribution of stroke peak currents

- **Lärchkopf:**
  The "Lärchkopf" is a 1515 m high eastern foothill of the mountain massif Leoganger Steinberge which is part of the Nördliche Kalkalpen. The "Lärchkopf" is about 5 km east of the highest summit of the Leoganger Steinberger named "Birnhorn" (2634 m). On 21st June 2007 ALDIS detected a bipolar flash with 27 strokes and an average peak current of -8 kA in the western proximity of "Lärchkopf" as shown in Figure 6.53. In the proximity of that wooded area are steep stony hillsides. A tree as well as the steep hillsides could be the trigger of that flash. The highest current amplitude exhibited stroke number 4 with -29.9 kA and two of the 27 strokes showed positive polarity as seen in Figure 6.54. But peak current of both of those positive strokes were smaller than +10 kA and possibly misclassified cloud discharges.

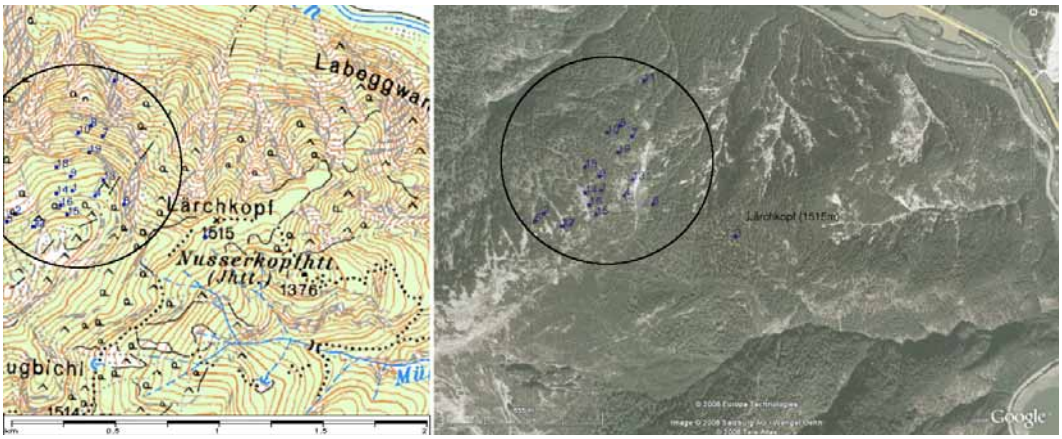

Figure 6.53: Map (left) and satellite image (right) of the proximity of the Lärchkopf showing the individual stroke locations

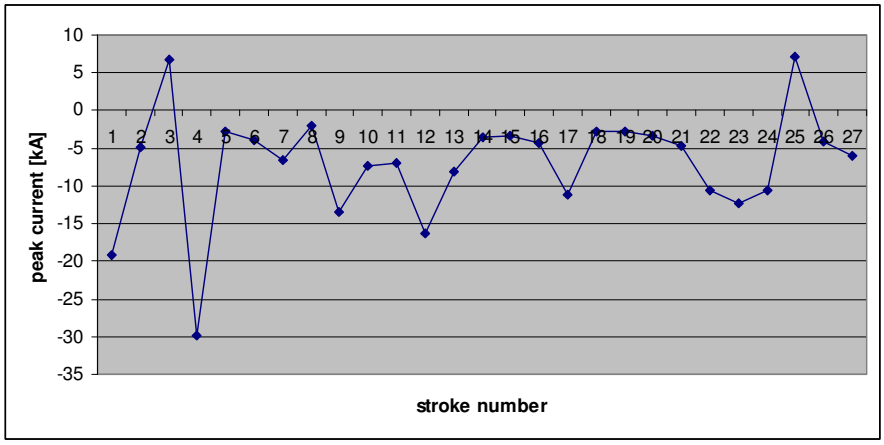

Figure 6.54: Distribution of stroke peak currents

- **Höllwand:**
  The Höllwand is a 2287 m high mountain with a cross on the top and characteristic steep hillsides about 4 km south of the village Schwarzach im Pongau. On 20th June 2007 ALDIS detected a bipolar flash with 32 strokes in the proximity of that summit as shown in Figure 6.55. The average peak current was -11.6 kA and the highest peak current exhibited stroke number 6 with -38.3 kA. Figure 6.56 shows that two strokes had opposite polarity, the characteristics of a bipolar flash. But those positive strokes were very small and probably misclassified cloud discharges.

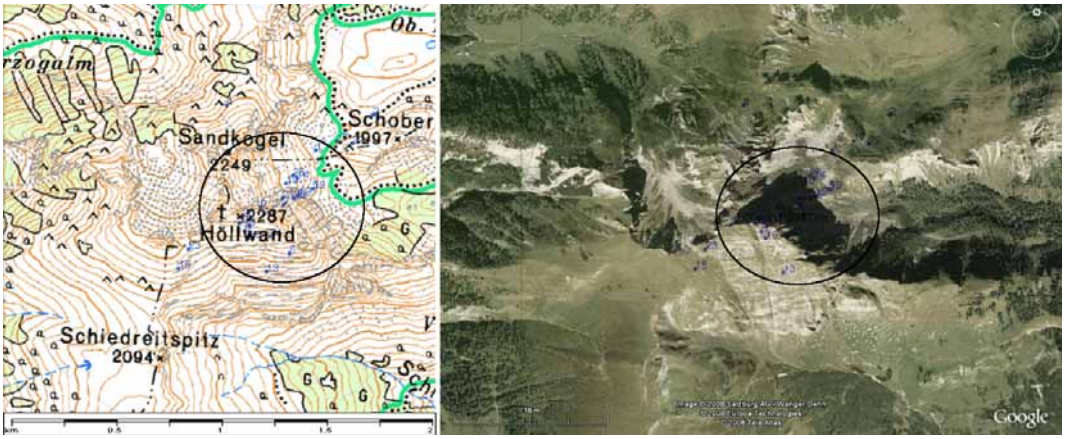

Figure 6.55: Map (left) and satellite image (right) of the proximity of the Höllwand showing the individual stroke locations

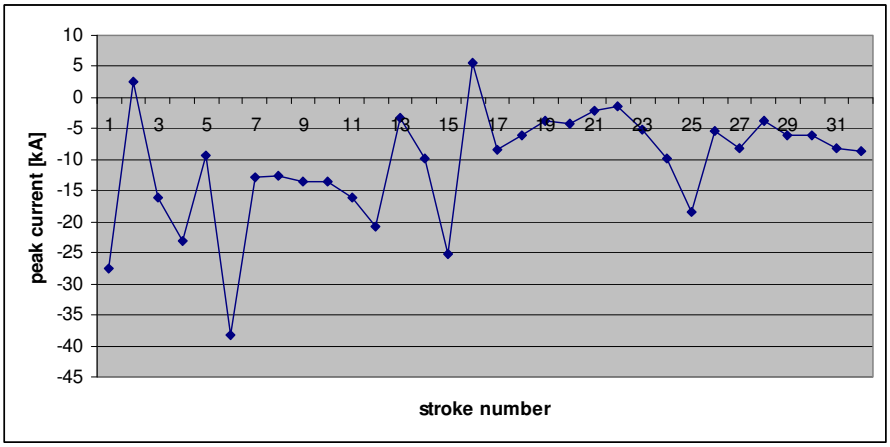

Figure 6.56: Distribution of stroke peak currents

- **Reißrachkopf:**
  The "Reißrachkopf" is a 2210 m high summit part of the ski-sport region Rauris. On the summit is a cross and a steep hillside and about 300 m east is a drag lift. One of those could have triggered that flash. On 24th June 2004 ALDIS detected a flash with a multiplicity of 28 and an average peak current of -8.2 kA in the eastern proximity of the Reißrachkopf. The highest peak current exhibited stroke number 1 with -22.9 kA.

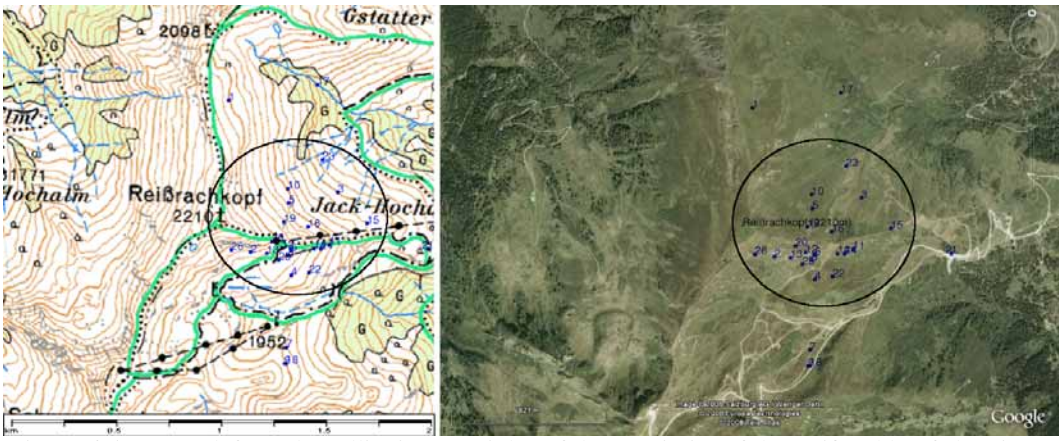

Figure 6.57: Map (left) and satellite image (right) of the proximity of the Reißrachkopf showing the individual stroke locations

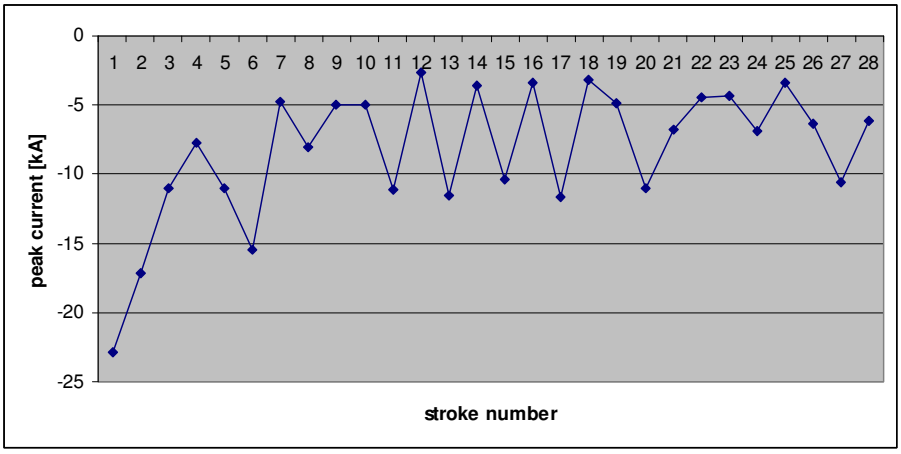

Figure 6.58: Distribution of stroke peak currents

- **Breitebenkopf:**
  The "Breitebenkopf" is a 2236 m high summit about 3.5 km south-west of the previously described "Reißrachkopf". Noteable is the cross on the top and the three ridges starting from the summit. On 21st July 2006 ALDIS detected a multiple-stroke flash in the eastern proximity of the "Breitebenkopf" as shown in Figure 6.59. This flash had a multiplicity of 28 and an average peak current of -9.3 kA. With -26.7 kA stroke number 3 had the highest peak current (see Figure 6.60).

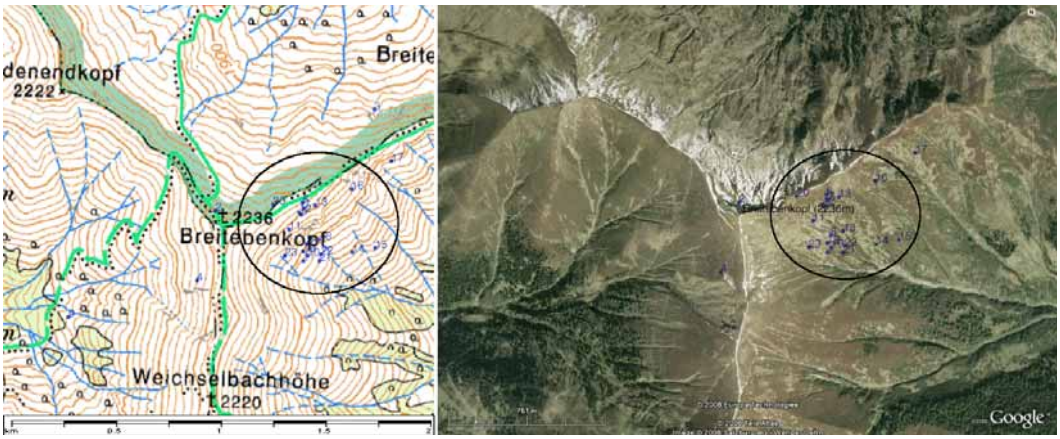

Figure 6.59: Map (left) and satellite image (right) of the proximity of the Breitebenkopf showing the individual stroke locations

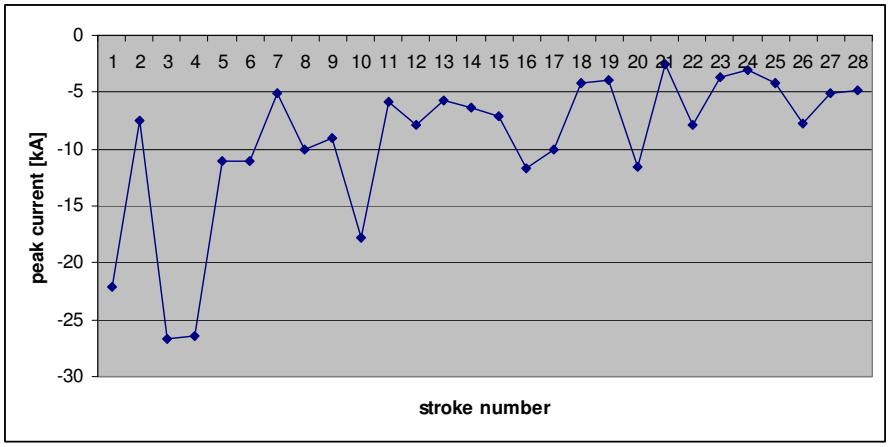

Figure 6.60: Distribution of stroke peak currents

- **Hochgolling:**
  The Hochgolling is with an altitude of 2862 m the highest summit of the mountain range Schladminger Tauern. On the top of the summit is a cross and the hillsides are steep. About 1 km north-west is a wind gap called "Gollingscharte". On 28th July 2006 ALDIS detected a bipolar flash with 26 strokes in the proximity of that wind gap as shown in Figure 6.61. The average peak current is -5.3 kA and the last stroke had the highest stroke peak current with -15.7 kA (see Figure 6.62). Figure 6.62 also shows that stroke number 11 was of opposite polarity. As this positive stroke was very small it is probably a misclassified cloud discharge.

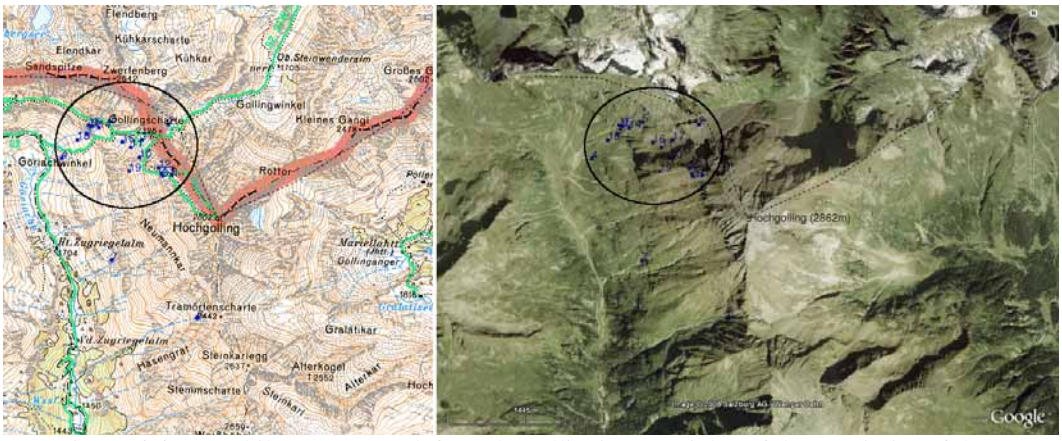

Figure 6.61: 4×4 kilometer map (left) and satellite image (right) of the proximity of the Hochgolling and the Gollingscharte showing the individual stroke locations

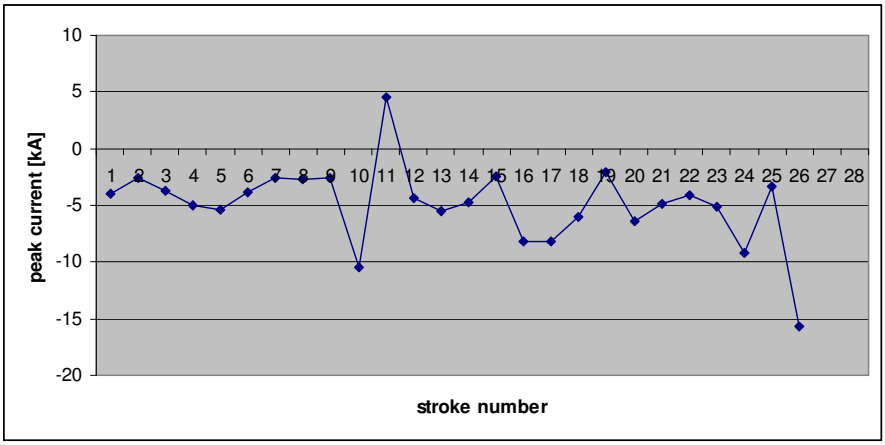

Figure 6.62: Distribution of stroke peak currents

- **Hirschwand / Himmelwand:**
  The "Hirschwand" (2099 m) and the "Himmelwand" (2055 m) are two steep rugged rocks on a wooded mountain plateau part of the Radstädter Tauern. On 25th May 2007 ALDIS detected a flash with 27 strokes and an average peak current of -8.4 kA in the proximity of those rocks as shown in Figure 6.63. With -20 kA stroke number 8 had the highest peak current as shown in Figure 6.64.

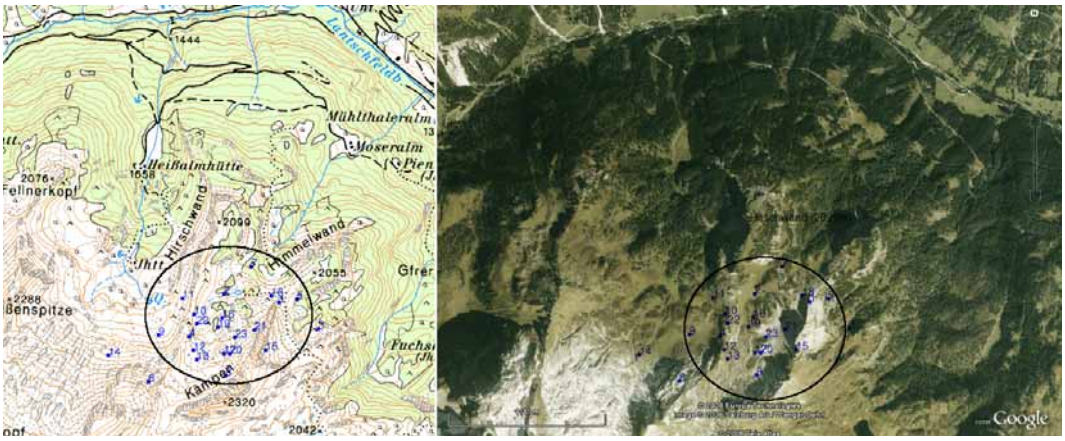

Figure 6.63: 3×3 kilometer map (left) and satellite image (right) of the proximity of the Hirschwand showing the individual stroke locations

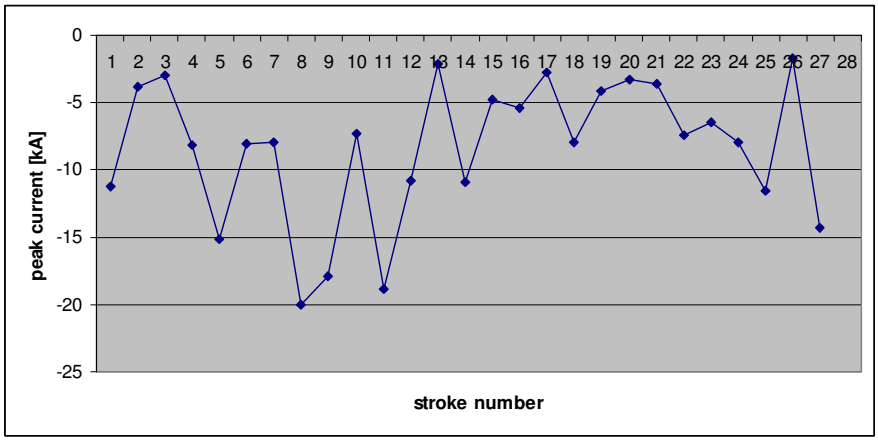

Figure 6.64: Distribution of stroke peak currents

- **Große Wiesbachhorn / Hoher Tenn:**
  On 21st July 2003 ALDIS detected a flash with 28 strokes in the surrounding of the Große Wiesbachhorn (3564 m). The first stroke was detected at this summit but the cluster of strike points of that multiple-stroke flash is about 2.5 km north at a mountain called Hoher Tenn with an altitude of 3368 m and a sharp ridge on the summit (see Figure 6.65). In the northern proximity of the Hoher Tenn is another summit called "Schneespitze" (3317 m) with a cross on the top. The detected flash had an average peak current of -6 kA and stoke number 22 exhibited the highest peak current with -13.3 kA as seen in Figure 6.66.

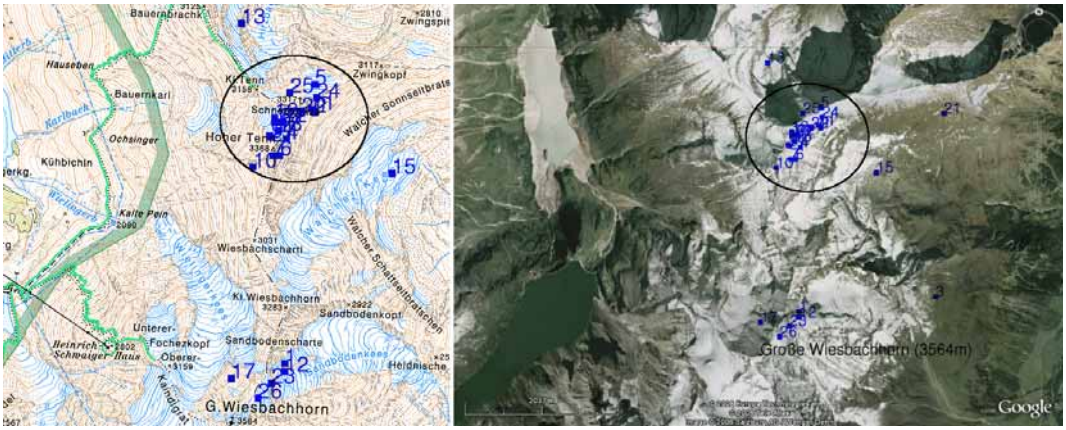

Figure 6.65: 4×4 kilometer map (left) and satellite image (right) of the proximity of the Große Wiesbachhorn and the Hoher Tenn showing the individual stroke locations

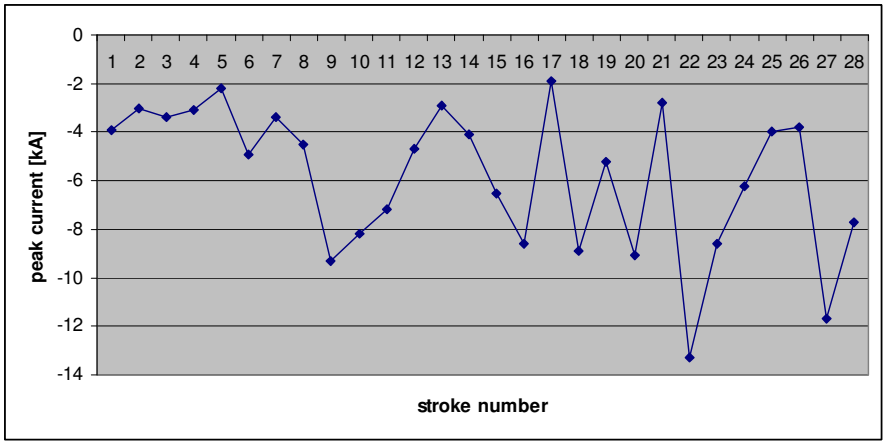

Figure 6.66: Distribution of stroke peak currents

- **Hocharn:**
  The Hocharn is a 3254 m high mountain part of the Goldberggruppe which is part of the mountain range Hohe Tauern. On 1st July 2003 ALDIS detected a flash with 28 strokes and an average peak current of -5.5 kA in the north-eastern proximity of the Hocharn as shown in Figure 6.67. Stroke number 26 exhibited with -11.2 kA the highest peak current as shown in Figure 6.68.

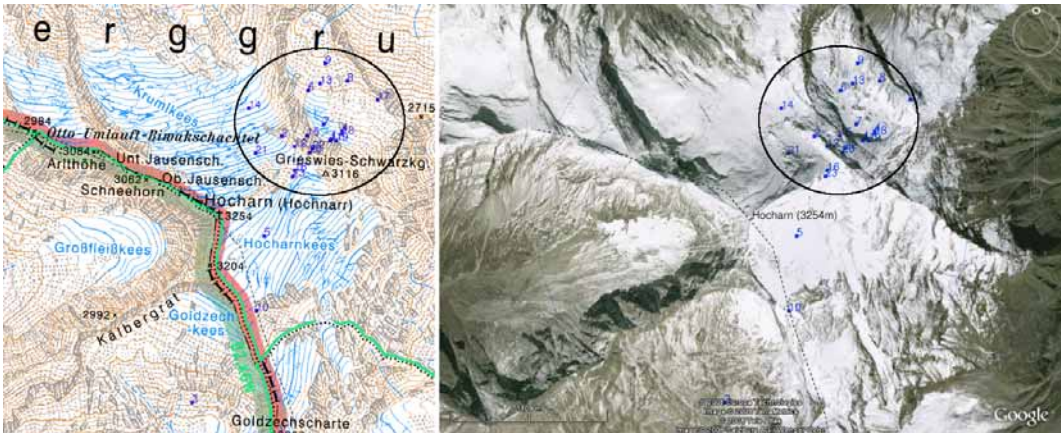

Figure 6.67: 3×3 kilometer map (left) and satellite image (right) of the proximity of the Hocharn showing the individual stroke locations

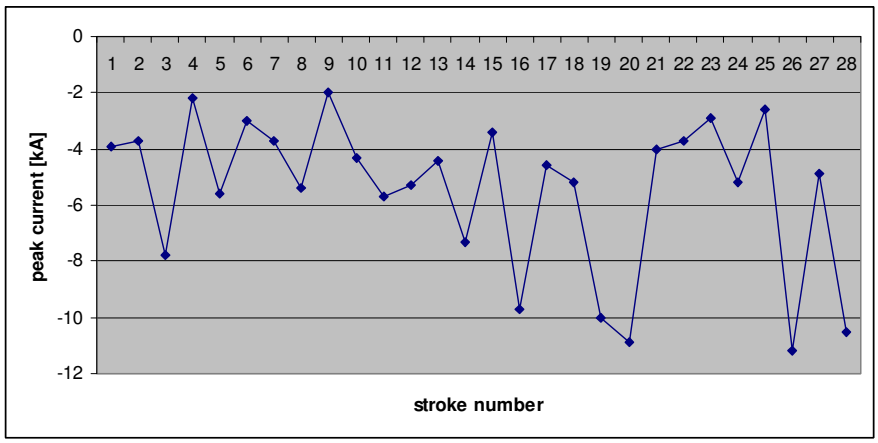

Figure 6.68: Distribution of stroke peak currents

- **Unnamed Summit 2107 m:**
  On 13th June 2007 ALDIS detected a 26 stroke flash with an average peak current of -11.3 kA in the ski-sport region Hinterglemm north-east of an unnamed summit with an altitude of 2107 m and a cross on the top. In the proximity of the stroke locations cluster are a drag lift and a shelter called Ellmau-Hochalm. Stroke number 7 with a peak current of -47.1 kA had one of the highest peak current values of all analysed multiple-stroke flashes. The most probable trigger of that flash is the local drag-lift.

Figure 6.69: Map (left) and satellite image (right) of the proximity of the unnamed summit (2107m) showing the individual stroke locations

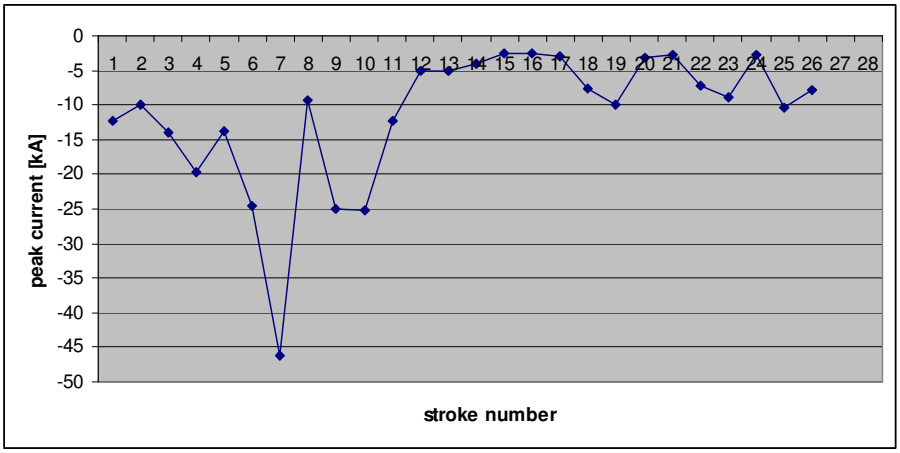

Figure 6.70: Distribution of stroke peak currents

6.8. Comparison and Conclusion

In the time interval from 2002 to 2007 a total of 55 flashes with a multiplicity greater than 25 were located by ALDIS in Austria. The flash of highest multiplicity with 45 strokes as well as the flash with multiplicity greater 25 and the highest stroke peak current of -66.8 kA occurred at the Dobratsch. Thus the Dobratsch is the most interesting area regarding multiplicity.

For the set of all analysed flashes listed in Table 6.4 the average multiplicity is 30.2 strokes per flash, the average peak currents is -8.1 kA and the average of the highest peak currents is -25 kA. Of all the detected 1662 strokes (sum over all flashes) in Table 6.4, 20 strokes (1.2%) were positive strokes as part of 13 bipolar flashes with one or maximum two positive strokes in a flash. Some of those positive strokes could be misclassified cloud discharges. The probability to be a misclassified cloud discharge for strokes with peak currents of less than +10 kA is high. All detected bipolar flashes[25], except two flashes, have positive peak currents of less than +10 kA. This is the reason of only using the negative strokes for the evaluation of the average peak current of a multiple-stroke flash. The two supposed real bipolar flashes occur at the Dobratsch (9th July.2007, 43 strokes) and the Wabnigspitz (29th June 2006, 26 strokes), respectively.

[25] The flash in the area of Mistelbach is excluded because of the ambiguity

Table 6.4 shows a summary and comparison of the detected multiple-stroke flashes including the strike location.

Table 6.4: Comparison of the individual multiple-stroke flashes

	altitude	multiplicity	date	average peak current [kA]	highest peak current [kA]	stroke number with the highest peak current	bipolar	Number of positive strokes	location properties	estimated trigger
Dobratsch	2166m	45	18.09.2007	-7.6	-17.3	41	no	0	radio transmitter tower, cable railway, chapel, shelter, cross, weather station, steep hillside	radio tower
Alkuser Rotspitze	3053m	44	09.07.2007	-6.5	-15.5	16	no	0	cross, ridge, steep hillside	cross / rock
Dobratsch	2166m	43	09.07.2007	-10.1	-66.8	23	yes	2	radio transmitter tower, cable railway, chapel, shelter, cross, weather station, steep hillside	radio tower
Dobratsch	2166m	38	02.07.2007	-5.8	-17.8	32	yes	1	radio transmitter tower, cable railway, chapel, shelter, cross, weather station, steep hillside	radio tower
Zirbitzkogel / Scharfes Eck	2364m	37	29.06.2006	-6.8	-14.7	2 and 5	no	0	weather radar station, radio transmitter tower, steep hillside	radio tower
Dobratsch	2166m	37	09.07.2007	-9.2	-23.9	32	no	0	radio transmitter tower, cable railway, chapel, shelter, cross, weather station, steep hillside	radio tower
Großer Speikkogel	2140m	36	24.09.2004	-8.8	-19.5	36	no	0	two radar stations, cross, steep hillside	radar station
Dobratsch	2166m	35	02.07.2007	-6.5	-14.8	12	no	0	radio transmitter tower, cable railway, chapel, shelter, cross, weather station, steep hillside	radio tower
Dobratsch	2166m	35	24.07.2007	-5.3	-14.5	28	yes	1	radio transmitter tower, cable railway, chapel, shelter, cross, weather station, steep hillside	radio tower
Großglockner	3798m	35	20.06.2007	-3.4	-6.6	23	no	0	cross, ridge, steep hillside	cross / rock
Dobratsch	2166m	34	02.07.2007	-9.5	-20.8	28	no	0	radio transmitter tower, cable railway, chapel, shelter, cross, weather station, steep hillside	radio tower
Dobratsch	2166m	33	04.10.2006	-5.3	-14.1	27	yes	2	radio transmitter tower, cable railway, chapel, shelter, cross, weather station, steep hillside	radio tower
Großer Speikkogel	2140m	32	04.07.2007	-5.6	-20.3	23	no	0	two radar stations, cross, steep hillside	radar station
Dobratsch	2166m	32	02.07.2007	-8	-21.7	28	no	0	radio transmitter tower, cable railway, chapel, shelter, cross, weather station, steep hillside	radio tower
Dobratsch	2166m	32	26.09.2007	-6.3	-14.6	24	no	0	radio transmitter tower, cable railway, chapel, shelter, cross, weather station, steep hillside	radio tower
Höllwand	2287m	32	20.06.2007	-10.6	-38.3	6	yes	2	cross, steep hillside	cross / rock
Goldeck	2142m	31	02.07.2007	-6.1	-13.5	21	no	0	radio transmitter tower, cross, ski lift, shelter	radio tower
Goldeck	2142m	31	02.07.2007	-6.1	-14	28	no	0	radio transmitter tower, cross, ski lift, shelter	radio tower
Sternwald I Wind Power Station	1000m	30	14.12.2003	-9	-30.7	25	no	0	wooded plateau, wind power plants	wind power turbine
Großer Speikkogel	2140m	30	24.09.2004	-8.1	-17.6	16	no	0	two radar stations, cross, steep hillside	radar station
Dobratsch	2166m	30	06.08.2003	-10.6	-17.3	12	no	0	radio transmitter tower, cable railway, chapel, shelter, cross, weather station, steep hillside	radio tower

Dobratsch	2166m	30	20.06.2004	-8.3	-29.4	29	no	0	radio transmitter tower, cable railway, chapel, shelter, cross, weather station, steep hillside	radio tower
Josefsberg / Mistelbach[26]	*257m*	*29*	*21.06.2007*		*33.7*	*2*	*yes*	*2*	*flat country, wind power plants*	wind power turbine
Lichtenberg	927m	29	11.11.2007	-8.1	-16.5	22	no	0	wooded elevation, viewing tower (20m), radio transmitter tower (156m)	radio tower
Gamsspitz	2057m	29	02.08.2007	-10.5	-40.6	12	no	0	steep hillside	rock
Dobratsch	2166m	29	16.07.2005	-12.1	-36.7	27	no	0	radio transmitter tower, cable railway, chapel, shelter, cross, weather station, steep hillside	radio tower
Schirchleralm	1321m	28	09.07.2006	-10	-36.7	6	yes	2	wooded hill	tree
Priedröf	1963m	28	14.06.2003	-8.6	-28.9	1	no	0	cross, two drag lifts	drag lift
Dobratsch	2166m	28	26.12.2004	-9	-17.8	28	no	0	radio transmitter tower, cable railway, chapel, shelter, cross, weather station, steep hillside	radio tower
Dobratsch	2166m	28	02.07.2007	-8.4	-16.9	24	no	0	radio transmitter tower, cable railway, chapel, shelter, cross, weather station, steep hillside	radio tower
Dobratsch	2166m	28	18.09.2007	-7.5	-23.1	26	yes	1	radio transmitter tower, cable railway, chapel, shelter, cross, weather station, steep hillside	radio tower
Gaisberg	1287m	28	16.12.2005	-10.6	-23.1	18	no	0	radio transmitter tower, cross, shelter	radio tower
Reißrachkopf	2210m	28	24.06.2004	-8.2	-22.9	1	no	0	cross, drag lift, steep hillside	drag lift
Breitebenkopf	2236m	28	21.07.2006	-9.3	-26.7	3	no	0	cross, ridge	cross / rock
Große Wiesbahhorn / Hoher Tenn	3368m	28	21.07.2003	-6	-13.3	22	no	0	cross, sharp ridge	cross / rock
Hocharn	3254m	28	01.07.2003	-5.5	-11.2	26	no	0	cross	rock
Sternwald I Wind Power Station	1000m	27	14.01.2004	-7.3	-15.4	12	no	0	wooded plateau, wind power plants	wind power turbine
Stuhleck	1782m	27	09.07.2007	-8.8	-21.3	11	yes	2	shelter, cross, chair lift	chair lift
Dobratsch	2166m	27	09.07.2007	-6.7	-13.9	19	no	0	radio transmitter tower, cable railway, chapel, shelter, cross, weather station, steep hillside	radio tower
Dobratsch	2166m	27	09.07.2007	-5.9	-19.1	25	no	0	radio transmitter tower, cable railway, chapel, shelter, cross, weather station, steep hillside	radio tower
Dobratsch	2166m	27	30.07.2007	-6	-20.9	22	yes	1	radio transmitter tower, cable railway, chapel, shelter, cross, weather station, steep hillside	radio tower
Goldeck	2142m	27	02.07.2007	-6.7	-18.4	23	no	0	radio transmitter tower, cross, ski lift, shelter	radio tower
Böseck	2834m	27	18.07.2005	-8.2	-28.8	8	no	0	ridge, steep hillside, lake, cottage	rock
Hochseiler	2793m	27	13.06.2007	-2.5	-4.5	16	no	0	cross, steep hillside	cross / rock
Lärchkopf	1515m	27	21.06.2007	-6.9	-29.9	4	yes	2	wooded foothill	rock
Hirschwand	2099m	27	25.05.2007	-8.4	-20	8	no	0	steep rugged rock	rock
Graz / St.Peter	377m	26	29.06.2006	-8.9	-47.5	1	no	0	urban region, church	church
Saualpe / Nameless summit	2029m	26	19.07.2004	-8.7	-16.4	9	no	0	alp with heaps of stones	heap of stones
Sapotnigofen	1474m	26	14.08.2007	-9.7	-47.3	1	no	0	wooded elevation, small village	tree
Pfannock	2254m	26	29.06.2006	-5.7	-18.1	21	no	0	cross, ridge, steep hillside	rock
Dobratsch	2166m	26	09.07.2007	-10.5	-22.4	13	no	0	radio transmitter tower, cable railway, chapel, shelter, cross, weather station, steep hillside	radio tower

[26] This flash is ambiguous as seen in chapter 6.2

Wabnigspitz	2773m	26	29.06.2006	-7	-44.6	1	yes	1	ridge, steep hillside	rock
Promos / Köderhöhe	2195m	26	29.08.2003	-12.2	-41.7	1	no	0	ridge, steep hillside	rock
Hochgolling	2862m	26	28.07.2006	-5	-15.7	26	yes	1	cross, ridge, steep hillside	rock
Unnamed summit (Hinterglemm)	2107m	26	13.06.2007	-11.3	-47.1	7	no	0	cross, drag lift	drag lift

I have tried to find out if there is a correlation between the multiplicity of a flash and the peak current of the strongest assigned stroke. A comparison between those two parameters of the individual multiple-stroke flashes, arranged according to the multiplicity value, is shown in Figure 6.71. Notable is that there is no correlation between these two parameters cognizable.

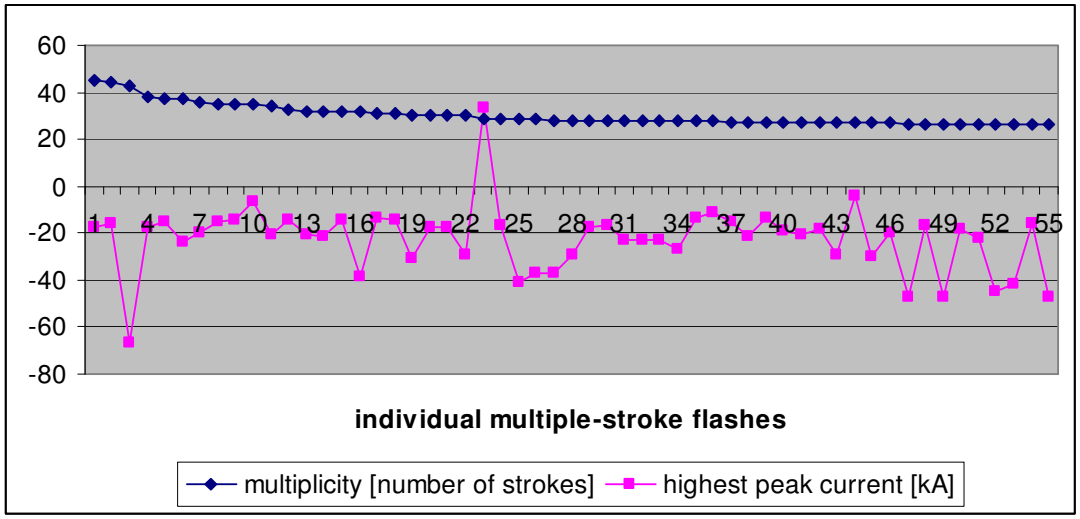

Figure 6.71: Comparison between multiplicity and belonging highest peak current

Figure 6.72 shows the distribution of the stroke peak currents of all analysed multiple stroke flashes. Clear recognizable is that the peak currents of high multiplicity flashes also follow a log normal distribution.

.

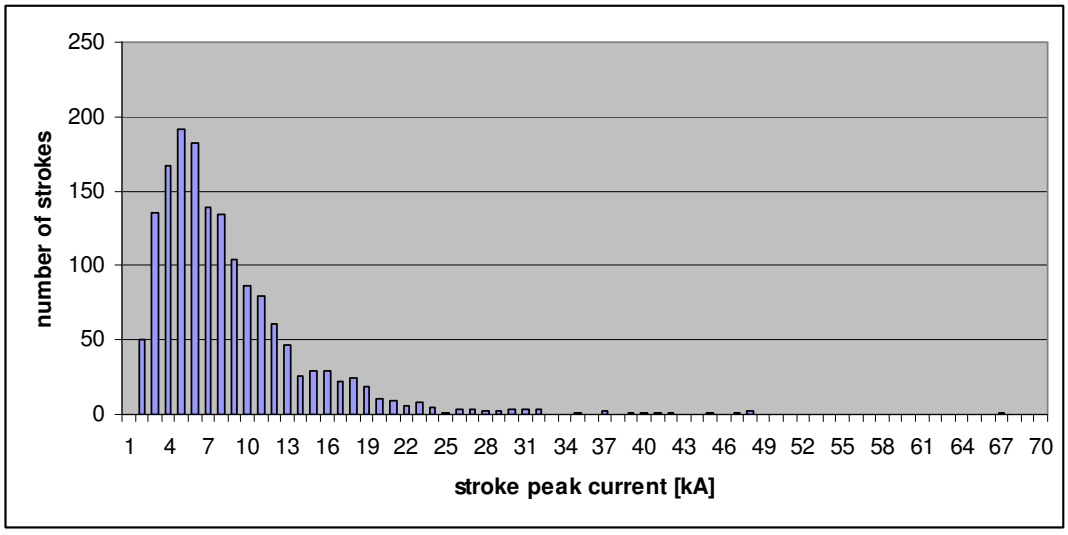

Figure 6.72: Distribution of stroke peak currents

Furthermore it is interesting to analyse the possible trigger structures of such multiple-stroke flashes. 58% of the analysed multiple-stroke flashes were detected in areas with a local radio transmitter tower, a radar station or wind turbine (category I) and 35% in mountain areas with a local cross, a ridge, a steep hillside, a shelter and/or chair/drag lift (category II). This means that only 7% (4 out of the 55 multiple-stroke flashes) were triggered by a tree, a church at ground level or other small objects like houses or even heaps of stones (category III). To those locations belong Schirchleralm, Graz/St.Peter, Saualpe/nameless summit and Sapotnigofen. The distribution is visualised in Figure 6.73. The highest multiplicities of the above described categories are given in Table 6.5.

Table 6.5: Categories

category	highest multiplicity	location
I	45	Dobratsch
II	44	Alkuser Rotspitze
III	28	Schirchleralm

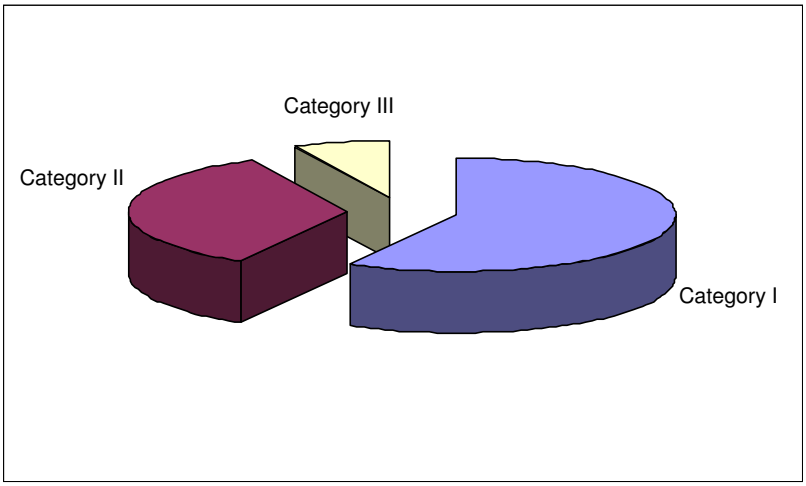

Figure 6.73: Distribution of multiple-stroke flashes regarding strike location category

In Figure 6.74 a distribution of estimated triggers of the multiple-stroke flashes under investigation is given. The top trigger are radio transmitter towers (26 flashes) followed by mountain rocks (9 flashes) and summit crosses (6 flashes). Four flashes were triggered by ski-lifts and three by radar stations and wind power turbines. Only two flashes were triggered by a tree and just one by a church and heaps of stones.

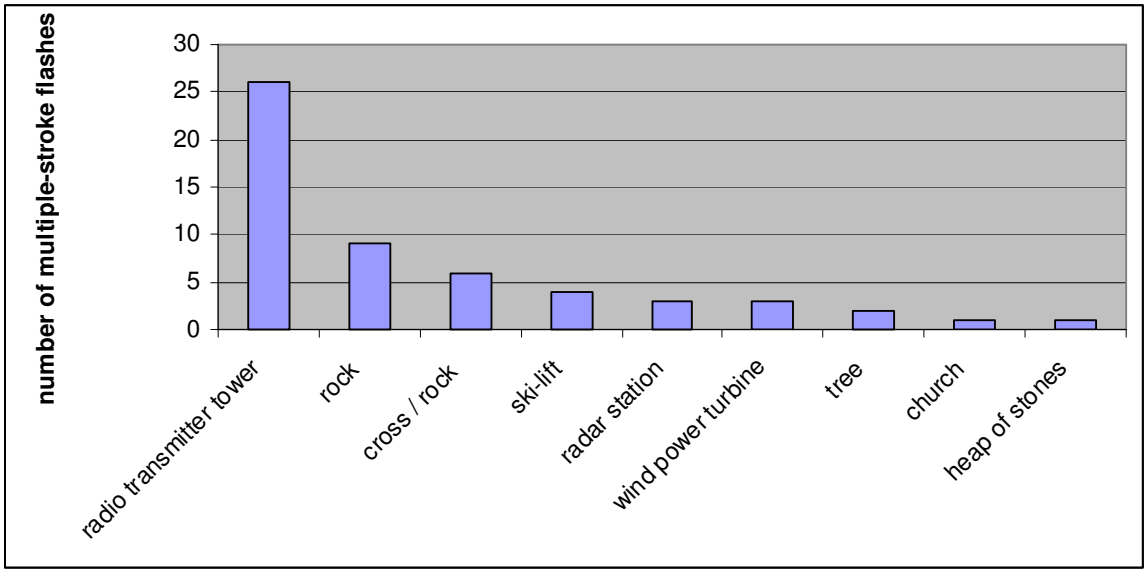

Figure 6.74: Distribution of estimated triggers of the investigated multiple-stroke flashes

Figure 6.75 shows the number of detected multiple-stroke flashes in the individual years of the time period under investigation. ALDIS detected 56% (31 of the 55) analysed flashes in the year 2007. The significant increase of the number of detected high multiplicity flashes in 2007 is probably related to an upgrade of the ALDIS LLS and the related higher detection efficiency.

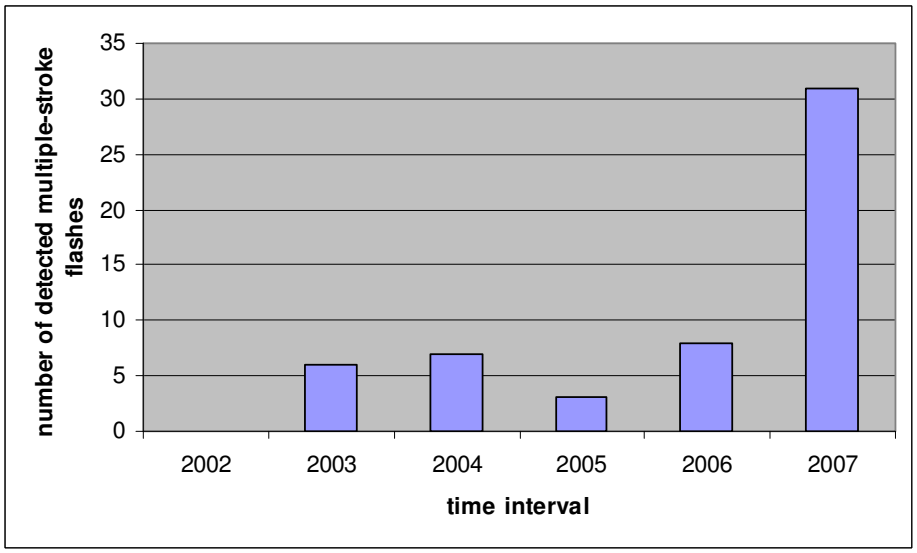

Figure 6.75: Distribution of detected multiple-stroke flashes in the individual years of the regarded time interval

A closer look on the monthly distribution of the regarded multiple-stroke flashes leads to Figure 6.76. Recognizable is, that the main activity is in summer and a smaller part in autumn. But there are also a few multiple-stroke flashes that occurred in winter thunderstorms.

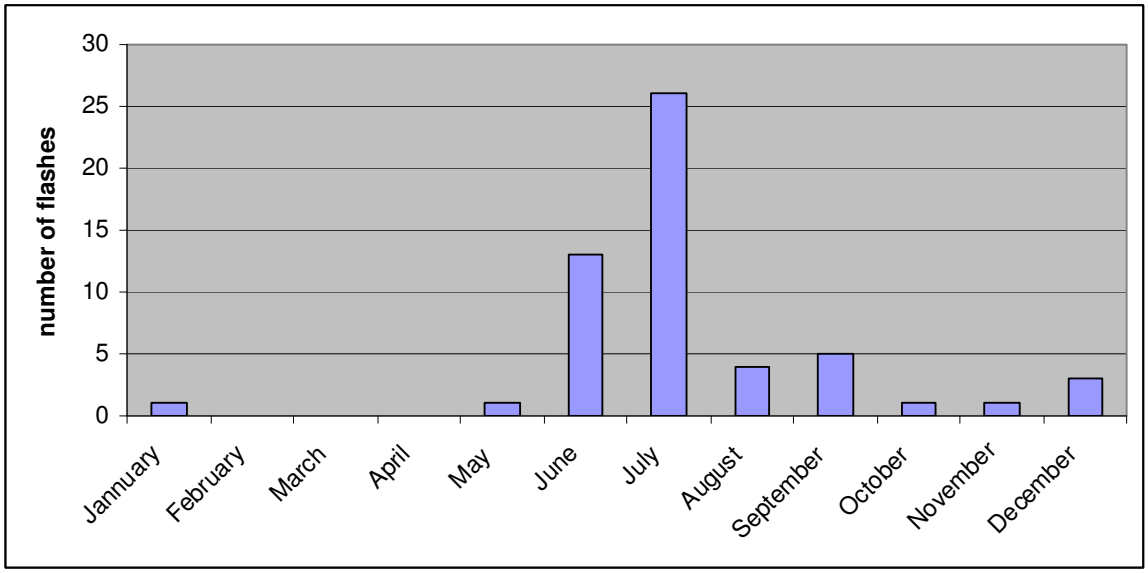

Figure 6.76: Monthly distribution of the regarded multiple-stroke flashes

7. Maximum Lightning Peak Currents

7.1. Introduction

In this chapter we make a fist attempt to examine strokes with very high peak currents in Austria and Middle Europe in the time interval between 2000 and 2007. Additionally the relation between the peak current and the number of sensors detecting the flash will be analysed. The sensors of a Lightning Location System are providing (depending on the sensor type) one (time), or two (time and angle) information for the location algorithm. The total number of measurements received by the central analyzer from all the sensors (angle and/or time) minus 3 (3 parameters are required to calculate the unknowns latitude, longitude and time) results in the value "degree of freedom" representing the amount of redundant information. The higher the degree of freedom the higher is the probability of an exact lighting detection. The problem of detecting a flash with a very high peak current is that nearby sensors will be overranged by the emitted high electromagnetic field or they send information about another peak of the complex field waveform close to the peak of the return stroke. In this first approach to select maximum peak current strokes the following measures represent the quality of a stroke detection:

- Number of sensors (should be high)
- Degree of freedom (should be high)
- χ^2 value (should be small)
- Semi major-axis of the error ellipse (should be small)

The aim of this chapter is to find the lightning stroke with the highest peak current and of sufficient high quality of detection to ensure that those amplitudes are real and not the result of any location errors. There is still some chance that the selected strokes are a result of located ionospheric reflexions or any other accidental correlations of sensor reports. A more detailed analysis of the individual flashes (e.g. reprocessing raw data, include sensor RNSS values as a quality criterion, etc.) is needed, but being outside of the scope of this thesis, to achieve a sufficient confidence in the resulting maximum peak current events.

The investigation of high peak current strokes was done for the time interval from 2000 until 2007. To visualize the information from each sensor, the program VISLOC, part of CATS software package, was used. In the plots produced by VISLOC the angle information is represented as straight-line and the time difference between two sensors as time-hyperbola.

7.2. Austria

In a first step I searched for strokes (negative and positive) with high peak current which occurred in the area of Austria and surrounding. In the given time interval 85 strokes with an absolute peak current greater than 300 kA were found. The 44 positive and 41 negative strokes with the most relevant detection parameters as amplitude [kA], date [dd.mm.yyyy], time [hh:mm:ss], number of strokes, stroke number, χ^2 value,

major-axis of the error ellipse [km], number of sensors and degree of freedom are listed in Appendix C: Maximum Lightning Currents

In Figure 7.1 the monthly distribution of detected high current strokes is given. Recognizable are the main activity from spring to autumn and the minor activity in winter. Figure 7.2 shows the distribution of detected strokes in the individual years of the regarded time interval. Notable is that the year 2005 was the year with the obviously highest number of strokes with a peak current greater than 300 kA.

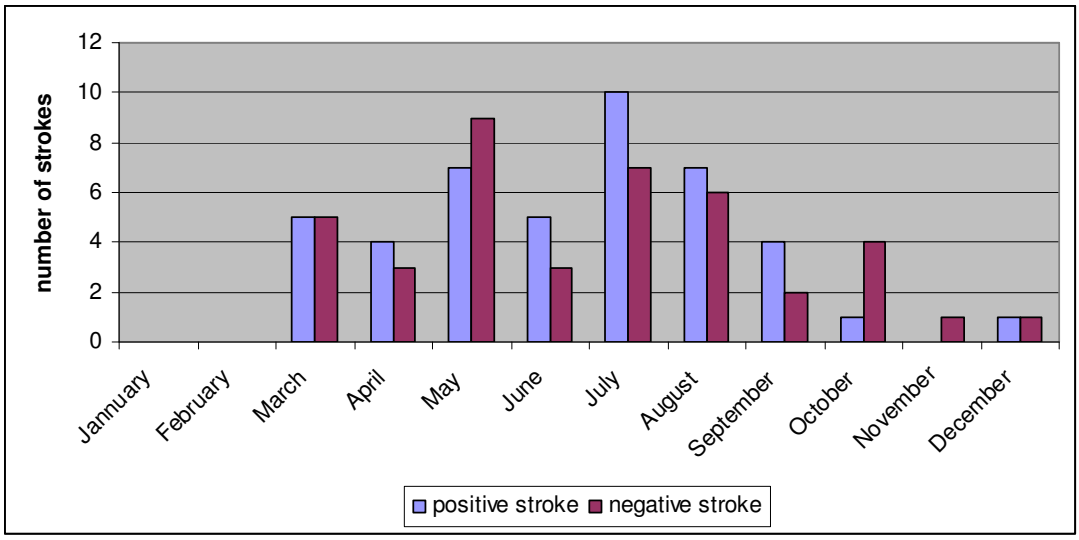

Figure 7.1: Monthly distribution of the detected high current strokes

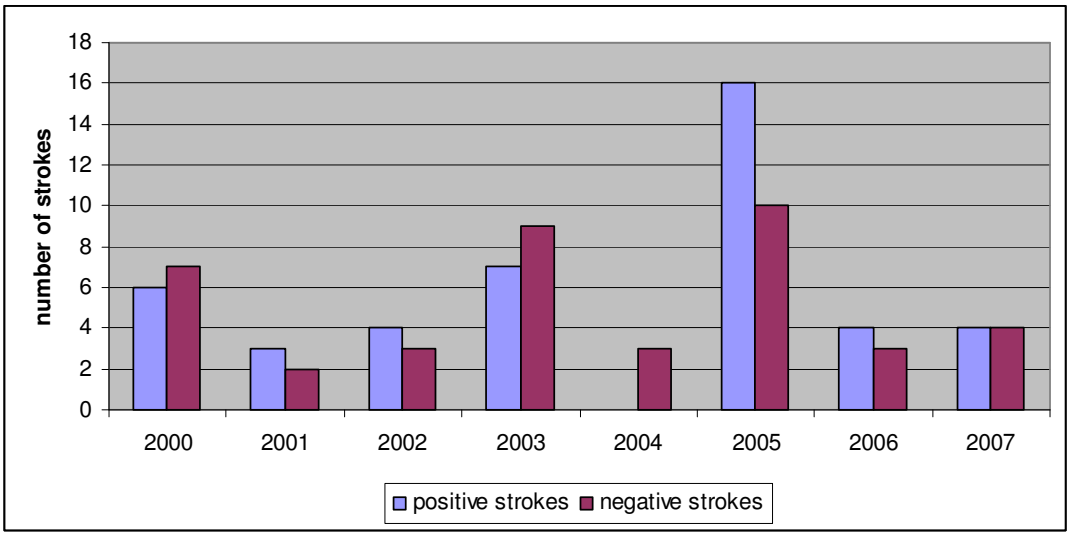

Figure 7.2: Distribution of detected high current strokes in the individual years of the regarded time interval

Based on the detection parameters and detailed analyses with the program VISLOC the following strokes have been selected as the events with the highest peak current and of sufficient location quality:

- 384.8 kA on 29th March 2005 at 16:40:10
- -385 kA on 18th August 2002 at 11:49:41

Figure 7.4 and Figure 7.5 shows the VISLOC analysis of the positive 384.8 kA stroke located about 20 km north-west of Udinese in Italy. That local area is very flat (see Figure 7.3) and the one-stroke-flash probably stroke into a tree or just to ground. The intersection of the straight lines (DF) and the hyperbolas (TOA) represent the estimated ground strike point of the high current lightning. Figure 7.5 shows only the direction to the stroke detected by the DFs without the hyperbolas. Please note that broken lines represents senor data which was removed by the detection algorithm. This stroke has been selected as a location of acceptable quality due to small values for the semi major-axis (0.3km) and χ^2 (1.2) as well as the relatively high number of sensors (12) and a degree of freedom of 12.

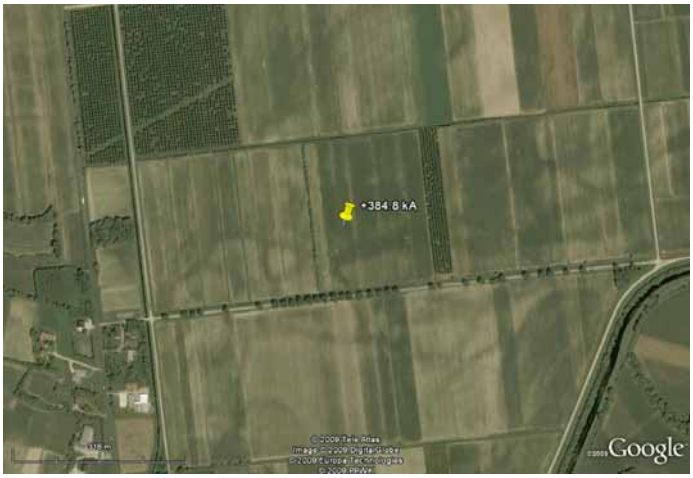

Figure 7.3: A Google Earth photography from the flat area where the +384.8 kA stroke was detected

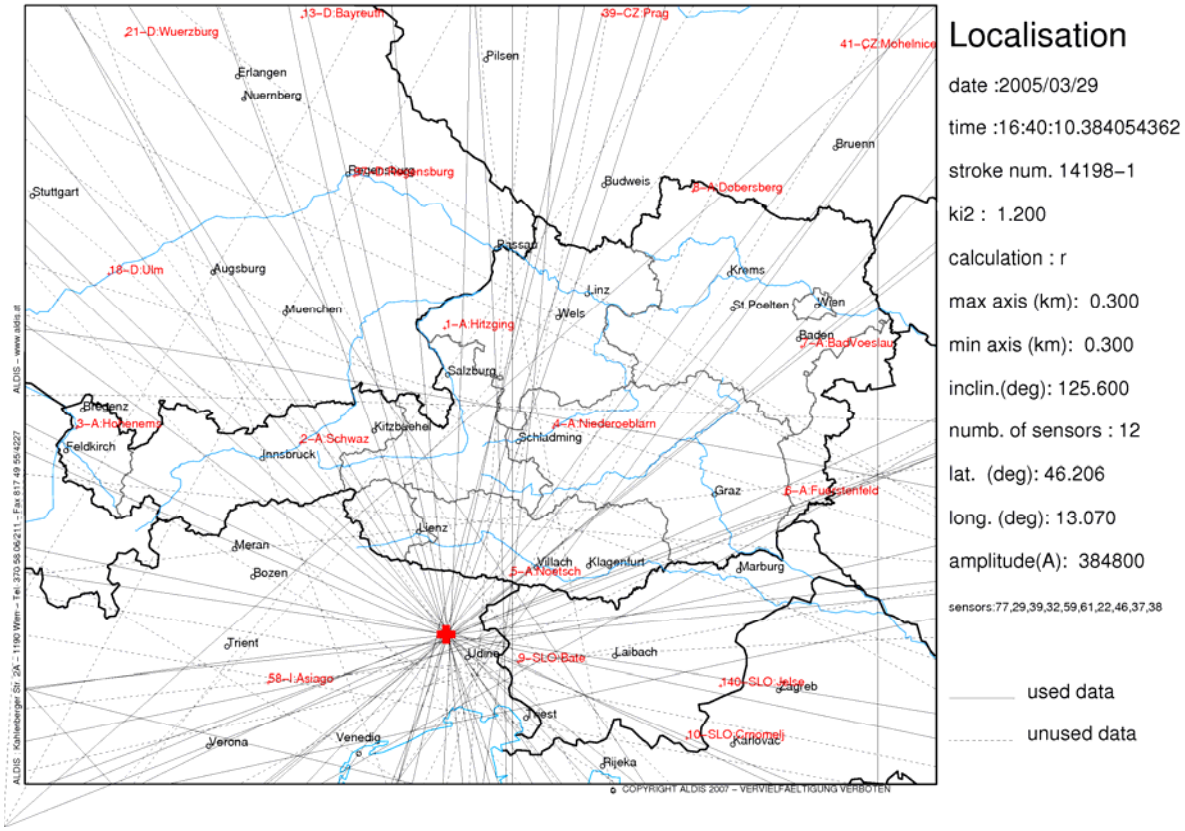

Figure 7.4: VISLOC analysis of the positive 384.8 kA stroke

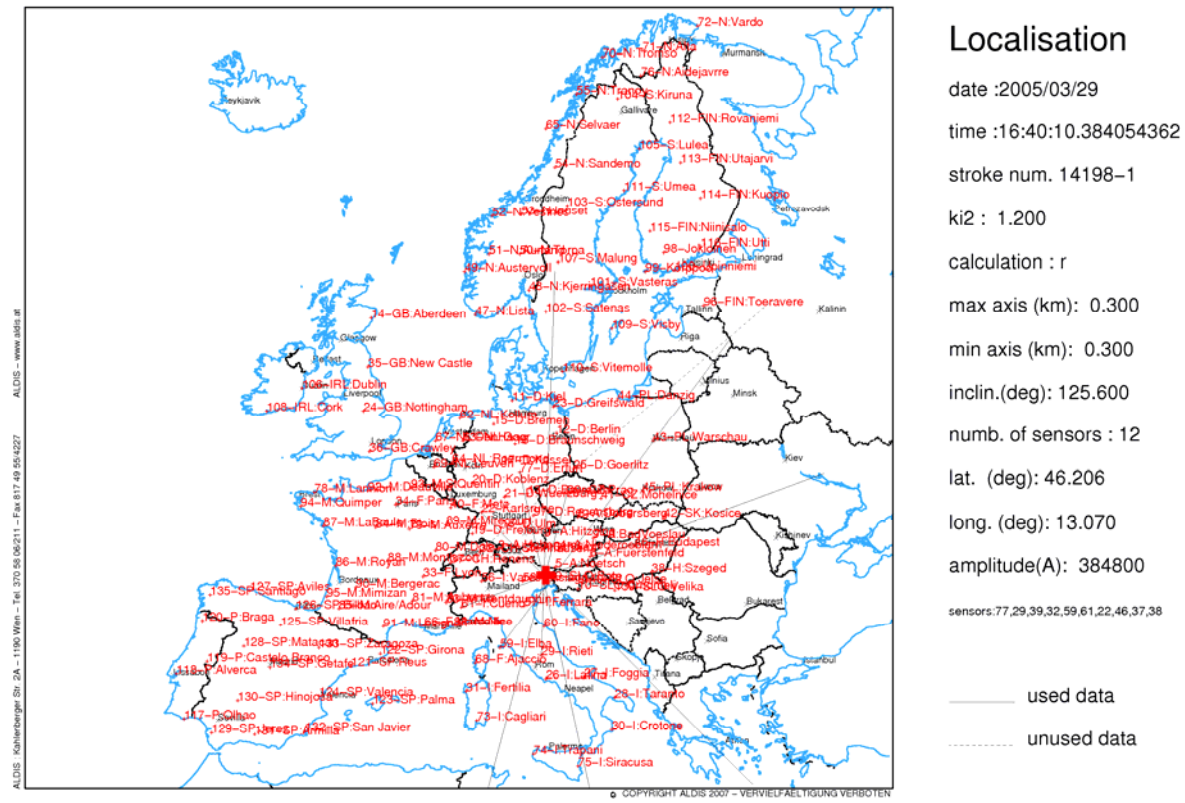

Figure 7.5: VISLOC analysis of the positive 384.8 kA stroke without plotted time-hyperbolas

The 384.8 kA stroke was detected by 12 sensors. Each of the sensors can provide only angle information, only time information or both of them. Additionally the detection algorithm will select only the sensor information needed to find the best estimation of the ground strike point. All the other information will be removed. All the sensor data used to locate the 384.8 kA stroke is shown in Table 7.1. The distance from sensor detecting the stroke to ground strike point varies from 365 km to 555 km with an average distances of about 470 km. Notable is that no sensor within a radius of 365 km around the ground strike point detected the stroke, indicating this stroke as a candidate of ionospheric reflection.

Table 7.1: Sensor data used to locate the 384.8 kA stroke

Date	time	nano	sensor number	angle [degree]	amplitude [LLP-Units]	angle information	time information	Distance to stroke location [km]
29.03.2005	16:40:10	385423541	77	167.44	2.12	X		555
29.03.2005	16:40:10	385456562	29	0.55	48.61	X	X	420
29.03.2005	16:40:10	385504722	39	176.69	50.31	X	X	435
29.03.2005	16:40:10	385526600	32	0	19.45		X	365
29.03.2005	16:40:10	385534524	59	33.89	39.13	X	X	445
29.03.2005	16:40:10	385602831	61	65.08	36.08	X	X	460
29.03.2005	16:40:10	385632395	22	126.96	67.04	X	X	470
29.03.2005	16:40:10	385635250	13	0	25.58			430
29.03.2005	16:40:10	385663750	46	0	23.59		X	480
29.03.2005	16:40:10	385672250	19	0	29.81			440
29.03.2005	16:40:10	385729000	37	0	17.98		X	500
29.03.2005	16:40:10	385863100	38	0	15.68		X	545

Figure 7.6 and Figure 7.7 shows the VISLOC analysis of the -385 kA stroke located in Styria in the proximity of a 1552 m high wooded summit called “Dirnberghöhe”. The trigger of this one-stroke-flash probably was a tree. The stroke was detected by 7 sensors and the degree of freedom equal to 7 seems acceptable. Additionally the major-axis (2.5 km) as well as the χ^2 value (1.7) is relatively small. Table 7.2 shows the sensor data used to locate the stroke. The distances from the sensor detecting the ground strike point varies from 190 km to 1050 km with an average distance of about 660 km.

Table 7.2: Sensor data of the -385kA stroke

date	time	nano	sensor number	angle [degree]	amplitude [LLP-Units]	angle information	time information	Distance to the strike point [km]
18.08.2002	11:49:41	240802000	8	199.37	-83.74	X	X	190
18.08.2002	11:49:41	241603400	25	177.26	-47.68	X	X	430
18.08.2002	11:49:41	241844500	22	112.09	-55.39	X	X	500
18.08.2002	11:49:41	241917200	77	153.3	-47			490
18.08.2002	11:49:41	242989400	11	149.02	-36.95	X	X	850
18.08.2002	11:49:41	243297800	110	177.95	-29.69		X	940
18.08.2002	11:49:41	243734200	74	6.5	-26.98	X		1050

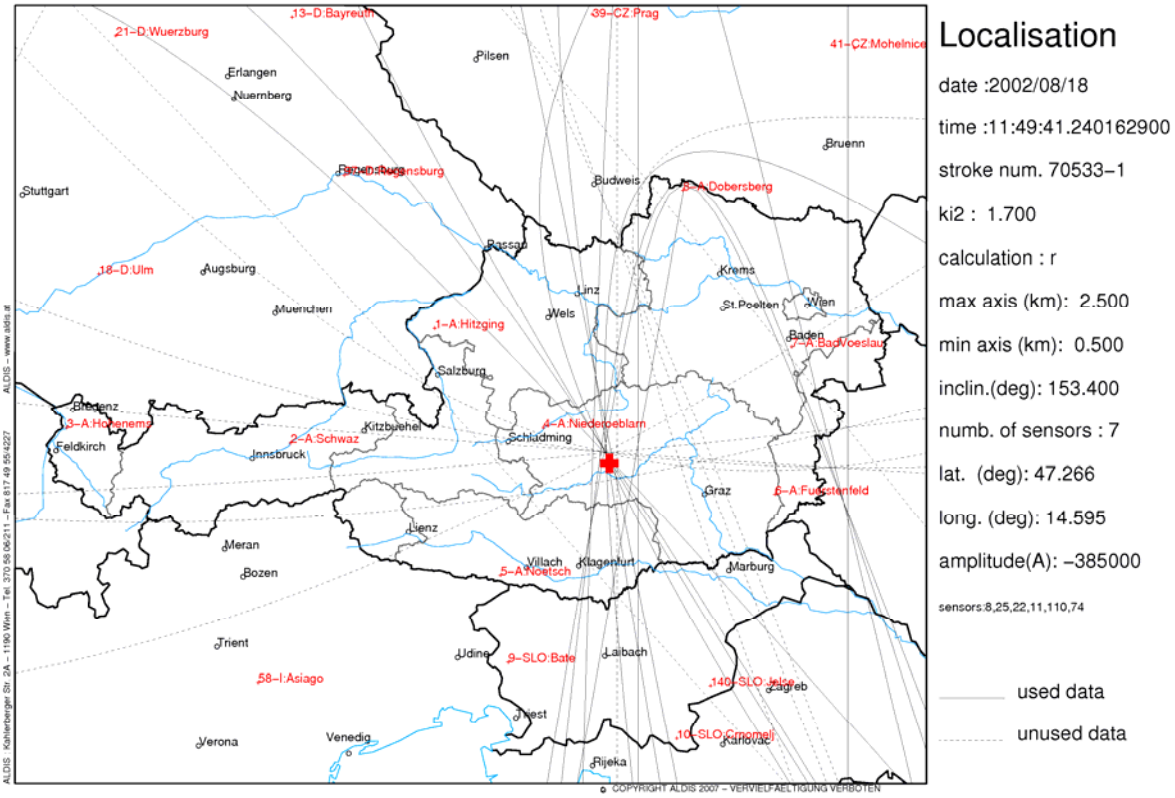

Figure 7.6: VISLOC analysis of the -385 kA stroke

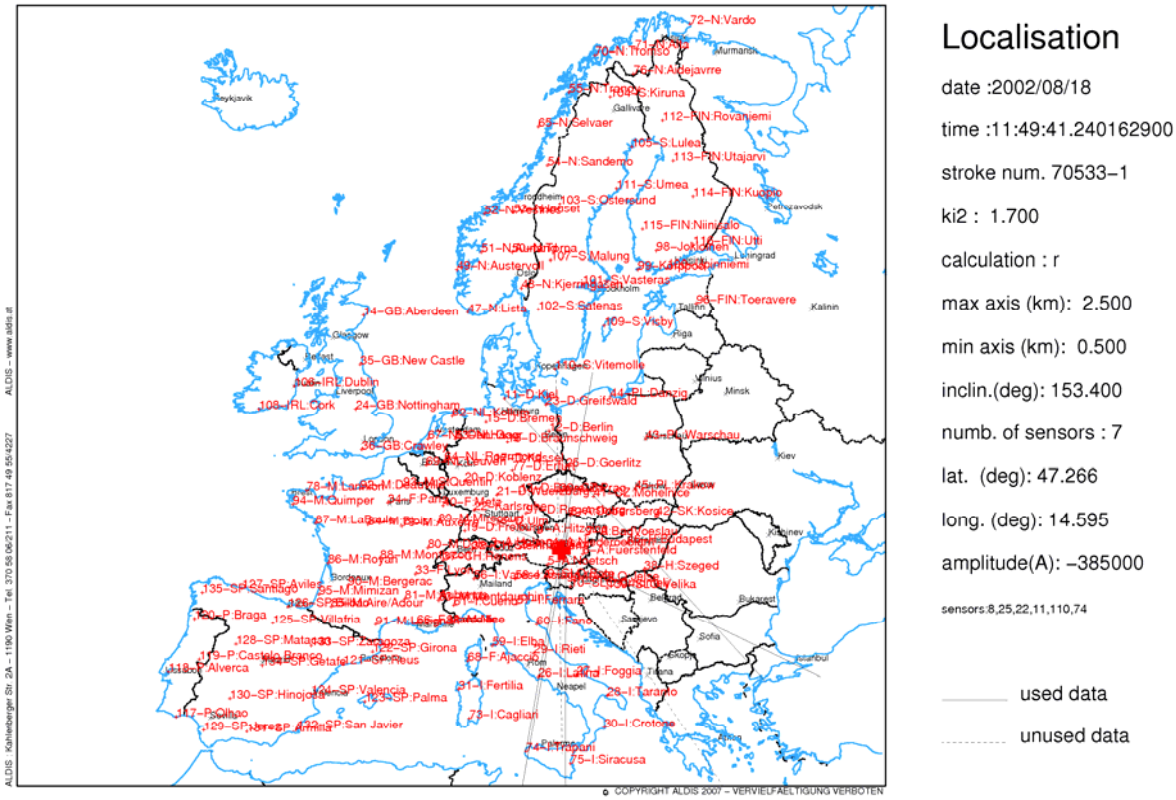

Figure 7.7: VISLOC analysis of the -385 kA stroke without plotted time-hyperbolas

7.3. Middle Europe

Next point is to find for each polarity the stroke with the highest peak current in Middle Europe. A database request resulted in 53 strokes with an absolute peak current greater than 400 kA and located in the given area at the given time interval. The 29 negative and the 25 positive strokes with the most important detection parameters are listed in Appendix C.

Based on the detection parameters and the analyses with the program VISLOC the following strokes have been selected as candidates of the highest peak current events:

- -473.1 kA on 24th October 2006 at 05:16:28
- 551.2 kA on 30th March 2005 at 16:45:59

The stroke with the highest negative peak current has an amplitude of -473.1 kA and was located in the water area of the English Channel. This stroke was detected by 26 sensors and the degree of freedom (17) is relatively high. The value of χ^2 (5.5) and the major-axis (3.8 km) are also in an acceptable range for detecting very high current strokes. Table 7.3 shows the sensor data used to detect the stroke and Figure 7.8 and Figure 7.9 show the VISLOC analyses of that stroke. The distances from sensor detecting the stroke to ground strike point varies from 560 km to 1620 km with an average distance of about 980 km. Notable is the very high average distance value of almost 1000 km.

Table 7.3: Sensor data of the -473.1kA stroke

date	time	nano	sensor number	angle [degree]	amplitude [LLP-Units]	angle information	time information	Distance to strike point [km]
24.10.2006	05:16:28	362111950	16	0	-38.06		X	560
24.10.2006	05:16:28	362302150	21	0	-22.52		X	615
24.10.2006	05:16:28	362395550	19	0	-32.88		X	645
24.10.2006	05:16:28	362432599	3	327.8	-4.15	X		785
24.10.2006	05:16:28	362604400	13	0	-24.95		X	710
24.10.2006	05:16:28	362710356	77	308.6	-6.59	X		620
24.10.2006	05:16:28	362711050	37	0	-16.7		X	740
24.10.2006	05:16:28	362794800	12	0	-26.39			770
24.10.2006	05:16:28	362844467	1	305.7	-2.94	X		910
24.10.2006	05:16:28	363299727	25	281.3	-21.6	X		885
24.10.2006	05:16:28	363323688	4	305.4	-0.99	X		1010
24.10.2006	05:16:28	363371133	9	295.9	-1.56	X		1100
24.10.2006	05:16:28	363420128	7	271.1	-1.59	X		1115
24.10.2006	05:16:28	363571405	5	282.4	-1.63	X		1060
24.10.2006	05:16:28	363598300	66	0	-3.24			1040
24.10.2006	05:16:28	363620996	101	236	-2.57	X		1180
24.10.2006	05:16:28	363678812	6	280.5	-2.92	X		1165
24.10.2006	05:16:28	363883137	125	356.7	-3.1	X		1225
24.10.2006	05:16:28	363947987	59	331.9	-3.08	X		1240
24.10.2006	05:16:28	363988995	60	328.9	-3.28	X		1250
24.10.2006	05:16:28	364233851	109	249.9	-10.28	X		1160
24.10.2006	05:16:28	364308950	45	0	-2.48			1250
24.10.2006	05:16:28	364362050	43	0	-5.5			1270
24.10.2006	05:16:28	364800800	42	0	-4.26			1400
24.10.2006	05:16:28	365005600	38	0	-2.99			1465
24.10.2006	05:16:28	365091681	111	227.2	-1.73	X		1620

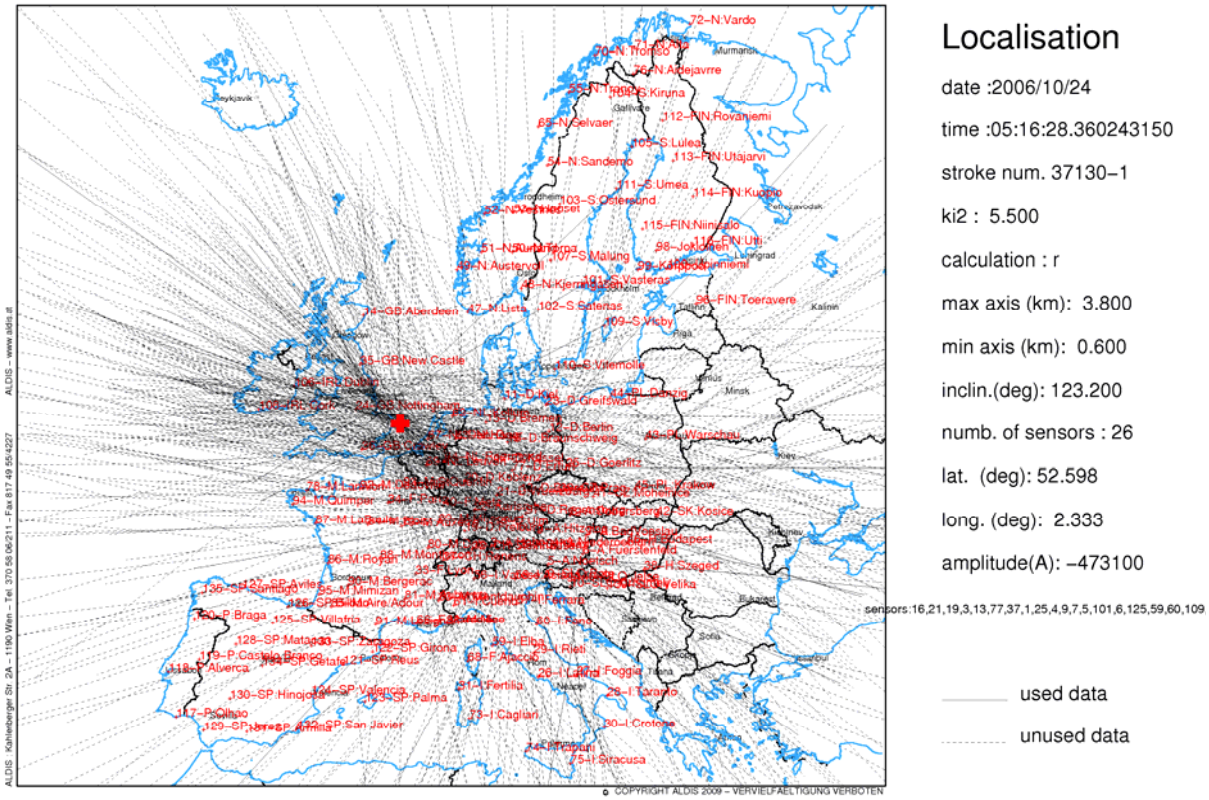

Figure 7.8: VISLOC analysis of the -473.1 kA stroke

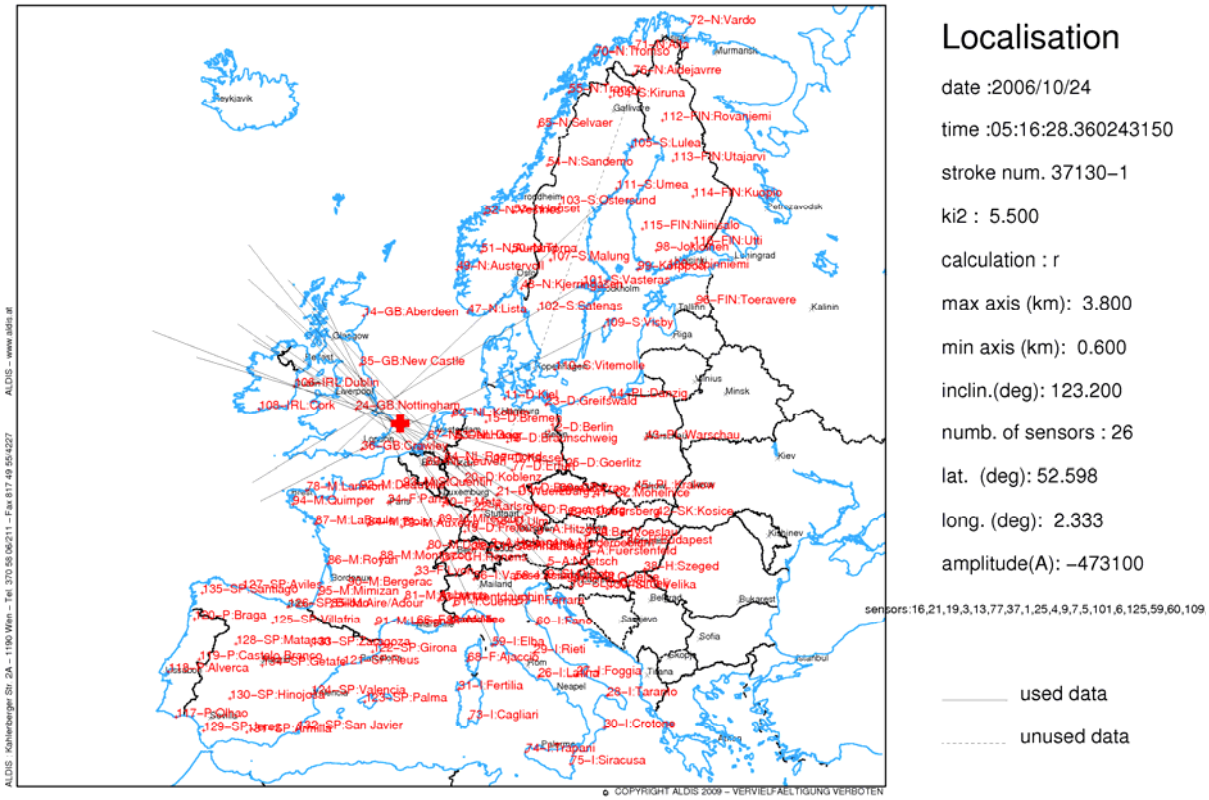

Figure 7.9: VISLOC analysis of the -473.1 kA stroke without plotted time-hyperbolas

The stroke with the highest positive peak current has an amplitude of 551.2 kA and was located about 25 km north-east of the city Parma in Italy. The proximity of the detected ground strike point is flat with a few villages in the surrounding (see Figure 7.10). Trigger of the stroke could be a tree, a house of just the earth. This stroke was detected by 11 sensors and the degree of freedom is 5. Additionally the χ^2 value (2.4) as well as the major-axis (0.8 km) are acceptable small. Table 7.4 shows the sensor data used to locate that stroke and Figure 7.11 shows the VISLOC analyses of the given stroke. The distances from sensor detecting the stroke to ground strike point varies from 350 km to 1500 km with an average distance of about 710 km.

Figure 7.10: A Google Earth photography from the flat area where the +551.2 kA stroke was detected

Table 7.4: Sensor data of the 551.2kA stroke

date	time	nano	sensor number	angle [degree]	amplitude [LLP-Units]	angle information	time information	Distance to strike point [km]
30.03.2005	16:45:59	43485164	73	70.03	2.59			645
30.03.2005	16:45:59	44958300	37	0	39.16		X	350
30.03.2005	16:45:59	45275092	1	210.38	89.25			395
30.03.2005	16:45:59	45579450	21	0	25.14		X	535
30.03.2005	16:45:59	45654700	13	0	31.11		X	560
30.03.2005	16:45:59	45910700	20	0	29.6		X	630
30.03.2005	16:45:59	46032428	39	187.27	82.58	X		635
30.03.2005	16:45:59	46113729	109	205.58	1.46	X		1500
30.03.2005	16:45:59	46194050	46	0	20.72		X	720
30.03.2005	16:45:59	46343900	38	0	1.39		X	770
30.03.2005	16:45:59	46459197	25	201.16	82.06			760

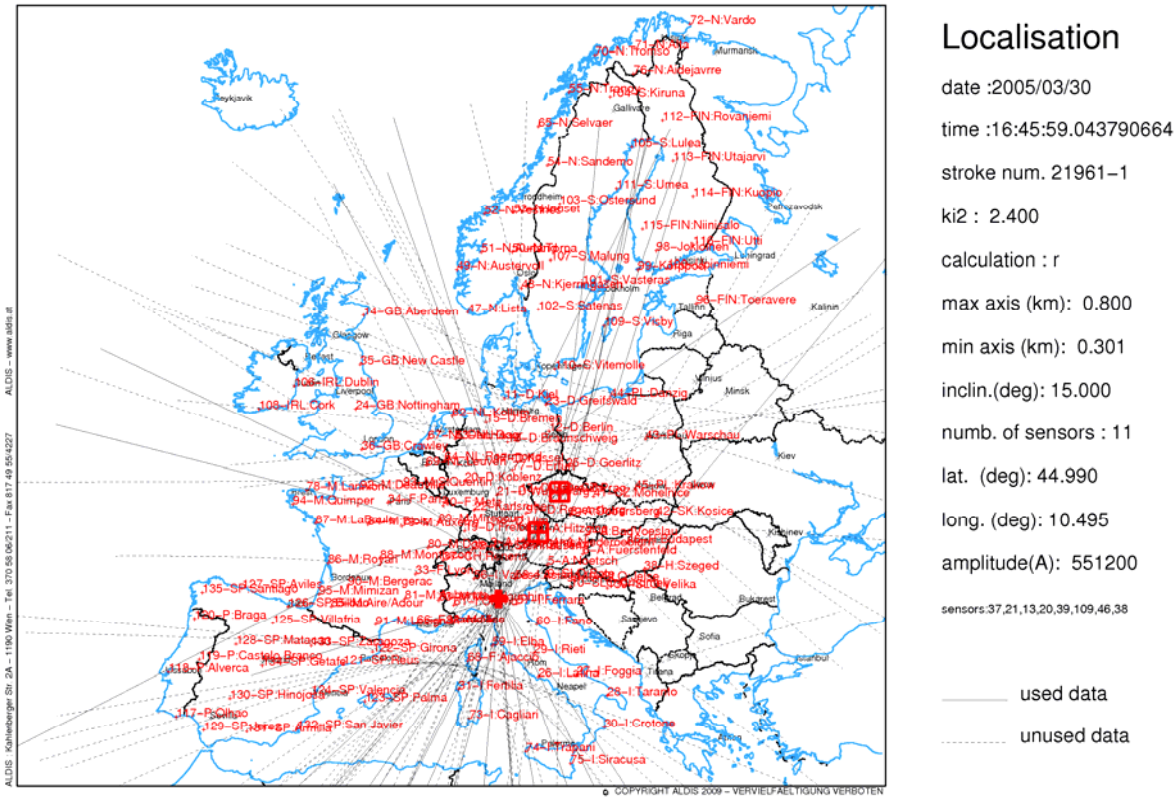

Figure 7.11: VISLOC analysis of the 551.2 kA stroke

An interesting point is to visualize the distribution of the strokes with a peak current greater than 200 kA that occurred in the time interval between 2000 and 2007 in Middle Europe (see Figure 7.12). In that figure we can see the confirmation of the theory that the higher the peak current of a stroke, in this range of peak currents, the smaller is the probability of occurrence. The distribution represents the decreasing part (tail) of a log normal distribution.

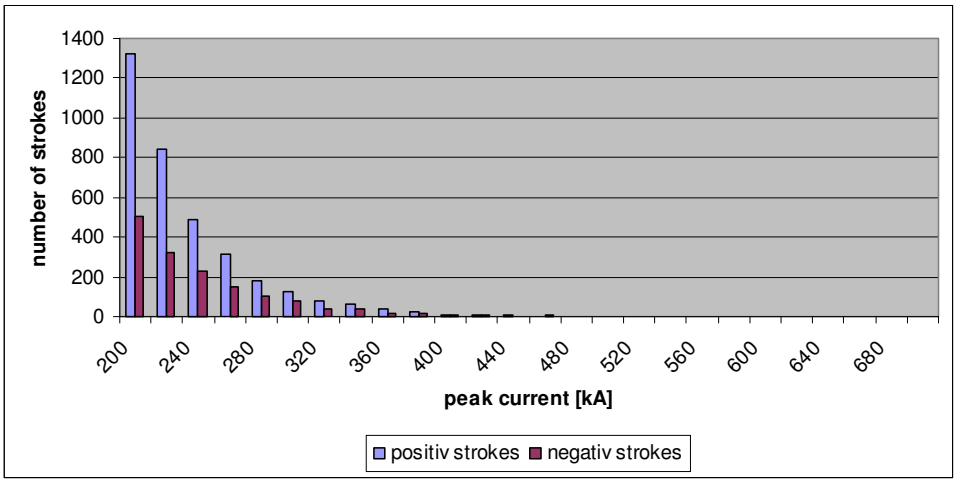

Figure 7.12: Number of strokes as a function of the peak current in middle Europe

A further point is the correlation between the peak current of those high peak current strokes and the number of sensors detecting that stroke as illustrated in the bar diagram in Figure 7.13. No clear correlation is recognizable in Figure 7.13.

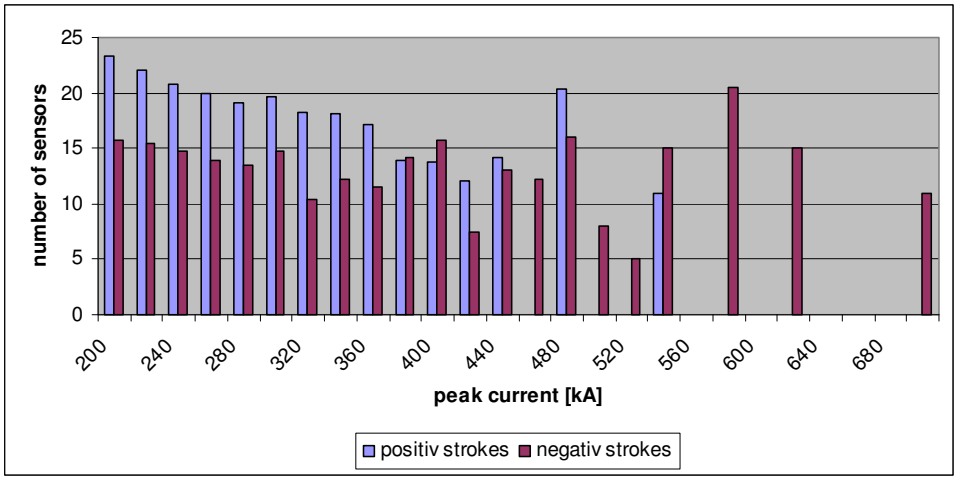

Figure 7.13: Number of reporting sensors as a function of peak current

Figure 7.14 shows a plot of the degree of freedom versus the peak current. Recognizable in that figure is that the higher the peak current of a stroke, the smaller is the degree of freedom and hence the quality of the detection decreases. *Cummins (2000)* explained a similar observation in the US network by the one or a combination of the following reasons:

(1) Saturation of nearby sensors - should be of minor effect, (2) nearby sensors get confused by strong leader pulses or large signals from intra-cloud discharges preceding the high peak current CG strokes, and (3) complexity of CG lightning waveforms is reduced at greater distances due to attenuation effects and hence only more distant sensors participate in the location.

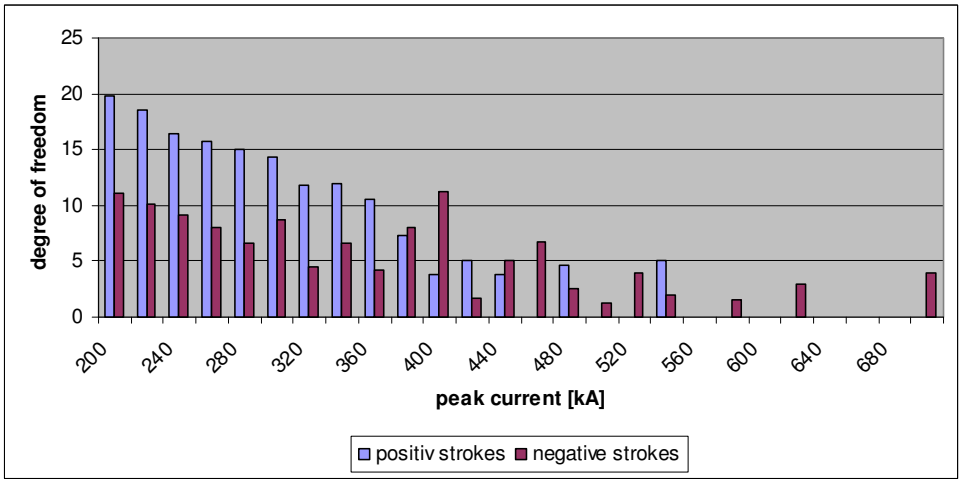

Figure 7.14: Degree of freedom as a function of the peak current

Another interesting part is that positive strokes with a peak current greater than 200 kA are not only more frequent than negative strokes (see Figure 7.12), they are also

detected by more sensors (see Figure 7.13) and with a higher degree of freedom (see Figure 7.14). Table 7.5 shows the average number of sensors and the average degree of freedom of all positive and negative strokes with a peak current higher than 200 kA. Summarizing a positive stroke with a high peak current is better to detect than a negative stroke.

Table 7.5: Comparison between the detecting of positive and negative strokes

	average number of sensors	average degree of freedom
positive strokes	20.1	30.8
negative strokes	14.8	9.3

7.4. Lightning Locating Inconsistencies

The EUCLID Lightning Location System sometimes detects high current strokes not being real. Reasons for such errors can be the detection of the ionospheric reflections of electromagnetic fields radiated by a stroke. These ionospheric reflections normally show (for the first reflection) the opposite polarity as the ground wave. The time difference between the ground wave and the ionospheric reflection is in a range of a few hundreds of microseconds. An example for such a detection is a -716.1 kA stroke that occurred on 11th March 2004 at 10:52:32.418595668. This stroke was detected by 11 sensors and the degree of freedom is 4. Table 7.6 shows also the details of the strokes that occurred about 110 µs before. We conclude that the probability is very high that the detection of the -716.1 kA stroke is a result of detection of the ionospheric reflections of the 121.1 kA stroke that occurred about 110 µs earlier. Figure 7.15 shows the location of both detections in the northern Adriatic Sea. The distance between the real stroke and the probable reflection is about 18 km.

Table 7.6: Reflexion of a stroke

date	time	nanosecond	flash number	latitude	longitude	amplitude [kA]	number of strokes	stroke number	ki2	major-axis [km]	number of sensors	degree of freedom
11.03.2004	10:52:32	418486980	3551	44.6390	12.9865	121.1	3	1	5.6	0.6	19	8
11.03.2004	10:52:32	418595668	3552	44.8019	12.9674	-716.1	1	1	3.4	3.8	11	4

Figure 7.15: A Google Earth photography from the northern Adriatic Sea where the two strokes were located

Another example of an unreal stroke detection is given in the following. Figure 7.16 shows a problem with the location algorithm in the past (and which is already solved since some years). The -597.6 kA stroke detected on 8th November 2000 at 02:46:32 is the result of such an algorithm error. The stroke was detected by 26 sensors and the degree of freedom (2) is obviously too small. The VISLOC analysis in Figure 7.16 shows clearly that the estimated ground strike point (red cross) is too far away from the intersection of majority of sensor data.

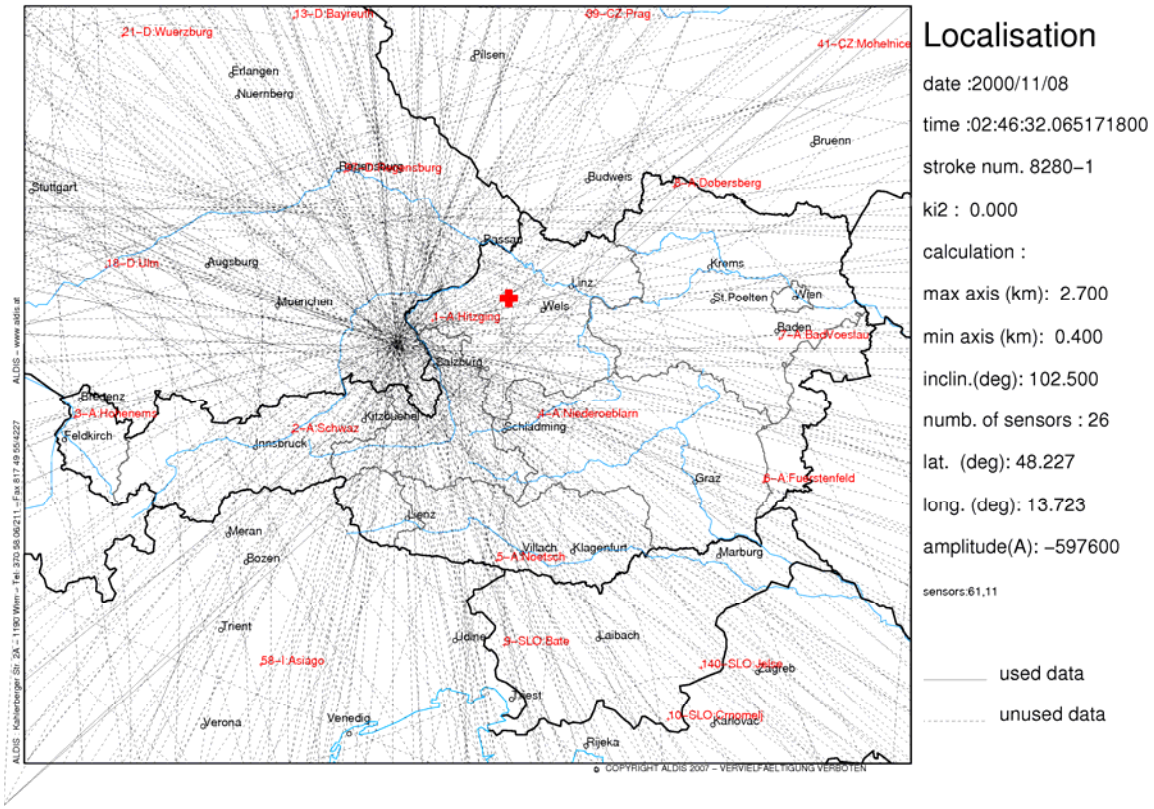

Figure 7.16: VISLOC analysis of the -597.6 kA stroke

8. Effect of the Gaisberg-Tower on the local ground flash density

This chapter has the aim to investigate the effect of an elevated radio transmitter tower on the lightning density of the surrounding area. A 20 km × 20 km area around the 1287 m high Gaisberg is analyzed because of the availability of direct current measurements at the tower since 1998. The map of the area is shown in Figure 8.1. In the western proximity is the city Salzburg and in the south-west is the mountain Untersberg with the summit “Salzburger-Hochfron” (1853 m) being the highest elevation in that square. In the remaining surrounding area there are just a few smaller mountains or hills.

Figure 8.1: Map (20 km × 20 km) of the Gaisberg surrounding

Figure 8.2: Satellite picture of the examined area around the Gaisberg

On the Gaisberg is a radio tower instrumented with a lightning current measurement system to record every lightning impact to the tower. Because of incomplete stroke records in the early operation years the investigation time interval was chosen from 2003 to 2007. The Lightning Location System ALDIS delivers the stroke density of that entire area. To see the effect of the tower the recorded tower impacts were subtracted from the total stroke density. With the help of the program EXCEL the examined area was divided in a 100 m and 500 m grid and every stroke was assigned to the appropriate grid cell. Hence it was possible to visualize the distribution of the located strokes.

Figure 8.3 shows the distribution (500 m grid) of all the strokes located in the examined area. Clearly recognizable is the high stroke density at the Gaisberg tower site. Due to the higher stroke density the Untersberg also appears in the south-west. Although the Untersberg is the highest object in that area (with a cross on the top and cable railway in the proximity), the stroke density at the Gaisberg tower is much higher. Hence the lightning triggering effect of the radio tower is obvious.

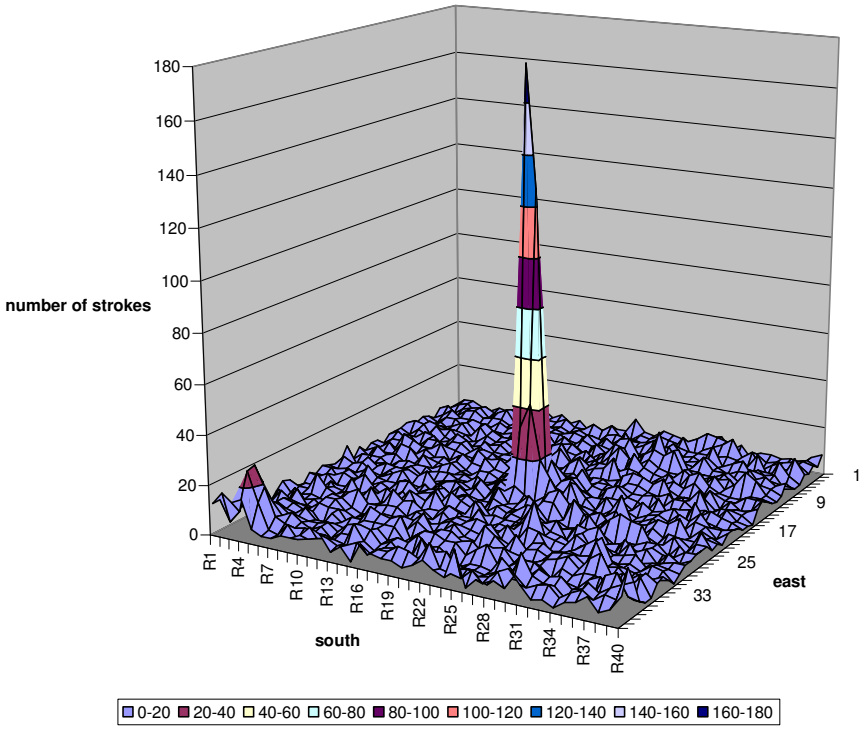

Figure 8.3: Distribution of the detected strokes by ALDIS in an area of 20 km × 20 km around the Gaisberg and based on a 500 m grid

Figure 8.4 shows the stroke distribution in the same area after eliminating all the recorded Gaisberg tower impacts. The interesting point is that now the stroke density at the Gaisberg tower is in the same range as at the Untersberg. We conclude that all the measured flashes at the tower do not have any significant effect on the ground flash density in the near vicinity of the tower.

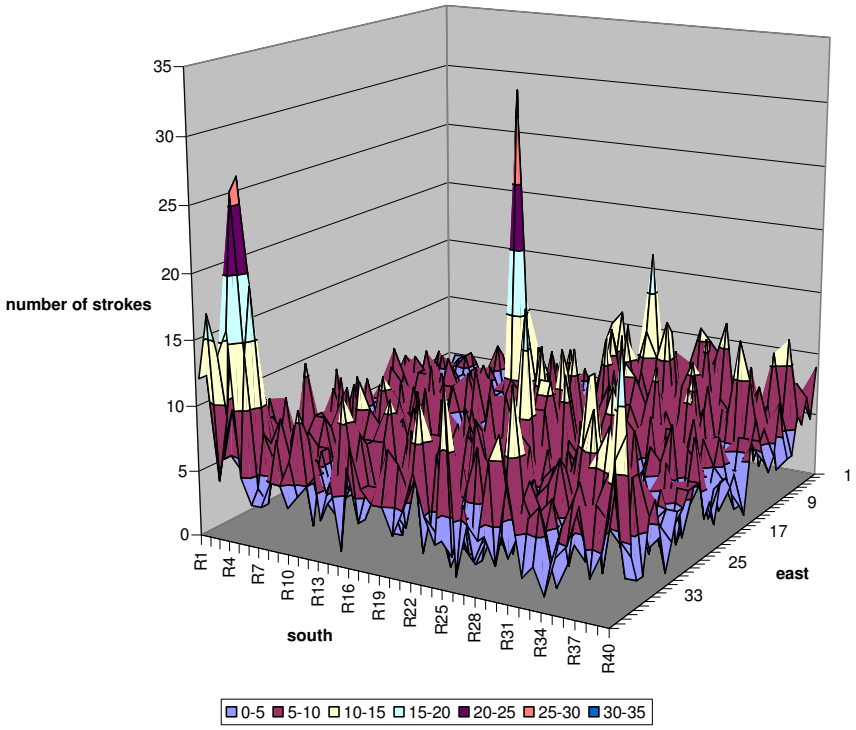

Figure 8.4: Distribution of the detected strokes by ALDIS when the strokes registered at the tower are eliminated

Analysing the distribution with the finer 100 m grid will help to prove that result. Table 8.1 and Table 8.2 show the evaluation in the proximity of the Gaisberg tower (2 km × 2 km around the Gaisberg tower; Figure 8.5). It is recognizable that despite the subtraction of the recorded tower impacts a few strokes remain in the area. This result could have the following reasons:

- The remaining strokes were tower impacts which were not recorded by the tower measurement system (unlikely)
- The remaining strokes did not strike the tower top and attached ground in the proximity (cross, building, tree, …) or nearby the shown area and were placed inside due to the existing location error

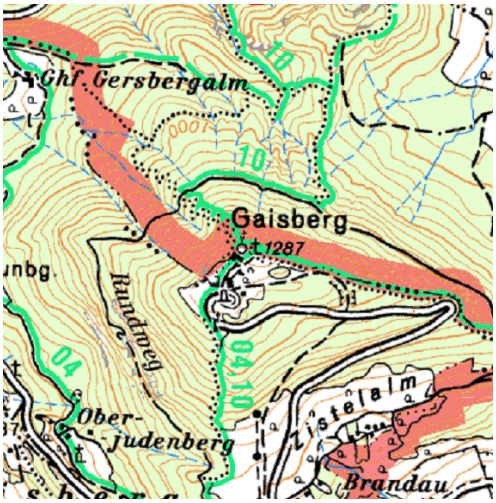

Figure 8.5: Map (2 km × 2 km) of the proximity of the Gaisberg summit

Table 8.1: Distribution of all strokes located by ALDIS in the proximity of the Gaisberg tower including events measured by the tower instrumentation

	-1000m	-900m	-800m	-700m	-600m	-500m	-400m	-300m	-200m	-100m	+100m	+200m	+300m	+400m	+500m	+600m	+700m	+800m	+900m	+1000m
+1000m	1	0	0	2	0	0	1	0	0	1	0	0	0	0	2	0	1	0	0	3
+900m	1	0	0	0	0	1	0	3	2	1	0	1	1	0	0	0	0	1	0	0
+800m	0	0	0	1	1	0	1	2	1	0	3	1	1	0	0	1	1	0	2	1
+700m	0	0	0	0	0	0	1	3	2	0	2	0	2	0	2	1	0	2	1	0
+600m	2	0	0	0	1	0	0	4	8	2	1	2	2	3	1	0	0	2	0	1
+500m	0	0	1	0	0	1	2	3	2	5	8	6	4	0	4	0	0	1	0	0
+400m	0	0	0	0	0	0	3	6	9	12	11	5	5	1	3	2	0	0	0	1
+300m	0	1	0	0	1	1	2	12	11	12	11	7	5	3	0	1	0	0	0	0
+200m	0	0	1	0	0	2	5	12	22	14	9	10	8	4	2	1	1	1	0	2
+100m	1	1	0	1	2	4	6	6	13	10	10	5	3	2	1	1	0	0	0	0
-100m	0	0	0	0	1	0	4	1	3	9	6	7	4	1	0	0	0	1	0	0
-200m	1	0	0	1	0	0	1	0	1	5	8	1	2	4	0	1	2	2	1	0
-300m	0	0	0	0	1	1	1	2	0	1	3	1	0	1	0	1	0	0	2	0
-400m	0	0	0	0	1	0	1	0	0	0	1	1	0	0	1	2	1	4	0	1
-500m	0	0	0	0	0	1	0	0	0	1	1	0	0	0	0	0	2	0	0	0
-600m	0	0	1	1	0	0	1	0	2	0	0	0	2	0	0	0	0	0	0	0
-700m	2	0	0	0	1	0	0	1	0	0	0	0	0	0	1	0	0	1	0	0
-800m	0	0	1	0	0	0	1	0	0	0	0	0	0	0	0	1	0	0	0	1
-900m	0	0	0	0	0	1	0	1	0	0	1	0	0	0	1	0	0	0	0	1
-1000m	0	0	0	0	0	0	0	1	1	0	0	0	0	0	1	0	0	0	0	0

Table 8.2: Distribution of the remaining strokes detected by ALDIS in the proximity of the Gaisberg summit when the registered flashes striking the tower are eliminated

	-1000m	-900m	-800m	-700m	-600m	-500m	-400m	-300m	-200m	-100m	+100m	+200m	+300m	+400m	+500m	+600m	+700m	+800m	+900m	+1000m
+1000m	1	0	0	0	0	0	1	0	0	0	0	0	0	0	1	0	1	0	0	1
+900m	1	0	0	0	0	1	0	2	1	1	0	0	1	0	0	0	0	1	0	0
+800m	0	0	0	1	1	0	1	0	0	0	1	0	1	0	0	1	0	0	1	0
+700m	0	0	0	0	0	0	0	1	1	0	1	0	0	0	0	0	0	0	0	0
+600m	2	0	0	0	1	0	0	1	6	1	0	0	0	0	1	0	0	1	0	0
+500m	0	0	0	0	0	0	0	0	1	1	1	0	1	0	1	0	0	1	0	0
+400m	0	0	0	0	0	0	0	1	2	3	3	1	0	0	0	0	0	0	0	1
+300m	0	1	0	0	0	1	1	3	3	0	1	0	0	0	0	1	0	0	0	0
+200m	0	0	1	0	0	1	1	3	2	1	0	1	1	2	0	1	1	1	0	2
+100m	1	1	0	1	2	0	1	2	2	3	1	0	1	0	0	1	0	0	0	0
-100m	0	0	0	0	1	0	1	1	1	2	0	0	1	1	0	0	0	1	0	0
-200m	0	0	0	1	0	0	0	0	1	0	2	0	1	0	0	1	0	1	0	0
-300m	0	0	0	0	1	0	1	0	0	0	1	1	0	0	0	0	0	0	1	0
-400m	0	0	0	0	1	0	1	0	0	0	0	0	0	0	1	1	0	1	0	1
-500m	0	0	0	0	0	1	0	0	0	1	1	0	0	0	0	0	1	0	0	0
-600m	0	0	1	1	0	0	1	0	2	0	0	0	2	0	0	0	0	0	0	0
-700m	2	0	0	0	1	0	0	1	0	0	0	0	0	0	1	0	0	1	0	0
-800m	0	0	1	0	0	0	1	0	0	0	0	0	0	0	0	1	0	0	0	1
-900m	0	0	0	0	0	1	0	1	0	0	1	0	0	0	1	0	0	0	0	1
-1000m	0	0	0	0	0	0	0	1	1	0	0	0	0	0	1	0	0	0	0	0

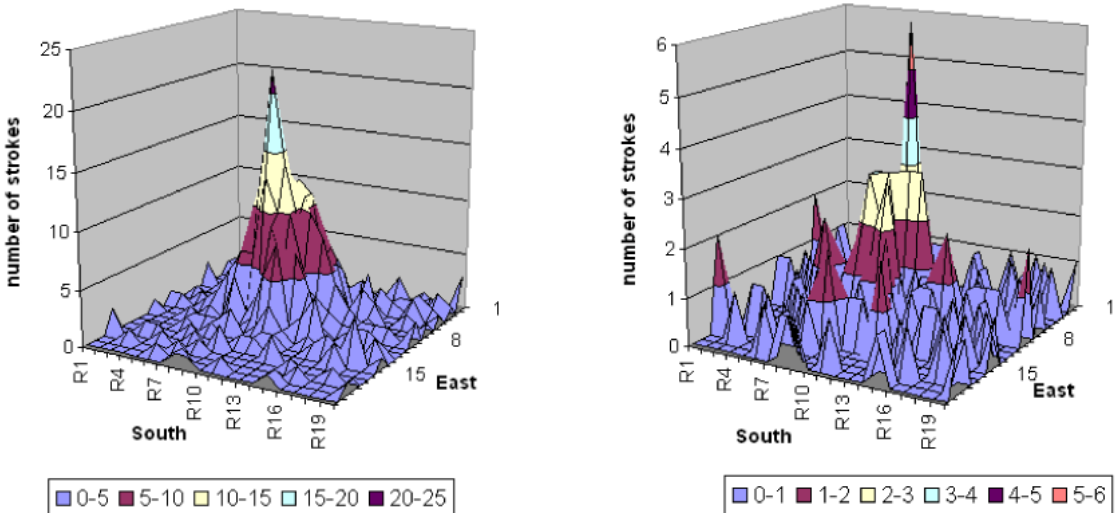

Figure 8.6: Visualization of the distribution given in Table 8.1 (left) and Table 8.2 (right). Note the difference in scaling in the two figures.

This comparison shows the significant influence of the tower to the lightning density in this area. It further shows that the tower does not collect all lightning in the area around it. Remaining flash density, after elimination of direct tower strikes, seems very similar to other mountains without any tower, where an increase of flash density with altitude is observed

9. Appendix A: Lightning Density

9.1. Lower Austria

- **Rax / Kaiserbrunnaussicht:**

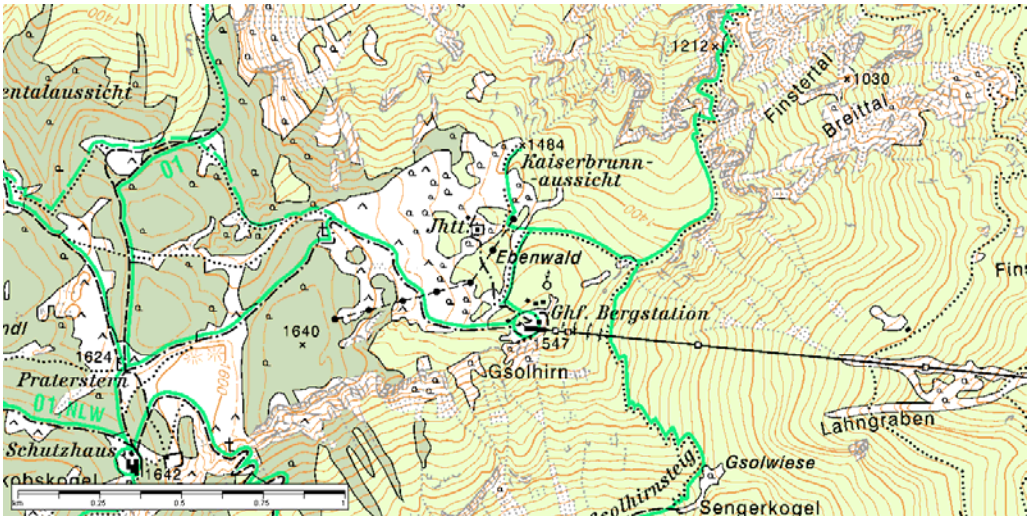

Figure 9.1: Map of the Kaiserbrunnaussicht (eastern part of the Rax) and surrounding

Figure 9.2: The eastern part of the Rax viewed from south-west [*Hubert Umprecht*]

Figure 9.3: The radio transmitter tower (left), the Gasthof Bergstation inclusive summit railway station (middle) and the drag lift on the Rax plateau (right) [*Hubert Umprecht*]

- **Sonnwendstein:**

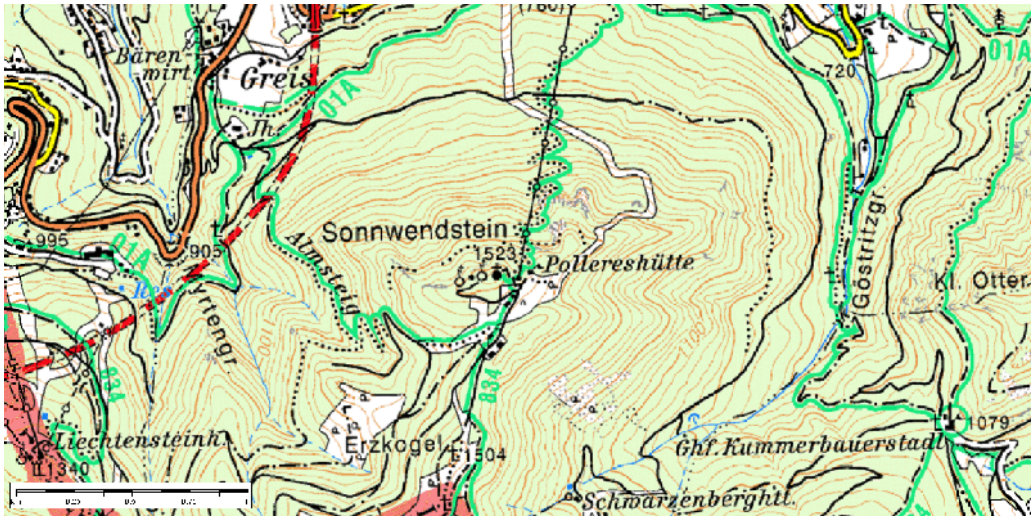

Figure 9.4: Map of the Sonnwendstein and surrounding


Figure 9.5: View to the summit of the Sonnwendstein from south [*www.wabweb.net*]

- **Hochschneeberg (Klosterwappen) / Waxriegel:**

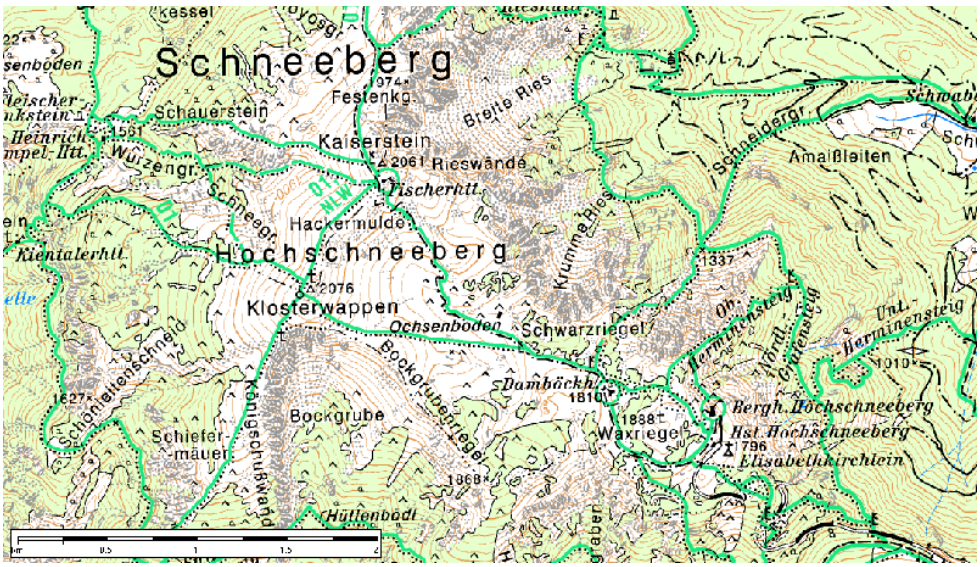

Figure 9.6: Map of the Schneeberg and surrounding

Figure 9.7: View to the Schneeberg from the south (left) [*www.wikipedia.org*] and the summit of the Hochschneeberg with the cross and the small radio transmitter mast (right) [*www.landschaftsfotos.at*]

Figure 9.8: The radar station next to the cross (left), the shelter Fischerhütte (middle) and the summit station of the rack railway next to the chapel Elisabethkirchlein on the Waxriegel (right) [*www.landschaftsfotos.at*]

Figure 9.9: View to the Klosterwappen (left) [*www.wikipedia.org*], view to the Waxriegel from the Hochschneeberg (middle) [*www.engelmaier.piranho.de*] and the cross on the Wayxriegel (right) [*www.engelmaier.piranho.de*]

9.2. Upper Austria

- **Katrin:**

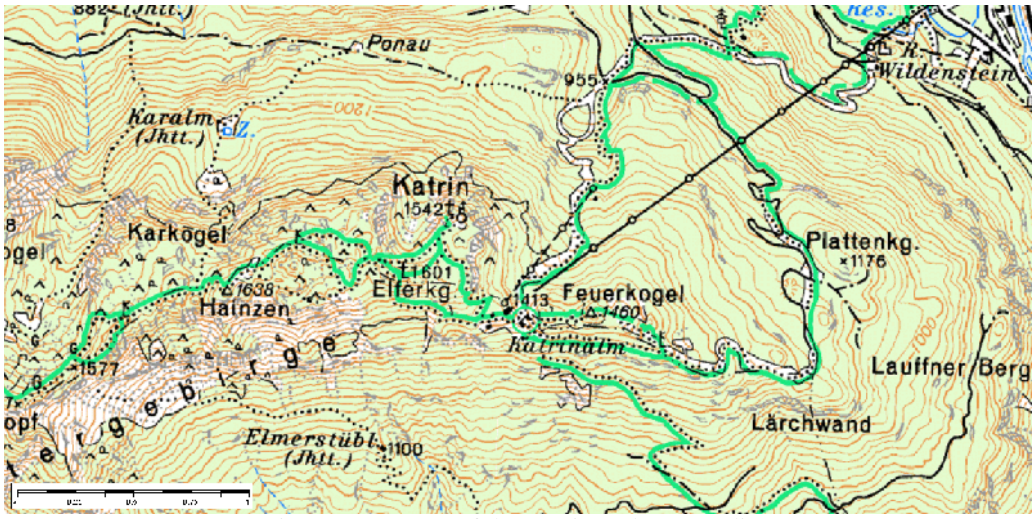

Figure 9.10: Map of the Katrin and surrounding

Figure 9.11: View to the summit with radio transmitter tower and cross from north [*Hubert Umprecht*]

Figure 9.12: Cross (left) and the top of it (right) [*Hubert Umprecht*]

Figure 9.13: Transmitter tower (left) and the highest point of the tower (right) [*Hubert Umprecht*]

Figure 9.14: The cable railway station (left) and the Katrinalm (right) in winter [*www.bergfex.at*]

9.3. Styria

- **Feistringstein / Kampl:**

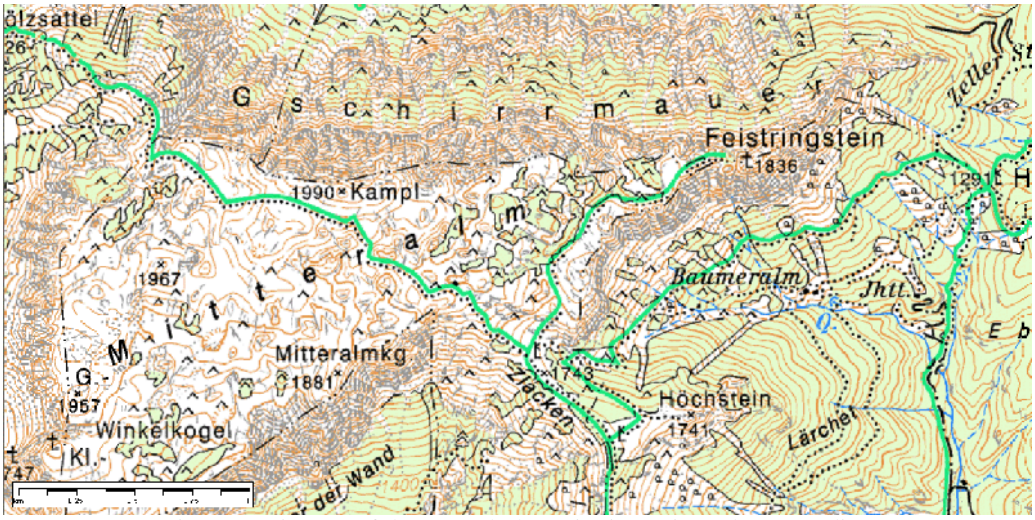

Figure 9.15: Map of the Kampl, the Feistringstein and surrounding

Figure 9.16: View to the Feistringstein and the Kampl from north [*www.panoramio.com*]

- **Lärchkogel:**

Figure 9.17: Map of the Lärchkogel and surrounding

Figure 9.18: View to the Windgrube and the Lärchkogel from the east (left) and the summit of the Windgrube inclusive skiing lifts (right) [*Hubert Umprecht*]

- **Schießlingalm:**

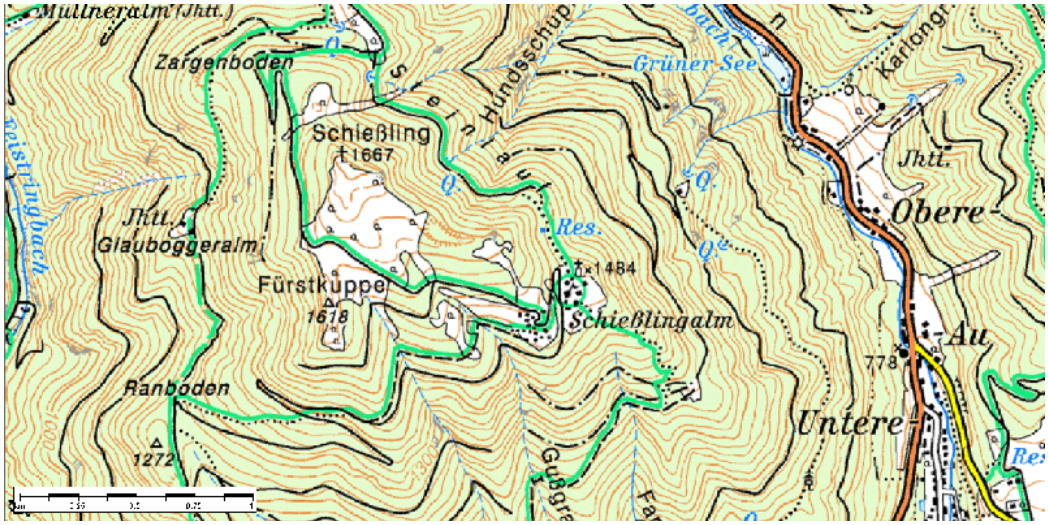

Figure 9.19: Map of the Schießlingalm and surrounding


Figure 9.20: The village at the Schießlingalm from different views [*Hubert Umprecht*]

- **Eisenerzer Reichenstein:**

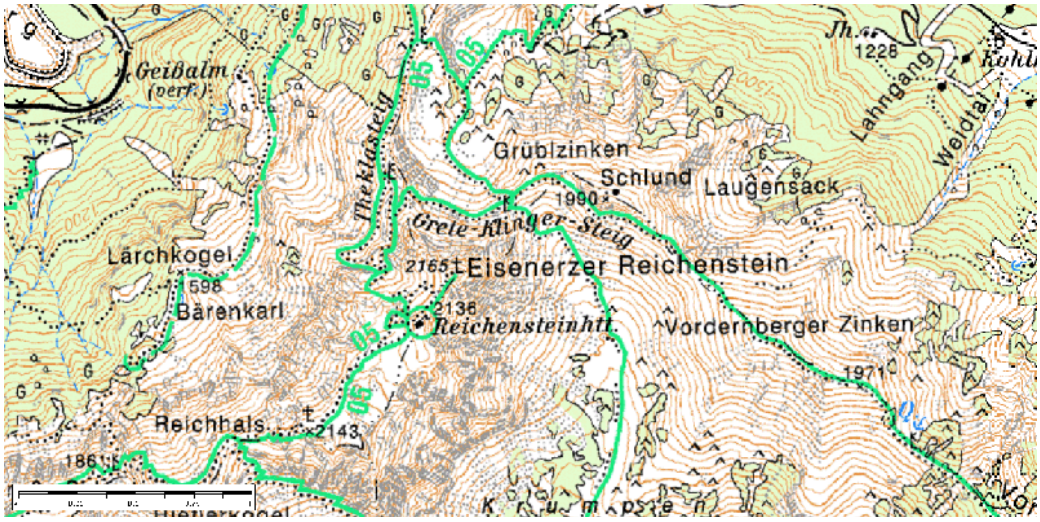

Figure 9.21: Map of the Eisenerzer Reichenstein and surrounding

Figure 9.22: The Eisenerzer Reichenstein (left) [*www.diplomingenieure.at*], the cross on the top (middle) [*Kurt Edegger*] and the summit include the shelter Reichensteinhütte (right) [*www.flickr.com*]

- **Reiting / Gößeck:**

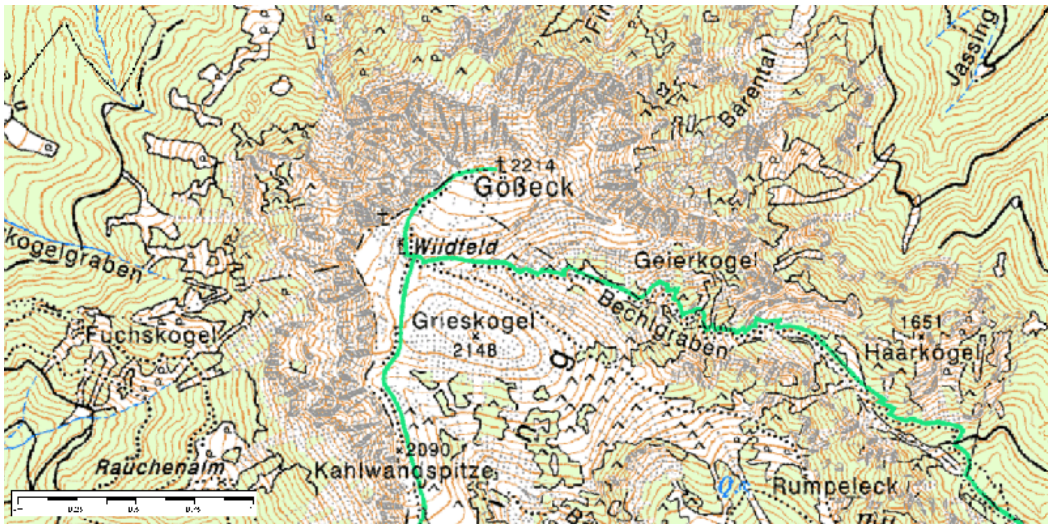

Figure 9.23: Map of the Gößeck and surrounding

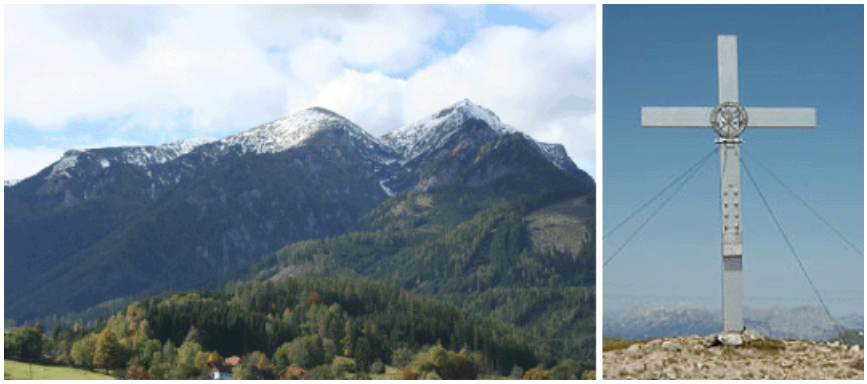

Figure 9.24: View to the Gößeck from the town Trofaiach in the east of the mountain (left). The right summit is named Gößeck and the more left one is the Grieskogel. On the right picture is the cross on the peak [*www.wandern.atspace.com*].

- **Stanglalpe:**

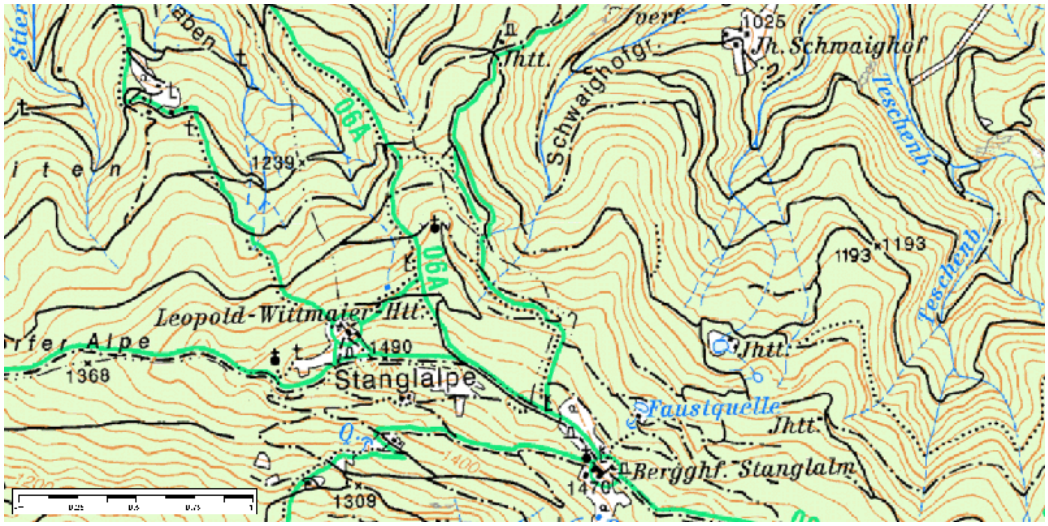

Figure 9.25: The Stanglalpe and surrounding


Figure 9.26: View to the wooded Stanglalpe from the south [*Hubert Umprecht*]

- **Kulmkogel (Sommeralm):**

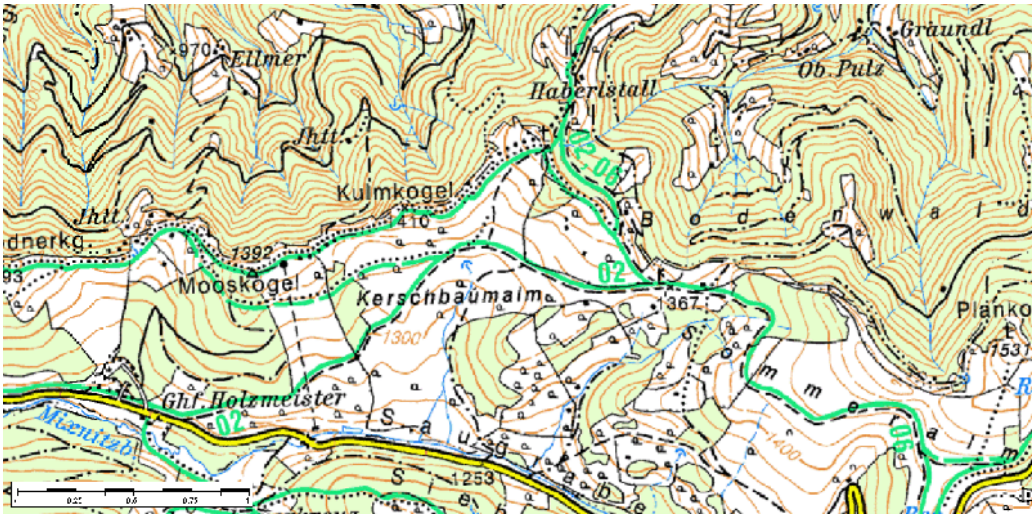

Figure 9.27: Map of the Kulmkogel and proximtiy

Figure 9.28: The Sommeralm (left) and the wind power turbine (right) [*www.panoramio.com*]

- **Heulantsch / Grubbauerkogel (Teichalm):**

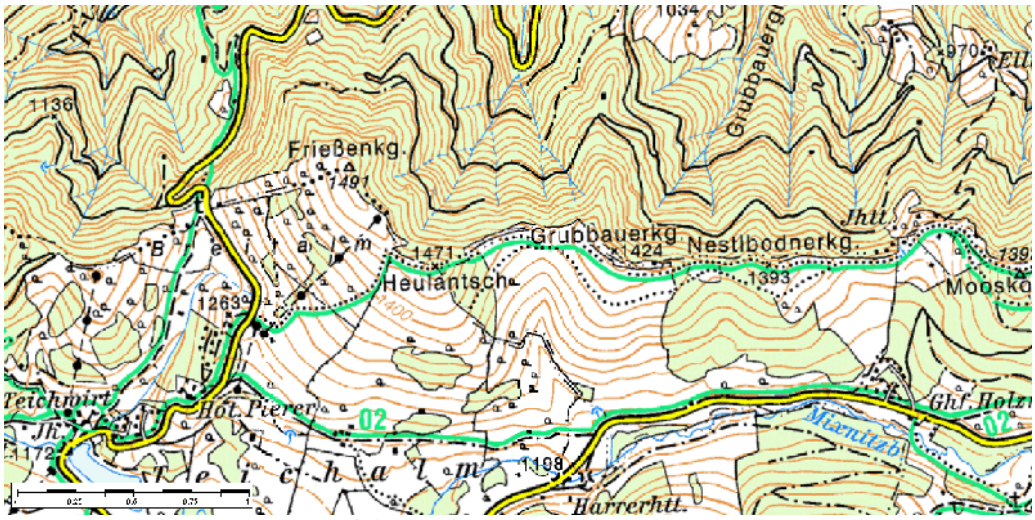

Figure 9.29: Map of the Heulantsch, Grubbauerkogel and surrounding

Figure 9.30: The surrounding of the Heulantsch viewed from the south [*www.panoramio.com*]

- **Schöckl:**

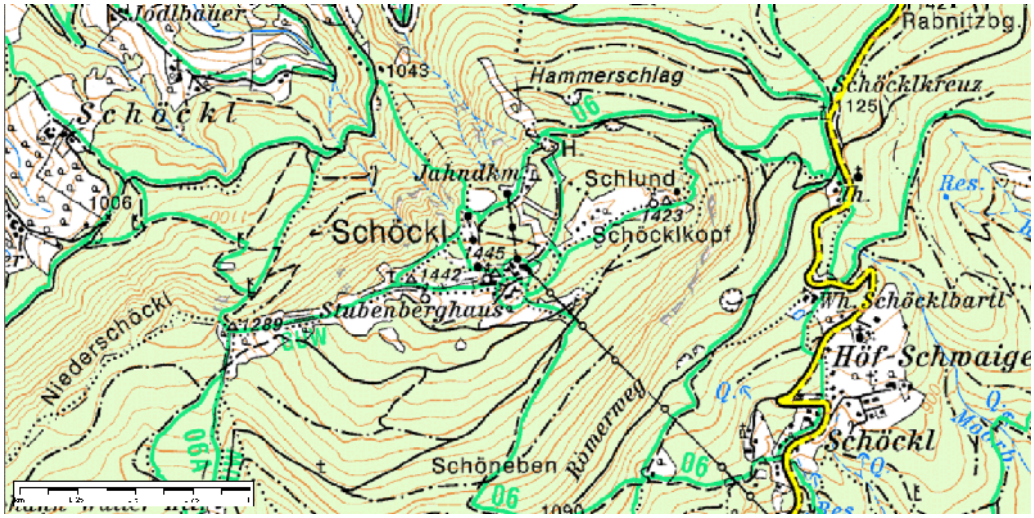

Figure 9.31: Map of the Schöckl and surrounding


Figure 9.32: The Schöckl (left) [*Müller Josef*] and the summit plateau (middle, right) [*www.panoramio.com*]


Figure 9.33: Three radio transmitter towers (left, middle) [*www.wabweb.net*] and the cross on the summit (right) [*www.panoramio.com*]

- **Schererkogel:**

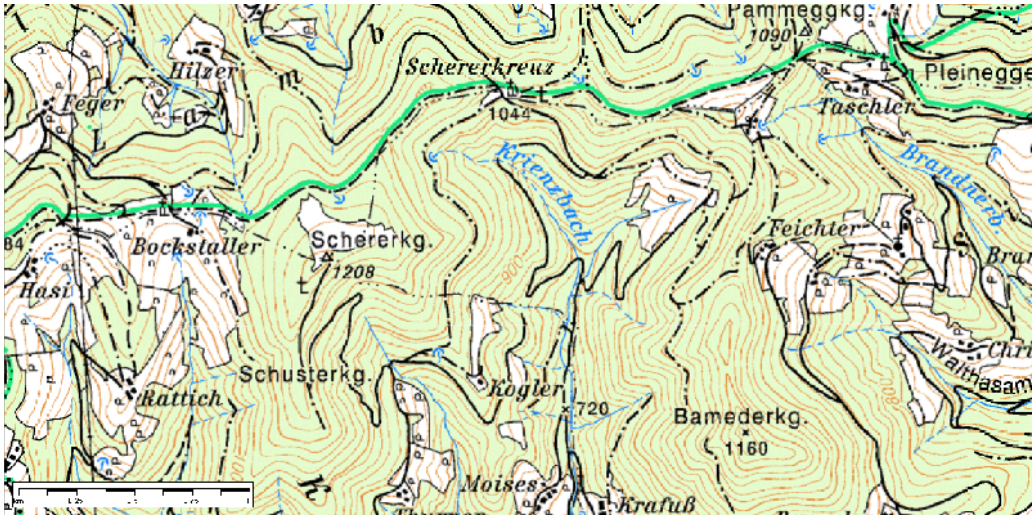

Figure 9.34: Map of the Schererkogel and surrounding


Figure 9.35: The surrounding of the wooded Schererkogel (left) and the summit where the Schererkreuz is located (right) [*Hubert Umprecht*]

- **Zirbitzkogel / Scharfes Eck:**

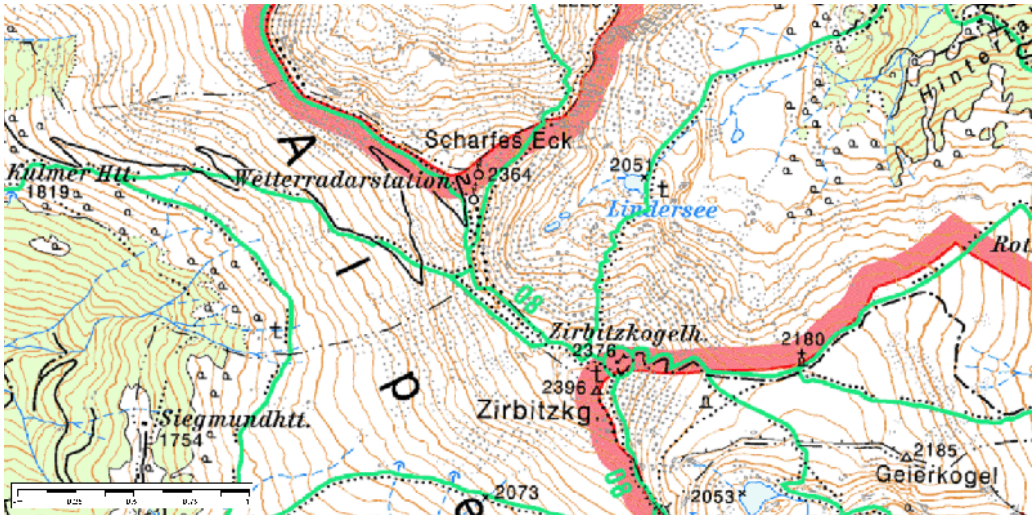

Figure 9.36: Map of the Zirbitzkogel, Scharfes Eck and surrounding

Figure 9.37: The Zirbitzkogel (left) [*www.hikr.org*], the shelter Zirbitzkogelhaus (middle) [*www.hribi.net*] and the cross on the summit (right) [*www.pbase.com*]

Figure 9.38: The summit of the Scharfes Eck (left), the weather radar (middle) and the radio transmitter tower (right) [*Hubert Umprecht*]

- **Grebenzen:**

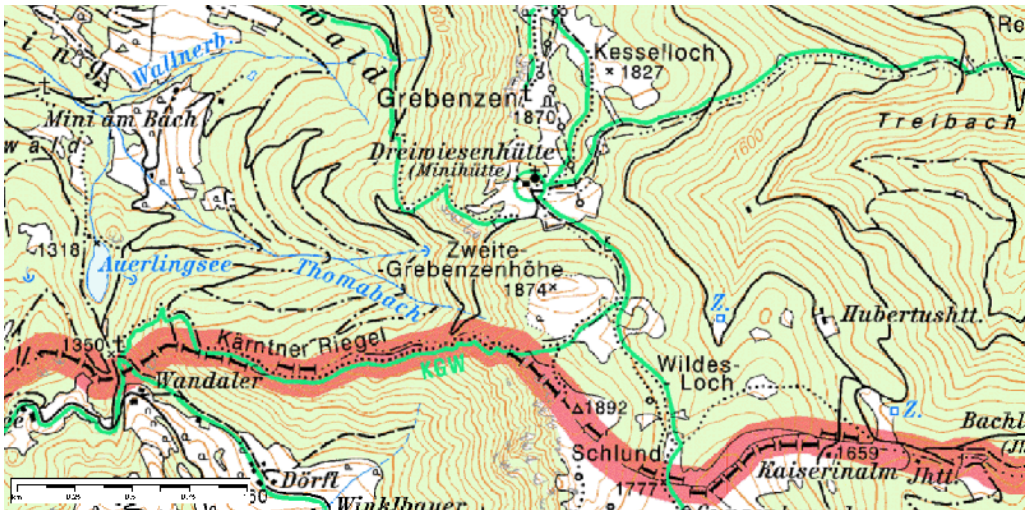

Figure 9.39: Map of the Grebenzen and surrounding

Figure 9.40: View to the Grebenzen from the town St.Lambrecht (left) [*www.panoramio.com*], the summit (middle) and the cross (right) [*Hubert Umprecht*]

Figure 9.41: View to the Zweite Grebenzenhöhe from the summit Grebenzen (left) [*Hubert Umprecht*], the shelter Dreiwiesenhütte (middle) and the chapel Hubertuskapelle (right) [*www.dreiwiesenhuette.at*]

9.4. Carinthia

- **Großer Speikkogel:**

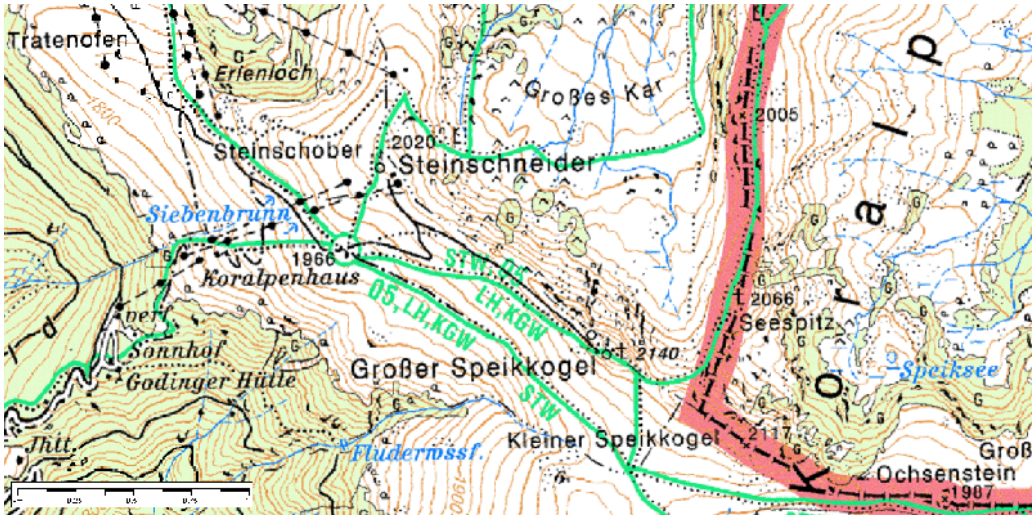

Figure 9.42: Map of the Großer Speikkogel and surrounding

Figure 9.43: The summit of the Großer Speikkogel (left) [*www.picasaweb.com*] and the two radar stations (right) [*Hubert Umprecht*]

Figure 9.44: The ridge and the cross of the summit Seespitz (left) and the cross on the Großer Speikkogel (right) [*Hubert Umprecht*]

- **Saualpe:**

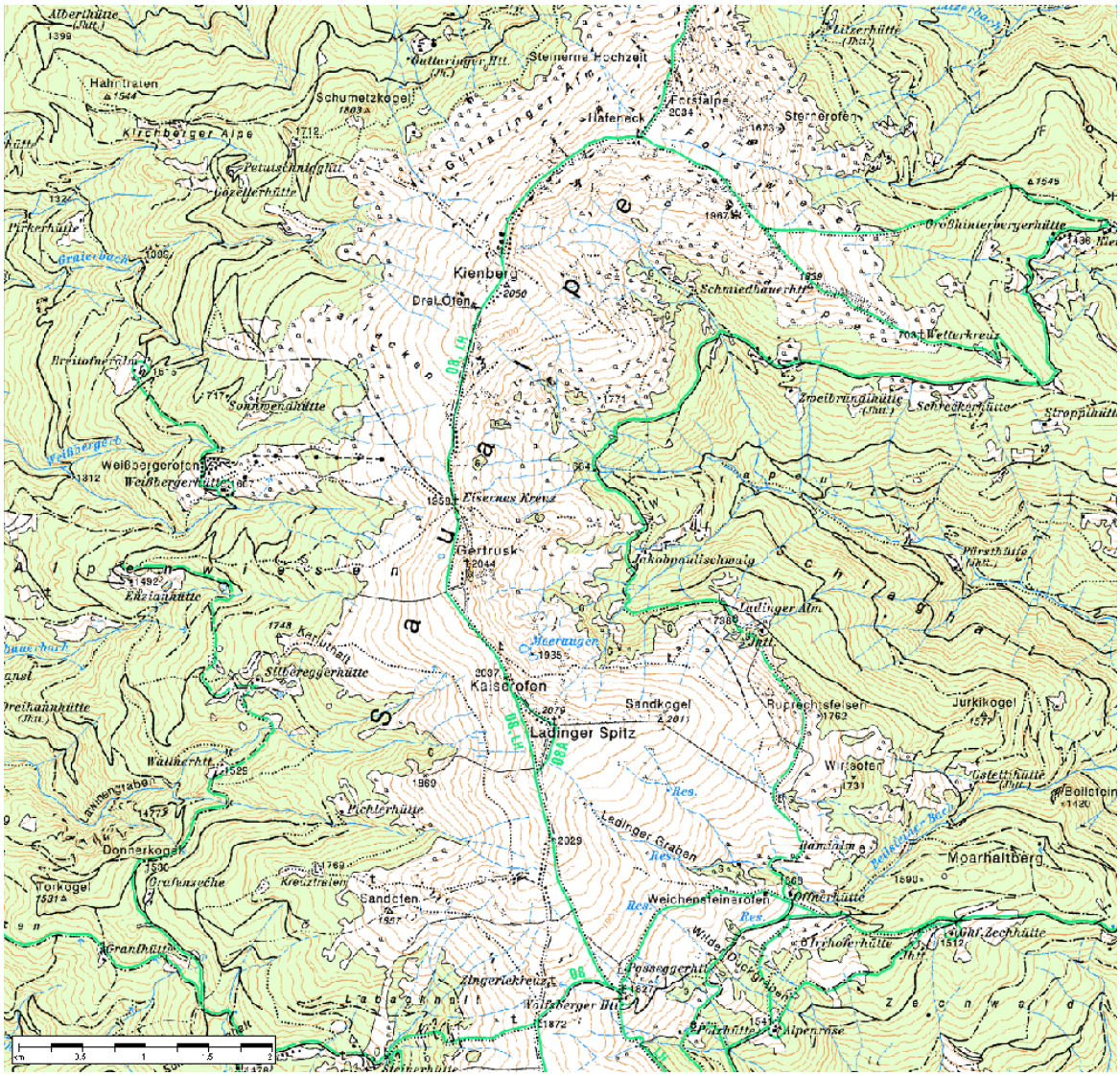

Figure 9.45: Map of the interesting part of the Saualpe

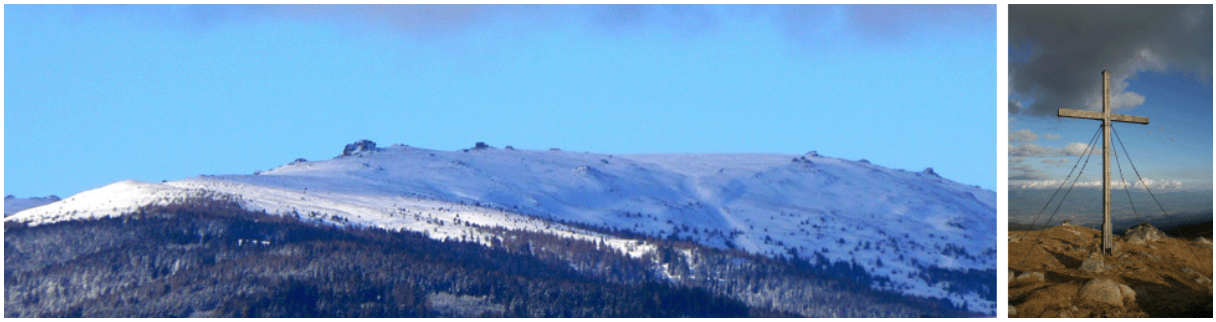

Figure 9.46: The Saualpe in winter (left) [*www.panoramia.com*] and the cross south of the unknown summit named Zingerlekreuz (right) [*Hubert Umprecht*]

Figure 9.47: The cross on the Ladinger Spitz (left), a southern view from the Ladinger Spitz (middle) and the shelter Wolfsberger Hütte (right) [*Hubert Umprecht*]

Figure 9.48: View to the summit Gertrusk (left) and the cross on it (middle) as well as the summits Kienberg and Forstalpe (right) [*Hubert Umprecht*]

- **Dobratsch:**

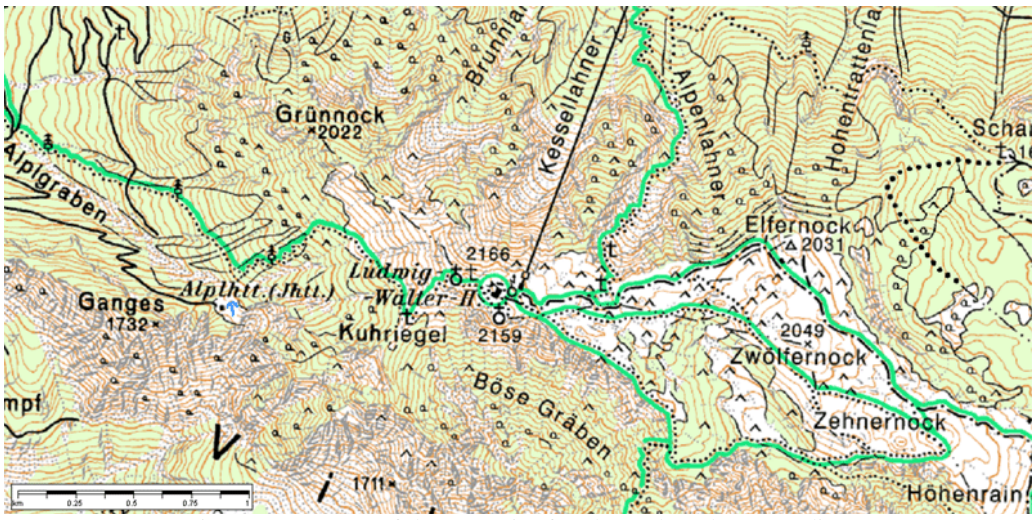

Figure 9.49: Map of the summit of Dobratsch and surrounding

Figure 9.50: The Villacher Alpe (left) [*Michael Kucher*], the summit of the Dobratsch (middle) and the top of the mountain with the transmitter tower and the chapel (right) [*www.wabweb.net*]

Figure 9.51: The small weather station and the cross on the summit (left), the shelter Ludwig-Walter Hütte (middle) [*www.panoramio.com*] and the ground station of the cable railway to the Dobratsch in the town Bad Bleiberg (right) [*Hubert Umprecht*]

- **Goldeck:**

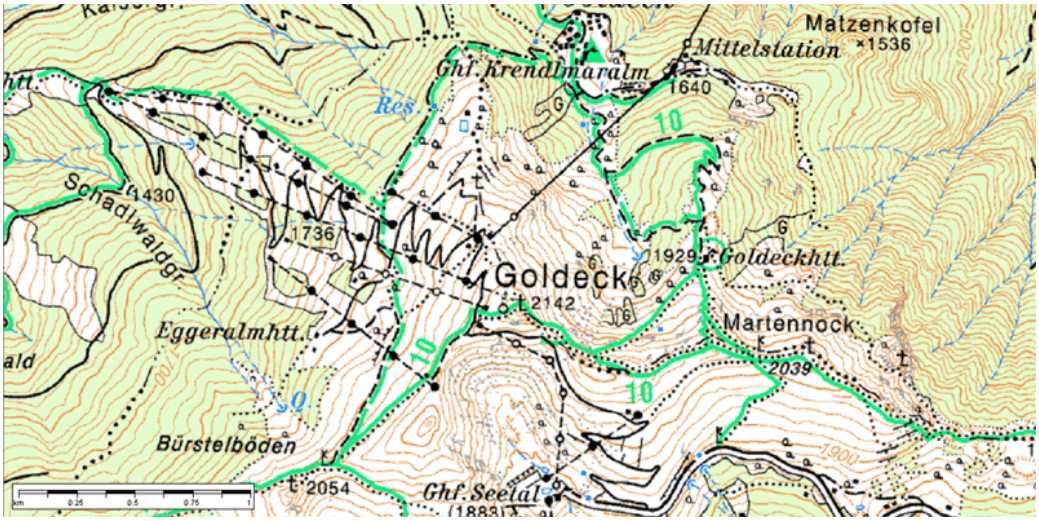

Figure 9.52: Map of the summit Goldeck and surrounding

Figure 9.53: The Goldeck winter sport area viewed from north (left) [*www.bergfex.at*], the ridge on the summit with the tower, different skiing lifts, cable railway station and shelters (middle) [*www.paragliding365.com*] and the radio transmitter tower with the cross on the top (right) [*www.goldeck-spittal.at*]

Figure 9.54: The summit viewed from south with the shelter Gasthof Seetal (left), the cross on the Goldeck (middle) and the cross on the Martennock (right) [*Hubert Umprecht*]

- **Hochwipfel:**

Figure 9.55: Map of the Hochwipfel and surrounding

Figure 9.56: The Hochwipfel (left and middle) [*Hubert Umprecht*] and the cross on the summit (right) [*www.panoramio.com*]

- **Hoher Trieb:**

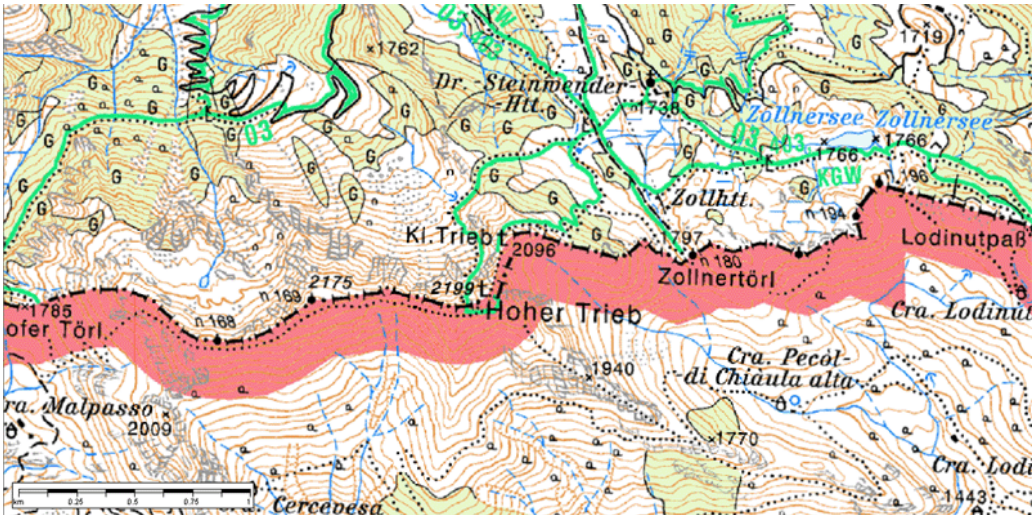

Figure 9.57: Map of the Hoher Trieb, Kleiner Trieb and surrounding

Figure 9.58: The Hoher Trieb and Kleiner Trieb (left) [*www.oeav-obergailtal.at*], the cross on the Kleiner Trieb (middle) and the shelter Dr.Steinwender Hütte with chapel (right) [*www.panoramio.com*]

- **Promos:**

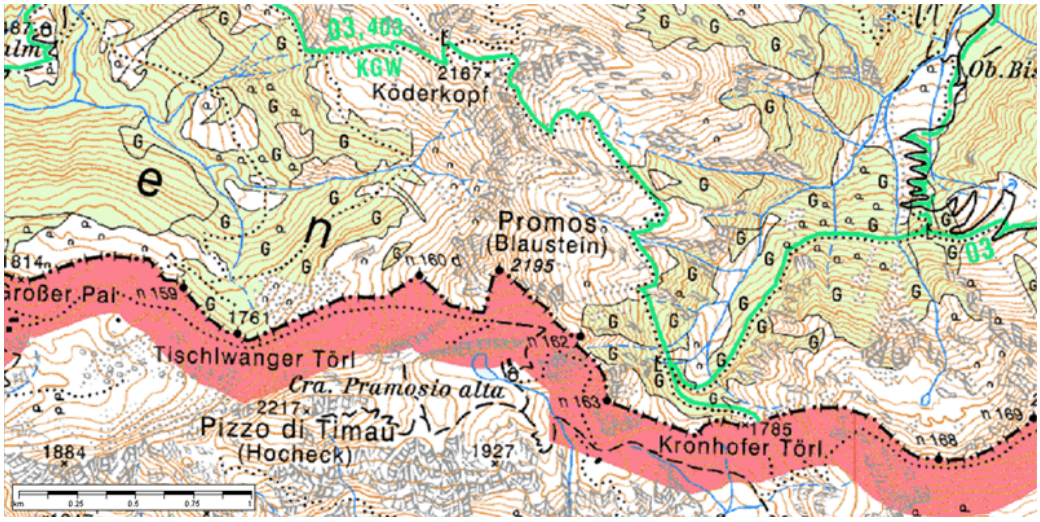

Figure 9.59: Map of the Promos, the Hocheck and surrounding

Figure 9.60: The Promos and the Pizzo Di Timau from the Austrian (left) [*www.panoramio.com*] and the Italian side (right) [*Hubert Umprecht*]

- **Polinik:**

Figure 9.61: Map of the Polinik and surrounding

Figure 9.62: The Polinik from south-west (left) [*Hubert Umprecht*] and the summit with the metal cross (right) [*www.panoramio.com*]

- **Hohe Warte:**

Figure 9.63: Map of the Hohe Warte, Kollinkofel and surrounding

Figure 9.64: Mountain massif Hohe Warte from north-west (left) [*www.summitpost.org*] and north-east (right) [*Hubert Umprecht*]

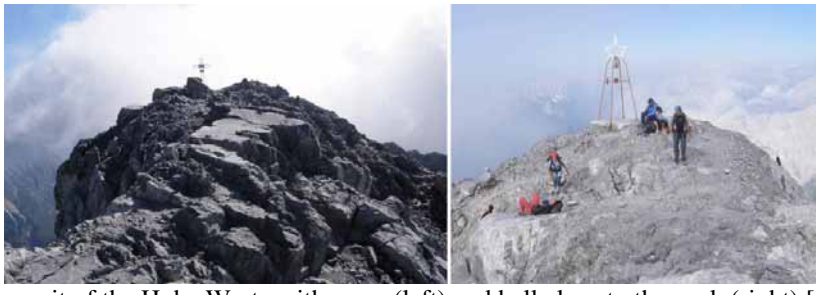

Figure 9.65: Summit of the Hohe Warte with cross (left) and bell close to the peak (right) [*www.hribi.net*]

- **Großglockner:**

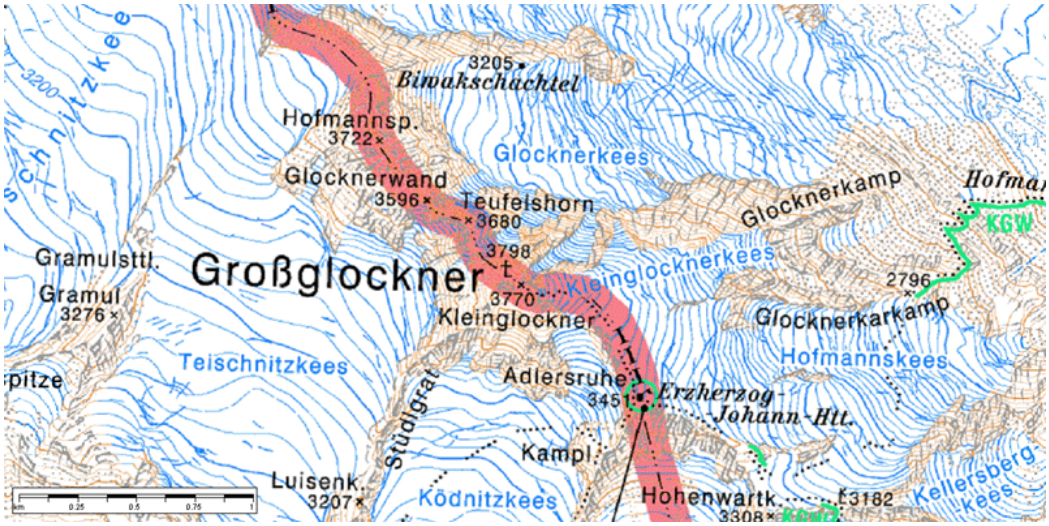

Figure 9.66: Map of the Großglockner and surrounding


Figure 9.67: The Großglockner viewed from north-east (left) [*Hermann Zauner*] and the summit with cross (right) [*www.panoramio.com*]


Figure 9.68: Cross on the peak (left) [*Dr. Wolfgang Schulz*] and the shelter Erzherzog-Johann Hütte (right) [*www.panoramio.com*]

9.5. East Tyrol

- **Niedere / Hoher Prijakt:**

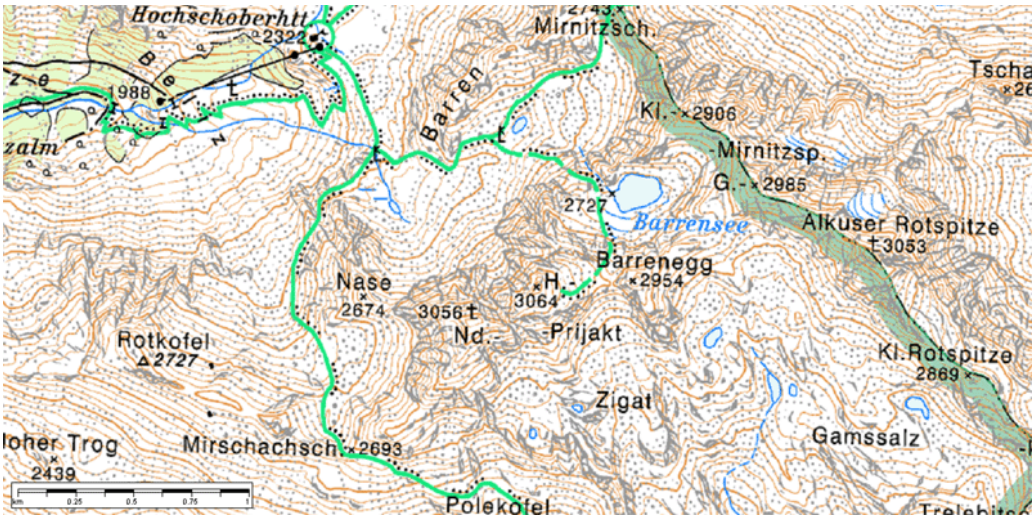

Figure 9.69: Map of the Niedere Prijakt, Hoher Prijakt and surrounding


Figure 9.70: The Niedere Prijakt and the Hoher Prijakt viewed from north (left) and the shelter Hochschoberhütte (right) [*www.panoramio.com*]

- **Rötspitze:**

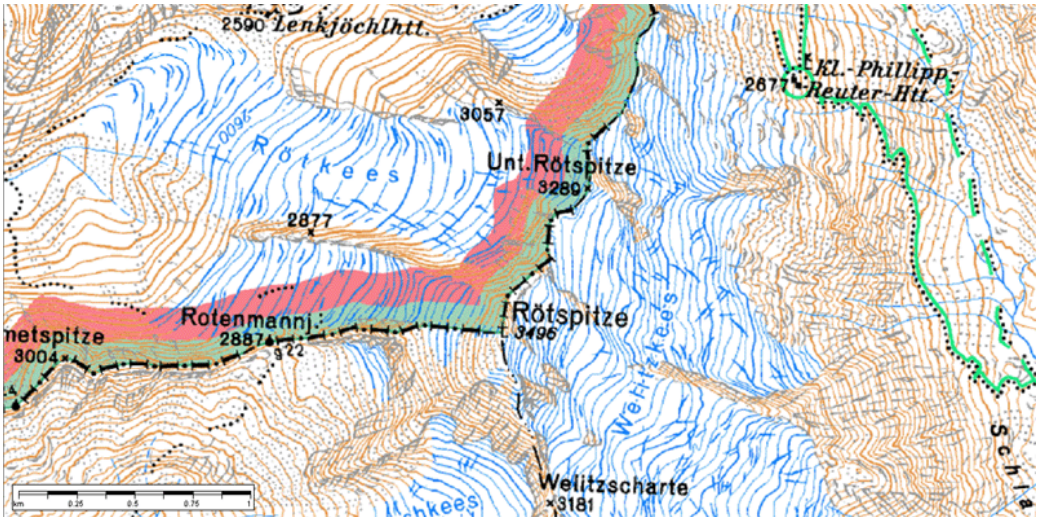

Figure 9.71: Map of the Rötspitze and surrounding

Figure 9.72: The Rötspitze viewed from the Austrian (left) and Italian (middle) side as well as the cross on the summit (right)

9.6. Salzburg

- **Große Wiesbachhorn:**

Figure 9.73: Map of the Große Wiesbachhorn and surrounding

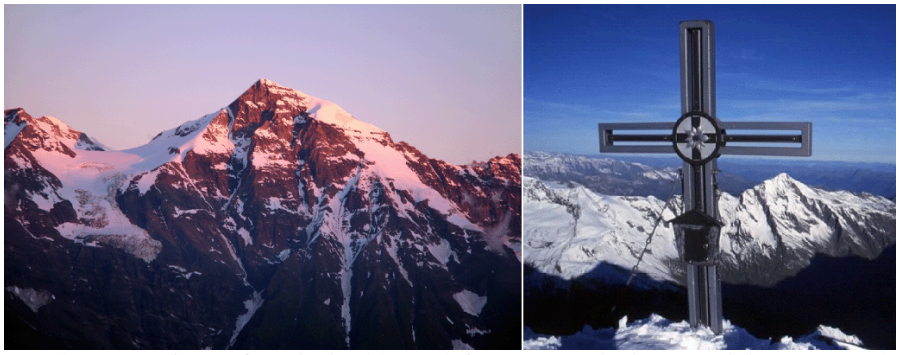
Figure 9.74: The mountain Große Wiesbachhorn (left) [*www.nightsky.at*] and the cross on the summit (right) [*Hermann Zauner*]

- **Gaisberg:**

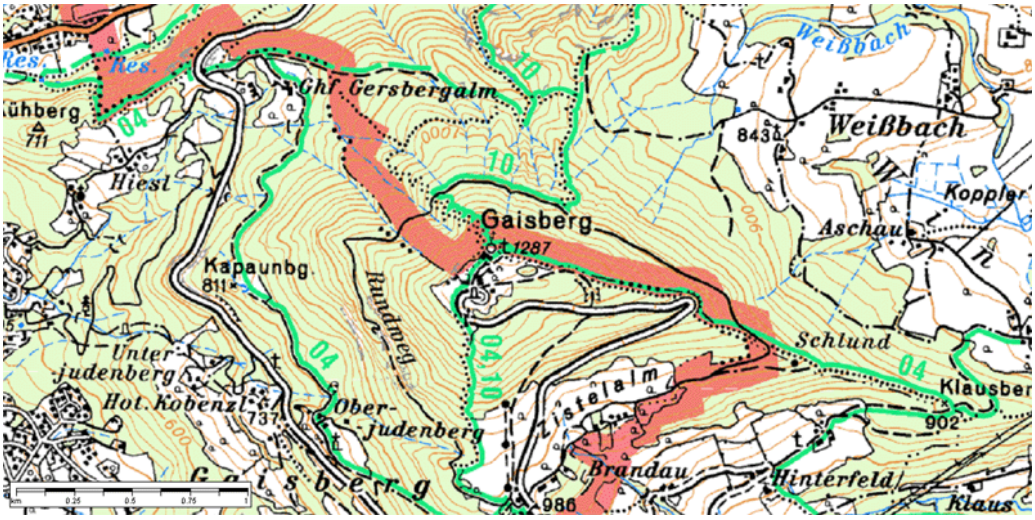

Figure 9.75: Map of the Gaisberg and surrounding


Figure 9.76: The Gaisberg (left) [*Hubert Umprecht*], the radio transmitter tower inclusive lightning measurement (middle) and the peak of the tower with the capture rods and measure resistance on the top (right) [*www.wabweb.net*]

Figure 9.77: The cross on the summit (left) and the signboard of the lightning measurement on the Gaisberg (right)

9.7. Tyrol

- **Kitzbühler Horn:**

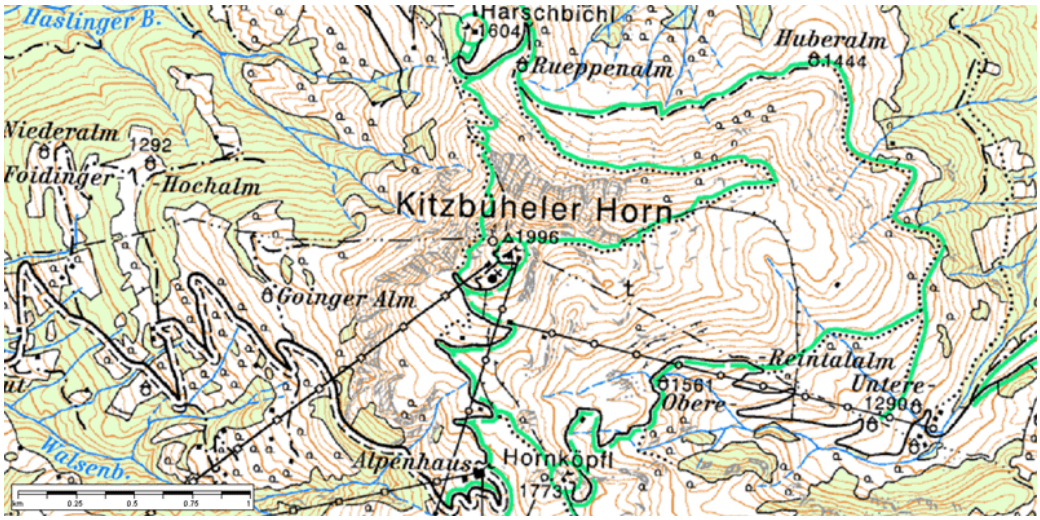

Figure 9.78: Map of the Kitzbühler Horn and surrounding

Figure 9.79: The mountain Kitzbühler Horn (left), the summit with the cable railway station and the radio transmitter tower (middle) [*www.wabweb.net*] and the tower next to the summit shelter (right) [*www.wabweb.net*]

Figure 9.80: The peak of the tower (left), the chapel (middle) and the cross next to the summit (right) [*Hubert Umprecht*]

- **Hohe Salve:**

Figure 9.81: Map of the Hohe Salve and surrounding

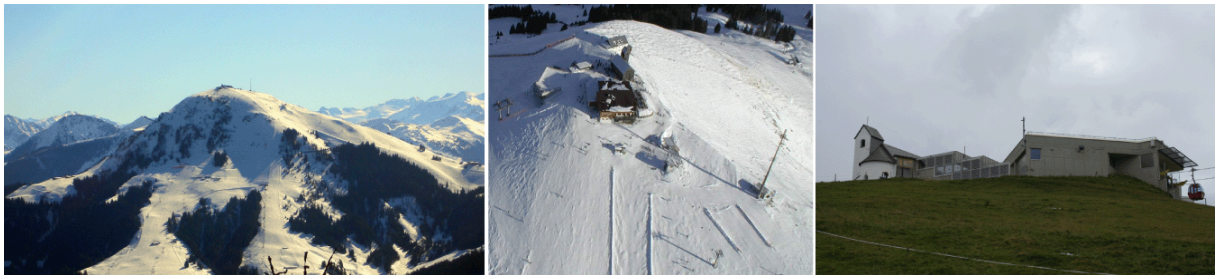
Figure 9.82: The mountain Hohe Salve (left) [*www.picasaweb.com*], an aerial view to the summit with two shelters, a chapel, a cable railway station, a drag lift and a transmitter tower (middle) [*www.panoramio.com*] and a close up of the chapel with one cable railway station (right) [*Hubert Umprecht*]


Figure 9.83: The summit with radio transmitter mast and cross (left), a close up of the tower (middle) and the top of it (right) [*Hubert Umprecht*]

- **Patscherkofel:**

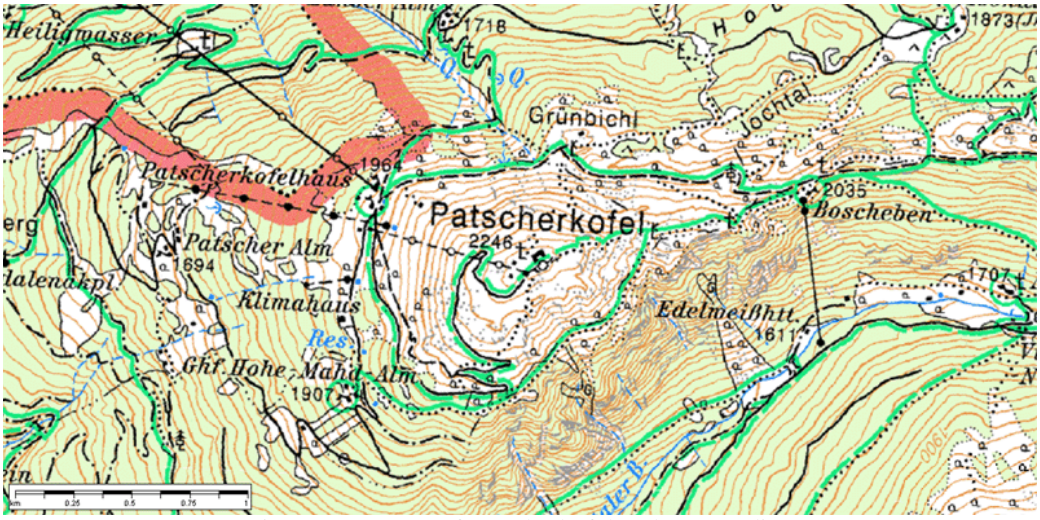

Figure 9.84: Map of Patscherkofel and surrounding

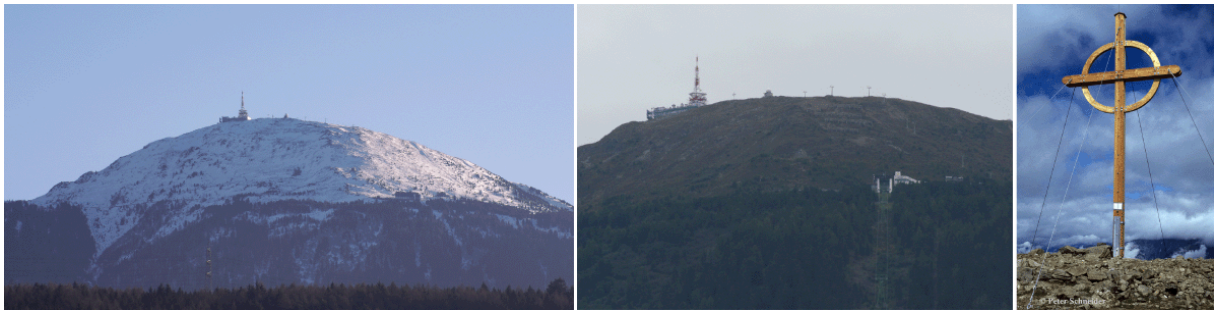
Figure 9.85: The Patscherkofel (left) [*www.wikipedia.org*], the summit inclusive the cable railway middle station (middle) [*Hubert Umprecht*] and the cross (right)


Figure 9.86: The summit with the radio transmitter towers (left), the weather radar and cross (right) and other sensors and buildings [*www.wabweb.net*]

Figure 9.87: The top of the two radio transmitter towers (left) [*www.wabweb.net*] and the peak of the higher one (right) [*Michael Kozubowski*]

- **Zugspitze:**

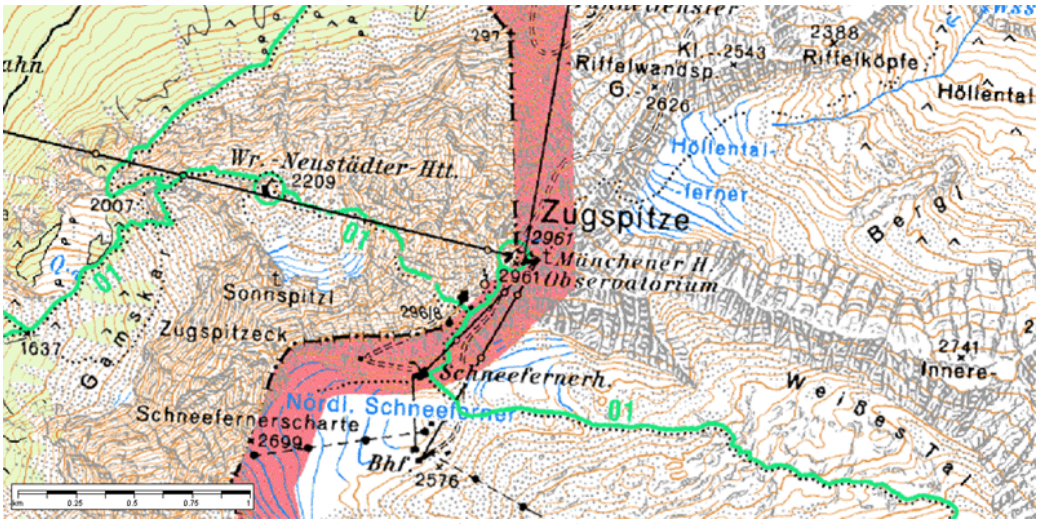

Figure 9.88: Map of the Zugspitze and surrounding

Figure 9.89: The west-wall of the Zugspitze massif (left) [*Wikipedia*], view from the German side (middle) [*www.h-i-g-h.de*] and the cross (right) [*www.sa-bri-na.de*]

Figure 9.90: The summit of the Zugspitze (left) [*www.zugspitze.at*], an aerial view (middle) [*Maximilian Dörrbecker*] and a close up of the building complex inclusive radio transmitter tower (right) [*www.senderfotos.de*]

10. Appendix B: Multiplicity

10.1. Lower Austria

- **Mistelbach / Josefsberg:**

Figure 10.1: The wind power park in the proximity of the north-eastern cluster point (left) and the radio transmitter tower on the highest point (right) [*Hubert Umprecht*]

Figure 10.2: The wind power park in the proximity of the south-western cluster point behind the village Schrick (left) and one of the wind power turbines (right) [*Hubert Umprecht*]

10.2. Upper Austria

- **Sternwald I wind power station:**

Figure 10.3: Wind Power Station V17708 [*Hubert Umprecht*]

- **Lichtenberg:**

Figure 10.4: The radio transmitter tower (left) [*www.wabweb.net*] and the viewing tower (right) [*www.av-linz.at*]

- **Gamsspitz:**

Figure 10.5: A view to the Gamsspitz from south [*Hubert Umprecht*]

10.3. Styria

- **Stuhleck:**

Figure 10.6: The Stuhleck (left) [*Josef Müller*] and the summit of the mountain viewed from east (right) [*www.modellflug-online.at*] inclusive chair lift and shelter

Figure 10.7: The metal cross with the chair lift in the background (left), the Alois-Günther-Haus on the summit (middle) and the chair lift (right) [*Hubert Umprecht*]

- **Graz – St.Peter:**

Figure 10.8: The church of St.Peter and surrounding (left) as well as the peak of the church (right) [*Hubert Umprecht*]

- **Zirbitzkogel / Scharfes Eck**

Photos of the Zirbitzkogel / Schafes Eck are seen in Appendix A: Lightning Density.

- **Schirchleralm**

Figure 10.9: The surrounding of the Schirchleralm [*Hubert Umprecht*]

10.4. Carinthia

- **Großer Speikkogel**

Photos of the Großer Speikkogel are seen in Appendix A: Lightning Density.

- **Saualpe – Nameless Summit 2029m**

Figure 10.10: Heap of stones on the 2029m summit with a small cross made of braches (left) and a view southward from the Ladinger Spitz (right) [*Hubert Umprecht*]

- **Sapotnigofen:**

Figure 10.11: A view to Sapotnigofen from south-west [*Hubert Umprecht*]

- **Pfannock:**

Figure 10.12: The Pfannock from the south (left) and the south-west ridge leading to the summit (right) [*www.summitpost.org*]

Figure 10.13: View from the summit to the south-west ridge (left) [*www.panoramio.com*] and the cross on the Pfannock (right) [*www.gipfelkreuz.de*]

- **Priedröf:**

Figure 10.14: The mountain Priedröf viewed from Bad Kleinkirchheim (left) [*www.picasaweb.com*] and the summit seen from the north (right) [*www.weissenboek.com*]

Figure 10.15: Summit View to north (left) [*www.panoramio.com*] and the cross on the Priedröf (right) [*www.weissenboek.com*]

- **Dobratsch:**

Photos of the Dobratsch are seen in Appendix A: Lightning Density.

- **Goldeck:**

Photos of the Goldeck are seen in Appendix A: Lightning Density.

- **Wabnigspitz:**

Figure 10.16: View to the Wabnigspitz from the north-eastern located mountain Säuleck [*www.bergfex.at*]

- **Böseck:**

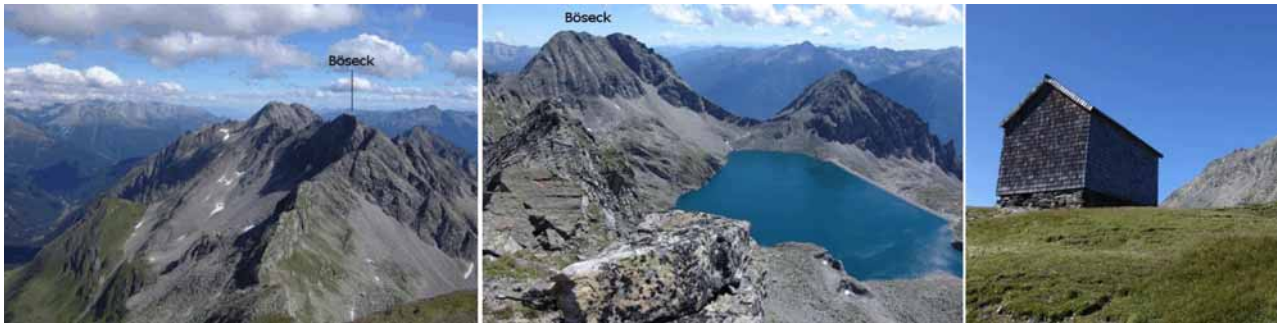

Figure 10.17: The Böseck viewed from north-east (left), the summit beneath the Oscheniksee (middle) and the cottage Böseckhütte (right) [*www.mallnitz.at*]

- **Promos / Köderhöhe:**

Figure 10.18: View from the Promos to the ridge in the north-west [*www.panoramio.com*]

- **Großglockner:**

Photos of the Großglockner are seen in Appendix A: Lightning Density.

10.5. East Tyrol

- **Alkuser Rotspitze:**

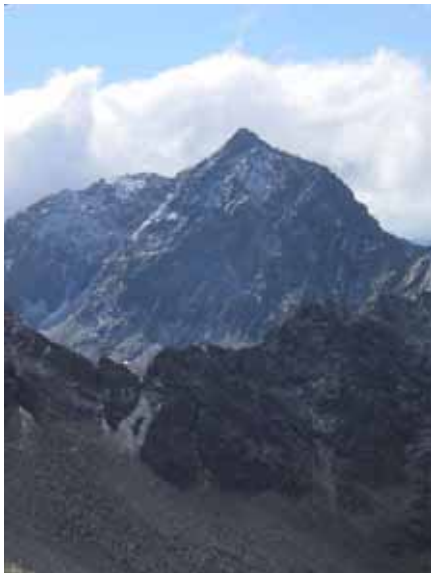

Figure 10.19: The Alkuser Rotspitze [*www.gibmirberge.at*]

10.6. Salzburg

- **Gaisberg:**

Photos of the Gaisberg are seen in Appendix A: Lightning Density.

- **Hochseiler:**

Figure 10.20: View to the Hochkönig massif from the south (left) [*www.wikipedia.org*] the summit Hochseiler (middle) [*www.picasaweb.com*] and the cross on the Hochseiler (right) [*www.alpintouren.com*]

- **Lärchkopf:**

Figure 10.21: The highest summits of the Leoganger Steinberge (left) [*www.wikipedia.org*] and the approximate location of the Lärchkopf in the Leoganger Steinberge (right)

Figure 10.22: The surrounding of the Lärchkopf where the flash was located [*Hubert Umprecht*]

- **Höllwand:**

Figure 10.23: The mountain Höllwand (left) [*www.hikr.org*], the summit (middle) [*www.wanderforum.at*] and the top with the cross (right) [*www.hikr.org*]

- **Reißrachkopf:**

Figure 10.24: The Reißrachkopf viewed from south-west (left), the summit with the cross (middle) and the drag-lift station 300m east of the summit (right) [*Hubert Umprecht*]

- **Breitebenkopf:**

Figure 10.25: The Breitebenkopf from north-east (left) [*Hubert Umprecht*], a view from the eastern village Wörth (middle) [*Hubert Umprecht*] and the cross on the top (right) [*www.bergwolf.at*]

- **Hochgolling:**

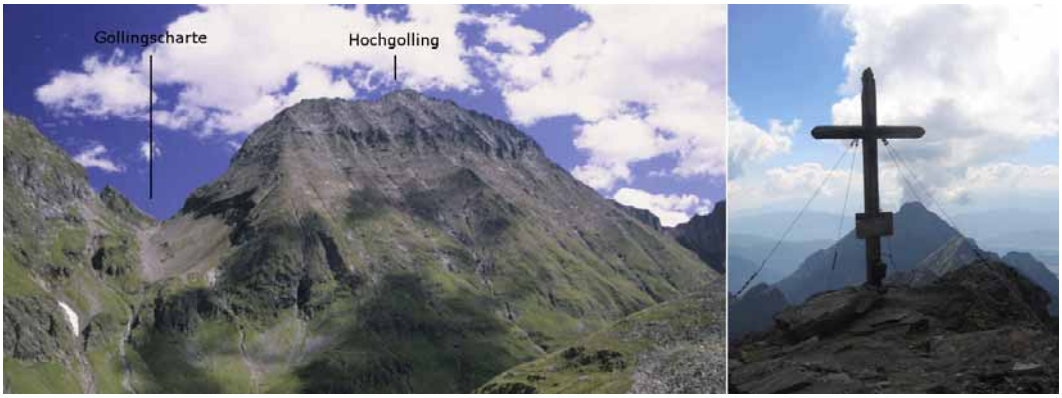

Figure 10.26: Gollingscharte and the mountain Hochgolling from south-west (left) [*www.wikipedia.org*] and the cross on the summit (right) [*www.panoramio.com*]

- **Hirschwand / Himmelwand:**

Figure 10.27: View to the Hirschwand (left rock) and the Himmelwand (right rock) from the north [*Hubert Umprecht*]

Figure 10.28: The Himmelwand (left) and the Hirschwand (right) [*Hubert Umprecht*]

- **Große Wiesbachhorn / Hoher Tenn:**

Figure 10.29: The Große Wiesbachhorn and the Hoher Tenn (left) [*Hubert Umprecht*] and the cross on the Schneespitze (right) [*www.picasaweb.com*]

- **Hocharn:**

Figure 10.30: The Hocharn viewed from north-east (left) [*www.pohori.supervht.com*] and the cross on the summit (right) [*www.panoramio.com*]

- **Unknown Summit 2107m / Hinterglemm:**

Figure 10.31: The interesting area where the flash was located (left), the drag-lift (middle) and the unknown summit with the cross on the top (right) [*Hubert Umprecht*]

11. Appendix C: Maximum Lightning Currents

11.1. Austria

Table 11.1: Flashes with a peak current higher than 300kA in Austria

amplitude [kA]	date	time	number of strokes	stroke number	χ^2	major-axis [km]	number of sensors	degree of freedom
494.5	22.05.2005	18:45:06	3	1	7.2	4.6	24	6
488.5	17.03.2001	19:24:12	1	1	3.1	0.5	29	2
443.8	29.04.2000	20:16:08	1	1	2	8.2	13	4
385.8	04.05.2000	17:08:41	1	1	5.5	24.5	2	1
384.8	**29.03.2005**	**16:40:10**	**1**	**1**	**1.2**	**0.3**	**12**	**12**
371.4	29.07.2002	12:58:20	1	1	0.6	16	5	1
360.9	29.03.2007	14:43:42	1	1	3.2	9.6	5	3
360.1	29.03.2005	16:35:44	2	1	3.6	0.5	28	19
357.6	04.10.2003	06:20:51	1	1	4.8	0.8	5	5
354.7	27.05.2003	14:02:50	2	1	6.9	11.1	8	1
352.8	06.12.2005	12:35:19	1	1	0.5	3.2	5	2
352.7	29.05.2003	15:42:10	2	1	2.1	1.4	4	5
346.2	20.08.2005	08:43:15	2	2	2.6	0.3	17	15
343.1	07.08.2005	09:49:16	1	1	6.4	13.4	3	1
336.7	28.07.2000	14:19:11	3	2	0.2	3.3	8	3
330.8	16.07.2005	23:25:56	1	1	3.6	0.9	32	26
328.6	03.05.2005	18:23:17	12	2	9.19	0.9	18	11
325.4	22.04.2003	14:15:50	1	1	2.6	7.9	2	1
324.3	26.07.2005	17:51:54	3	1	1.7	1.1	9	2
324.3	28.08.2006	18:09:09	1	1	2.8	0.4	28	10
322.5	27.09.2005	02:05:54	1	1	8.5	0.5	36	27
322.5	17.05.2006	03:08:52	1	1	2.1	0.8	27	5
319.3	25.08.2002	15:03:42	3	1	0.1	4.6	3	1
317.6	06.06.2001	16:32:09	1	1	4	1.4	21	10
317.3	31.07.2002	19:17:21	3	1	0.6	0.5	21	22
316.7	23.04.2006	12:09:06	3	2	4.7	0.6	26	15
314.8	29.04.2000	18:40:17	1	1	0	10.9	9	1
313.7	22.07.2005	18:19:55	2	1	0.8	0.4	32	16
313.1	07.07.2005	23:02:42	1	1	3.1	0.3	36	24
312.9	30.08.2007	05:35:48	1	1	1	0.8	23	12
312.8	03.09.2002	00:20:54	1	1	2.8	1.5	3	2
311.8	11.09.2003	11:24:44	1	1	0.3	1.6	7	3
311.2	29.06.2007	18:26:41	1	1	4.3	0.3	33	17
311.1	18.08.2005	16:14:31	1	1	0.9	9.89	8	3
310.6	10.08.2006	17:40:59	1	1	1.1	0.3	10	11
306.9	04.09.2000	11:50:53	2	1	2.5	0.4	6	3
306.7	15.07.2001	15:14:31	1	1	2.6	0.5	3	2
306.4	04.05.2000	17:13:37	1	1	1.7	0.7	30	14

amplitude [kA]	date	time	number of strokes	stroke number	χ^2	major-axis [km]	number of sensors	degree of freedom
-597.6	08.11.2000	02:46:32	1	1	0	2.7	26	2
-416.3	13.07.2004	14:53:26	1	1	2.29	1.2	6	3
-398.4	30.03.2005	17:48:55	3	1	3.9	2	8	6
-398.2	23.07.2004	08:18:13	1	1	1.6	3.2	5	6
-398	29.03.2005	02:33:02	4	2	9.5	1.6	9	2
-395.2	04.10.2003	20:44:18	2	2	3.5	5	9	3
-385	**18.08.2002**	**11:49:41**	**1**	**1**	**1.7**	**2.5**	**7**	**7**
-379.9	25.07.2005	15:21:07	1	1	3.7	0.5	8	3
-368.6	06.05.2001	13:00:36	1	1	1	1.9	6	1
-364.8	01.05.2000	18:58:25	1	1	1.1	3.9	18	1
-353.6	09.10.2004	23:31:43	1	1	2.29	0.9	12	11
-352.4	20.08.2005	07:40:54	1	1	3.8	0.7	9	9
-349.3	30.03.2005	12:05:00	1	1	3.1	1.6	8	2
-346.7	26.06.2003	17:35:55	2	2	1.9	1.2	4	3
-346.4	30.03.2003	17:53:26	1	1	2.4	0.5	6	3
-346.4	09.05.2003	10:33:52	1	1	2.6	2.8	5	4
-346.2	17.03.2001	19:24:12	1	1	1.3	2	6	2
-345	04.06.2003	13:44:52	1	1	5.8	1.8	7	4
-342.5	19.04.2005	14:12:30	1	1	1	0.5	9	11
-332.2	22.07.2005	18:19:55	2	2	8.9	3.4	2	1
-332.1	27.07.2006	17:20:24	1	1	4.9	10.3	3	1
-329.4	01.05.2000	13:41:39	1	1	0.5	8.4	4	1
-327.7	01.07.2005	05:36:42	2	1	1.2	2.4	9	10
-326.2	10.05.2006	16:49:10	1	1	3.4	3	7	6
-324.2	27.08.2005	14:54:50	1	1	3.1	0.7	4	3
-322.7	03.09.2002	02:45:22	3	1	6.2	1.9	3	1
-321.7	18.10.2002	07:44:53	1	1	1.7	1.3	5	6
-321.6	15.12.2000	18:25:01	1	1	1	9.9	19	1
-320.1	30.08.2000	15:45:58	2	1	1.9	1.7	6	2
-318.8	01.05.2000	18:58:25	1	1	2.8	3.3	4	3
-314.5	09.05.2003	19:50:21	1	1	0.1	9.5	3	2
-313.4	20.08.2005	07:42:13	2	2	4.59	2.2	12	13
-312.4	06.10.2007	01:07:50	5	1	0.2	3.7	22	3
-309.2	23.04.2003	11:15:27	2	1	5.8	0.5	5	2
-308.4	26.04.2007	16:22:10	4	1	1.6	0.6	14	9
-305.5	31.05.2003	12:18:43	2	1	1.8	0.4	28	18
-304.9	20.08.2007	04:25:49	1	1	1.8	1.2	6	2
-304.6	03.07.2003	09:58:11	2	2	1.3	0.6	4	3

303.7	29.03.2005	16:43:13	1	1	1.4	0.3	26	15
302.7	04.06.2007	13:02:46	7	2	0.6	5.9	10	3
302.5	28.07.2003	19:40:51	1	1	3.6	0.8	26	8
302	24.06.2005	15:58:14	3	1	6.6	12	9	5
301.9	01.07.2005	12:49:43	1	1	3.6	2.2	21	9
301.3	27.06.2003	10:26:42	6	1	1.2	2.3	8	1

-303.5	28.06.2006	03:47:36	1	1	1.7	0.6	6	6
-302.3	20.09.2000	16:41:35	1	1	3.8	1.8	9	4
-301.2	15.05.2007	11:04:01	1	1	8.3	0.5	10	8

11.2. Middle Europe

Table 11.2: Flashes with a peak current higher than 400kA in Middle Europe

amplitude [kA]	date	time	number of strokes	stroke number	ki2	major-axis [km]	number of sensors	degree of freedom
-716.1	11.03.2004	10:52:32	1	1	3.4	3.8	11	4
-620	03.11.2000	04:24:38	1	1	2.9	2.2	15	3
-597.6	08.11.2000	02:46:32	1	1	0	2.7	26	2
-586.2	26.11.2000	00:15:23	1	1	0.3	19.3	15	1
-543.7	20.11.2000	13:06:43	1	1	0	8.9	15	2
-521.9	08.05.2005	21:02:59	4	2	0.4	4.4	5	4
-514.4	23.03.2001	18:49:51	1	1	0.3	22.9	9	1
-509.2	29.03.2005	16:31:14	1	1	2.29	2.4	8	2
-502	29.10.2000	04:44:51	1	1	0.5	12.9	7	1
-495.3	06.06.2007	22:21:00	1	1	3.9	4.69	16	3
-486.6	09.11.2001	00:26:01	1	1	0	7.2	16	2
-479.6	06.04.2000	14:50:29	1	1	0.1	4.5	6	2
-473.1	**24.10.2006**	**05:16:28**	**1**	**1**	**5.5**	**3.8**	**26**	**17**
-468.6	25.05.2007	18:48:28	1	1	2.5	0.9	8	5
-460.6	23.04.2007	13:03:44	1	1	9.6	6.4	9	3
-458.5	12.06.2004	18:23:40	1	1	1.4	0.6	8	11
-458	08.11.2001	22:21:43	1	1	8.2	12.3	16	1
-448.2	03.11.2000	14:49:15	1	1	0	7.8	15	3
-436.5	11.10.2000	22:24:34	1	1	8.3	12.5	5	1
-434.9	20.04.2005	10:06:24	1	1	2	3.6	13	3
-425.5	06.04.2000	14:42:17	1	1	0.2	5.2	7	1
-424.4	10.06.2000	16:47:31	1	1	5.1	6.1	4	1
-422.8	20.08.2005	00:58:10	1	1	0.8	4.3	11	3
-422	04.10.2003	15:25:49	1	1	0.7	20.29	5	1
-416.3	13.07.2004	14:53:26	1	1	2.29	1.2	6	3
-412.1	29.03.2005	14:31:27	1	1	1.1	5.2	6	3
-409.5	29.10.2000	04:42:36	1	1	0	12.7	9	2
-403.1	02.06.2003	05:28:56	3	1	5.8	2.5	13	1
-400.1	16.04.2005	20:35:16	2	1	3.1	0.3	45	47

amplitude [kA]	date	time	number of strokes	stroke number	ki2	major-axis [km]	number of sensors	degree of freedom
551.2	**30.03.2005**	**16:45:59**	**1**	**1**	**2.4**	**0.8**	**11**	**5**
494.5	22.05.2005	18:45:06	3	1	7.2	4.6	24	6
488.5	17.03.2001	19:24:12	1	1	3.1	0.5	29	2
482.6	11.08.2005	11:25:42	5	1	3.1	0.7	8	6
459.9	17.04.2005	15:13:50	6	1	8.19	0.6	16	6
456.9	04.04.2006	14:15:03	5	1	0.5	2.7	20	3
454.7	22.04.2006	17:52:15	1	1	3.9	15.4	8	2
443.8	29.04.2000	20:16:08	1	1	2	8.2	13	4
439	27.12.2004	03:05:31	1	1	3.7	2.09	12	7
432.7	29.10.2000	04:35:44	1	1	5.5	20.4	7	1
428.6	06.04.2005	19:00:46	1	1	2.6	0.6	17	7
428	09.07.2007	15:15:44	1	1	0.8	2.2	6	2
424.2	09.11.2001	00:22:29	1	1	0.1	21.9	9	1
421.9	21.04.2003	15:32:40	2	1	1.8	1.4	11	2
421.8	07.12.2006	19:56:52	1	1	1.7	0.7	21	10
420.9	31.03.2003	14:51:03	1	1	0.8	0.8	14	11
416.6	26.03.2003	15:27:30	1	1	0.4	21	15	1
416.6	08.11.2001	21:28:03	1	1	1.4	21.6	9	1
415	29.03.2005	01:15:01	3	1	1.5	2.4	21	8
412.3	04.08.2000	14:30:08	1	1	2.6	12	23	1
405	03.11.2000	03:49:38	1	1	0	4.8	12	2
404.5	10.07.2007	12:38:34	2	1	0.2	2.3	8	2
403	09.01.2004	13:33:52	2	1	1.3	5.2	11	1
402.9	07.12.2005	05:59:05	1	1	1.2	0.7	17	12
400	05.12.2005	11:30:42	2	1	1.3	2	8	6

12. References

ALDIS *www.aldis.at*, March 2009

Anderson R., Bjornsson S., Blanchard D.C., Gathman S., Hughes J., Jonasson S., Moore C.B., Survilas H.J. and Vonnegut 1965, *Electricity in Volcanic Clouds*, Science 148, pp. 1179-1189

Berger K. 1978, *Blitzstromparameter von Aufwärtsblitzen*, Bull. Schweiz. Elektrotechn. Ver., 69, pp. 353-360

Brook M., Moore C.B. and Segurgenssen J. 1974, *Lightning in Volcanic Clouds*, J. Geophys. Res. 79, pp. 472-475

Byrne G.J., Few A.A. and Weber M.E. 1983, *Altitude, Thickness and Charge Concentration of Charged Regions of Four Thunderstorms during Trip 1981 Based Upon in Situ Ballon Electric Field Measurements*, Geophys. Res. Lett., 10, pp. 39-42

CIGRE, Diendorfer G., Bernardi M., Cummins K., De La Rosa F., Hermoso B., Hussein A., Kawamura T., Rachidi F., Rakov V., Schulz W., and Torres H. 2008, *CLOUD-TO-GROUND LIGHTNING PARAMETERS DERIVED FROM LIGHTNING LOCATION SYSTEMS*

Cummins K.L., Krider E.P. and M.D. Malone 1998, *The U.S. National Lightning Detection Network and Applications of Cloud-to-Ground Lightning by Electric Power Utilities,* IEEE Transactions on Electromagnetic Compatibility, Vol. 40, No. 4, pp. 465-480

Cummins, K.L., 2000: *Continental-scale detection of cloud-to-ground lightning,* T.IEE Japan, Vol. 120-B, No. 1

Diendorfer G. and Schulz W. 1998, *Lightning Characteristics Based on Data from the Austrian Lightning Locating System,* IEEE-EMC Transactions, Vol. 40, No. 4

Diendorfer G. 2007, *Lightning Location Systems (LLS),* IX International Symposium on Lightning Protection (SIPDA), Foz do Iguaçu, Brazil

EUCLID *www.euclid.org*, March 2009.

Finkelstein D. and Powell J. 1970, *Earthquake Lightning*, Nature (London), 228, pp. 759-760

Gardner R.L., Frese M.H., Gilbert J.L., and Longmire C.L. 1984, *A Physical Model of Nuclear Lightning*, Phys. Fluids, 27, pp. 2694-2698

Gary C. 1995, *La Foudre: Des methodologies antiques à la recherche moderne*, Masson, Paris-France

Gotthardt E. 1968, *Einführung in die Ausgleichsrechnung,* Herbert Wichmann Verlag, Karlsruhe

Grover M.K. 1981, *Some Analytical Models for Quasi-Static Source Region EMP: Aplication to Nuclear Lightning*, IEEE Trans. Nucl. Sci., NS-28, pp. 990-994

Hasse Peter, Wiesinger Johannes and Wolfgang Zischank 2006, *Handbuch für Blitzschutz und Erdung*, Richard Pflaum Verlag GmbH & Co KG Munich, Germany.

Hill R.D. 1973, *Lightning Induced by Nuclear Bursts*, J. Geophys. Res., 78, pp. 6355-6358

Horner F. 1957, *Very-low-frequency propagation and direction finding,* Proc. IEEE, 101B, pp. 73-80

Jayaratne E.R. and Saunders C.P.R., 1984, *The Rain Gush, Lightning, and the Lower Positiv Charge Center in Thunderstorms*, J. Geophys. Res., 89, pp. 816-818

Kamra A.K. 1972, *Measurements of the Electrical Properties of Dust Storms*, J. Geophys. Res., 77, pp. 5856-5869

Krider E.P., Noggle R.C., Pifer A.E., Vance D.L. 1980, *Lightning direction-finding systems for forest fire detection*, J. Appl. Meteor

Malan D.J. and Schonland B.F.J. 1951, *The Distribution of Electricity in Thunderclouds*, Proc. Soc. London Ser. A, 209, pp. 158-177

Marshall T.C. and Winn W.P. 1982, *Measurements of Charged Precipitations in a New Mexico Thunderstorm: Lower Positive Charge Centers*, J. Geophys. Res., 87, pp. 7141-7157

ORS *www.ors.at*, 19.11.2008

Rachidi F., Bermudez J.L. Rubinstein M. and Rakov V.A. 2004, *On the estimation of lightning peak currents from measured fields using lightning location systems*, Journal of Electrostatics, Vol.60, pp. 121-129

Rakov V.A. and Uman M.A. 2003, *Lightning Physics and Effects*, Cambridge University Press, U.S.

Sartor J.D., 1967, *The Role of Particle Interactions in the Distribution of Electricity in Thunderstorms*, J. Atmos. Sci., 24, pp. 601-613

Schneebergbahn *www.schneebergbahn.at*, 27.11.2008

Schulz W. 1997, *Performance evaluation of lightning location systems*, PhD thesis, 136 pp, Technical University of Vienna

Schulz W. und Diendorfer G. 2000, *Evaluation of a lightning location algorithm using an elevation model*, 25th International Conference on Lightning Protection (ICLP), Rhodos

Schulz W. und Diendorfer G. 2003, *Bipolar flashes detected with lightning location systems and measured on an instrumented tower*, Int. Symposium on Lightning Protection, Curitiba, Brazil

Uman M.A., Seacord D.F., Price G.H. and Pierce E.T. 1972, *Lightning Induced by Thermonuclear Detonations*, J. Geophys. Res, 77, pp. 1591-1596

Uman M.A., D.K. McLain and E.P. Krider 1975, *The electromagnetic radiation from a finite antenna*, Am. J.Phys.43

Uman M.A. 1986, *All About Lightning*, Dover Publications, Inc., New York, U.S.

Uman M.A. 1987, *The Lightning Discharge*, Academic Press, Inc., Orlando

Pounder C. 1980, *Weather*, 35, pp. 357-360

Wagner P.B. and Telford J.V. 1981, *Charge Dynamics and a Electric Charge Separation Mechanism in Convective Clouds*, J. Rech. Atmos., 15, pp. 97-120

Weber M.E., Christian H.J., Few A.A. and Stewart M.F. 1982, A Thundercloud Electric Field Sounding: Charge Distribution and Lightning, J. Geophys. Res., 87, pp. 7158-7169